

University of Alberta

**The Effect of Skin and Soft Tissue on Spinal
Frequency Response Measurements**

by

Colleen Patricia Decker

A thesis submitted to the Faculty of Graduate Studies and Research
in partial fulfillment of the requirements for the degree of

Master of Science

Department of Biomedical Engineering

©Colleen Patricia Decker

Fall 2010

Edmonton, Alberta

Permission is hereby granted to the University of Alberta Libraries to reproduce single copies of this thesis and to lend or sell such copies for private, scholarly or scientific research purposes only. Where the thesis is converted to, or otherwise made available in digital form, the University of Alberta will advise potential users of the thesis of these terms.

The author reserves all other publication and other rights in association with the copyright in the thesis and, except as herein before provided, neither the thesis nor any substantial portion thereof may be printed or otherwise reproduced in any material form whatsoever without the author's prior written permission.

Examining Committee

Greg Kawchuk, Faculty of Rehabilitation Medicine – Department of Physical Therapy

Jason Carey, Faculty of Engineering – Department of Mechanical Engineering

Gary Faulkner, Faculty of Engineering – Department of Mechanical Engineering

I would like to dedicate my thesis to my parents, Pat and Bob,
who have always supported me whole heartedly in
every endeavor I have chosen in my life.

Abstract

Introduction: This study sought to investigate the effects of soft tissue on measurements of a spinal vibration response using skin-mounted accelerometers and a non-invasive contact tip.

Methods: Vibration was applied to the spine of porcine and human cadavers. Measurements of the spinal vibration response were taken from needle, skin, and bone-mounted accelerometers. Several skin-mounted accelerometer placements dorsal to a spinous process were tested, and 6 different non-invasive contact tip shapes were used to explore sources of variance in the signals.

Results: Vibration measured from skin-mounted accelerometers had altered signal patterns compared to bone-mounted accelerometers. The measured FRF was found to be sensitive to accelerometer positioning. No significant difference in skin-bone correlation was attributed to contact tip shape or vertebral level.

Conclusion: The use of a non-invasive contact tip excites vibration in the soft tissues which overlay the spine, in addition to the vertebral column. This vibration interferes with skin sensor measurements of vertebral vibration response, with the effect diminishing as distance from the contact tip increases. Small changes in contact tip shape do not affect the correlation between skin and bone signals.

Acknowledgements

I would like to sincerely thank the following people for helping me succeed in completing this thesis:

Will Mason, my fiancé – Through the best and worst times of this journey, your unconditional love has helped me reach my goal.

Bob and Pat Decker, my parents – thank you for always encouraging me to pursue my dreams and always be the best person I can be.

Dr. Greg Kawchuk, my supervisor – You have taught me so much, not just about research, but about living life to the fullest and loving every minute of it. Thank you for being a wonderful role model and mentor.

Dr. Jason Carey – Thank you for your invaluable input to the direction my work has taken, and for helping me remember what I came here for.

Dr. Gary Faulkner – Thank you for your input as a teacher and expert, right from the beginning of my program.

Michèle Vaillant – My lab partner in crime. How can I ever thank you enough for your emotional and technical support. From being my guinea pig to harboring us flood refugees to becoming an unwitting comedian with your English-isms, you have helped make this experience both worthwhile and entertaining.

Dr. Narasimha Prasad – My statistics advisor. I am grateful for your patience with my seemingly endless questions and excellent advice.

Paula Mosbrucker – Thank you for always being there for me. I am glad we went through this journey together.

Brian Decker – I know I am lucky to have one of the most wonderful and supportive brothers in the world. Thank you for being there.

To my lab family - Arnold, Tiffany, Grayson, Riikka, and Maxi – Thank you for providing technical support, editing, advice, laughs, and wonderful conversations.

Maisie Goh, Benu Bawa, Debbie Pietrzykowski, and Cheryl Low – Thank you for keeping me on track in my program (and also answering my inane administrative questions).

Table of Contents

Chapter 1:	Introduction	1
1.1	Overview	1
1.2	Background and Rationale	2
1.2.1	Prevalence and Impact of Low Back Pain	2
1.2.2	Mechanical Dysfunction as a Cause of Low Back Pain.....	3
1.2.3	Diagnosing Low Back Disorders	3
1.3	Potential Solution for Non-Invasive Functional Analysis of the Spine.....	4
1.3.1	Precedent for use of Vibration in Medical Diagnostics.....	5
1.4	The Effects of Soft Tissue in Live Vibration Testing	6
1.5	Problem Statement.....	7
1.6	Purpose	8
1.7	Goals	8
1.7.1	Protocol 1 Goals	8
1.7.2	Protocol 2 Goals	9
1.8	Hypotheses	9
1.8.1	Protocol 1 Hypotheses	10
1.8.2	Protocol 2 Hypotheses	10
1.9	Statement on Research Ethics	11
1.10	Thesis Outline.....	12
1.11	References	13
Chapter 2:	Literature Review	19
2.1	Introduction	19
2.2	Lumbar Spine Structure and Anatomy.....	20
2.3	Low Back Disorders.....	23
2.3.1	Epidemiology.....	23
2.3.2	Socio-Economic Effects of LBDs	24
2.3.3	Dysfunction of the Spine.....	25
2.4	Diagnosing Low Back Disorders	30
2.4.1	Diagnostic Techniques	30

2.4.2	Disadvantages and Limitations of Current Diagnostic Techniques.....	34
2.4.3	Pain as a Confounder in Diagnosis of Spinal Dysfunction.....	38
2.4.4	Summary on Diagnostics.....	39
2.5	Vibration and Dynamics.....	40
2.6	Structural Damage Detection	44
2.6.1	Current Standard Uses of Structural Damage Detection.....	48
2.6.2	Structural Damage Detection as a Medical Diagnostic Technique	48
2.6.3	Experimental Factors in Structural Damage Detection for Medical Applications.....	57
2.7	Skin and Soft Tissue Effects.....	59
2.7.1	Anatomy of the Skin.....	60
2.7.2	Mechanics of the Skin	61
2.7.3	Skin Thickness Effects	63
2.7.4	Effects of Time-Variant Factors on Skin Properties	64
2.7.5	Other Soft Tissue Effects.....	66
2.7.6	Accuracy of Bone Motion Measurements by Skin Mounted Sensors	66
2.7.7	Methods of Correcting Error in Skin Mounted Sensors.....	68
2.8	Signal Analysis Techniques.....	71
2.8.1	Global Shape and Amplitude Criteria.....	72
2.8.2	Principal Component Analysis.....	73
2.8.3	The D-statistic	76
2.8.4	Transmissibility	78
2.9	Literature Review Summary.....	79
2.10	References	81
Chapter 3: Protocol 1 – Determining Skin Effects Using Invasive and Non-Invasive Contact Tips.....		
3.1	Overview	100
3.2	Introduction	100
3.2.1	Protocol Goals and Hypotheses	102
3.3	Methods.....	104
3.3.1	Animal Preparation	104
3.3.2	Application of Equipment	106

3.3.3	Vibration Input.....	109
3.3.4	Repeatability of Tests.....	110
3.3.5	Accelerometer Position Tests (Non-invasive Contact Tip).....	110
3.3.6	Needle-mounted Accelerometer Technique Validation.....	111
3.3.7	Invasive and Non-Invasive Contact Tip Comparison.....	113
3.3.8	Accelerometer Position Tests (Invasive Contact Tip).....	115
3.3.9	Data Analysis Techniques.....	115
3.4	Results.....	117
3.4.1	Repeatability of Tests - Single Transducer Results	117
3.4.2	Repeatability of Tests - Multiple Transducer Results	119
3.4.3	T-9 Accelerometer Placement Results.....	122
3.4.4	Results of Replacement Tests	130
3.4.5	Comparison of T-10 Needle and Bone Mounted Accelerometer Signals.....	133
3.4.6	Statistical Results Summary	136
3.5	Discussion.....	137
3.5.1	Signal Smoothing.....	137
3.5.2	Repeatability of Measured Signals.....	138
3.5.3	T-9 Accelerometer Placement	138
3.5.4	Replacement of A-A'	145
3.5.5	Needle and Bone Vibration Response Measurement Comparisons.....	146
3.6	Conclusions	150
3.7	References	152
Chapter 4: Protocol 2 – Effect of Contact Tip Shape on Correlation between Skin and Bone Vibration Response Signals.....		157
4.1	Overview	157
4.2	Introduction	158
4.2.1	Protocol Goals and Hypotheses	159
4.3	Methods.....	161
4.3.1	Porcine Cadaver Setup.....	161
4.3.2	Human Cadaver Setup	162
4.3.3	Equipment Setup	163
4.3.4	Experiment Procedure	166

4.3.5	Data Analysis Techniques.....	168
4.4	Results.....	169
4.4.1	Repeatability of Tests.....	169
4.4.2	Skin and Needle Mounted Accelerometer Correlations.....	175
4.4.3	Replaceability of Skin-Mounted Accelerometers	181
4.4.4	ANOVA Results Summary.....	184
4.5	Discussion.....	185
4.5.1	Repeatability of Measured Signals.....	185
4.5.2	Effect of Distance between Contact Tip and Accelerometer.....	185
4.5.3	Contact Tip Shape Effect.....	188
4.5.4	Correlation of Skin and Bone signals in Porcine vs. Human Cadavers....	191
4.5.5	Replaceability of Skin-Mounted Accelerometers	195
4.6	Conclusions	196
4.7	References	198
Chapter 5:	Discussion of Overall Results	201
5.1	Introduction	201
5.2	Discussion of Overall Results	201
5.2.1	Signal Attenuation Due to Soft Tissues.....	201
5.2.2	Signal Correlation Methods	206
5.2.3	Comparison of Skin and Reference Signals.....	210
5.3	Strengths and Weaknesses of the Study	216
5.3.1	Strengths.....	216
5.3.2	Weaknesses	217
5.4	Influence of Study Assumptions	220
5.5	Significance of the Study.....	222
5.6	Future Considerations.....	224
5.7	References	226
Chapter 6:	Summary of Conclusions.....	230
6.1	Protocol 1 Conclusions.....	230
6.2	Protocol 2 Conclusions.....	231
6.3	Overall Conclusions.....	231
Appendix A:	Principal Component Analysis Calculation.....	233

Appendix B: Compression-Spring Force Gage	238
Appendix C: Vibration System Technical Background.....	241
Appendix D: Human Cadaver Ethics Documents.....	249
Appendix E: Porcine Cadaver Tissues Permission	266
Appendix F: Calculation of Accelerometer Weight Factor.....	269

List of Tables

Table 3.1: Mean GSC and GAC on global sensor system using the non-invasive contact tip, averaged over position tests.	120
Table 3.2: Mean GSC and GAC on global sensor system using the invasive contact tip, averaged over position tests.	121
Table 3.3: Percentage of variance accounted for by PC1 in each subject.....	125
Table 3.4: Description of mean placement FRF features, and signal effect represented by PC1, for the non-invasive contact tip.....	126
Table 3.5: Description of mean placement FRF features, and signal effect represented by PC1, for the invasive contact tip	126
Table 3.6: Non-invasive contact tip D-statistic values between mean skin-mounted accelerometer and 95% confidence interval on bone-mounted accelerometer signals.	129
Table 3.7: Invasive contact tip D-statistic values between mean skin-mounted accelerometer and 95% confidence interval on bone-mounted accelerometer signals.....	130
Table 3.8: D-Statistic values comparing Position A and Position A'	132
Table 3.9: D-statistic results for all subject using both the non-invasive and invasive contact tips, comparing the needle-mounted accelerometer signal to bone-mounted accelerometer signal.	135
Table 3.10: Summary of statistical tests run in Protocol 1. Significant results are indicated by *. All ANOVAs were run at $\alpha=0.05$	136

Table 4.1: Results of GSC and GAC for the global accelerometer system in cadaveric porcine experiments.....	173
Table 4.2: Results of GSC and GAC for the global accelerometer system in cadaveric human experiments.....	174
Table 4.3: D-statistic values comparing mean skin-mounted accelerometer FRF to the mean needle-mounted accelerometer FRF in porcine cadaver subjects. ...	176
Table 4.4: D-statistic values comparing mean skin-mounted accelerometer FRF to the mean needle-mounted accelerometer FRF in human cadaver subjects.	177
Table 4.5: D-statistic on replacements of the skin-mounted accelerometer to its original position in human cadaver subjects.	183
Table 4.6: Summary of RM ANOVA findings for Protocol 2 results. Significant results are indicated by *. All ANOVAs were run at $\alpha=0.05$	184
Table C.1: Excitation Signal Characteristics (Adapted from Allemang [Allemang et al])	246

List of Figures

Figure 2.1: The human vertebral column. Image from Gray's Anatomy (1918). .	21
Figure 2.2: The stabilizing structures of the spine. The three systems work together to control the function of the spine. Image from Panjabi (1992)	22
Figure 2.3: Dysfunction of the spinal stability system. (1) Injury, degeneration and/or disease may decrease the (2) passive stability and/or the (3) active stability. (4) The neural control unit attempts to remedy the stability loss by increasing the stabilizing function of the remaining spinal components: (5) passive and (6) active. This may lead to (7) accelerated degeneration, abnormal muscle loading, and muscle fatigue. If these changes cannot adequately compensate for the stability loss, a (8) chronic dysfunction or pain may develop. Caption and image from Panjabi (1992).....	27
Figure 2.4: Basic spring-mass vibration system, with mass m , damping coefficient c , spring constant k , and displacement x	41
Figure 2.5: A basic structural health monitoring system utilizing a shaker[Brown et al.].....	46
Figure 2.6: An example of a frequency response function (FRF). The amplitude response ratio is graphed on the y axis against input frequency on the x axis....	47
Figure 2.7: Basic structures of human skin.....	60
Figure 2.8: Mechanical wave travelling through the skin can cause localized areas of tension (T) and compression (C).....	62
Figure 2.9: Behaviour of the basic elastic components of skin with increasing strain. Figure adapted from [Dellaleau et al 2008]and [Holzapfel et al 2001].....	62

Figure 2.10: The effect of adding (+) and subtracting (-) a multiple of each PC to the mean temperature curve. Figure from [Ramsay and Silverman, 2005]..... 75

Figure 2.11: Calculation of the d-statistic on two signals. The dashed lines represent the confidence bounds of the 'baseline' data, while the dotted line represents the mean of the 'experimental' signal. A) D-statistic of 51.56 B) d-statistic of 100. Figure adapted from Zennaro et al. [Zennaro et al., 2002] 77

Figure 3.1: Cadaver positioning setup. A) Rope-hoist system; B) Lateral clamping wood; C) Hinged locking bracket; D) Cross-brace plank; E) Adjustable lift table105

Figure 3.2: i) Schematic of non-invasive contact tip with skin-mounted accelerometers only. A: Shaker B: Stinger rod. C: Impedance head. D: Static load cell. E: Non-invasive contact tip. F: T8 Vertebra. G: T9 vertebra. H: T10 vertebra. I: Accelerometer. J: skin and soft tissue 108

Figure 3.3: Aerial view of experimental setup with accelerometer placements (A-E). 1: Shaker and in-line vibration input components. 2: T10 spinous process (under skin/soft tissue). 3: Placement of T10 accelerometer. Placement A' is the same as placement A. 111

Figure 3.4: Setup of non-invasive contact tip with skin-mounted accelerometers and needle mounted accelerometer. A: Shaker B: Stinger rod. C: Impedance head. D: Static load cell. E: Non-invasive contact tip. F: T8 Vertebra. G: T9 vertebra. H: T10 vertebra. I: Accelerometer. J: Skin and soft tissue. K: Hypodermic needle inserted into T10 vertebra with affixed accelerometer..... 112

Figure 3.5: i) Setup of invasive contact tip with skin-mounted accelerometers and needle mounted accelerometer. A: Shaker B: Stinger rod. C: Impedance head. D: Static load cell. E: Invasive contact tip. F: T8 Vertebra. G: T9 vertebra. H: T10 vertebra. I: Skin-mounted accelerometer. J: Skin and soft tissue. K: Hypodermic needle inserted into T10 vertebra with affixed accelerometer 114

Figure 3.6: Repeated FRFs obtained from Subject 1, T9 Position A, using the non-invasive contact tip	117
Figure 3.7 : Mean repeated test (FRF) with standard deviation on the 5 repeated measures for subject 1, T9 Position A, using the non-invasive contact tip.....	118
Figure 3.8: Repeated tests obtained from subject 1, T9 Position A, using the invasive contact tip.	118
Figure 3.9: Mean repeated test (FRF) with standard deviation on the 5 repeated measures for subject 1, T9 Position A, using the non-invasive contact tip.....	118
Figure 3.10: Repeated tests obtained from subject 1, T9 Position C, using the non-invasive contact tip.....	119
Figure 3.11: Mean position tests (FRFs) at T-9 vertebra taken using the non-invasive contact tip. Black signals indicate the accelerometer in position A, green indicates positions lateral to position A, and red indicates positions rostro-caudally located to position A.....	122
Figure 3.12: Figure 3.11 truncated to 800 Hz to show detail in low frequency vibration response	123
Figure 3.13: Mean position tests (FRFs) at T-9 vertebra taken using the invasive contact tip. Black signals indicate the accelerometer in position A, green indicates positions lateral to position A, and red indicates positions rostro-caudally located to position A.....	123
Figure 3.14: Figure 3.13 truncated to 300 Hz to show detail in low frequency vibration response	124
Figure 3.15: Mean non-invasive contact tip placement test with PC1 loading vector added and subtracted. Data taken from subject 1.....	124

Figure 3.16: Mean invasive contact tip placement test with PC1 loading vector added and subtracted. Data taken from subject 1.....	125
Figure 3.17: Comparison of position A skin-mounted to confidence interval on corresponding bone-mounted accelerometer signals, using the non-invasive contact tip. D-statistic is 0.12%.....	127
Figure 3.18: Enlargement of Figure 3.37 to 800 Hz to show low frequency detail	128
Figure 3.19: Comparison of position A skin-mounted to confidence interval on corresponding bone-mounted accelerometer signals, using the invasive contact tip. D-statistic is 4.24%.....	128
Figure 3.20: Enlargement of Figure 3.39 to 400 Hz to show low frequency detail	129
Figure 3.21: Vibration response of the T9 vertebra using the non-invasive contact tip. Measurements were taken with the skin-mounted accelerometer Position A, and at Position A again (A') after all other placements had been completed. Data taken from subject 1.....	131
Figure 3.22: Vibration response of the T9 vertebra using the invasive contact tip. Measurements were taken with the skin-mounted accelerometer Position A, and at Position A again (A') after all other placements had been completed. Data taken from subject 1.....	131
Figure 3.23: D-Statistic values comparing Position A and Position A'	132
Figure 3.24: D-statistic on the measurement of the T-10 vibration response using the non-invasive contact tip. The statistic was calculated using the mean needle-mounted FRF and the 95% confidence interval on the FRFs measured from the bone-mounted accelerometer. D= 0.12%	134

Figure 3.25: D-statistic on the measurement of the T-10 vibration response using the invasive contact tip. The statistic was calculated using the mean needle-mounted FRF and the 95% confidence interval on the FRFs measured from the bone-mounted accelerometer. D= 9.99%	134
Figure 3.26: The 5 repeated measures taken of the T-10 bone signal using the non-invasive contact tip in subject 2.	135
Figure 3.27: Comparison of measured skin and bone T-9 vibration response using the non-invasive contact tip	143
Figure 3.28: Comparison of measured skin and bone T-9 vibration response using the invasive contact tip.....	143
Figure 4.1 Porcine cadaver setup. A) Rope-hoist system; B) Lateral clamping wood; C) Hinged locking bracket; D) Cross-brace plank; E) Adjustable lift table	162
Figure 4.2 :i) Setup of non-invasive contact tip with skin-mounted accelerometers and needle mounted accelerometers. A: Shaker B: Stinger rod. C: Impedance head. D: Static load cell. E: Non-invasive contact tip. F: L1 Vertebra. G: L2 vertebra. H: L3 vertebra. I: L4 vertebra. J: Skin and soft tissue. K: Hypodermic needle inserted into vertebra with affixed accelerometer. L: Skin mounted accelerometer	165
Figure 4.3: Contact tip shapes used in the Protocol 2 experiments.....	167
Figure 4.4: The 5 repeated tests measured at the L2 skin mounted accelerometer. Data taken from porcine subject 1.....	170
Figure 4.5: Mean FRF and standard deviation on the 5 repeated tests in Figure 4.4	170
Figure 4.6: The 5 repeated tests measured at the L2 skin mounted accelerometer. Data taken from human subject 1.....	171

Figure 4.7: Mean FRF and standard deviation on the 5 repeated tests in Figure 4.6	171
Figure 4.8: The five repeated measures FRFs taken from pig Subject 4, L2 skin-mounted accelerometer using contact tip B. Test 5 shows an outlier response.	172
Figure 4.9: D-statistic on the measurement of the L4 vibration response using contact tip A in human subject 1. The figure shows the mean needle-mounted accelerometer FRF of the 5 repeated tests and the 95% confidence interval on the bone-mounted accelerometer FRFs of the 5 repeated tests. D=0.5%.....	179
Figure 4.10: D-statistic on the measurement of the L4 vibration response using contact tip B in human subject 1. The figure shows the mean needle-mounted accelerometer FRF of the 5 repeated tests and the 95% confidence interval on the bone-mounted accelerometer FRFs of the 5 repeated tests. D=2.62%.....	179
Figure 4.11: D-statistic on the measurement of the L4 vibration response using contact tip C in human subject 1. The figure shows the mean needle-mounted accelerometer FRF and the 95% confidence interval on the bone-mounted accelerometer FRFs. D=4.49%	180
Figure 4.12: D-statistic on the measurement of the L4 vibration response using contact tip D in human subject 1. The figure shows the mean needle-mounted accelerometer FRF and the 95% confidence interval on the bone-mounted accelerometer FRFs. D=1.87%	180
Figure 4.13: D-statistic on the measurement of the L4 vibration response using contact tip E in human subject 1. The figure shows the mean needle-mounted accelerometer FRF of the 5 repeated tests and the 95% confidence interval on the bone-mounted accelerometer FRFs of the 5 repeated tests. D=2.00%.....	181

Figure 4.14: D-statistic on the measurement of the L4 vibration response using contact tip F in human subject 1. The figure shows the mean needle-mounted accelerometer FRF of the 5 repeated tests and the 95% confidence interval on the bone-mounted accelerometer FRFs of the 5 repeated tests. D=4.00%..... 181

Figure 4.15: Three replacement signals obtained from the L4 skin-mounted accelerometer. Orig. Pl. is the original signal, where replacement 1 and replacement 2 are signals obtained after removing and replacing the accelerometer to the skin..... 182

Figure 4.16: The 95% confidence interval on the original signal, compared to the first replacement signal (Rep. 1). D= 36.45 %..... 182

Figure 4.17: The 95% confidence interval on the original signal, compared to the second replacement signal (Rep. 2). D= 4.24 %..... 183

Figure 4.18: Measured vibration response at L2, L3, and L4 by skin-mounted accelerometers. Data taken from porcine subject 1, using contact tip A. 186

Figure 4.19: L2 Skin-mounted accelerometer (blue) and bone-mounted accelerometer (orange) mean FRF of the 5 repeated tests using contact tip A. The mean of all tests is shown for both signals..... 187

Figure 4.20: L3 Skin-mounted accelerometer (blue) and bone-mounted accelerometer (orange) mean FRF of the 5 repeated tests using contact tip A. The mean of all tests is shown for both signals..... 187

Figure 4.21: L4 Skin-mounted accelerometer (blue) and bone-mounted accelerometer (orange) mean FRF of the 5 repeated tests using contact tip A. The mean of all tests is shown for both signals..... 188

Figure 4.22: Signals taken from human subject 1 at the L2 vertebra for each of the contact tips used. Data shown to 500 Hz. 189

Figure 4.23: Signals taken from human subject 1 at the L3 vertebra for each of the contact tips used. Data shown to 500 Hz.	189
Figure 4.24: Signals taken from human subject 1 at the L4 vertebra for each of the contact tips used. Data shown to 500 Hz.	189
Figure 4.25: Evolution of contact tip shapes used by Thompson et al. and Steele et al. [Thompson et al. 1976]. Tips a) and b) were found to be painful and induced secondary resonances of the skin. Tip c) eliminated this problem, but tips d) e) and f) were found to attain the highest repeatability in data. Figure taken from Steele et al. [Steele et al. 1988]	190
Figure 5.1: Amplitude response of a perfectly oscillating signal under various damping conditions. Increasing damping ratio ζ decreases the time taken to reach a steady response.	204
Figure 5.2: Mean skin-mounted accelerometer FRF graphed with 95% confidence interval on the needle-mounted accelerometer measurements at L4 using contact tip C in human cadaver subject 1. D=1.12%	207
Figure 5.3: Comparison of T-9 bone-mounted accelerometer response taken using the non-invasive (blue) and invasive (green) contact tips. Data taken from subject 1, Protocol 1 porcine data.....	219
Figure 5.4: T-9 bone-mounted accelerometer vibration response at two time intervals. Blue - skin-mounted accelerometer was placed at position A. Green – skin-mounted accelerometer was placed replaced, position A'	221
Figure B.1: Compression spring force gauge.	238
Figure B.2: Calibration curve of the compression spring used in the force gauge	239
Figure B.3: Compression spring force gauge in its experimental setup state.	240

Figure C.1: Electrodynamic shaker schematic. Image from Labworks [Labworks, 2010] 243

List of Abbreviations

LBD – low back disorder

LBP – low back pain

MRI – magnetic resonance imaging

CT – computed tomography

sEMG – surface electromyography

FRF – frequency response function

SDD – structural damage detection

SHM – structural health monitoring

FFT – Fast Fourier Transform

RCT – randomized controlled trial

PCA – principal component analysis

GSC – global shape criteria

GAC – global amplitude criteria

List of Equations

$m\ddot{x} + kx = 0$ (1)	41
$x(t) = x_0 \cos \omega_n t + \frac{v_0}{\omega_n} \sin \omega_n t$ (2)	42
$\omega_n = \sqrt{\frac{k}{m}}$ (3)	42
$m\ddot{x} + kx = p_0 \cos \theta t$ (4)	43
$X = \frac{p_0}{k - m\theta^2}$ (5)	43
$X_0 = \frac{p_0}{k}$ (6)	43
$\frac{X}{X_0} = \frac{1}{1 - r^2}$ (7)	44
$r = \frac{\theta}{\omega_n}$ (8)	44
$GSC = \frac{ H_{x1}(\omega)H_{x2}(\omega) ^2}{(H_{x1}(\omega)H_{x1}(\omega))^H (H_{x2}(\omega)H_{x2}(\omega))^H}$ (9)	72
$GAC = \frac{2 H_{x1}(\omega)H_{x2}(\omega) }{(H_{x1}(\omega)H_{x1}(\omega))^H + (H_{x2}(\omega)H_{x2}(\omega))^H}$ (10)	72
$T = \frac{H(\omega)_2}{H(\omega)_1}$ (11)	78
$\zeta = \frac{c}{2\sqrt{km}}$ (12)	203
$k = \frac{F}{x}$ (13)	203
$X_{n \times p} = U_{n \times n} \Sigma_{n \times p} V_{p \times p}^T$ (14)	234
$A\vec{v} = \lambda\vec{v}$ (15)	234

$$\vec{v} = \begin{bmatrix} x_1 \\ \vdots \\ x_{n,p} \end{bmatrix} \quad (16) \dots\dots\dots 234$$

$$C^2 = \frac{\|\hat{u} - \bar{u}\|^2}{n} \quad (17) \dots\dots\dots 236$$

Chapter 1: Introduction

1.1 Overview

Low back pain (LBP) is a serious medical condition with a lifetime prevalence estimated to be between 59-85% in the adult population [Cassidy et al. 1998;Carragee and Cohen 2009;Walker 2000]. In 85-90% of cases, no obvious identifiable cause of the LBP is present [Manek and MacGregor 2005;Deyo et al. 1991].

Many different causes of LBP have been proposed, given the range of tissues, disease processes, and injury mechanisms that exist in the low back. While many of these proposed etiologies may be valid given the wide range of symptoms associated with low back disorders (LBDs), recent research has shown that LBDs may frequently be caused by mechanical dysfunction, or altered natural activity of the spine [Grabias and Mankin 1979;Adams and Dolan 1995;Riihimaki 1991;Panjabi 1992]. Unfortunately, mechanical dysfunction has been difficult to assess due to a lack of objective, reliable functional diagnostic techniques.

A new technique has been developed to attempt to overcome known challenges in assessing mechanical dysfunction of the spine. [Kawchuk et al. 2008;Kawchuk et al. 2009]. The technique uses the engineering approach of structural damage detection (SDD) to identify the location and severity of mechanical dysfunctions of the spine.

Previous experiments performed by Kawchuk et al. have shown the viability of the technique when implemented invasively in cadaveric pigs [Kawchuk et al. 2008;Kawchuk et al. 2009]. The technique is now being developed for non-invasive use in live human subjects, requiring that various sensors and vibration input mechanisms on the skin are implemented with minimal impact on the patient. Consequently, the experiments that comprise this thesis explore the influence of skin and soft tissues on the implementation of the vibration technique.

1.2 Background and Rationale

1.2.1 Prevalence and Impact of Low Back Pain

Low back pain is a common condition, experienced by 59-85% of the population, with recurrence rates varying from 20-44% [Cassidy et al. 1998;Carragee and Cohen 2009;Walker et al. 2004;Andersson 1999]. Despite these statistics, only 10-15% of all cases have an identifiable source of these painful symptoms. These sources are generally attributed to acute injury, fracture, or other 'red flag' conditions [Deyo et al. 1991;Manek and MacGregor 2005].

The prevalence of LBP also creates a significant financial impact. Indirect costs associated with lost work days contributed to an estimated loss of at least \$19.8 billion over a year in the United States alone, according to a recent study [Stewart et al. 2003]. Additionally, the direct costs of LBP treatments, therapies, medications, and diagnostic testing have been estimated to be anywhere from \$12-90 billion per year [Dagenais et al. 2008].

1.2.2 Mechanical Dysfunction as a Cause of Low Back Pain

The spine is a dynamic mechanical structure meant to bear mostly compressive loads, while giving structure and providing flexibility and movement to the torso. Unfortunately, this complex structure is often a source of pain for many adults. The cause of LBP has become a highly debated and researched topic. While numerous potential causes have been postulated, many believe that LBP is caused by mechanical dysfunction of the spine [Panjabi 1992]. Specifically, the stability of the spine has been identified as significantly altered in patients with LBP symptoms [Kirkaldy-Willis and Farfan 1982; Magee 2008]. Changes in stability of the spine can produce abnormal, higher than maximal stresses, and altered muscle recruitment patterns [McGill 2002]. This, in turn, can cause pain and precipitate further dysfunction [Panjabi 1992]. Given these findings, it is generally thought that instability of the spine is a major cause of LBP [Panjabi 1992]

1.2.3 Diagnosing Low Back Disorders

Diagnosing the cause of pain in the low back is a difficult task, due to the non-specific nature of the symptoms [Deyo and Phillips 1996]. Frequently, the diagnosis a patient receives from a physical assessment can vary [van Trijffel et al. 2005]. To aid in the diagnostic process, clinicians often use imaging procedures, namely x-ray, computed tomography (CT), and magnetic resonance imaging (MRI) to view the anatomic structure of the spine. Unfortunately,

studies have delineated a number of problems with imaging. X-ray images can show abnormalities in bony structures, but are generally poor at imaging soft tissues [Jarvik and Deyo 2002;Lateef and Patel 2009]. Images obtained by CT or MRI are excellent for viewing soft tissues injuries. However, even being able to detect a structural anomaly may not be enough, as subjects complaining of back pain may not have any in the perceived symptomatic area. Conversely, soft tissue damage (degeneration, herniations) can often be found in asymptomatic subjects [Tong et al. 2006;Boden et al. 1990]. Imaging can only create an anatomical perspective of the spine, and does not give any information about spinal function. As an alternative to imaging, surface electromyography, or sEMG, has been used to detect dysfunction of trunk musculature in LBP subjects [Hodges and Richardson 1998;Radebold et al. 2000]. However, the protocols for using sEMG are poorly defined for the broader diagnostic community, and therefore the use of sEMG to detect dysfunction may not be reliable [Ambroz et al. 2000].

Given the above, if back pain and back disorders are thought to be caused by mechanical dysfunction, a diagnostic technique that helps detect areas of dysfunction would be a significant advantage in the diagnostic process.

1.3 Potential Solution for Non-Invasive Functional Analysis of the Spine

A new technique is being developed at the University of Alberta Spinal Function Lab to diagnose functional problems of the spine. This method adapts structural damage detection, a well known engineering technique used to diagnose functional problems in large structures such as bridges or aircraft for use in the

human spine. Briefly, when an object is given an input of vibration, it responds to that vibration according to its structural properties (mass, damping properties, moment of inertia, etc.) [Craig and Kurdila 2006]. This response is known as the frequency response. When the object is vibrated at a number of frequencies, the frequency response at each is recorded, to create the frequency response function, or FRF. This function is a signature of that object given its particular structural properties as changes in the structural conditions cause changes in the elasticity and damping of the system. When the structural conditions change, the FRF will change [Ewins 2000;Farrar and Worden 2007]. As a result of these observations, it is thought that changes in the FRF may be analyzed to detect changes in spinal function [Kawchuk et al. 2008;Kawchuk et al. 2009].

1.3.1 Precedent for use of Vibration in Medical Diagnostics

Structural damage detection, or parts of the structural damage detection process have been used in recent years in the field of medical diagnostics. A number of investigators have postulated that vibration could be used to detect mechanical spinal dysfunction. Keller and Colloca developed a device using vibration to analyze the stiffness of the spine, and found that stiffness increased with increasing vibration frequency [Keller and Colloca 2007]. Conza et al attempted unsuccessfully to use SDD to detect changes in the pelvic ligaments [Conza et al. 2007]. However, their unsuccessful result was thought to be influenced by a number of different factors including experimental setup.

Kawchuk et al. developed a new method to test whether SDD could be used as a tool to identify lumbar spine dysfunction [Kawchuk et al. 2008;Kawchuk et al.

2009]. Using an invasive setup in a cadaveric pig model, the spine was vibrated up to 2000 Hz after inducing sequential systematic injuries. Measurements of the vertebral response to this vibration were taken. The obtained FRFs from each vibration test were successfully 'diagnosed' using a neural networking program, with a minimum sensitivity of 0.994 and a specificity of 1.000.

Though this experimental implementation was successful, it was highly invasive to the spine, and therefore not suitable for use in clinical settings. As a result, focus in this project has shifted to adapting the technique for non-invasive application of vibration and measurement in a live human subject.

1.4 The Effects of Soft Tissue in Live Vibration Testing

Potentially, one of the most significant issues when performing non-invasive measurements of skeletal motion is the effect of the soft tissue overlaying the spine. The effects of soft tissue have frequently gone unaccounted for or ignored in non-invasive vibration testing, where sensors are typically placed on the skin covering the bone of interest [Keller and Colloca 2007;Li et al. 1996;Georgiou and Cunningham 2001]; therefore, the effect of skin and soft tissue on the measurements of underlying bone vibration response are largely unknown.

The properties of skin and soft tissues are extremely variable from person to person. Skin properties, which dictate how vibration is transferred through the skin, can be affected by factors such as hydration levels, subject age, and body composition [Potts et al. 1984;Potts et al. 1983;Davis et al. 1989]. To further

complicate matters, the skin is visco-elastic, and has non-linear behaviour at higher strain/strain rate levels [Delalleau et al. 2008].

Because skin can move independently of the bone to some degree, the accuracy of skin mounted sensor measuring an underlying bone's movement may vary. Most studies investigating the accuracy of skin mounted markers have concluded that a significant amount of motion artifact from the skin exists in the signals [Holden et al. 1997;Kuo et al. 2003]. The majority of these experiments were performed in the extremities of the body. However, full structural damage detection experiments have not been conducted in the spine to the author's knowledge; therefore, the influences of motion artifacts in spinal vibration testing are unknown. Due to the potentially significant influence of motion artifacts on the measured signal, it is important to investigate their significance in order to accurately measure the spinal vibration response.

1.5 Problem Statement

Given the potential that exists in understanding LBD etiology through this technique, this thesis will seek understanding in a number of areas where important knowledge is deficient. First, the effect of small changes in placement of the skin mounted accelerometer on the measurement of the bone vibration signal requires definition. Second, the role of skin and soft tissues on the alteration of the input vibration, as well as on the measurements obtained from skin mounted accelerometers is unknown. Finally, the effect of altering the contact tip shape on the measurement of the vertebral vibration response, from a skin-mounted accelerometer is unknown.

1.6 Purpose

The purpose of these experiments was to investigate the effect of skin on the non-invasive measurement of the vertebral vibration response in the context of structural damage detection.

1.7 Goals

The goals of this project were addressed through two protocols.

1.7.1 Protocol 1 Goals

1. Determine the repeatability of measurements of the spinal vibration response, obtained with non-invasive equipment.
2. Vary the position of a skin-mounted accelerometer placed posterior to a vertebra of interest, and determine the effects of these position changes on the measured vibration response of the vertebra.
3. Compare the vibration response signal measured from a skin-mounted accelerometer to the signal measured from the same position after removing and replacing the original accelerometer.
4. To determine the viability of using an accelerometer attached atop a hypodermic needle, implanted dorsally through the skin into the spinous process of a vertebra, as a method of measuring the vibration response of the vertebra.
5. For each of these goals, determine the effect of a non-invasive or invasive contact tip on the results.

1.7.2 Protocol 2 Goals

1. Quantify the signal correlation between skin mounted accelerometer and a needle mounted accelerometer in measuring vertebral vibration.
2. Given the above, determine whether the vertebral level, and hence distance from the contact tip, is a significant factor in the degree of signal correlation.
3. Determine, through signal correlations, which contact tip shape allows for the highest correlation of the needle-mounted accelerometer and skin mounted accelerometer signals.
4. Determine whether similar levels of signal correlation and contact tip performance were achieved in porcine and human cadavers.
5. Determine the correlation between the mean signal obtained from a skin-mounted accelerometer, and the mean signal from the same accelerometer once removed and replaced to the same position. Performance of this test at 3 different vertebral levels of increasing distance from the contact tip will determine whether replaceability of the accelerometer is affected by distance from the contact tip.

1.8 Hypotheses

Hypotheses have been proposed for each of the two sets of experiments.

1.8.1 Protocol 1 Hypotheses

1. Measurements of the spinal vibration response will be highly repeatable, yielding good correlation values.
2. Variations in placement of the skin mounted accelerometer over the vertebral body affect the measured FRF significantly.
3. The vibration response measured from an initial position will have a good degree of correlation to that of the signal measured by the accelerometer upon replacing it to the initial position.
4. The vibration response measured from an accelerometer affixed directly to a vertebra will have good correlation with that of an accelerometer mounted to a hypodermic needle that is implanted directly into the spinous process of the vertebra.
5. A non-invasive contact tip will affect the measured vibration response of a vertebra by transmitting inputted vibrations through the soft tissues it contacts.

1.8.2 Protocol 2 Hypotheses

Goals 1 and 2 are summarized in hypothesis 1. All other hypotheses correspond to the single goals listed.

1. Increasing distance between the vertebral level and contact tip input point will increase the correlation between a skin-mounted accelerometer and a needle-mounted accelerometer signal.

2. Alteration of the contact tip shape parameters will significantly affect the degree of correlation between the FRF obtained from a skin mounted accelerometer, and that of a bone mounted accelerometer.
3. The overall correlation between skin-bone mounted accelerometers in human cadavers will improve over that of porcine cadavers due to the increase in compliance and elasticity of human skin; however, the variance in correlation values will increase due to the heterogeneity in human cadaver specimens.
4. A high correlation will occur between two FRFs from skin-mounted accelerometer measurements, taken before and after removing and replacing the accelerometer to the same position.

1.9 Statement on Research Ethics

Strict ethics protocols were adhered to for the entirety of this thesis work. An online course in ethics, mandatory for all graduate students as dictated by the Faculty of Graduate Studies and Research, was completed, as well as a full day of research and ethics training provided by the Faculty of Medicine and Dentistry.

The use of porcine spine tissues from regularly euthanized animals at the Swine Research and Technology Centre was approved by the Faculty of Agriculture, Forestry, and Home Economics' Animal Policy Welfare Committee, as well as the Health Sciences Animal Policy and Welfare Committee (Appendix E). Specific protocols for experiments performed in human cadavers were reviewed and approved by the Health Research Ethics Board Panel B of the University of Alberta (Appendix D).

1.10 Thesis Outline

This thesis is written in a mixed-format. First, the relevant literature will be reviewed. The following two chapters will be presented in a scientific paper format, each describing one of the two experiments performed. Finally, a unifying chapter will be presented to discuss the overall results and outcomes of the thesis.

1.11 References

Adams MA, Dolan P. Recent advances in lumbar spinal mechanics and their clinical significance. "Clin Biomech (Bristol 1995;10(1):3-19.

Ambroz C, Scott A, Ambroz A, Talbott EO. Chronic low back pain assessment using surface electromyography. J Occup Environ Med 2000;42(6):660-669.

Andersson GBJ. Epidemiological features of chronic low-back pain. Journal Article 1999;354(9178):581-585.

Boden SD, Davis DO, Dina TS, Patronas NJ, Wiesel SW. Abnormal magnetic-resonance scans of the lumbar spine in asymptomatic subjects. A prospective investigation. J Bone Joint Surg Am 1990;72(3):403-408.

Carragee EJ, Cohen SP. Lifetime asymptomatic for back pain: the validity of self-report measures in soldiers. Spine 2009;34(9):978-983.

Cassidy JD, Carroll LJ, Côté P. The Saskatchewan health and back pain survey. The prevalence of low back pain and related disability in Saskatchewan adults. Spine 1998;23(17):1860-6; discussion 1867.

Conza NE, Rixen DJ, Plomp S. Vibration testing of a fresh-frozen human pelvis: the role of the pelvic ligaments. J Biomech 2007;40(7):1599-1605.

Craig RR, Kurdila A, editor. Fundamentals of structural dynamics. 2 ed. Wiley; 2006. 728 p.

Dagenais S, Caro J, Haldeman S. A systematic review of low back pain cost of illness studies in the United States and internationally. *Spine J* 2008;8(1):8-20.

Davis BR, Bahniuk E, Young JK, Barnard CM, Mansour JM. Age-dependent changes in the shear wave propagation through human skin. *Exp Gerontol* 1989;24(3):201-210.

Delalleau A, Josse G, Lagarde JM, Zahouani H, Bergheau JM. A nonlinear elastic behavior to identify the mechanical parameters of human skin in vivo. *Skin Res Technol* 2008;14(2):152-164.

Deyo RA, Cherkin D, Conrad D, Volinn E. Cost, controversy, crisis: low back pain and the health of the public. *Annu Rev Public Health* 1991;12:141-156.

Deyo RA, Phillips WR. Low back pain. A primary care challenge. *Spine* 1996;21(24):2826-2832.

Ewins DJ, editor. Modal testing. Wiley; 2000. 562 p.

Farrar CR, Worden K. An introduction to structural health monitoring. *Philos Transact A Math Phys Eng Sci* 2007;365(1851):303-315.

Georgiou AP, Cunningham JL. Accurate diagnosis of hip prosthesis loosening using a vibrational technique. *Clin Biomech (Bristol)* 2001;16(4):315-323.

Grabias SL, Mankin HJ. Pain in the lower back. Bull Rheum Dis 1979;30(8):1040-1045.

Hodges PW, Richardson CA. Delayed postural contraction of transversus abdominis in low back pain associated with movement of the lower limb. J Spinal Disord 1998;11(1):46-56.

Holden JP, Orsini JA, Siegel KL, Kepple TM, Gerber LH, Stanhope SJ. Surface movement errors in shank kinematics and knee kinematics during gait. Gait and Posture 1997;5:217-227.

Jarvik JG, Deyo RA. Diagnostic evaluation of low back pain with emphasis on imaging. Ann Intern Med 2002;137(7):586-597.

Kawchuk GN, Decker C, Dolan R, Carey J. Structural health monitoring to detect the presence, location and magnitude of structural damage in cadaveric porcine spines. J Biomech 2009;42(2):109-115.

Kawchuk GN, Decker C, Dolan R, Fernando N, Carey J. The feasibility of vibration as a tool to assess spinal integrity. J Biomech 2008;41(10):2319-2323.

Keller TS, Colloca CJ. Dynamic dorsoventral stiffness assessment of the ovine lumbar spine. J Biomech 2007;40(1):191-197.

Kirkaldy-Willis WH, Farfan HF. Instability of the lumbar spine. Clin Orthop Relat Res 1982;(165):110-123.

Kuo LC, Cooney WP, Oyama M, Kaufman KR, Su FC, An KN. Feasibility of using surface markers for assessing motion of the thumb trapeziometacarpal joint. "Clin Biomech (Bristol 2003;18(6):558-563.

Lateef H, Patel D. What is the role of imaging in acute low back pain? Current reviews in musculoskeletal medicine 2009;2(2):69-73.

Li PL, Jones NB, Gregg PJ. Vibration analysis in the detection of total hip prosthetic loosening. Med Eng Phys 1996;18(7):596-600.

Magee DJ. Orthopedic physical assessment. 4 ed. W B Saunders Co; 2008. 1138 p.

Manek NJ, MacGregor AJ. Epidemiology of back disorders: prevalence, risk factors, and prognosis. Curr Opin Rheumatol 2005;17(2):134-140.

McGill S. Low Back Disorders: Evidence Based Prevention and Rehabilitation. Windsor, Ontario: Human Kinetics; 2002.

Panjabi MM. The stabilizing system of the spine. Part I. Function, dysfunction, adaptation, and enhancement. J Spinal Disord 1992;5(4):383-9; discussion 397.

Potts RO, Buras EM, Chrisman DA. Changes with age in the moisture content of human skin. J Invest Dermatol 1984;82(1):97-100.

Potts RO, Chrisman DA, Buras EM. The dynamic mechanical properties of human

skin in vivo. J Biomech 1983;16(6):365-372.

Radebold A, Cholewicki J, Panjabi MM, Patel TC. Muscle response pattern to sudden trunk loading in healthy individuals and in patients with chronic low back pain. Spine 2000;25(8):947-954.

Riihimaki H. Low-back pain, its origin and risk indicators. Eur J Radiol 1991;17(2):81-90.

Stewart WF, Ricci JA, Chee E, Morganstein D, Lipton R. Lost productive time and cost due to common pain conditions in the US workforce. JAMA 2003;290(18):2443-2454.

Tong H, Carson J, Haig A, Quint D, Phalke V, Yamakawa K, Miner J. Magnetic resonance imaging of the lumbar spine in asymptomatic older adults. J Neuroimaging 2006;19:67-72.

Walker BF. The prevalence of low back pain: a systematic review of the literature from 1966 to 1998. J Spinal Disord 2000;13(3):205-217.

Walker BF, Muller R, Grant WD. Low back pain in Australian adults. health provider utilization and care seeking. J Manipulative Physiol Ther 2004;27(5):327-335.

Wu JZ, Dong RG, Smutz WP, Schopper AW. Nonlinear and viscoelastic characteristics of skin under compression: experiment and analysis. Biomed Mater Eng 2003;13(4):373-385.

van Trijffel E, Anderegg Q, Bossuyt PMM, Lucas C. Inter-examiner reliability of passive assessment of intervertebral motion in the cervical and lumbar spine: a systematic review. *Man Ther* 2005;10(4):256-269.

Chapter 2: Literature Review

2.1 Introduction

Low back disorders (LBDs) are a common ailment among adults of all ages [Guo et al., 1999]. This literature review outlines the causes of low back disorders, along with their prevalence and socio-economic impact. It next discusses current methods of diagnosing the causes of low back disorders, and the difficulties and limitations these methods pose. The chapter then delves into the basics of vibration theory, to outline the mechanisms which make vibration a potentially viable diagnostic tool. Previous studies that have attempted to use vibration as a diagnostic technique are summarized, along with discussion of their benefits and drawbacks. Further to this, invasive vibration response studies performed by our lab are reviewed in-depth.

An invasive technique to detect the location and magnitude of imposed injuries to the lumbar spine has been developed at the Spinal Function Lab at the University of Alberta. Current work on this project is focused on adapting the previously developed invasive apparatus into a non-invasive technique suitable for use in live human testing. Previous studies, discussed in this review, have shown that soft tissue can significantly affect the accuracy of non-invasive measurements of skeletal function [Holden et al., 1997]. A discussion of the accuracy of skin mounted markers, as well as the merit of methods to overcome

these issues is given. Finally, a discussion of viable signal analysis techniques, along with their deficiencies and merits is given.

2.2 Lumbar Spine Structure and Anatomy

The spine, the support column of the human body, is shown in Figure 2.1. It gives structure and movement to the torso, bears compressive loads, and protects the spinal cord and neural structures which run through it [Panjabi, 1992]. The low back, or lumbar spine, is comprised of the lowest five independent vertebrae, and their intervertebral discs.

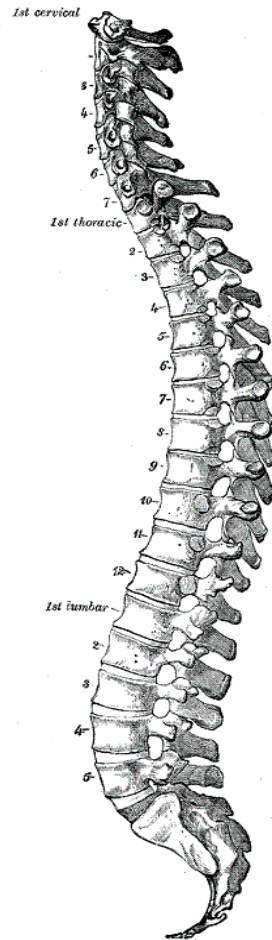


Figure 2.1: The human vertebral column. Image from Gray's Anatomy (1918).

The spine is comprised of 3 types of structures: active structures, passive structures, and neural structures [Panjabi, 1992]. These structures work together closely to control the motion of the spine, as illustrated in Figure 2.2.

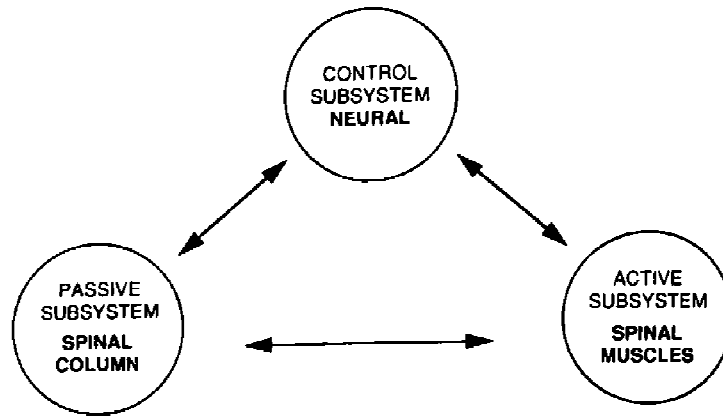


Figure 2.2: The stabilizing structures of the spine. The three systems work together to control the function of the spine. Image from Panjabi (1992)

The purpose of the passive structures of the spine is to limit the end range of spinal motion [Panjabi, 1992]. Similar in function to guy-wires, they are not involved in the direct positioning or movement of the spine, but provide stability and support to the structure, as well as act as ‘transducers’ to detect spinal position. Passive structures include ligaments, cartilage, intervertebral discs, bones (vertebrae), and fascia. The muscles of the spine and their associated tendons comprise the active structures. Muscles generate forces to move the spine into different positions, and dynamically stabilize and stiffen the spine. Finally, the neural system in the spine consists of the peripheral nerves, the spinal cord, and the brain. The neural structures of the spine interact with both the active and passive structures by receiving information transmitted from them about the spine’s orientation and the stresses placed upon it. They then transmit feedback information to the active structures to control the spine’s motion [Panjabi, 1992].

2.3 Low Back Disorders

Injury, disease, or damage to any one of the three systems can be a source of low back disorders (LBDs). LBDs are a medical issue with multiple potential origins, often painful symptoms, and sometimes serious implications. These issues are discussed in the following section.

2.3.1 Epidemiology

Worldwide, the reported incidence of LBDs and related low back pain (LBP) is considerable. Its manifestation and impact can range from mild discomfort to severe debilitation. Cassidy et al. report a lifetime prevalence of 84.1% of LBP in the Saskatchewan adult population [Cassidy et al., 1998]. Further studies of populations in Australia, the United Kingdom, and the United States report lifetime incidence rates of 64.6%, 59% and 84%, respectively [Walker et al., 2004; Papageorgiou et al., 1995; Carragee and Cohen, 2009]. However, a systematic review of literature from 1966-1998 on the prevalence of LBP by Walker et al. suggests the incidence rate in developed countries varies from 13.8% - 84% [Walker, 2000]. These discrepancies are due to the widely varying definition of LBP, and demographic of populations in the studies under review (occupation, gender, other health factors). Nonetheless, even at the lowest estimated lifetime prevalence of 13.8%, LBP affects a substantial proportion of the adult

population. The worldwide presence of LBP makes it an extremely important global health issue.

It is important to bring context to these statistics. In the 1996/97 National Population Health (NPH) survey of the impact of chronic illness in Canada, Statistics Canada reports that 14.1% of respondents reported having back pain at that time [Schultz and Kopec, 2003], similar to the 12-33% point prevalence cited in the international systematic review by Walker [Walker, 2000]. In the same NPH survey, 3.9% of respondents reported having heart disease, 1.5% reported having cancer, and 3.2 % reported having diabetes. These studies confirm that LBP has a significantly wider prevalence than other major disorders in Canada.

2.3.2 Socio-Economic Effects of LBDs

The physical impact of LBDs translates to significant economic consequences. Costs due to loss of work productivity, performing assessment and diagnosis, patient therapy, and lost wages are all a significant economic burden to patients and health care systems. The physical effects of LBDs force many to take a significant amount of time off of work. A study utilizing the National Centre for Health Statistics' 1988 National Health Interview Survey in the United States reported that approximately 4.6% of respondents with LBP missed work due to their pain, at an average of 6.8 workdays per episode [Guo et al., 1999]. This translates to approximately 149.1 million lost work days. A similar study by Stewart et al. of the American Productivity Audit's 2003 Work and Health Interview estimated the cost of missed work days or reduced productivity due to

back pain to be \$19.8 billion and 3.84 billion lost work hours [Stewart et al., 2003]. Assuming an 8 hour work day, this translates to 480 million lost work days per year. A systematic review of articles examining the costs of LBP from 1995-2003 produced estimates of both direct and indirect costs [Dagenais et al., 2008]. Direct costs such as therapy, surgery, imaging, or pharmaceuticals were estimated from \$14-90 billion, while indirect costs such as sick leave or early retirement were estimated from \$7.4-28 billion (U.S.).

The numbers produced by these studies highlight the socio-economic burden of LBDs. Discrepancies in estimates can be attributed to inflation rates, source of data (societal/governmental perspective, insurance perspective), and methods of determining costs (direct calculations, indirect calculation by collected survey statistics). However, with numbers in the billions of dollars, the money lost due to low back disorders has a large impact.

2.3.3 Dysfunction of the Spine

The structure of the spine is highly complex. The active, passive, and neural systems must all work together to control the motion of this multi-bodied system. Injury, damage, or disruption of any one of these components has the potential to cause instability of this dynamic system [Panjabi, 1992; Norris, 1995; Grabias and Mankin, 1979; Adams and Dolan, 1995; Riihimaki, 1991; Fritz et al., 1998].

It is thought that patients with LBDs have altered functional ability in their spine. A function of an object may be thought of as its purpose, or the natural activity of an object [Oxford University Press, 2008]. Functional instability of the spine is thought to be one of the major causes of low back disorders [Kirkaldy-Willis and Farfan, 1982; Norris, 1995; Panjabi, 1992; Porterfield and DeRosa, 1991]. The definition proposed by Panjabi describes instability as “the loss of the spine’s ability to maintain its patterns of displacement under physiologic loads so there is no initial or additional neurologic deficit, no major deformity, and no incapacitating pain” [Panjabi, 2003]. This definition emphasizes the loss of control over the standard function of the spine which does not incite pain. It should be noted that the term ‘dysfunction’ does not necessarily imply injury or degeneration to the spine; it implies abnormality of the regular mechanics of the spine, with or without a perceived structural anomaly. A study by Carragee et al. tracked 200 asymptomatic or minimal LBP subjects over 5 years, taking a baseline MRI at the start of the study [Carragee et al., 2006]. Of these subjects, 51 had a total of 67 secondary MRIs taken at various points in the 5 years, due to reported LBP. Upon reviewing the follow up MRIs, 88% of these subjects showed no structural changes from their original MRIs. This study emphasizes the point that structural changes do not need to occur for new LBP symptoms to arise; hence, functional changes in the spine should be investigated.

2.3.3.1 Spinal Instability and Dysfunction Mechanisms

It has long been hypothesized that spinal instability caused by injury, disease, or degeneration may be the source of LBDs [Panjabi, 1992; Panjabi, 2003;

Nachemson, 1985]. Additionally, it is thought that instability of the spine could in turn contribute or perpetuate injury, disease, and degeneration in the spine. Figure 2.3 shows Panjabi's proposed cyclic dysfunction system [Panjabi, 1992].

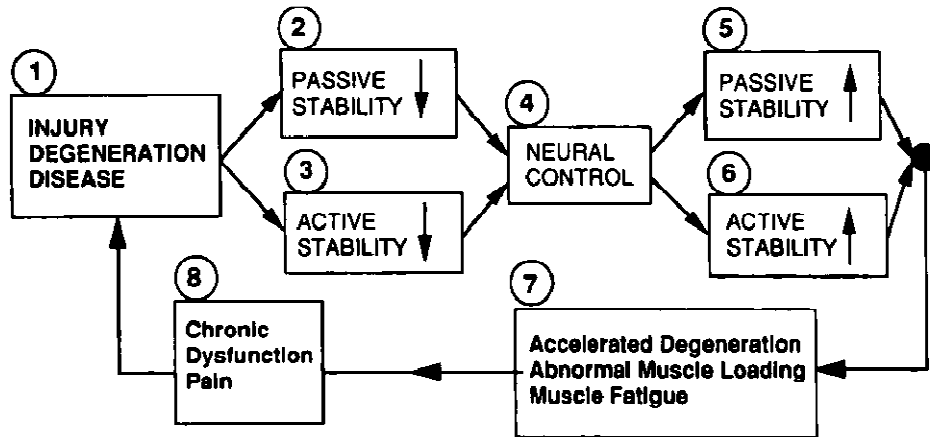


Figure 2.3: Dysfunction of the spinal stability system. (1) Injury, degeneration and/or disease may decrease the (2) passive stability and/or the (3) active stability. (4) The neural control unit attempts to remedy the stability loss by increasing the stabilizing function of the remaining spinal components: (5) passive and (6) active. This may lead to (7) accelerated degeneration, abnormal muscle loading, and muscle fatigue. If these changes cannot adequately compensate for the stability loss, a (8) chronic dysfunction or pain may develop. Caption and image from Panjabi (1992)

Studies have suggested that intervertebral disc degeneration [Devereaux, 2004], musculoskeletal injury or trauma such as sprains, strains and ligament damage [Riihimaki, 1991; Devereaux, 2004; Jarvik and Deyo, 2002], disc prolapses or herniations [Kelsey and White, 1980] may be the most common changes in the spine leading to dysfunction. For example, a degenerating disc loses flexibility,

which increases the local stiffness and causes surrounding joints to take on stresses the disc can no longer bear. This also places additional stresses on the discs immediately above and below it. Conversely, laxity in ligaments can produce a decrease in stiffness. This laxity may cause joint movements outside the normal range, placing high stresses on joint interfaces and instigating degenerative changes [Porterfield and DeRosa, 1991; McGill, 2002; Niosi and Oxland, 2004].

Changes in spinal stiffness (hypo- or hypermobility) have also been linked to pain symptoms in the low back. A study of subjects with and without back pain revealed that those with LBP had significantly higher postero-anterior (PA) stiffness [Latimer et al., 1996]. Additionally, when LBP subjects reached 80% reduction in pain, re-testing showed a significant decrease in PA stiffness. Similarly, in a more recent study by Fritz et al., 71% of subjects with LBP were found to have hypomobility in at least one vertebral level, and 11% of subjects with LBP were found to have hypermobility [Fritz et al., 2005]. 2.3% of subjects were found to have hyper and hypomobile regions of the lumbar spine. Upon receiving interventions of manipulation in the hypomobile group, or stabilization in the hypermobile group, Oswestry Disability Questionnaire scores (with higher scores indicating more severe back pain) were significantly decreased.

When one element of the spine dysfunctions, the other passive, neural, and muscular structures work together to accommodate this injury, allowing the spine's continued operation [Porterfield and DeRosa, 1991; Brumagne et al., 2008]. However, adaptation to this dysfunction, or changes in the control over spinal function can cause altered spinal system mechanics [Kirkaldy-Willis and Farfan, 1982; Fritz et al., 1998]. A number of studies have used surface

electromyography, or sEMG, to show delayed or altered recruitment of various muscle groups in LBP subjects. Studies by Hodges and Richardson showed that LBP subjects had delayed recruitment of transversus abdominis and obliquus internus abdominis muscles in preparation for movement of the upper limbs [Hodges and Richardson, 1996; Hodges and Richardson, 1998; Hodges and Richardson, 1999]. Radebold et al. found a delay in recruitment of the erector spinae muscles in response to a sudden jolting of the torso [Radebold et al., 2000]. In a study by van Dieën et al., subjects performed both trunk movements in the sagittal, frontal, and transverse planes, as well as isometric contractions in both left and right lateral bending, flexion, and extension [van Dieën et al., 2003]. In non-specific LBP patients, the ratio of activation of lumbar to thoracic erector spinae muscles was significantly higher than in asymptomatic subjects for both bending and isometric contraction tests. The alteration of the muscle recruitment patterns of the spine imply modified spinal function.

Low back pain due to an LBD can be a chronic, cyclic process, as illustrated in Figure 2.3. Liszka-Hackell et al define chronic back pain as pain for >6 months, and acute back pain as resolved within two weeks [Liszka-Hackzell and Martin, 2004]. Many others also follow the definition of chronic back pain as greater than 3-6 months, and acute back pain as resolved within 1-2 weeks [Von Korff and Saunders, 1996].

Injury or dysfunction of the spine may be the cause of chronic pain. Conversely, chronic pain can alter spinal muscle mechanics through subconscious fear-avoidance behaviors such as muscle guarding. Muscle guarding occurs when a patient alters their normal muscle activation pattern to avoid inciting pain or re-injuring a previously damaged structure. The patient may begin to use muscle

guarding to limit the elicitation of a pain response, thus invoking abnormal movements of the spine and disuse of the damaged system [Lundy-Ekman, 2002; O'Sullivan, 2005]. This alteration of normal spinal mechanics is thought to contribute to abnormal loading and instability of the spine [O'Sullivan, 2005]. As previously mentioned, chronic pain may also contribute to degeneration of spinal structures. Chronic low back pain sufferers have been shown to have decreased cross sectional area of the paraspinal muscles compared to acute sufferers, implying atrophy of the muscles [Cooper et al., 1992]. It is thought that this atrophy may occur because of altered muscle recruitment patterns, contributing to instability of the spine.

Functional changes such as hyper or hypomobility, changes in muscle recruitment patterns, or injuries and degenerative changes in spinal structures can all lead to instability of the spine, and hence to LBP. It is clear that functional assessment of the spine is essential in determining the cause of this painful disorder.

2.4 Diagnosing Low Back Disorders

2.4.1 Diagnostic Techniques

The ability to diagnose the cause of low back disorders is a contentious issue. Traditionally, a patient will first see a practitioner. Upon physical examination, red flags or systemic problems will first be ruled out (cancer, bowel disease, etc.). The practitioner may then begin a course of action to determine the cause

of the low back disorder. It is estimated that up to 85-90% of the time, no obvious cause is present [Deyo et al., 1991; Manek and MacGregor, 2005]. Clinicians then begin a manual assessment of the patient. This can include testing for range of motion, observation of posture and gait, palpation, and assessing joint play [Magee, 2008]. This testing can determine a general pattern of dysfunction for which there are a number of treatment paths. If no specific diagnosis can be established through observation and manual physical tests, a practitioner may order imaging studies for the patient [Wing, 2001]. These most often include radiography (x-ray), magnetic resonance imaging (MRI), or computed tomography (CT). These techniques, as well as the lesser used surface EMG and discography are discussed below.

2.4.1.1 Radiography (x-ray)

Radiography is used to image hard structures of the body, namely bone [Freund and Sartor, 2006]. As such, its usefulness is mostly limited to detecting bony defects, bone density issues, or secondary inferences on soft tissues such as viewing the height of intervertebral discs by measuring distances between vertebrae [Lateef and Patel, 2009; Jarvik and Deyo, 2002]. Studies have shown that radiographs used for diagnostic purposes are not linked to an improved outcome for LBP patients, and may in fact be correlated to worsening of pain and longer recovery times [Kendrick et al., 2001]. Nonetheless they are still frequently performed as initial diagnostic tools. A randomized controlled trial (RCT) of 141 LBP subjects, along with 427 non-randomized patients with non-specific low back pain followed the subjects' physical and emotional recovery

through one year after their initial doctor's visit [Kerry et al., 2002]. It was found that patients referred for x-rays had no improvement in pain or functional ability, in both the RCT subjects and the uncontrolled group. Subjects referred for x-rays had slightly improved psychological/depression scores over those not referred. This study provides evidence that radiographs for non-specific low back pain, while providing some psychological effect, are not correlated with improved pain, disability, or functional outcomes for patients. It is unknown whether this is due to the radiograph providing poor diagnostic information, or whether treatment based on the diagnostic information provided was ineffective. Due to the poor association of x-ray with improved clinical outcomes, many studies now recommend bypassing x-ray use when investigating non-specific low back pain [Jarvik and Deyo, 2002; Lateef and Patel, 2009].

2.4.1.2 MRI and CT Imaging

MRIs and CT scans can provide a more in-depth look at the spinal anatomy, including soft tissues such as intervertebral discs and spinal ligaments. While the detail they can achieve is far greater than x-rays, they too have disadvantages. MRI aligns protons in soft tissues with a large magnetic field, thus utilizing proton densities to discriminate between the tissues. 'Slices' (images) are taken through the body in one axis, which can then be re-organized to view the body in a corresponding perpendicular axis. While useful, MRI has the opposite effect of x-ray; it is generally poor at achieving high quality bone images but produces superior soft tissue views. CT scans use a similar 'slice' technique to be able to view the body in multiple axes, and provide better imaging quality of bone than

MRIs. The ability of MRI and CT scans to discover spinal abnormalities is not debated; they are capable of detecting irregularities such as herniations or degeneration in the intervertebral discs, narrowing of the spinal canal (canal stenosis), nerve root impingement, and ligamentous thickening.

2.4.1.3 Discography

Needle techniques to diagnose the structural source of LBP are somewhat controversial [Nachemson, 1989; Nachemson and Vingard, 2002]. Discography is a technique used by clinicians to specifically determine whether the disc is the source of pain, by injecting a radiopaque dye into the disc in specific areas. In doing so, the clinician hopes to both view possible abnormalities in the structure of the disc, as well as replicate the pain experienced by the patient through distention of the disc [Bogduk, 1996]. The usefulness of discography is debated. Nachemson et al. argue that, while discography provides detail for disc degeneration, it is not useful for showing disc herniations. MRI provides a non-invasive, highly accurate alternative for both of these problems, making the need for discography questionable [Nachemson and Vingard, 2002]. Discography also requires the use of CT imaging to view the radiopaque dye, exposing the patient to potentially unnecessary radiation. Discography is not used frequently due to its questionable utility and the invasiveness of the procedure [Magee, 2008]

2.4.1.4 *Surface Electromyography (sEMG)*

Some clinicians and researchers have used sEMG to characterize functional muscular disorders in the spine. As previously discussed in Section 2.3.3, altered muscle recruitment or activation patterns can occur in patients with LBP. In these studies, sEMG was used as a non-invasive method for measuring muscle activity levels in the low back area. The parameters compared included timing and levels of activation/contraction, as well as time to provoke muscle fatigue [Hodges and Richardson, 1996; Hodges and Richardson, 1998; Hodges and Richardson, 1999; van Dieën et al., 2003; Radebold et al., 2000; Candotti et al., 2008; Ambroz et al., 2000; Ahern et al., 1990].

By measuring the level and timing of the muscle activation, comparisons between LBP patients and healthy control subjects can be made to determine in which muscles dysfunction is occurring. Additionally, therapists may use this sEMG information to determine which muscles show altered recruitment patterns or early fatigue, and re-train these muscles to normal function [Hu et al., 2010; Candotti et al., 2008].

2.4.2 Disadvantages and Limitations of Current Diagnostic Techniques

Clinicians are responsible for preliminary physical examination of LBD/LBP patients. These practitioners come from a wide variety of training backgrounds, and may use a large range of tests in the diagnostic process. However, the

reliability of inter-examiner physical assessments has been the subject of debate. Studies have shown that even clinicians with similar training backgrounds can have inconsistent evaluations of the degree of mobility of the spine [Gonnella et al., 1982], or even at which vertebral level the dysfunction exists [Qvistgaard et al., 2007]. A systematic review of 10 studies investigating the reliability of passive assessment of the spine (ex: using flexion, extension, rotation motions) showed an average poor to fair inter-rater reliability, with studies reporting poor to excellent results [van Trijffel et al., 2005] . However, the authors of the study noted that significant methodological issues, such as correct blinding of examiners or vague reporting of study protocol existed in all but two studies. Therefore, the ability of clinicians to accurately and consistently diagnose spinal dysfunctions based solely on physical assessments is debatable.

Imaging using CT and x-ray for the low back are somewhat controversial, as they both use radiation to produce images. However, CT scans typically use a significantly higher dose of radiation than regular x-rays [Shrimpton et al., 2005]. The pelvic region, containing delicate and vital reproductive and digestive organs, is exposed to this radiation when these types of images are produced for the low back, making the use of CT and x-ray a resource that should be used only when necessary.

Apart from the risks associated with high doses of radiation, these imaging methods may not necessarily aid in accurately diagnosing the LBD. It is not uncommon to find abnormalities in MRI or CT scans of asymptomatic subjects with no history or current occurrence of pain. In a study by Tong et al., 33 asymptomatic subjects, 55 years and older, had MRIs taken of their low back [Tong et al., 2006]. Almost all subjects had at least one abnormality, with 85%

showing bulging discs, 75% showing at least one degenerated facet joint, ligamentous thickening in 66% of subjects, and two subjects showing severe canal stenosis. A further study by Boden et al. of asymptomatic subjects categorized by age group showed similar results [Boden et al., 1990]. In fifty-three subjects below 60 years of age, 22% had herniated discs, and one showed canal stenosis. In 14 subjects 60-80 years of age, 36% of subjects had herniated discs, while 21% showed significant canal stenosis. In a study by Silfies et al., subjects were recruited based on abnormalities detected by MRI in passive structures of the spine, such as degenerated discs. The study did not find conclusive evidence that these abnormalities caused direct dysfunction of the trunk muscle recruitment, and therefore may not have been the cause of the subjects' LBP. The prevalence of abnormalities of the spine in asymptomatic subjects appears to be quite common. The findings of these studies prove that anatomic anomalies found by imaging studies do not necessarily correlate to reported pain or dysfunction. This causes difficulty and confusion for the clinician in discerning the source of pain by providing irrelevant or erroneous information. Therefore, the subject's clinical history must be reviewed heavily in conjunction with the image [Jensen et al., 1994].

When considering the proposed causes of the LBD, it is clear that imaging may not be an optimal diagnostic aid. Specifically, traditional imaging provides a static picture of a subject's anatomy. There is no way to tell from this image whether a spinal segment is hypo- or hypermobile, or how components of the spine may be functioning together. Given that LBP is thought to be a disorder of functional ability of the spine, static diagnostic information obtained through imaging may not be an optimal diagnostic aid.

The sEMG method of detecting muscle dysfunction may not be applicable in all cases of LBP. In a study by Jalovaara et al., subjects with 3 different LBP symptoms were tested for sEMG activation of the paraspinal muscles; one group with sciatica, one group with disc herniations, and one group with localized low back pain [Jalovaara et al., 1995]. Additionally, a control group with no back pain was tested. Subjects were further categorized as to whether they had pain at the time of sEMG recording or not. Of those subjects reporting pain at the time of testing, only localized LBP subjects had significantly increased paraspinal activation from the control group. Furthermore, subjects in all 3 symptomatic groups who reported 'no pain' at the time of testing did not have significantly increased activation from the control group. This study showed that while sEMG may be able to detect dysfunction in some diagnostic groups, it may not be sensitive enough to define LBP subgroups with different underlying pathologies.

Ambroz et al. point out that, while there are many studies that report negative findings in using sEMG to diagnose dysfunction, the reasons for this may be due to a lack of defined protocol in this area [Ambroz et al., 2000]. They note that, frequently, most studies do not adjust for body fat or BMI, or classification of pain type, two factors that when accounted for show positive results for sEMG as a diagnostic tool. Therefore, while sEMG may be useful, the protocols for this type of testing are not yet clearly or adequately defined for the broader diagnostic community.

Furthermore, while sEMG may be somewhat successfully used to determine postural dysfunction or specific dysfunctional muscles, it is unknown whether this dysfunction is the cause of back pain, or whether back pain causes this dysfunction [O'Sullivan, 2005]. van Dieën et al. caution that altered muscle

recruitment patterns may be compensation techniques for stabilizing the spine and may not be the cause of the pain. Therefore, normalizing these recruitment patterns may not have an effect on the subject's pain [van Dieën et al., 2003]. Therefore, while the dysfunction may be detected, the root cause of the LBD may not.

Should the clinician rely heavily on the imaging study to create their diagnosis, it could lead to unnecessary and potentially life-changing treatments such as surgery, without fixing the true source of pain [Boden et al., 1990] [Lateef and Patel, 2009].

2.4.3 Pain as a Confounder in Diagnosis of Spinal Dysfunction

In addition to the drawbacks discussed in each of the previous sections, the diagnostic process can be further complicated by the complex issue of pain invocation. Many structures of the spine are highly innervated, providing significant opportunity for a pain response to be invoked [Bogduk, 1983; Siddall and Cousins, 1997]. When nociceptive pain occurs, it may be due to irregular mechanical dysfunction causing unwanted direct stimulation of the nerves [Bogduk, 2009]. Unfortunately, other pain mechanisms which can also be produced via this dysfunction such as referred pain, radicular pain, and radiculopathy can lead to symptoms at sites remote from the dysfunction.

It is increasingly thought that the inflammatory process adds to the difficulty in diagnosing a specific cause of LBDs [Porterfield and DeRosa, 1991]. Studies have

shown that a constricted nerve segment is affected both during physical compression, and after the compression has been removed. Watanabe and Parke have shown in rabbits that this may be caused by a metabolic deficiency due to constriction of blood flow [Watanabe and Parke, 1986]. This reduction in nutrients and oxygen has been associated with increasing nervous pain. Compressed nerves have been shown to be extremely sensitive to mechanical pressures long after compression is removed, producing pain at a much lower threshold [Parke, 1991; Howe et al., 1977], physical nerve damage such as demyelination [Rydevik and Nordborg, 1980], dysfunction such as slowed conduction [Garfin et al., 1990], and referred pain to other areas of the body [Zimmermann, 2001]. These neural experiments show that nerves can remain sensitive, dysfunctional and damaged long after the physical irritation or spinal loading has been removed. The absence of an apparent anatomic anomaly in the presence of continued LBP can add further complexity to the diagnostic process. As previously discussed in Section 2.3.3, dysfunction of the spine may occur in the absence of a physical injury or abnormality. Because of the potential confounding pain symptoms, it is important to determine not the anatomic deficiencies of the spine, but the functional deficiencies.

2.4.4 Summary on Diagnostics

The diagnostic difficulties associated with low back disorders are numerous. Though clinicians are well trained in standard assessment techniques, the reliability of diagnoses by manual techniques has been shown to be debatable. Furthermore, while imaging is somewhat effective at determining most

structural abnormalities, the abnormalities detected do not always correlate to a patient's reported pain, and are frequently found in fully asymptomatic subjects. From these studies, it is apparent that simply viewing the spine statically from an anatomical standpoint is not an effective method of determining the source of low back pain. In addition to reliability issues, subjects receiving CT scans or plain radiographic imaging are exposed to harmful radiation. Finally, though LBDs are considered to be functional in nature, static images do not give information about the function of the spine. These issues provide reason for alternative diagnostic techniques to be explored.

One such alternative method being explored is the use of structural damage detection as a diagnostic technique. The proceeding section discusses basic vibration theory to delineate for the reader the reasons for choosing to explore vibration in this capacity.

2.5 Vibration and Dynamics

Vibration is an often complex relationship between an object, its structural properties, and oscillating forces applied to that object. To understand more about how the functional and structural characteristics of an object affect how it vibrates, a basic exploration of these properties are discussed in the following section.

A simplified vibrating system can be characterized by an undamped oscillating mass, shown in Figure 2.4.

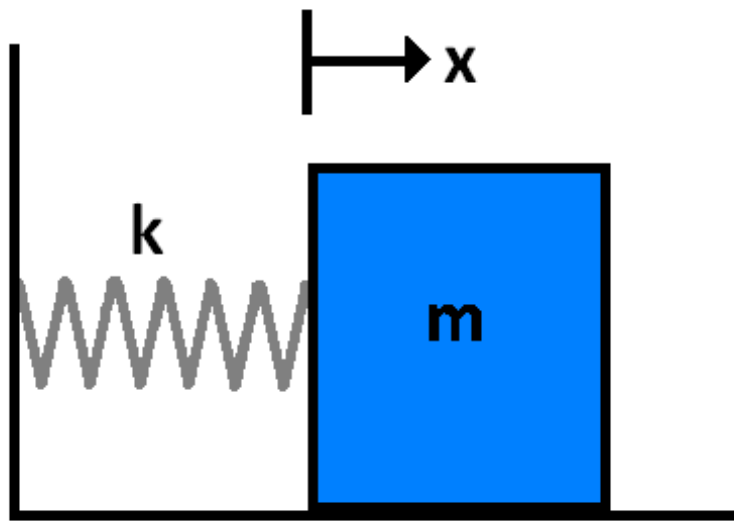


Figure 2.4: Basic spring-mass vibration system, with mass m , damping coefficient c , spring constant k , and displacement x .

The force balance for this system is:

$$m\ddot{x} + kx = 0$$

(1)

Where m is the mass of the object, \ddot{x} is the acceleration of the object, k is the spring constant, and x is the displacement of the mass from a neutral spring position. The solution to this equation is:

$$x(t) = x_0 \cos \omega_n t + \frac{v_0}{\omega_n} \sin \omega_n t$$

(2)

Where:

$$\omega_n = \sqrt{\frac{k}{m}}$$

(3)

Where $x(t)$ is the position of the object at time t , ω_n is the undamped natural (rotational) frequency, x_0 is the initial position of the object, v_0 is the initial velocity of the object [Craig and Kurdila, 2006]. The natural frequency of an object is defined as the frequency an object freely vibrates at, given an input of energy [Craig and Kurdila, 2006]. Equation (3) shows that the natural frequency of an object is a function of its structural properties; that is, its elastic properties and its mass. The derivation of equation (2) is not shown here, but can be found in any basic dynamics textbook. This equation is included for the reader to note that the motion of the mass at any point in time can be characterized by its natural frequency, and its structural boundary conditions.

Though this is a very simplified and idealized system, all other objects can be analyzed using the same principles; namely, that the way an object vibrates is a function of the forces applied to it, and its physical conditions. These properties help define how an object moves with time and space. In more complicated

situations, factors such as friction, inertial properties, and damping are taken into account.

A more complicated input to the system can give further information about how an object vibrates. A sinusoidal force p_0 acting on an object has the equation of motion:

$$m\ddot{x} + kx = p_0 \cos \theta t$$

(4)

Where p_0 is the force input amplitude and θ is the forcing frequency. The object reaches a steady-state response in reacting to the input force, given as:

$$X = \frac{p_0}{k - m\theta^2}$$

(5)

Where X is the steady state response amplitude. The initial amplitude (displacement of the object under a static force p_0) of the object is given by:

$$X_0 = \frac{p_0}{k}$$

(6)

By re-arranging for p_0 in (6) and substituting (6) into (5), we obtain:

$$\frac{X}{X_0} = \frac{1}{1-r^2}$$

(7)

Where r , the frequency ratio, is defined as:

$$r = \frac{\theta}{\omega_n}$$

(8)

The relation of $\frac{X}{X_0}$ is known as the non-dimensionalized frequency response function (FRF), or $H(r)$. Equation (7) shows that this ratio is defined by r , and is inherently a function of a major physical property of the system: the natural frequency. From Equation (3), it is known that the natural frequency is defined by the mechanical properties of the system. Therefore, it can be concluded that changes in the structural properties of an object will change its response to an energy input.

2.6 Structural Damage Detection

Vibration testing can be used to characterize the physical nature of a structure. As demonstrated in Section 2.5, the response of a system to an input vibration, or *vibration response*, changes when the structural properties of that system change.

Engineers have used this relationship between structural properties and vibration response to their advantage for many years [Ewins, 2000; Farrar and Worden, 2007]. Today, vibration testing is a standard accepted technique with a wide variety of applications. One such application involves using the vibration response of an object to determine whether its structural properties are changing. In particular, it is used to detect damage and monitor structural integrity. This is known as *structural damage detection (SDD)* or *structural health monitoring (SHM)* [Farrar and Worden, 2007]. Ewins defines structural damage detection as “the process involved in testing (SHM) components or structures with the objective of obtaining a mathematical description of their dynamic or vibration behavior” [Ewins, 2000].

To perform a structural damage detection test on an object, a number of components are required. The components described here were used in the experiments performed for this thesis, and are only one of many different types of setups that may be required depending on the scale of the object and the testing goals. A basic structural damage detection system is shown below in Figure 2.5.

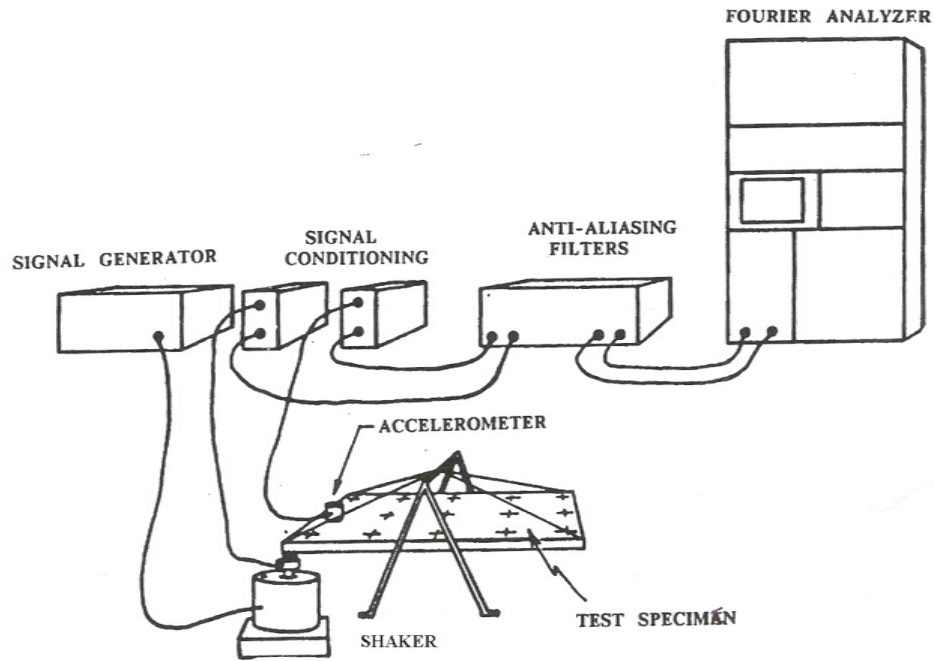


Figure 2.5: A basic structural health monitoring system utilizing a shaker[Brown et al.].

A signal generator is required to generate the desired input vibration signal. This signal is carried to an amplifier. The amplifier then transmits the signal to an electrodynamic shaker. The shaker is connected to the object via a semi-rigid rod known as a stinger, which allows the transfer of the vibration from the shaker to the object. Sensors (in Figure 2.5, accelerometers) are placed on the object, and measure the object's vibration response. These time signals are relayed back to the computer. Software on the computer performs a fast fourier transform (FFT) on the time data to produce the FRF. An example of an FRF is shown below in Figure 2.6.

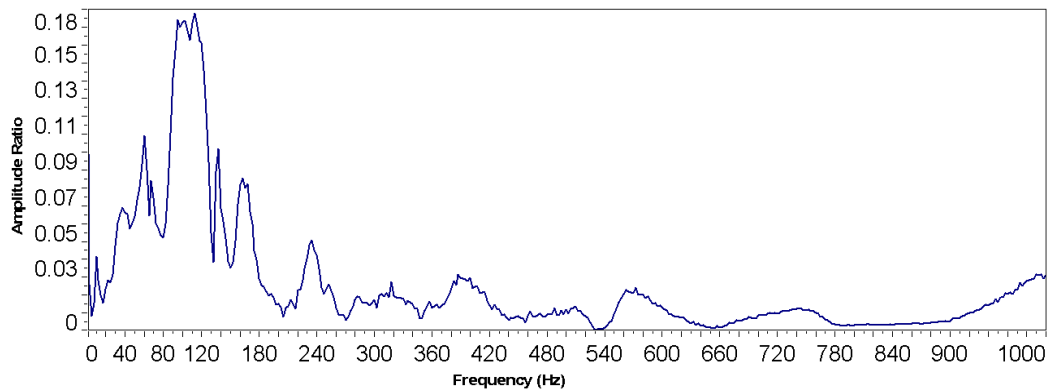


Figure 2.6: An example of a frequency response function (FRF). The amplitude response ratio is graphed on the y axis against input frequency on the x axis.

The FRF has significant impact when viewed graphically. The function is plotted with input frequency on the x-axis, and amplitude response ratio (magnitude) on the y-axis. This graph is an indication of the behavior of the object under vibration. It is a signature response of that object under its current particular conditions. High response ratios indicate the object is close to or at a resonant frequency ($\theta = \omega_n$), where low response ratios indicate the object may be close to an anti-resonance frequency ($\frac{x}{x_0} = 0$). In the context of this thesis, the response ratio or amplitude ratio is a ratio of acceleration/force, also known as ‘accelerance’. Analysis of changes in this signature frequency response curve may indicate that the structural or functional properties of the object are changing. This type of analysis is termed *modal analysis*, where the term ‘mode’ refers to a resonant frequency. The terms *structural health monitoring* and *structural damage detection* are roughly synonymous, and are frequently used interchangeably.

2.6.1 Current Standard Uses of Structural Damage Detection

Structural damage detection has been developed over the last 30 years as a tool to monitor for damage or flaws in objects of interest. It is heavily used in aerospace, civil and infrastructure engineering industries. Bridges, pipelines and airplane wings are all examples of objects that are frequently subjected to structural damage detection testing [Farrar and Worden, 2007]. Vibration is applied to these structures at given time intervals. The vibration responses can be compared using statistical analysis to determine whether structural changes are occurring in the object. This tool allows engineers to detect location and magnitude of cracks or warping, determine remaining useable life of parts, or simply monitor the condition of an intact object.

2.6.2 Structural Damage Detection as a Medical Diagnostic Technique

It can be argued that the use of SDD for medical diagnostics can be traced back to doctors' use of tuning forks to attempt to diagnose many different ailments in the late 19th/ early 20th century [Stritch, 1902]. A vibrating tuning fork was placed on the body to locate points of pain or different tissue densities. As early as 1969, more sophisticated apparatus were being developed to investigate the use of vibration as a diagnostic tool for osteoporosis and diabetes [Jurist, 1970] [Jurist, 1970].

Vibration has been investigated in many diagnostic areas, such as patellofemoral crepitus (crackling, popping, or grating sounds in the knee) for osteoarthritis or disruptions of the meniscus [Kernohan et al., 1986; McCoy et al., 1987], or as previously mentioned, the diagnosis of fractures in long bones. A few applications with more mature development are discussed in the following sections.

2.6.2.1 *Dental Applications*

Structural damage detection has been investigated for a number of medical applications. Dental applications of the technique have been significantly developed. Huang et al. applied vibration up to 20,000 Hz to determine the natural frequency of a dental implant as a means of assessing implant stability and osseointegration [Huang et al., 2000]. The amount of force applied to clamp the implant was varied, as well the length of unclamped implant available for free vibration. This *in vitro* study showed the natural frequency linearly varied with changing free length and clamping force, and could potentially be used as a predictor of osseointegration. The effect of soft tissue damping was not taken into consideration. Meredith et al. also initiated clinical trials with a small transducer affixed directly to the implant [Meredith et al., 1996]. It was shown that measurements of resonance frequencies of dental implants *in vivo* could be easily performed. A follow-up clinical trial demonstrated that the natural frequency of the implant was significantly correlated with implant stability and eventual failure/rejection of the implant [Glauser et al., 2004]. The successes and

failures of research in this arena should be built on in applying this technique to other areas of the body.

2.6.2.2 *Applications in the Hip*

SDD techniques have also been applied to monitoring hip implants for loosening and failure. The first *in vivo* studies were performed in 1989 by Rosenstein et al. Vibration tests up to 1000 Hz were performed on human femurs with artificial hip implants installed in loose and secure manners, post mortem [Rosenstein et al., 1989]. The loose implants had significantly more harmonic resonances than the secure implants. Additionally, a pilot clinical study was carried out on live subjects admitted for suspected loosening of previously installed implants. An accelerometer was held in place at the greater trochanter of the hip, and a sinusoidal signal was applied at the lateral lower extremity via a hand held shaker, pre-operatively. A signal with multiple harmonics, indicating loosening of the implant was detected in all 5 subjects, which was confirmed during the implant revision surgery. The authors note that soft tissue interference did not significantly alter the ability to correctly diagnose a loose implant, however they did not address what effects might be present. They also did not address any variability due to the hand-held nature of the shaker and accelerometer device.

Since this paper, others have attempted to further research in this area. A more recent yet similar study conducted by Georgiou and Cunningham also utilized a hand-held system to diagnose hip implant loosening in 23 patients [Georgiou and Cunningham, 2001]. Their detection system had a sensitivity of 80%, and a

specificity of approximately 88%, but was only tested on subjects with extreme signs of loosening. The effect of soft tissue was also not discussed.

2.6.2.3 *Applications in the Spine and Pelvis*

An area that has also received attention is the pelvis and spine. Due to the difficulty in diagnosing the source of nonspecific low back pain, structural damage detection has been viewed as a potential technique to aid clinicians in this process. Various aspects of full structural damage detection protocols have been implemented.

A number of researchers have investigated the use of vibration as a stimulus to invoke pain in the back, thereby locating the source of pain [Yrjämä and Vanharanta, 1994; Yrjämä et al., 1997; Takalo-Kippola et al., 1995], however, no measurements of input vibration or spinal response to those vibrations were taken.

Keller and Colloca [Keller and Colloca, 2007] have used vibration to analyze the stiffness of the spine, a factor associated with low back pain, degeneration of spinal structures, and decrease in range of motion [Latimer et al., 1996]. A set of experiments performed *in vivo* in an ovine model vibrated the spine at 2, 6, and 12 Hz steady oscillation, as well as from 0.6-19.7 Hz using a swept-sine mode of vibration. Using a custom-made dynamic mechanical testing apparatus, the force and displacement response of the L3 vertebra to the vibrations was measured. It was found that the stiffness of the spine roughly increased with increasing

excitation frequency. This study measured a single vertebral response at the mechanical driving point, and did not characterize the remaining vertebral responses. Furthermore, the low frequencies used in this study limit the diagnostic ability of the device, as others have obtained viable information at much higher frequencies [Kawchuk et al., 2009; Conza et al., 2007].

A great deal of work in the use of vibration in the spine has come from a group investigating the sacro-iliac joint as a source of low back pain. Low frequency mechanical vibrations were measured by both ultrasound and accelerometry in the human pelvis/sacrum as a means of detecting abnormalities. Ultrasonic methods of measurement were first investigated [Vlaanderen et al., 2005; Conza, 2005]. The subject lay in a prone position on a patient table. An electro-mechanical shaker protruded from underneath the table to contact the anterior iliac crest via a small plastic disc, and created excitement frequencies of 100 and 200 Hz. An ultrasound transducer was placed at the left posterior iliac crest, and over the second sacral vertebra to measure the vibration response. Using the ultrasound, displacement measurements of the underlying bone were taken to determine the vibration response of the system. The system was able to successfully measure movement of the pelvis and sacrum down to the sub-micrometer level. However, the authors noted that, as the measurement consisted of displacement data, they would be highly unrepeatable when the transducer head was moved, and were dependent on the exact transducer head angle.

The variables needing to be accounted for in setting up and performing these ultrasound measurements were numerous, considering the measurement precision could reach the sub-micrometer level. As such, the method of

accelerometry was tested. These experiments are discussed in-depth here due to their similarities with the experiments performed by the Spinal Function Lab at the University of Alberta. Conza et al. tested an excised fresh-frozen human pelvis, with both sacroiliac joint and spine up to L4 intact [Conza et al., 2007]. The pelvis was suspended via rubber bands, and 13 L-platforms to hold the accelerometers were screwed into holes drilled into the bone at key measurement locations. The pelvis was vibrated over 7 runs from 10-340 Hz using a sine sweep signal, using two accelerometers and switching their placement to a new location after each run. Upon completion of the 7 runs, the sacrospinous and the sacrotuberous ligaments were resected on both sides of the pelvis, and the pelvis was vibrated only 3 times, measuring at 6 locations, in the same manner. The same method was performed after the iliolumbar ligaments were resected. In the unresected pelvis, resonant frequencies were found at 133, 226, and 244Hz. After resection of the sacrospinous and sacrotuberous ligaments, the resonant frequencies shifted slightly to 132, 226 and 245 Hz. Finally, after iliolumbar ligament resection, the resonant frequencies were determined to be 132, 226 and 246 Hz. The small amount of variation in these resonant frequencies led the researchers to conclude that the resected ligaments did not contribute to the dynamic response of the pelvis to the inputted vibrations. This conclusion implies that abnormalities of the ligaments would not be detected using vibration as a diagnostic tool.

The system described above simulates a 'free' supported structure, in which the system is essentially suspended in space [Ewins, 2000]. In this type of modal testing, rigid body modes are most likely to be found, and bending or flexing of the pelvis are not as likely to occur. Free-support testing does not appear to be

the optimal choice for testing in the pelvis. The sacro-iliac joint, as well as the pubic symphysis provide compliant interfaces between the bones to allow the pelvis to vibrate as a multi-body system. In rigid body testing, the mass and inertial properties are what defines how an object vibrates [Ewins, 2000]. Resection of the ligaments would do very little to change these properties. This is likely the main reason why the modes of vibration of the system changed very little over the course of the experiment. A more appropriate choice for testing may have been to treat the system as a multi-body system tested *in situ*, as the behavior of a structure in a free vibration situation is very different from that of an installed situation [Ewins, 2000].

2.6.2.4 Experiments in the Spine Performed at the Spinal Function Lab

The Spinal Function Lab at the University of Alberta has investigated the use of vibration to identify mechanical dysfunctions of the lumbar spine. Two sets of experiments were performed. The first set investigated the plausibility of the use of vibration as a repeatable measure of spinal function. The second set of experiments utilized the same technique to attempt to determine the location and magnitude of damage imparted to the spine. These experiments are described and discussed here in detail due to their close relationship with and impact on the work performed in this thesis

As previously mentioned, experiments were performed in five cadaveric, eviscerated pigs to determine whether vibration could be used to detect changes in the structure of the lumbar spine [Kawchuk et al., 2008]. Triaxial

accelerometers were embedded directly in the spinous processes of each lumbar vertebra. A pincer clamp was secured to the L3 vertebra to rigidly input vibrations using a random burst protocol. The spinal response to 10 bursts containing multiple frequencies between 0-2000 Hz were averaged to create a mean response FRF. Two bone screws, which had been installed in the L3 and L4 vertebrae, had a rod tightened securely between them. Five repeated measures of mean FRFs were taken of the spine in this condition. Five repeated measures were further taken under the following damage state conditions: a loosened scoliosis rod, scoliosis rod removed, bone screws removed (non-damaged/baseline), and disc transections progressively from L1-2, L4-5, L2-3 and L3-4.

Each of the 5 repeats in a set was compared to one another by the frequency response assurance criteria (FRAC), a method developed and utilized by many to correlate FRFs [Heylen and Lammens, 1996]. Reliability between repeats was calculated using the intraclass correlation coefficient on the FRAC values [Shrout and Fleiss, 1979; Weir, 2005]. The reliability of the repeats was found to be acceptably good (0.68-0.99). The FRAC was also used to calculate the correlation of each of the damage states with the non-damaged condition. Damage states incurred closer to the baseline state had higher FRAC values. FRAC values tended to decrease with damage states incurred further away (time-wise) from the baseline condition. These experiments showed that changes in the structural health of the spine caused changes in its functional vibration response.

The second set of experiments was performed to further the hypothesis that SDD could detect the location and magnitude of structural damage to the spine. Experiments were performed in 6 cadaveric, eviscerated pigs [Kawchuk et al.,

2009]. Bone screws were installed in each of the L1-L5 vertebrae. Triaxial accelerometers were installed in the spinous processes of each of the same. 'Damage' states were created to alter the mechanics of the lumbar spine, alternated with 'healthy' states, in which the spine was returned to its presumed normal condition. The same random burst protocol was utilized as in the preliminary experiments. Ten mean FRFs were obtained for the healthy states, while five mean FRFs were obtained for damage states. Damage states performed included: cable ties tightened between two pedicle screws to bind two adjacent vertebrae together, performed at each of the L1-L2, L2-L3, L3-L4 and L4-L5. Linkages of L1-2 and L3-4, L1-2 and L4-5, and L2-3 and L4-5 employed simultaneously were also measured. After each set of 5 measurements, cable ties were removed and the spine was returned, allowing the spine to return to a 'normal' state. Finally, irreversible damages were created in the intervertebral discs. First, a scalpel stab at the midline of the L1-L2 disc was created, and 5 repeated tests were performed. This was performed at the L4-L5, L2-L3, and L3-L4 discs. Next, the scalpel stab was widened to transect half the intervertebral disc at each of the previously injured discs. Finally, the whole disc was transected. Five repeated tests were performed after each half or full transection.

An adapted version of the previously used FRAC, the global shape criteria (GSC) and global amplitude criteria (GAC) developed by Zang et al., was used to correlate the shape and amplitude features, respectively, of the FRFs [Zang et al., 2003] [Zang et al., 2003]. The GSC and GAC values were analyzed by a neural networking program. A total of 5040 comparisons resulted in only 10 misclassifications of the data to the correct healthy or damaged state and its

location, when all 3 axes of data were taken into consideration. This significant result heralded sensitivity values of 0.994-1.000 and specificity values at 1.000.

These experiments utilized the full capabilities of SDD theory to perform identifications, employing a single input multiple output (SIMO) experimental setup, coupled with a neural networking program for analysis. They clearly demonstrate that structural damage detection may be a viable option for detecting the location and magnitude of spinal dysfunctions.

2.6.3 Experimental Factors in Structural Damage Detection for Medical Applications

2.6.3.1 Shaker Considerations

There has been very little discussion in most of the previously reviewed experimental papers examining the method of connection or attachment of the accelerometers and vibration input contact point to the body. Craig and Ewins both note that electrodynamic or electromechanical shakers must be supported rigidly when inputting vibration to the system [Ewins, 2000; Craig and Kurdila, 2006]. Lack of support for the shaker can cause large displacements of the shaker body, particularly at low frequencies. Displacements of the shaker body reduce the force of the vibrations imparted to the structure, decreasing the effective signal imparted to the object under vibration. A number of the previously described experiments [Rosenstein et al., 1989; Kernohan et al., 1986; McCoy et al., 1987; Georgiou and Cunningham, 2001; Yrjämä et al., 1997; Yrjämä

and Vanharanta, 1994; Takalo-Kippola et al., 1995] involving vibration testing do not address this issue.

Vlaanderen et al. do not adequately describe the interface between the shaker and the body in their article on ultrasonic techniques [Vlaanderen et al., 2005]. The article describes a plastic disc that contacts the anterior superior iliac crest, but does not mention how the disc is secured to the subject to maintain contact and prevent slippage, nor what the pre-loading conditions on the disc were. Furthermore, the size of the disc is not described, making it difficult to determine the precision of the vibration input to the pelvis.

2.6.3.2 *Transducer Considerations*

A similar issue exists with the attachment of transducers meant to measure the vibration response of the object. A signal obtained from a transducer (ex: accelerometer) is typically presumed to accurately represent the motion of the object to which it is mounted. However, a number of studies neglect this important consideration in their testing apparatus. Takalo-Kippola et al. designed a hand held vibration device used to detect painful areas in the lumbar spine [Takalo-Kippola et al., 1995; Yrjämä et al., 1997; Yrjämä and Vanharanta, 1994]. While the ultimate goal of this device was not to perform a full structural damage detection test, the hand-held nature of the device did not allow the examiners to standardize the force applied, or maintain the device in a rigid position while vibration was applied to the spine.

As previously mentioned, experiments performed in the hip face similar problems; both Georgiou and Rosenstein used a non-invasive hand-held shaker and accelerometer [Georgiou and Cunningham, 2001; Rosenstein et al., 1989]. The problem here is two-fold; holding the shaker or accelerometer on by hand adds compliance (ie, non-rigid fixture) from the tester's body, and neither paper addresses the impact of the soft tissue between the bone and the equipment of the patient on the results.

Conza et al. concluded that vibration could not be used to detect changes in the ligaments of the pelvis [Conza et al., 2007]. They adequately discussed both the shaker attachment and accelerometer attachment to the pelvis. However, as previously noted in the discussion of that paper, the 'free' setup of the pelvis may not have been the appropriate setup choice, and may have diminished their results.

2.7 Skin and Soft Tissue Effects

The effects of skin and soft tissue in vibration testing are largely unknown, and often overlooked, as evidenced by Section 2.6. However, researchers have investigated the issue in depth in work on biomechanics and human kinematics. This section will explore the differences in properties of porcine and human skin. Discussion on the methods of attachment of sensors to the skin, and issues associated with those methods will be given.

2.7.1 Anatomy of the Skin

The skin is a multi-layered organ, comprised of cells, elastic tissues, and highly specialized features such as hair and hair follicles, glands, and pores, while housing arteries, veins, and nerves. Figure 2.7 shows the basic structure of skin.

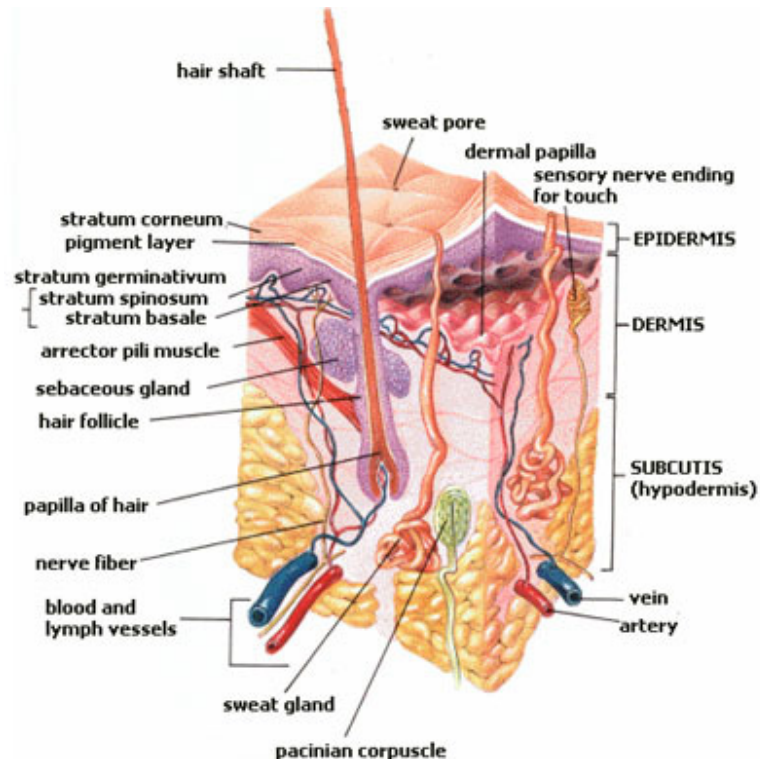


Figure 2.7: Basic structures of human skin

The properties and structure of the skin of an animal vary greatly depending on the region of the body they cover [Montagna and Yun, 1964; Cua et al., 1990; Diridollou et al., 2000], the age of the subject [Cua et al., 1990; Sanders, 1973], and the hydration level of the skin [Cua et al., 1990]. Furthermore, the

differences in skin properties between humans and pigs, both tested during this thesis, are also very distinct in many ways. While the exact mechanical properties of the skin seem to vary greatly from subject to subject, sometimes in orders of magnitude [Greenleaf et al., 2003], certain generalized characteristic statements can be made. Montagna et al. outline a number of main differences in the mechanical and physiological properties of domestic pig skin to that of human skin, demonstrating one reason for the necessity of validating previous porcine results in human subjects [Montagna and Yun, 1964]. Importantly for this study is the notably increased thickness and density of the stratum corneum layer of the epidermis, and potentially the decreased vascularization of the dermis in the pig, which may contribute to the elasticity of the skin. The importance of these differences on the measurement of vibration in the spine is discussed in the following sections.

2.7.2 Mechanics of the Skin

The non-linear behaviour of skin is well known. The elasticity of skin has been shown to significantly change under loading in both compression and tension in both FEA models, as well as *in vitro* [Wu et al., 2003; Delalleau et al., 2008]. Potentially, mechanical waves imparted to the tissue by vibration would place the skin under both mild tension and compression during wave propagation, invoking non-linear behavior. This is demonstrated in Figure 2.8.

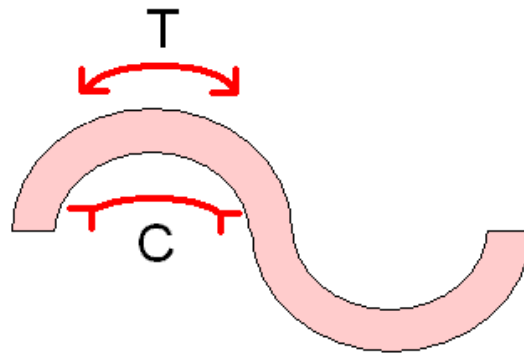


Figure 2.8: Mechanical wave travelling through the skin can cause localized areas of tension (T) and compression (C).

Non-linear behavior in the skin is attributed to the uncoiling of disordered collagen fibers, as shown in Figure 2.9, while the viscous nature of the skin can be explained by interstitial fluid and frictional interactions between tissue elements [Delalleau et al., 2008; Oomens et al., 1987; Holzapfel, 2001].

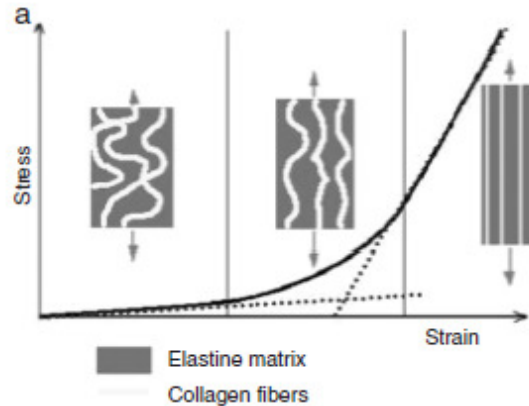


Figure 2.9: Behaviour of the basic elastic components of skin with increasing strain. Figure adapted from [Dellaleau et al 2008] and [Holzapfel et al 2001]

The bulk of studies determining the mechanism of propagation of vibration through the skin have been in the ultrasonic range, in the field of elastography

[Greenleaf et al., 2003]. However, one study did attempt to employ low frequency vibration to determine skin properties. A study performed by Zhang et al. investigated the propagation of surface waves in various locations on the body, including the mid-back [Zhang et al., 2008]. A small shaker was applied to the skin to impart vibrations at 100, 200, 300 and 400 Hz in 11 male volunteers, age 25-66. A laser vibrometer was used to measure the vibration of the skin from 2-12 mm away from the vibration input, at 2mm intervals. These methods allowed the authors to measure the propagation of the wave. The experiment showed a non-linear relationship between increasing frequency and subsequent vibration wave speed; however, the authors do not discuss this effect in detail. The authors do not mention the effects of preloading (or lack of preloading) the shaker to the skin, the significance of the range of volunteers' ages, or composition of the body's underlying tissues. The results of this study show that vibration travels through different anatomical regions of skin differently.

2.7.3 Skin Thickness Effects

A study by Dellaleau et al. looked at different mathematical models to describe the behavior of the skin [Delalleau et al., 2008]. Deflection of skin of 3 different thicknesses was measured using a standard skin suction test. The authors first confirmed the 3-stage non-linear behavior of the skin, as shown in Figure 2.9. Next, a mathematical model was developed to predict the behavior of the skin under suction, using a modified Hooke's law. Excellent agreement between the mathematical model and the experimental skin deformation behavior was found, but only when skin thickness was taken into account. This study showed

the importance of accounting for non-linear behavior and variation of skin parameters (thickness) between individuals.

2.7.4 Effects of Time-Variant Factors on Skin Properties

Studies have been conducted to characterize the vibration propagation properties of the skin. Potts et al. created an *in vivo* device consisting of two transducers lightly rested on the skin, to test the propagation of shear waves in wet and dry skin of men aged 24-63 [Potts et al., 1983; Potts et al., 1984]. The device transmitted vibrations to the back of the hand from 8-1016 Hz, with input measured by the first transducer at the driving point, and transmission measured by the second transducer at a known distance from the driving point. The velocity of the transmission was calculated by the change in phase from the input to the output wave. The damping of the transmission was calculated as the change in amplitude of the wave. This research produced a number of very important results. First, it was found that the age of the skin was a significant factor in the transmission of vibration through the skin. A positive linear relationship was found between increasing age and increasing frequency of vibration for both wave velocity and damping. Second, differences in vibration transmission were found to be maximal at low frequencies and minimal within high frequencies when comparing wet and dry skin tests in each subject. This important result suggests that low frequencies are carried through the stratum corneum, the outermost layer of the skin which is affected by water content, while higher frequencies are carried at deeper tissue levels. These results highly impact data presented in this thesis, further suggesting that the amount and

frequencies of vibration transmitted through the skin are highly dependent on skin age (presumably age-related changes in elasticity and composition) and water content. However, certain subject dependent factors such as measurements of skin thickness or body fat, as well as potential transmission of vibration through the bone were not considered or discussed at a satisfactory level.

Studies have been developed based upon this protocol to investigate factors such as sex, sun damage and variations in skin thickness. Pereira et al. performed experiments using the equipment described by Potts et al. [Potts et al., 1983] to further investigate the effect of age on the transmission of shear waves [Pereira et al., 1990]. A number of single layered silicon sheets of known varying moduli and thickness, as well as a dual layered mathematical model were used to simulate the skin. A frequency input of 0-2000 Hz was used. The authors concluded that vibrations were highly influenced by skin properties at low frequencies (<1000 Hz). This experiment had many assumptions that may have affected the validity of the results; namely, the modeling of a single layer of tissue only, and the assumption that skin is a linear visco-elastic, homogeneous, isotropic substance. Davis et al. further studied the propagation of shear waves through skin on the underside of the forearm, also using the Potts device up to 2000 Hz [Davis et al., 1989]. A questionnaire was given to correlate wave propagation with sun exposure, height, weight, smoking, level of exercise, skin pigmentation class, and hand dominance. The only significant correlation found was between age and propagation velocity. However, the measure of sun damage may have been poor, as the underside of the forearm generally does not get much sun exposure.

The results of these studies show that skin is a highly complex organ. Skin has been shown to be an anisotropic, non-linear substance, with variation in skin properties being influenced by age, water content, and skin thickness. These properties make non-invasive measurement of skeletal motion exceptionally difficult because of the variable nature in which vibration is transferred through the skin.

2.7.5 Other Soft Tissue Effects

The effect of skin on surface marker measurements of spinal movement has been reviewed by many. However, there have been no papers which have reviewed the effect of other soft tissues, such as cartilage, ligaments, and fascia. The tips of the spinous processes are cartilaginous, and are connected by the supraspinous ligament and interspinous ligament. The dorsolumbar fascia also connects over top of the spinous processes. These tissues all have different compliances, but their direct effects on testing using surface markers has not been quantified or delineated from that of the skin.

2.7.6 Accuracy of Bone Motion Measurements by Skin Mounted Sensors

Much work has been done concerning the attachment of sensors to the human body non-invasively. Biomechanists have been using skin mounted optical

markers and accelerometers for many years in attempts to measure body kinematics and motion. However, discrepancies exist between the perceived bone movement measured by a skin mounted sensor, and the true underlying bone movement. This is due to difficulties in mounting the sensors to the skin, as well as the significant deformation effects of the skin and underlying soft tissues during skeletal movement.

A number of groups have utilized markers on bone pins to measure kinematics of various body parts [Holden et al., 1997; Nester et al., 2007; Panjabi et al., 1986; Fuller et al., 1997]. While these results were successful in measuring skeletal movements, they were invasive in nature, and thus were not appropriate in the adaptation of a non-invasive vibration device for spinal diagnostics.

Holden et al. provide a comprehensive summary of 17 studies performed prior to 1997 in the introduction to their experiment on measuring displacements of skin markers/sensors compared to bone-embedded markers/sensors [Holden et al., 1997]. The results of all of the reviewed studies showed significant movement of skin mounted markers (8 mm - 40 mm) in comparison to their original positions, depending on their location on the body. A similar conclusion was drawn by Kuo et al. [Kuo et al., 2003]. They studied the accuracy of skin mounted markers on the thumb. Even in such a small body part, a movement error of 4.9° and 2.8 mm occurred. Consistently, these studies showed that surface measurements do not accurately reflect the underlying bone movement. None of these studies discussed the effect of small changes or adjustments in the placement of the skin-mounted sensors on the measurement signal.

2.7.7 Methods of Correcting Error in Skin Mounted Sensors

2.7.7.1 Physical Corrections

A number of methods have been suggested to overcome the effects of skin on the measurement of skeletal movements. Physical improvements to systems have been explored, but with limited success. Lafortune et al. placed accelerometers on a thin sheet of balsa wood, which was then glued to the skin over the tibia and elastically secured to the leg [Lafortune et al., 1995]. Accelerometers were also attached to intracortical pins, which were inserted directly into the tibia. Among five subjects running at 4.5 m/s, they found excellent agreement between skin and bone mounted accelerometers in two, fair agreement in two, and poor agreement in one. They devised a transfer function to describe the difference between the skin and bone mounted accelerometers; however, it did not apply to the subject with poor agreement between sensors, and could only moderately account for discrepancies in the two subjects with 'fair' agreement in signals. The authors could not cite a cause for this discrepancy, and concluded that the signal distortion was not a systematic feature. No comments were made about possible contributions of the balsa wood or elastic strap to the resonance, or inertia of the system. It was noted that 'subject morphology' was not a factor in the discrepancies, but this statement is not elaborated on.

Researchers have also attempted to use sensors mounted on plates to reduce skin artifacts in signals. Nester et al. compared walking gait patterns measured from a number of markers on the foot, mounted in 3 different methods: mounted directly to the skin, mounted on rigid plates over the skin, and

mounted on bone pins directly inserted in the skin [Nester et al., 2007]. Over the 6 subjects tested, neither skin mounting of sensors nor plate mounting of sensors emerged as the superior technique when compared to the bone mounted sensors. Leknius et al. devised a thin plate interface between the accelerometer and the skin as a stabilizer for the sensor, to measure temporomandibular joint sounds and movements [Leknius and Kenyon, 2005]. The influence of the plate was not evaluated, and no experimental data was given.

2.7.7.2 Mathematical Corrections

Mathematical methods have also been investigated to post-process data from skin mounted transducers, in an effort to align them with true bone response. As previously discussed, Lafortune et al. devised a transfer function method, which was only successful in accurately correcting 40% of measured skin signals [Lafortune et al., 1995].

Kitazaki and Griffin proposed a mathematical correction by modeling the skin as a single degree of freedom spring and damper system for both the normal and shear directions of the skin [Kitazaki and Griffin, 1995]. They used an inverse acceleration transfer function with local system parameters (damping and mass of accelerometer and skin) as a correction to signals measured from a skin mounted marker over top of the L3 vertebra. This method was somewhat effective, but a number of issues impede its usefulness. The authors did not measure true bone movement in their subjects, and thus could not directly compare their corrected data to a direct measurement. Their correction method

was compared to data from data from other authors, who measured spinal movement from sensors on Kirchner wires embedded in the vertebrae. While a somewhat acceptable correlation occurred between the three studies' data, the data was only viewed up to 15 Hz. However, data presented earlier in the Kitazaki study showed that no correction was needed for data at such low frequencies. Therefore, the *in vivo* validity of this correction has not been fully proven. Additionally, standardized correction functions could not be created for the 8 subjects tested, due to the heterogeneity of the subjects. Finally, as discussed in Section 2.6.2.3, measurements at such low frequencies would only cover rigid body modes of vibration. Thus, the validity of the correction has not been proven at higher frequencies.

A somewhat successful technique has been developed by Andriacchi et al, termed the Point Cluster Technique (PCT) [Andriacchi et al., 1998; Alexander and Andriacchi, 2001]. Eight reflective markers were uniformly distributed across a limb segment. Each point was given an arbitrary mass (ie: weighting). From these masses, an inertia tensor of the marker system was calculated. The eigenvalues of this matrix represented the rigid body motion principal moments of inertia, and the eigenvectors represented the axes of inertia. When non-rigid body motion was measured by the markers, the eigenvectors and the eigenvalues changed. The transformation matrix representing this shift was used on the experimental data to reduce the skin artifact. Results showed that the PCT provided a substantial beneficial correction in the measurement of the thigh and femur movement [Andriacchi et al., 1998]. However, the corrected data was not compared to bone mounted sensor data obtained from the same experiment, but to data obtained in an experiment by Lafortune et al [Lafortune et al., 1992].

The correlation between the Andriacchi and Lafortune data is considered excellent in some cases (leg flexion), but poor in others (internal/external rotation, abduction/adduction). The PCT correction does appear to have some merit as shown by the excellent correlation of leg flexion data. Comparisons to bone mounted sensor data obtained in the same experiment would strengthen this conclusion. Unfortunately, the PCT correction is not likely a useful tool for measurements in the spine, due to the high number of markers required to be mounted to a single bone.

A number of methods of mounting sensors to the skin, and correcting for skin artifacts in the obtained signals have been discussed here. From this discussion, it can be seen that the skin still poses a very difficult problem in the non-invasive measurement of human kinetics. Much of this research has been performed in the extremities of the body. The effect of the skin on the measurement of the spine in the context of structural damage detection testing is currently unknown.

2.8 Signal Analysis Techniques

A wide variety of analysis techniques have been used to analyze functional data such as FRFs. Different techniques each have their own merits and deficiencies, which will be discussed here.

2.8.1 Global Shape and Amplitude Criteria

A measure known as the Modal Assurance Criteria (MAC) was originally developed in 1982 by Brown and Allemang as a method to assess the correlation between two structural health states in an object [Allemang and Brown, 1982]. Many variations of this measure have been created since, with the Global Shape Criteria (GSC) and Global Amplitude Criteria (GAC) being some of the latest. The GSC and GAC were developed by Zang et al., and allow the user to delineate the correlation in signal shape and signal amplitude, respectively [Zang et al., 2007]. The GSC and GAC are shown below in equations (9) and (10):

$$GSC = \frac{|\{H_{x1}(\omega)\}^H \{H_{x2}(\omega)\}|^2}{(\{H_{x1}(\omega)\}^H \{H_{x1}(\omega)\})(\{H_{x2}(\omega)\}^H \{H_{x2}(\omega)\})}$$

(9)

$$GAC = \frac{2|\{H_{x1}(\omega)\}^H \{H_{x2}(\omega)\}|}{(\{H_{x1}(\omega)\}^H \{H_{x1}(\omega)\}) + (\{H_{x2}(\omega)\}^H \{H_{x2}(\omega)\})}$$

(10)

Where $H_x(\omega)$ denotes the complex FRF of time data X, ω denotes the measurement frequency, the subscripts 1 and 2 denote reference and experimental data, respectively, and the superscript H denotes the hermitian transpose of the FRF [Zang et al., 2007].

A note should be made about the definition of 'shape' and 'amplitude'. Shape does not refer to the mode shape of an individual FRF; rather, it refers to the 'spatial shape' of the vibration response of the object, and the relative amplitude of the sensor measurements within each FRF. The measurement of amplitude is an absolute comparison of the values in each FRF to each other.

The GSC and GAC provide useful information in determining the specific shape and amplitude correlation of sets of signals; however, as can be seen from these equations, the GSC or GAC functions require a matrix of sensor responses, recorded simultaneously, as input. A single vector used as input produces a GSC or GAC of 1. Therefore, they cannot be used to correlate the signal from one sensor to that of another.

2.8.2 Principal Component Analysis

Principal component analysis (PCA) is typically implemented for large data sets to reduce the size of matrices for speeding up computation or reducing required memory storage space, without losing important information [Rao, 1964].

To perform PCA, a matrix of measured functional data (X) is created, where each column represents an individual function. The mean value of each function is next subtracted from the function's data points, to centre the mean of the function at zero. Next, singular value decomposition (SVD) is performed on the matrix to obtain the eigenvectors and eigenvalues of the matrix. The eigenvectors of the X matrix represent an orthogonal basis upon which the X

data is projected. The first principal component, or PC1, represents the highest mode of variance, PC2 the second highest mode, etc. The eigenvalues of each eigenvector represent how much variance in the data set each PC accounts for. The eigenvectors are the principal components, representing the largest sources of variance and most important changes in the previous X data set.

The PCs of the X matrix can provide information about how a set of signals, such as FRFs, are varying or shifting. PC1 represents the greatest source of variance in the data; however, it is only a vector. To visualize the meaning of this vector, a multiple of the PC1 vector is added and subtracted from the average measured FRF. This allows us to visualize the singled out mode of variance within the data set. In an example using temperatures measured over a year for 10 years, the investigator would like to know how temperatures fluctuate. Using the previously described graphing technique, the PCs with the highest percentage of variance associated are graphed with the mean data curve, shown in Figure 2.10.

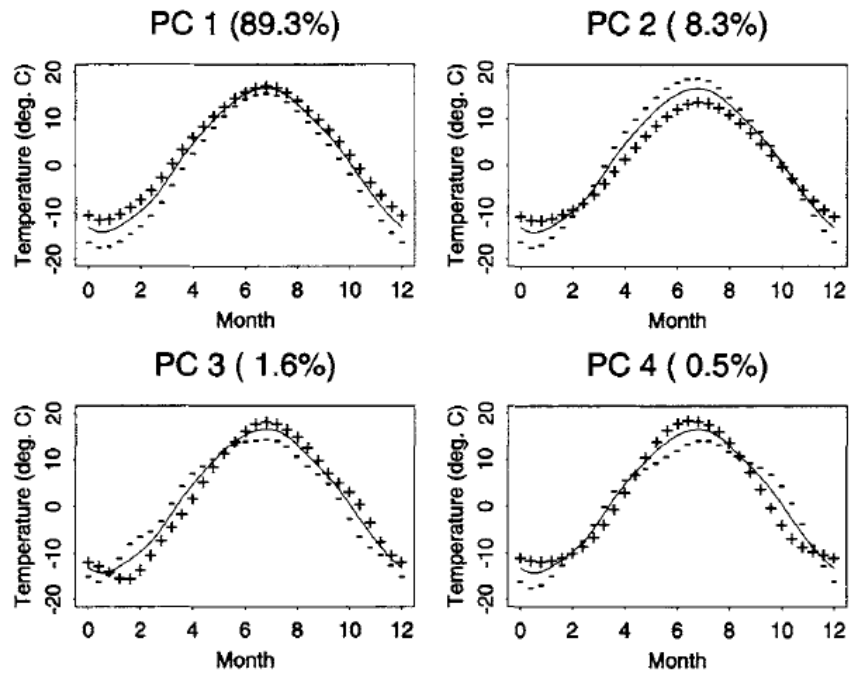


Figure 2.10: The effect of adding (+) and subtracting (-) a multiple of each PC to the mean temperature curve. Figure from [Ramsay and Silverman, 2005]

PC1, accounting for 89.3% of the variance in the data, shows that a simple amplitude effect in the winter months causes the most variance in the curves. PC2 shows that a decrease in the temperature over the summer months is the next highest mode of curve variance. PC 3 shows a shifting of the peak temperature to later in the summer, while PC 4 shows spring beginning later and fall ending earlier [Ramsay and Silverman, 2005].

PCA can provide a wealth of information concerning a set of signals, their modes of variance, and how large an effect each mode of variance has on the data. It presents an excellent method of both quantifying and qualifying the differences

in a set of signals. PCA is one of the most popular multivariate statistical analysis methods for large data sets. It has been used in many applications in almost every scientific field. Examples in medicine include detecting differences in the gait of subjects with and without disease [Deluzio and Astephen, 2007; Reid et al., 2010; Duhamel et al., 2006], or detecting carotid artery disease [Sherriff et al., 1982]. In addition to simply detecting differences in gait patterns, Deluzio et al. [Deluzio and Astephen, 2007] used the visual PCA method described by Ramsay et al. [Ramsay and Silverman, 2005] to determine the overall effect of the PCs on the variance in their data. PCA has also been used specifically with FRFs to reduce data sets, such as those measured from buildings under earthquake conditions [Ni et al., 2006], or from FRF data sets representing healthy and damaged states in aircraft wings [Trendafilova et al., 2008]. Ramsay et al.'s visual method has not been used to describe changes specifically in FRFs, to this author's knowledge.

For complete information on the calculation of principal components, please see Appendix A.

2.8.3 The D-statistic

The d-statistic is a simple calculation used to quantify shape similarities between signals [Zennaro et al., 2002]. To obtain the D-statistic, the 95% confidence interval on a 'baseline' population of repeated sample signals is calculated. Next, a mean signal of a different 'experimental' population of repeated sample signals is calculated. The percentage of the experimental signal that falls within the 95%

confidence bounds of the baseline signals is the D-statistic value. An example of the D-statistic is shown in Figure 2.11.

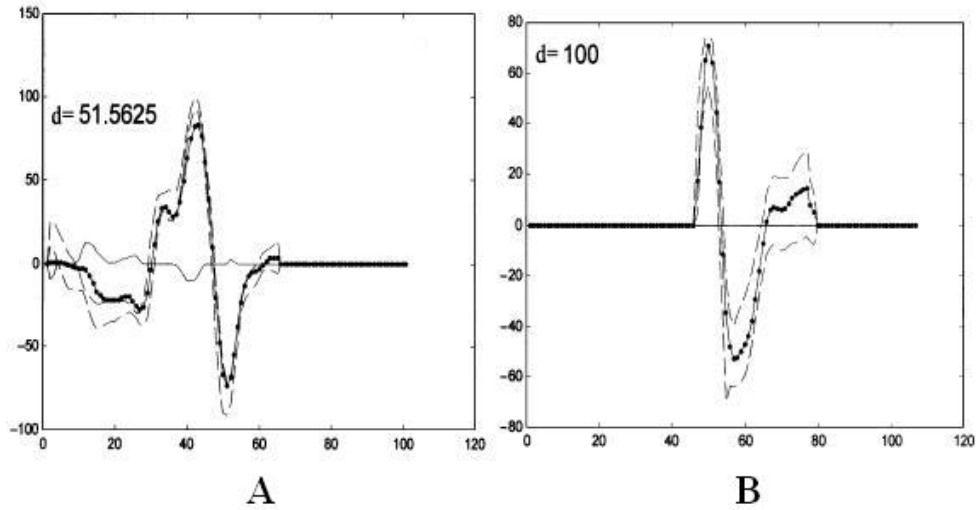


Figure 2.11: Calculation of the d -statistic on two signals. The dashed lines represent the confidence bounds of the 'baseline' data, while the dotted line represents the mean of the 'experimental' signal. A) D -statistic of 51.56 B) d -statistic of 100. Figure adapted from Zennaro et al. [Zennaro et al., 2002]

Though simplistic in nature, it gives a general idea of how well two signals match. Unfortunately, the D -statistic can be misleading due to its insensitivity. If the 95% confidence bands are large, this can allow for significant shape differences in the mean signals to occur undetected.

2.8.4 Transmissibility

Transmissibility is another simple calculation describing the ratio of one FRF to another. Traditionally, it is used to calculate the effectiveness of damping mechanisms on a mechanical system [Ungar and Dietrich, 1966]. However, we may also use the transmissibility to calculate the relationship between any input signal and a measured output signal, such as the effect of the skin on a vibration signal, measured from a skin mounted accelerometer and a bone mounted accelerometer. Equation 11 shows the transmissibility, T, calculation.

$$T = \frac{H(\omega)_2}{H(\omega)_1}$$

(11)

Where $H(\omega)_x$ represents the frequency response function, and x denotes the bone (1) or skin (2) signal.

For a signal with a large number of data points, such as an FRF, window averaging of the transmissibility may be used to reduce the data size and create a more meaningful data output. However, this reduction of data may be misleading. For example, a transmissibility of 0.5 and 1.5 average to fool the user to thinking there is a perfect transmissibility of 1. An additional disadvantage of the transmissibility calculation may be its simplicity. This simple ratio takes only amplitude into effect, and cannot tell the user whether two FRFs may be similar in shape.

Calculation of transmissibility has been effectively used to determine the effectiveness of transmission of simple single frequency sinusoidal vibrations to the spine [Rubin et al., 2003] and other areas of the body [Bressel et al., 2010].

2.9 Literature Review Summary

Mechanical low back pain has been shown to be a significant problem for the adult population [Walker et al., 2004; Papageorgiou et al., 1995; Cassidy et al., 1998]. LBP is thought to be caused by dysfunction of the spine [Panjabi, 1992; Kirkaldy-Willis and Farfan, 1982; Norris, 1995]. Current diagnostic techniques are proficient in imaging the anatomic features of the spine; however, they do not adequately describe the mechanical function of the spine. It has been shown that anatomic anomalies do not always correlate with reported symptoms, or lack thereof, in subjects [Jensen et al., 1994; Tong et al., 2006; Deyo, 1994].

It is thought that vibration may be used to characterize the function of the spine. Structural damage detection (SDD) is an engineering technique that utilizes vibration to detect damage or dysfunction in structures such as bridges or industrial machinery [Craig and Kurdila, 2006; Ewins, 2000]. A new technique is being developed which employs SDD techniques for detecting the location and magnitude of functional anomalies in the spine. The technique has been proven accurate in damage detection in an invasive porcine model [Kawchuk et al., 2008; Kawchuk et al., 2009].

Adaptation of the technique for use in a non-invasive human model has been undertaken. The effect of the spinal soft tissues, namely the skin, on the measurement of the spinal vibration response, is an issue that must be investigated [Andriacchi et al., 1998]. Currently, very few techniques have been successful in overcoming the interference of skin on the measurement of underlying bone movement, in both physical and mathematical corrections [Taylor et al., 2005; Andriacchi et al., 1998].

This thesis aims to further investigate and characterize this skin effect in the context of the vibration testing techniques under development.

2.10 References

Adams MA, Dolan P. 1995. Recent advances in lumbar spinal mechanics and their clinical significance. "Clin Biomech (Bristol 10:3-19.

Ahern DK, Hannon DJ, Goreczny AJ, Follick MJ, Parziale JR. 1990. Correlation of chronic low-back pain behavior and muscle function examination of the flexion-relaxation response. Spine 15:92-95.

Alexander EJ, Andriacchi TP. 2001. Correcting for deformation in skin-based marker systems. J Biomech 34:355-361.

Allemang R, Brown D. 1982. A Correlation Coefficient for Modal Vector Analysis. Proceedings of the First International Modal Analysis Conference, Union Coll, Schenectady, NY, USA, Orlando, Florida.

Ambroz C, Scott A, Ambroz A, Talbott EO. 2000. Chronic low back pain assessment using surface electromyography. J Occup Environ Med 42:660-669.

Andriacchi TP, Alexander EJ, Toney MK, Dyrby C, Sum J. 1998. A point cluster method for in vivo motion analysis: applied to a study of knee kinematics. J Biomech Eng 120:743-749.

Boden SD, Davis DO, Dina TS, Patronas NJ, Wiesel SW. 1990. Abnormal magnetic-

resonance scans of the lumbar spine in asymptomatic subjects. A prospective investigation. *J Bone Joint Surg Am* 72:403-408.

Bogduk N. 2009. On the definitions and physiology of back pain, referred pain, and radicular pain. *Pain* 147:17-19.

Bogduk N. 1983. The innervation of the lumbar spine. *Spine* 8:286-293.

Bogduk N. 1996. Needle Techniques in the Diagnosis of Low Back Pain. In: Weinstein JN, Gordon SL, editor. *Low Back Pain: A Scientific and Clinical Overview*. Rosemont, IL: American Academy of Orthopedic Surgeons.

Bressel E, Smith G, Branscomb J. 2010. Transmission of whole body vibration in children while standing. *Clin Biomech (Bristol)* 25:181-186.

Brown D, Allemang R, Avitabile P. *Modal Analysis: Theory and Application*. International Modal Analysis Conference XXVII, Society for Experimental Mechanics, 2009.

Brumagne S, Janssens L, Janssens E, Goddyn L. 2008. Altered postural control in anticipation of postural instability in persons with recurrent low back pain. *Gait Posture* 28:657-662.

Candotti CT, Loss JF, Pressi AMS, Castro FADS, La Torre M, Melo MDO, Araújo LD, Pasini M. 2008. Electromyography for assessment of pain in low back muscles. *Phys Ther* 88:1061-1067.

Carragee EJ, Cohen SP. 2009. Lifetime asymptomatic for back pain: the validity of self-report measures in soldiers. *Spine* 34:978-983.

Carragee E, Alamin T, Cheng I, Franklin T, van den Haak E, Hurwitz E. 2006. Are first-time episodes of serious LBP associated with new MRI findings? *Spine J* 6:624-635.

Cassidy JD, Carroll LJ, Côté P. 1998. The Saskatchewan health and back pain survey. The prevalence of low back pain and related disability in Saskatchewan adults. *Spine* 23:1860-6; discussion 1867.

Conza NE, Rixen DJ, Plomp S. 2007. Vibration testing of a fresh-frozen human pelvis: the role of the pelvic ligaments. *J Biomech* 40:1599-1605.

Conza N. 2005. Ultrasound Detection System for Musculoskeletal Disorders. *Experimental Techniques* 29:54-57.

Cooper RG, St Clair Forbes W, Jayson MI. 1992. Radiographic demonstration of paraspinal muscle wasting in patients with chronic low back pain. *Br J Rheumatol* 31:389-394.

Craig RR, Kurdila A, editor. 2006. *Fundamentals of structural dynamics*. Wiley. 728 p.

Cua AB, Wilhelm KP, Maibach HI. 1990. Frictional properties of human skin:

relation to age, sex and anatomical region, stratum corneum hydration and transepidermal water loss. *Br J Dermatol* 123:473-479.

Dagenais S, Caro J, Haldeman S. 2008. A systematic review of low back pain cost of illness studies in the United States and internationally. *Spine J* 8:8-20.

Davis BR, Bahniuk E, Young JK, Barnard CM, Mansour JM. 1989. Age-dependent changes in the shear wave propagation through human skin. *Exp Gerontol* 24:201-210.

Delalleau A, Josse G, Lagarde JM, Zahouani H, Bergheau JM. 2008. A nonlinear elastic behavior to identify the mechanical parameters of human skin in vivo. *Skin Res Technol* 14:152-164.

Deluzio KJ, Astephen JL. 2007. Biomechanical features of gait waveform data associated with knee osteoarthritis: an application of principal component analysis. *Gait Posture* 25:86-93.

Devereaux MW. 2004. Low back pain. *Eur J Radiol* 31:33-51.

Deyo RA. 1994. Magnetic resonance imaging of the lumbar spine. Terrific test or tar baby? *N Engl J Med* 331:115-116.

Deyo RA, Cherkin D, Conrad D, Volinn E. 1991. Cost, controversy, crisis: low back pain and the health of the public. *Annu Rev Public Health* 12:141-156.

Diridollou S, Black D, Lagarde JM, Gall Y, Berson M, Vabre V, Patat F, Vaillant L. 2000. Sex- and site-dependent variations in the thickness and mechanical properties of human skin in vivo. *International journal of cosmetic science* 22:421-435.

Duhamel A, Devos P, Bourriez J, Preda C, Defebvre L, Beuscart R. 2006. Functional Data Analysis for Gait Curves Study in Parkinson's Disease. *Stud Health Technol Inform* 124:469-574.

Ewins DJ, editor. 2000. *Modal testing*. Wiley. 562 p.

Farrar CR, Worden K. 2007. An introduction to structural health monitoring. *Philos Transact A Math Phys Eng Sci* 365:303-315.

Freund M, Sartor K. 2006. Degenerative spine disorders in the context of clinical findings. *Eur J Radiol* 58:15-26.

Fritz JM, Erhard RE, Hagen BF. 1998. Segmental instability of the lumbar spine. *Phys Ther* 78:889-896.

Fritz JM, Whitman JM, Childs JD. 2005. Lumbar spine segmental mobility assessment: an examination of validity for determining intervention strategies in patients with low back pain. *Arch Phys Med Rehabil* 86:1745-1752.

Fuller J, Liu L, Murphy M, Mann R. 1997. A comparison of lower-extremity skeletal kinematics measured using skin-mounted and pin-mounted markers.

Hum Mov Sci 16:219-242.

Garfin SR, Cohen MS, Massie JB, Abitbol JJ, Swenson MR, Myers RR, Rydevik BL. 1990. Nerve-roots of the cauda equina. The effect of hypotension and acute graded compression on function. *J Bone Joint Surg Am* 72:1185-1192.

Georgiou AP, Cunningham JL. 2001. Accurate diagnosis of hip prosthesis loosening using a vibrational technique. *Clin Biomech (Bristol)* 16:315-323.

Glauser R, Sennerby L, Meredith N, Rée A, Lundgren A, Gottlow J, Hämmerle CHF. 2004. Resonance frequency analysis of implants subjected to immediate or early functional occlusal loading. Successful vs. failing implants. *Clin Oral Implants Res* 15:428-434.

Gonnella C, Paris SV, Kutner M. 1982. Reliability in evaluating passive intervertebral motion. *Phys Ther* 62:436-444.

Grabias SL, Mankin HJ. 1979. Pain in the lower back. *Bull Rheum Dis* 30:1040-1045.

Greenleaf JF, Fatemi M, Insana M. 2003. Selected methods for imaging elastic properties of biological tissues. *Annu Rev Biomed Eng* 5:57-78.

Guo HR, Tanaka S, Halperin WE, Cameron LL. 1999. Back pain prevalence in US industry and estimates of lost workdays. *Am J Public Health* 89:1029-1035.

Heylen W, Lammens S. 1996. FRAC: A consistent Way of Comparing Frequency Response Functions. Proceedings of the International Conference on Identification in Engineering Systems, Innisbruck, Australia.

Hodges PW, Richardson CA. 1996. Inefficient muscular stabilization of the lumbar spine associated with low back pain. A motor control evaluation of transversus abdominis. Spine 21:2640-2650.

Hodges PW, Richardson CA. 1998. Delayed postural contraction of transversus abdominis in low back pain associated with movement of the lower limb. J Spinal Disord 11:46-56.

Hodges PW, Richardson CA. 1999. Altered trunk muscle recruitment in people with low back pain with upper limb movement at different speeds. Arch Phys Med Rehabil 80:1005-1012.

Holden JP, Orsini JA, Siegel KL, Kepple TM, Gerber LH, Stanhope SJ. 1997. Surface movement errors in shank kinematics and knee kinematics during gait. Gait and Posture 5:217-227.

Holzappel G. 2001. Biomechanics of Soft Tissue. In: Lemaître J, editor. Handbook of materials behavior models. Academic Press. p 1200.

Howe JF, Loeser JD, Calvin WH. 1977. Mechanosensitivity of dorsal root ganglia and chronically injured axons: a physiological basis for the radicular pain of nerve root compression. Pain 3:25-41.

Hu Y, Siu SHF, Mak JNF, Luk KDK. 2010. Lumbar muscle electromyographic dynamic topography during flexion-extension. *J Electromyogr Kinesiol* 20:246-255.

Huang HM, Pan LC, Lee SY, Chiu CL, Fan KH, Ho KN. 2000. Assessing the implant/bone interface by using natural frequency analysis. *Oral Surg Oral Med Oral Pathol Oral Radiol Endod* 90:285-291.

Jalovaara P, Niinimäki T, Vanharanta H. 1995. Pocket-size, portable surface EMG device in the differentiation of low back pain patients. *Eur Spine J* 4:210-212.

Jarvik JG, Deyo RA. 2002. Diagnostic evaluation of low back pain with emphasis on imaging. *Ann Intern Med* 137:586-597.

Jensen MC, Brant-Zawadzki MN, Obuchowski N, Modic MT, Malkasian D, Ross JS. 1994. Magnetic resonance imaging of the lumbar spine in people without back pain. *N Engl J Med* 331:69-73.

Jurist JM. 1970. In vivo determination of the elastic response of bone. I. Method of ulnar resonant frequency determination. *Phys Med Biol* 15:417-426.

Jurist JM. 1970. In vivo determination of the elastic response of bone. II. Ulnar resonant frequency in osteoporotic, diabetic and normal subjects. *Phys Med Biol* 15:427-434.

Kawchuk GN, Decker C, Dolan R, Carey J. 2009. Structural health monitoring to detect the presence, location and magnitude of structural damage in cadaveric porcine spines. *J Biomech* 42:109-115.

Kawchuk GN, Decker C, Dolan R, Fernando N, Carey J. 2008. The feasibility of vibration as a tool to assess spinal integrity. *J Biomech* 41:2319-2323.

Keller TS, Colloca CJ. 2007. Dynamic dorsoventral stiffness assessment of the ovine lumbar spine. *J Biomech* 40:191-197.

Kelsey JL, White AA. 1980. Epidemiology and impact of low-back pain. *Spine* 5:133-142.

Kendrick D, Fielding K, Bentley E, Kerslake R, Miller P, Pringle M. 2001. Radiography of the lumbar spine in primary care patients with low back pain: randomised controlled trial. *BMJ* 322:400-405.

Kernohan WG, Beverland DE, McCoy GF, Shaw SN, Wallace RG, McCullagh GC, Mollan RA. 1986. The diagnostic potential of vibration arthrography. *Clin Orthop Relat Res* :106-112.

Kerry S, Hilton S, Dundas D, Rink E, Oakeshott P. 2002. Radiography for low back pain: a randomised controlled trial and observational study in primary care. *Br J Gen Pract* 52:469-474.

Kirkaldy-Willis WH, Farfan HF. 1982. Instability of the lumbar spine. *Clin Orthop*

Relat Res :110-123.

Kitazaki S, Griffin MJ. 1995. A data correction method for surface measurement of vibration on the human body. *J Biomech* 28:885-890.

Kuo LC, Cooney WP, Oyama M, Kaufman KR, Su FC, An KN. 2003. Feasibility of using surface markers for assessing motion of the thumb trapeziometacarpal joint. *Clin Biomech (Bristol)* 18:558-563.

Lafortune MA, Cavanagh PR, Sommer HJ, Kalenak A. 1992. Three-dimensional kinematics of the human knee during walking. *J Biomech* 25:347-357.

Lafortune MA, Henning E, Valiant GA. 1995. Tibial shock measured with bone and skin mounted transducers. *J Biomech* 28:989-993.

Lateef H, Patel D. 2009. What is the role of imaging in acute low back pain? *Current reviews in musculoskeletal medicine* 2:69-73.

Latimer J, Lee M, Adams R, Moran CM. 1996. An investigation of the relationship between low back pain and lumbar posteroanterior stiffness. *Physiother Res Int* 19:587-591.

Latimer J, Lee M, Adams R, Moran CM. 1996. An investigation of the relationship between low back pain and lumbar posteroanterior stiffness. *J Manipulative Physiol Ther* 19:587-591.

Leknius C, Kenyon BJ. 2005. Stable accelerometer attachment to the skin surface. *J Prosthet Dent* 94:466-467.

Liszka-Hackzell JJ, Martin DP. 2004. An analysis of the relationship between activity and pain in chronic and acute low back pain. *Anesth Analg* 99:477-81, table of contents.

Lundy-Ekman L, editor. 2002. *Neuroscience: Fundamentals for Rehabilitation*. Philadelphia, PA: W.B. Saunders Company.

Magee DJ. 2008. *Orthopedic physical assessment*. W B Saunders Co. 1138 p.

Manek NJ, MacGregor AJ. 2005. Epidemiology of back disorders: prevalence, risk factors, and prognosis. *Curr Opin Rheumatol* 17:134-140.

McCoy GF, McCrea JD, Beverland DE, Kernohan WG, Mollan RA. 1987. Vibration arthrography as a diagnostic aid in diseases of the knee. A preliminary report. *J Bone Joint Surg Br* 69:288-293.

McGill S. 2002. *Low Back Disorders: Evidence Based Prevention and Rehabilitation*. Windsor, Ontario: Human Kinetics.

Meredith N, Alleyne D, Cawley P. 1996. Quantitative determination of the stability of the implant-tissue interface using resonance frequency analysis. *Clin Oral Implants Res* 7:261-267.

Montagna W, Yun JS. 1964. The Skin of the Domestic Pig. *J Invest Dermatol* 42:11-21.

Nachemson A. 1985. Lumbar spine instability. A critical update and symposium summary. *Spine* 10:290-291.

Nachemson A. 1989. Lumbar discography--where are we today? *Spine* 14:555-557.

Nachemson A, Vingard E. 2002. Assessment of Patients with Neck and Back Pain: A Best-Evidence Synthesis. In: Nachemson A, Jonsson E, editor. *Neck and Back Pain: The Scientific Evidence of Causes, Diagnosis, and Treatment*. Philadelphia, PA: Lippincott Williams & Wilkins. p 189-236.

Nester C, Jones RK, Liu A, Howard D, Lundberg A, Arndt A, Lundgren P, Stacoff A, Wolf P. 2007. Foot kinematics during walking measured using bone and surface mounted markers. *J Biomech* 40:3412-3423.

Ni Y, Zhou X, Ko J. 2006. Experimental investigation of seismic damage identification using PCA-compressed frequency response functions and neural networks. *Journal of Sound and Vibration* 290:242-263.

Niosi CA, Oxland TR. 2004. Degenerative mechanics of the lumbar spine. *Spine J* 4:202S-208S.

Norris CM. 1995. *Spinal Stabilisation 1. Active Lumbar Stabilisation - Concepts*.

Physiotherapy 81:61-63.

O'Sullivan P. 2005. Diagnosis and classification of chronic low back pain disorders: maladaptive movement and motor control impairments as underlying mechanism. *Man Ther* 10:242-255.

Oomens CW, van Campen DH, Grootenboer HJ. 1987. A mixture approach to the mechanics of skin. *J Biomech* 20:877-885.

2008. Compact Oxford English Dictionary. Oxford University Press. 1264 p.

Panjabi MM. 1992. The stabilizing system of the spine. Part I. Function, dysfunction, adaptation, and enhancement. *J Spinal Disord* 5:383-9; discussion 397.

Panjabi MM, Andersson GB, Jorneus L, Hult E, Mattsson L. 1986. In vivo measurements of spinal column vibrations. *J Bone Joint Surg Am* 68:695-702.

Panjabi MM. 2003. Clinical spinal instability and low back pain. *J Electromyogr Kinesiol* 13:371-379.

Papageorgiou AC, Croft PR, Ferry S, Jayson MI, Silman AJ. 1995. Estimating the prevalence of low back pain in the general population. Evidence from the South Manchester Back Pain Survey. *Spine* 20:1889-1894.

Parke WW. 1991. The significance of venous return impairment in ischemic

radiculopathy and myelopathy. *Orthop Clin North Am* 22:213-221.

Pereira JM, Mansour JM, Davis BR. 1990. Analysis of shear wave propagation in skin; application to an experimental procedure. *J Biomech* 23:745-751.

Porterfield JA, DeRosa C, editor. 1991. *Mechanical Low Back Pain*. USA: W.B. Saunders Company.

Potts RO, Buras EM, Chrisman DA. 1984. Changes with age in the moisture content of human skin. *J Invest Dermatol* 82:97-100.

Potts RO, Chrisman DA, Buras EM. 1983. The dynamic mechanical properties of human skin in vivo. *J Biomech* 16:365-372.

Qvistgaard E, Rasmussen J, Laetgaard J, Hecksher-Sørensen S, Bliddal H. 2007. Intra-observer and inter-observer agreement of the manual examination of the lumbar spine in chronic low-back pain. *Eur Spine J* 16:277-282.

Radebold A, Cholewicki J, Panjabi MM, Patel TC. 2000. Muscle response pattern to sudden trunk loading in healthy individuals and in patients with chronic low back pain. *Spine* 25:947-954.

Ramsay JO, Silverman BW, editor. 2005. *Functional data analysis*. Springer Us. 426 p.

Rao CR. 1964. *The Use and Interpretation of Principal Component Analysis in*

Applied Research. Sankhyā: The Indian Journal of Statistics 26:329-358.

Reid SM, Graham RB, Costigan PA. 2010. Differentiation of young and older adult stair climbing gait using principal component analysis. *Gait Posture* 31:197-203.

Riihimaki H. 1991. Low-back pain, its origin and risk indicators. *Eur J Radiol* 17:81-90.

Rosenstein AD, McCoy GF, Bulstrode CJ, McLardy-Smith PD, Cunningham JL, Turner-Smith AR. 1989. The differentiation of loose and secure femoral implants in total hip replacement using a vibrational technique: an anatomical and pilot clinical study. *Proc Inst Mech Eng [H]* 203:77-81.

Rubin C, Pope M, Fritton JC, Magnusson M, Hansson T, McLeod K. 2003. Transmissibility of 15-hertz to 35-hertz vibrations to the human hip and lumbar spine: determining the physiologic feasibility of delivering low-level anabolic mechanical stimuli to skeletal regions at greatest risk of fracture because of osteoporosis. *Spine* 28:2621-2627.

Rydevik B, Nordborg C. 1980. Changes in nerve function and nerve fibre structure induced by acute, graded compression. *J Neurol Neurosurg Psychiatry* 43:1070-1082.

Sanders R. 1973. Torsional elasticity of human skin in vivo. *Pflugers Arch* 342:255-260.

Schultz SE, Kopec JA. 2003. Impact of chronic conditions. *Health Rep* 14:41-53.

Sherriff SB, Barber DC, Martin TR, Lakeman JM. 1982. Use of principal component factor analysis in the detection of carotid artery disease from Doppler ultrasound. *Med Biol Eng Comput* 20:351-356.

Shrimpton P, Hillier M, Lewis M, Dunn M. 2005. Doses from Computed Tomography (CT) Examinations in the UK - 2003 Review. National Radiological Protection Board

Shrout PE, Fleiss JL. 1979. Intraclass correlations: uses in assessing rater reliability. *Psychol Bull* 86:420-428.

Siddall PJ, Cousins MJ. 1997. Spinal pain mechanisms. *Spine* 22:98-104.

Stewart WF, Ricci JA, Chee E, Morganstein D, Lipton R. 2003. Lost productive time and cost due to common pain conditions in the US workforce. *JAMA* 290:2443-2454.

Stritch G. 1902. The tuning fork as an aid in diagnosis. *The Lancet* 160:1353-1354.

Takalo-Kippola H, Lappalainen P, Yrjiima M, Vanhciranta H. 1995. A Novel Vibrator for the Diagnosis of Spinal Intradiscal Pain. *IEEE-EMBC and CMBEC*,

Taylor WR, Ehrig RM, Duda GN, Schell H, Seebeck P, Heller MO. 2005. On the influence of soft tissue coverage in the determination of bone kinematics using

skin markers. *J Orthop Res* 23:726-734.

Tong H, Carson J, Haig A, Quint D, Phalke V, Yamakawa K, Miner J. 2006. Magnetic resonance imaging of the lumbar spine in asymptomatic older adults. *J Neuroimaging* 19:67-72.

Trendafilova I, Cartmell M, Ostachowicz W. 2008. Vibration-based damage detection in an aircraft wing scaled model using principal component analysis and pattern recognition. *Journal of Sound and Vibration* 313:560-566.

Ungar E, Dietrich C. 1966. High-frequency vibration isolation. *Journal of Sound and Vibration* 4:224-241.

Vlaanderen E, Conza NE, Snijders CJ, Bouakaz A, De Jong N. 2005. Low back pain, the stiffness of the sacroiliac joint: a new method using ultrasound. *Ultrasound Med Biol* 31:39-44.

Von Korff M, Saunders K. 1996. The course of back pain in primary care. *Spine* 21:2833-7; discussion 2838.

Walker BF. 2000. The prevalence of low back pain: a systematic review of the literature from 1966 to 1998. *J Spinal Disord* 13:205-217.

Walker BF, Muller R, Grant WD. 2004. Low back pain in Australian adults. health provider utilization and care seeking. *J Manipulative Physiol Ther* 27:327-335.

- Watanabe R, Parke WW. 1986. Vascular and neural pathology of lumbosacral spinal stenosis. *J Neurosurg* 64:64-70.
- Weir JP. 2005. Quantifying test-retest reliability using the intraclass correlation coefficient and the SEM. *J Strength Cond Res* 19:231-240.
- Wing PC. 2001. Rheumatology: 13. Minimizing disability in patients with low-back pain. *CMAJ* 164:1459-1468.
- Wu JZ, Dong RG, Smutz WP, Schopper AW. 2003. Nonlinear and viscoelastic characteristics of skin under compression: experiment and analysis. *Biomed Mater Eng* 13:373-385.
- Yrjämä M, Tervonen O, Kurunlahti M, Vanharanta H. 1997. Bony vibration stimulation test combined with magnetic resonance imaging. Can discography be replaced? *Spine* 22:808-813.
- Yrjämä M, Vanharanta H. 1994. Bony vibration stimulation: a new, non-invasive method for examining intradiscal pain. *Eur Spine J* 3:233-235.
- Zang C, Friswell MI, Imregun M. 2007. Structural Health Monitoring and Damage Assessment Using Frequency Response Correlation Criteria. *Journal of Engineering Mechanics* 133:981-993.
- Zang C, Friswell MI, and Imregun M. 2003. Structural health monitoring and damage assessment using measured FRFs from multiple sensors. I: The indicator

of correlation criteria.”. 245:131-139.

Zang C, Friswell MI, and Imregun M. 2003. Structural health monitoring and damage assessment using measured FRFs from multiple sensors. II: Decision making with RBF networks. 245:141-148.

Zennaro D, Laubli T, Wellig P, Krebs D, Schnoz M, Klipstein A, Krueger H. 2002. A method to test reliability and accuracy of the decomposition of multi-channel long-term intramuscular EMG signal recordings. *International Journal of Industrial Ergonomics* 30:211-224.

Zhang X, Kinnick RR, Pittelkow MR, Greenleaf JF. 2008. Skin viscoelasticity with surface wave method. *Proceedings - IEEE Ultrasonics Symposium* 2008:651-653.

Zimmermann M. 2001. Pathobiology of neuropathic pain. *Eur J Pharmacol* 429:23-37.

van Dieën JH, Cholewicki J, Radebold A. 2003. Trunk muscle recruitment patterns in patients with low back pain enhance the stability of the lumbar spine. *Spine* 28:834-841.

van Trijffel E, Anderegg Q, Bossuyt PMM, Lucas C. 2005. Inter-examiner reliability of passive assessment of intervertebral motion in the cervical and lumbar spine: a systematic review. *Man Ther* 10:256-269.

Chapter 3: Protocol 1 – Determining Skin Effects Using Invasive and Non-Invasive Contact Tips

3.1 Overview

This chapter covers protocols performed in pig cadavers using both an invasive and non-invasive contact tip for vibration input to the spine. Previously, a fully invasive technique was developed that could determine the location and magnitude of simulated injuries to a cadaveric pig spine. The goal of the present investigation was to determine the role of the skin and soft tissues in adapting the previously developed technique to a non-invasive format.

3.2 Introduction

The need for a new, non-invasive diagnostic technique to assess spinal function was discussed in-depth in the literature review (Chapter 2). To attain this goal, the Spinal Function Lab at the University of Alberta has begun to adapt the technique of structural damage detection (SDD) for use in detecting dysfunction of the low back [Kawchuk et al. 2008;Kawchuk et al. 2009]. It was shown in these studies that an invasive technique that applied vibration directly to the vertebrae, while also measuring the spinal vibration response through bone-mounted accelerometers, could detect the location and magnitude of mechanically imposed damage to the spine.

The technique is now being adapted for non-invasive use in this thesis. While there have been many attempts to use vibration as a diagnostic tool in other areas of the body such as testing long bones stiffness characteristics [Jurist 1970;Steele et al. 1988], dental implant stability [Meredith et al. 1996;Glauser et al. 2004], and hip implant stability [Rosenstein et al. 1989;Georgiou and Cunningham 2001], few have attempted full scale diagnostics in the spine. Yrjama et al. used vibration as a stimulus to invoke intradiscal pain in the back to locate the source of pain [Yrjämä and Vanharanta 1994;Yrjämä et al. 1997]. This testing provided only a binary response as to whether pain was invoked at a site, and did not provide further information concerning the dysfunction of the spine. Keller and Colloca used vibration as a tool to successfully analyze the stiffness of the spine at low frequencies [Keller and Colloca 2007]. This testing did not provide any further information as to the potential location of the dysfunction, or the specific structure/tissue which may be implicated in the increased stiffness. Therefore, while appearing promising, the use of vibration as a fully non-invasive diagnostic technique remains undeveloped.

It is thought that vibration may be inputted to the spine via a non-invasive contact tip to elicit a vibration response, which may then be measured using skin-mounted accelerometers. Skin-mounted sensors have been used by biomechanists for many years in attempts to measure human skeletal motion. However, most have found that discrepancies do exist between measurements taken from skin-mounted sensors and bone-mounted sensors [Holden et al. 1997]. Typically in SDD testing, accelerometers and vibration input mechanisms such as electrodynamic shakers are affixed rigidly and directly to the test object [Ewins 2000]. While the spine is comprised partly of quasi-rigid vertebrae, it is linked by non-rigid soft tissues such as intervertebral discs, cartilage, ligaments and tendons, and is protected by the soft tissues such as skin, muscles, and

fascia. The effect of these soft tissues on the ability to both input and measure vibration in the spine is unknown.

The behaviour of soft tissue in response to a random burst vibration used in these experiments is also unknown. Holzapfel describes the soft tissues of the body as exhibiting a non-linear elastic behavior in response to loading [Holzapfel 2001], while Wu et al. have described the skin as having a non-linear response and varied Poisson's ratio in response to loading rates [Wu et al. 2003]. The loading rate on the skin caused by a random burst of vibration could cause significant variations in the measurement of the underlying bone vibration response. The effect of these soft tissues on the non-invasive techniques used to create and detect the spinal vibration response has not been fully determined.

3.2.1 Protocol Goals and Hypotheses

There were multiple goals to be achieved in performing this protocol:

1. Determine the repeatability of measurements of the spinal vibration response, obtained with non-invasive equipment.
2. Vary the position of a skin-mounted accelerometer placed posterior to a vertebra of interest, and determine the effects of these position changes on the measured vibration response of the vertebra.
3. Compare the vibration response signal measured from a skin-mounted accelerometer to the signal measured from the same position after removing and replacing the original accelerometer.
4. Determine the viability of using an accelerometer attached atop a hypodermic needle, implanted dorsally through the skin into the

spinous process of a vertebra, as a method of measuring the vibration response of the vertebra.

5. For each of these goals, determine the effect of a non-invasive or invasive contact tip on the results.

For each of these goals, a hypothesis was formulated.

1. Measurements of the spinal vibration response will be repeatable and yield good correlation values between repeats.
2. Variations in placement of the skin mounted accelerometer over the vertebral body cause large changes the measured FRF.
3. The vibration response measured from an initial accelerometer position will have a good degree of correlation to that of the signal measured by the accelerometer upon replacing it to the initial position.
4. The vibration response measured from an accelerometer affixed directly to the vertebral bone will have good correlation with that of an accelerometer mounted to a hypodermic needle that is implanted directly into the spinous process of the same vertebra.
5. A non-invasive contact tip will affect the measured vibration response of a vertebra by transmitting inputted vibrations through the soft tissues it contacts.

3.3 Methods

3.3.1 Animal Preparation

Five cadaveric pigs of crossbreed Large White x Landrace or Duroc x (Large White x Landrace), each of 50-60 kg, were used. Permission to use cadaveric porcine tissues was obtained from the Animal Policy and Welfare Committee of the Faculty of Agriculture, Forestry, and Home Economics at the University of Alberta (Appendix E). Each pig was euthanized and eviscerated following protocols approved by the University of Alberta Swine Research and Technology Centre. Evisceration was performed for the purpose of accessing the ventral side of the spine. Protocols were performed at approximately room temperature immediately after euthanization of each animal, lasting approximately 6 hours each. Rigor mortis in adult pigs begins at approximately 12-24 hours after death [Ranken et al. 1997]. While the extent of the rigor in each animal was unknown, it is unlikely that it was present during testing.

In each animal, excess skin tissue was removed from the lateral and ventral sides of the abdominal cavity to allow for access to the ventral spine during each experiment. In addition, the psoas major and minor muscles were removed to allow further access to the intervertebral discs. Finally, the ventral 3-4 inches of each rib of the T9-T14 was removed to increase the amount of independent motion available to the thoracic vertebrae.

The cadaver was then placed in a restraint and support system to maintain its position and orientation, shown in Figure 3.1.

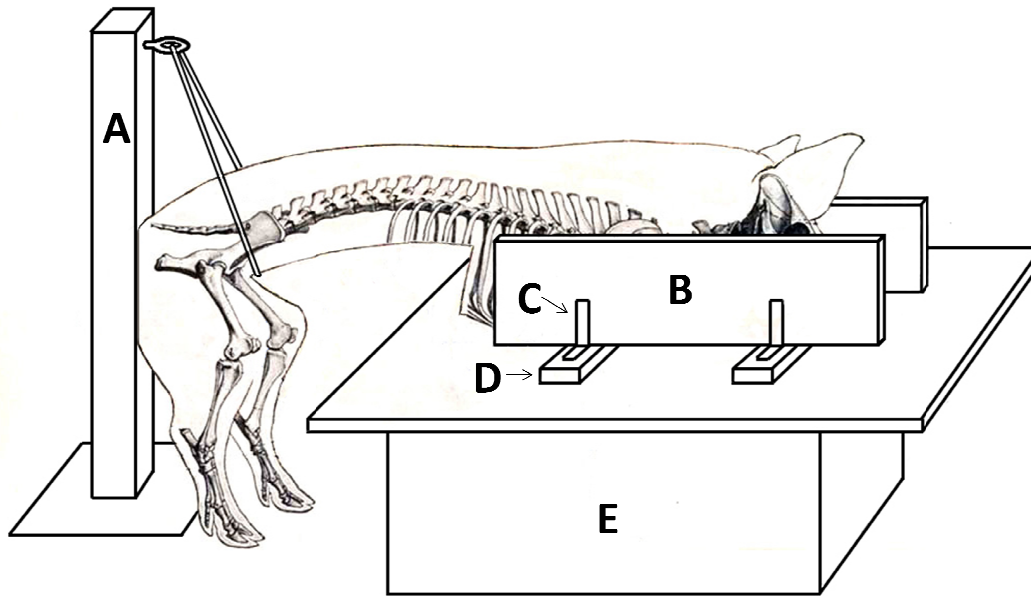


Figure 3.1: Cadaver positioning setup. A) Rope-hoist system; B) Lateral clamping wood; C) Hinged locking bracket; D) Cross-brace plank; E) Adjustable lift table

Specifically, the thoracic and cranial section of the cadaver was placed on an adjustable lift table, with the rear legs overhanging the end of the table. To secure the cadaver in place, a clamping restraint system was devised that consisted of two lateral planks. The clamp was applied to the thoracic section of the cadaver, leaving the thoracic spine unrestrained from T7 inferiorly. A rope-hoist system was used to lift and support the cadaver's pelvis, at the crease of the hip.

The skin overlaying the T8-T10 vertebrae was shaved and cleaned using rubbing alcohol pads. The investigator palpated the spine to locate the spinous processes of the T8-T10 vertebrae, and the locations were marked on the skin using a permanent marker. The locations were visually confirmed by mobilizing the vertebrae in a dorso-ventral manner, while the resulting motion was viewed

from the ventral side where the vertebrae could be accurately viewed and identified.

3.3.2 Application of Equipment

Figure 3.2 shows the experimental setup described in this section. Uniaxial accelerometers (Model 352A24, PCB Piezotronics, Depew, NY) were used to measure the vertebral response to vibration. The sensors were glued to the skin over the centre of each of the previously marked T9 and T10 spinous processes using cyanoacrylate. A breakout box was used to relay the individual accelerometer signals to the computer.

Additional accelerometers were next affixed directly to the vertebral bodies ventrally. This process involved several steps. First, to ensure the bone-mounted accelerometers were angularly aligned with the skin-mounted accelerometers, a protractor with a built in level was used to measure the angle of the skin-mounted accelerometer from the horizontal in the rostral-caudal direction of the cadaver. A Dremel tool (400 Series XPR, bit #932, Robert Bosch Tool Corporation, Mt. Prospect, IL, USA) was attached to an incline plane that had been adjusted to the measured horizontal angle. The tool was used to shave the ventral side of each vertebra to create a flat surface to which the bone-mounted accelerometer was affixed. The lateral angle of the accelerometers was not matched as their central positioning over the spine axis did not produce large angles ($<1^{\circ}$) in this direction.

Control of the vibration input was executed by PUMA Vibration Control and Analysis Software (Spectral Dynamics, San Jose, CA, USA). The vibration input signals were sent from the computer to a linear power amplifier (PA-138,

Labworks, Costa Mesa, CA, USA), which relayed the signals to an electrodynamic shaker (LW- 126-13, Labworks, Costa Mesa, CA, USA). The shaker was mounted to the crossbar of a large, heavy frame, centered over top of the spine. A stainless steel stinger approximately 30 cm in length was screwed into the shaker. The following components were attached in series with the stinger: an impedance head to measure the dynamic input force and acceleration (Model 288D01, PCB Piezotronics, Depew, NY, USA), a static load cell to measure the static preload of the system on the spine (Model ELFS-T3, Entran Sensors & Electronics, Fairfield, NJ, USA), and a Lexan contact tip. The tip was used to interface the system with the spine. The static load cell was connected to an oscilloscope (Model TDS 3014B, Tektronix, Inc., Beaverton, OR, USA) to measure the static preload. The impedance head transmitted the measured dynamic load signals to the computer.

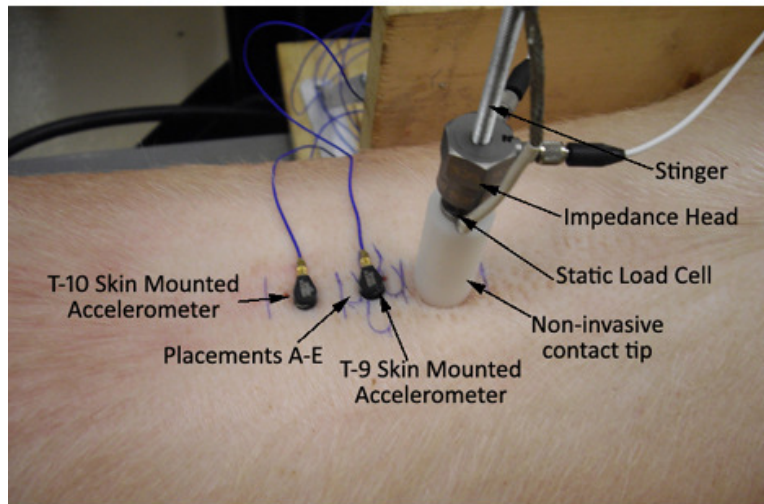
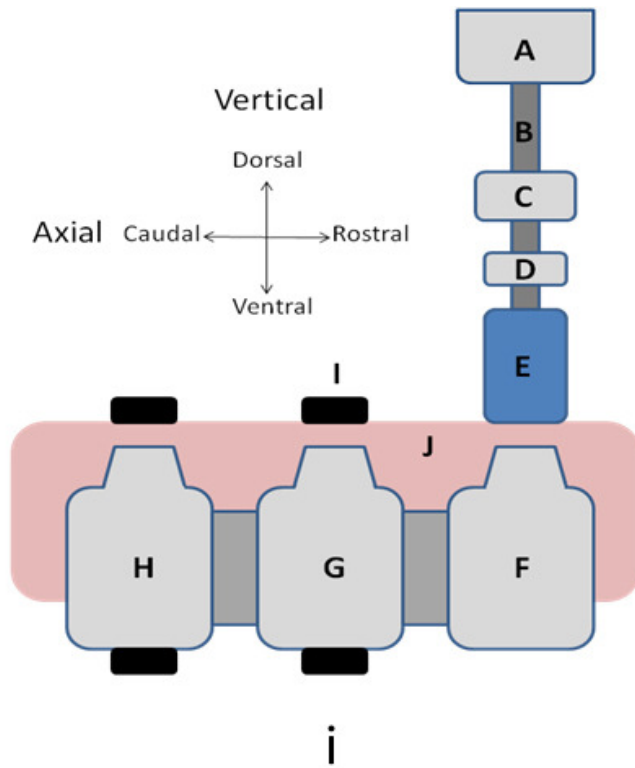


Figure 3.2: i) Schematic of non-invasive contact tip with skin-mounted accelerometers only. A: Shaker B: Stinger rod. C: Impedance head. D: Static load cell. E: Non-invasive contact tip. F: T8 Vertebra. G: T9 vertebra. H: T10 vertebra. I: Accelerometer. J: skin and soft tissue

ii) Photo of in-situ setup

3.3.3 Vibration Input

The non-invasive contact tip contacted the T8 spinous process with a preload of 30 N. A preload of 30 N was chosen to compress the underlying soft tissues and ensure constant contact with the underlying vertebrae during the vibration input. Keller and Colloca used a preload of 13 N and peak load of 48 N in an ovine model in a non-invasive vibration testing setup [Keller and Colloca 2007]. However, 30 N was used in this protocol for the reasons previously listed. Preload was calculated by measuring the voltage output from the static load cell through the oscilloscope, and multiplying by the load cell's previously calculated linear calibration constant of 7.35 N/V.

To obtain the vibration response of the spine, 10 shaker excitation bursts of random frequencies from 0-2000 Hz were applied to the spine via the contact tip. A resolution of 800 frames was used, meaning measurements of frequencies were taken every 2.5 Hz. Due to the burst nature of the vibration input, windowing of the signal was not required. Each accelerometer measured the vibration at its location, with the information recorded by the computer. This measured response of the spine to the burst of input frequencies was recorded and averaged over the 10 bursts using a PUMA built-in exponential averaging algorithm. The average signal from these 10 bursts is herein referred to as one 'test'.

Additional information pertaining to technical details of vibration testing can be found in Appendix C.

3.3.4 Repeatability of Tests

In the following sections, descriptions of the accelerometer placements tests are described. In each of these accelerometer placements, the repeatability of a measured test signal was determined. This was done by performing 5 tests at each placement to gather signal repeatability data.

3.3.5 Accelerometer Position Tests (Non-invasive Contact Tip)

To test the effect of varying the position of the skin mounted accelerometer (over top of the spinous process) on the measured vibration response, the T9 skin-mounted accelerometer was placed in 5 different positions in relation to the centre of the T9 spinous process: A) Centralized axially and laterally, B) Axially caudal and laterally central, C) Laterally left and axially central, D) Axially rostral and laterally central, E) Laterally right and axially central. After vibration testing was completed at each of the mentioned positions, the accelerometer was placed back to the original A position, denoted herein by A' and again 5 repeated measures were taken. During these tests, the accelerometers mounted to the bone at T-9 and T-10, as well as the skin at T-10 remained affixed in their original positions. These positions are shown in Figure 3.3.

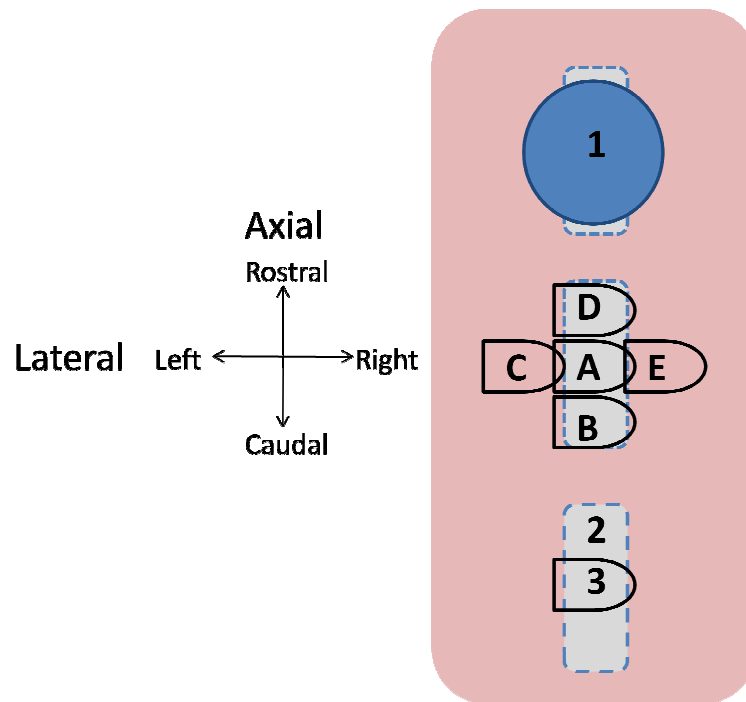


Figure 3.3: Aerial view of experimental setup with accelerometer placements (A-E). 1: Shaker and in-line vibration input components. 2: T10 spinous process (under skin/soft tissue). 3: Placement of T10 accelerometer. Placement A' is the same as placement A.

3.3.6 Needle-mounted Accelerometer Technique Validation

The accelerometers mounted ventrally to the vertebral bodies were presumed to be attached rigidly to the bone, and therefore measured the response of the bone to the vibration input directly. While this preparation can be considered to be a reference standard for comparison with skin-based vibration signals, it is a highly invasive preparation that would be difficult or impossible to implement in cadaveric or live human subjects. Therefore, an alternative, minimally invasive technique was investigated for use in future experiments. Specifically, the skin mounted accelerometer over the T-10 vertebra was first removed, and the skin cleaned before a hypodermic needle (21 gauge, 1.5 in, BD, Franklin Lakes, NJ,

USA) was inserted dorsally into the spinous process of the T-10 vertebra, directly centered over the position of the previously removed skin-mounted accelerometer. To ensure the secure implantation of the needle in the spinous process, the hub of the needle was tapped with a hammer to drive the needle into the bone. The previously removed T-10 skin-mounted accelerometer was then glued to the hub of the needle using cyanoacrylate. The setup is shown below in Figure 3.4.

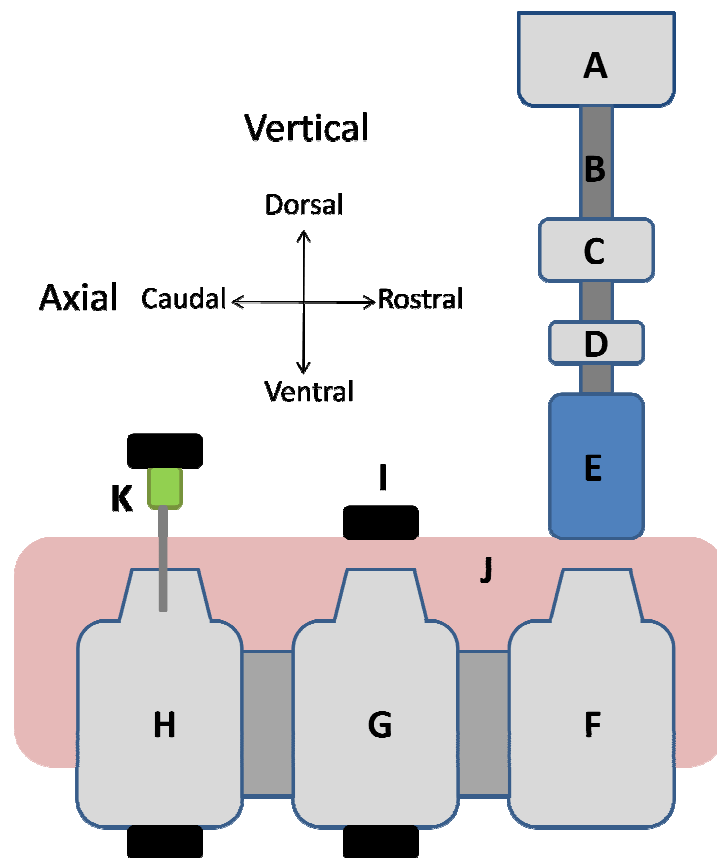


Figure 3.4: Setup of non-invasive contact tip with skin-mounted accelerometers and needle mounted accelerometer. A: Shaker B: Stinger rod. C: Impedance head. D: Static load cell. E: Non-invasive contact tip. F: T8 Vertebra. G: T9 vertebra. H: T10 vertebra. I: Accelerometer. J: Skin and soft tissue. K: Hypodermic needle inserted into T10 vertebra with affixed accelerometer

3.3.7 Invasive and Non-Invasive Contact Tip Comparison

Next, to determine the ability of the non-invasive contact tip to input vibration to the spine during the positioning part of the protocol, the non-invasive contact tip was removed, and was replaced with the original invasive contact tip used in previous experiments performed at the Spinal Function Lab at the University of Alberta [Kawchuk et al. 2008;Kawchuk et al. 2009]. When employed, this tip makes direct contact with the spinous process by clamping onto its lateral surfaces. To install this invasive tip, a small 0.75 inch x 0.75 inch (approximate surface dimension) section of skin, muscle, and soft tissue was removed dorsally from the T-8 spinous process. The tip's pincer clamp was then applied to the spinous process and tightened maximally by hand. Figure 3.5 shows this setup.

The needle-mounted accelerometer assembly remained installed in the bone to obtain measurements using the invasive contact tip.

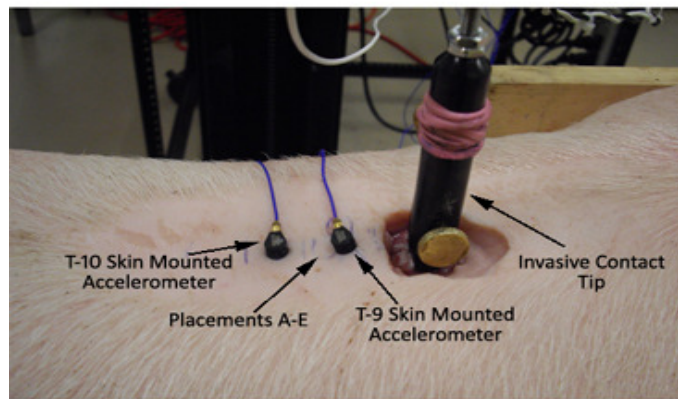
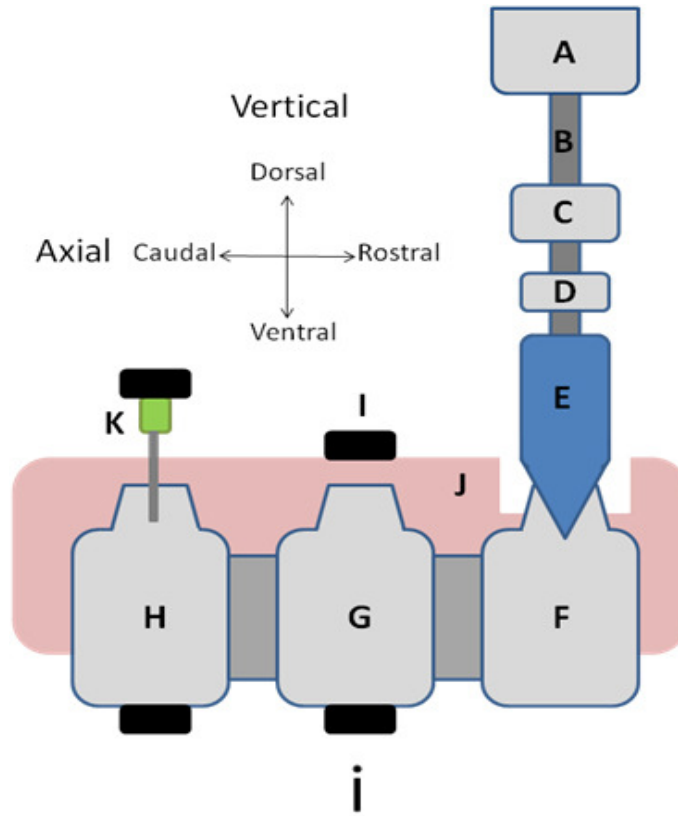


Figure 3.5: i) Setup of invasive contact tip with skin-mounted accelerometers and needle mounted accelerometer. A: Shaker B: Stinger rod. C: Impedance head. D: Static load cell. E: Invasive contact tip. F: T8 Vertebra. G: T9 vertebra. H: T10 vertebra. I: Skin-mounted accelerometer. J: Skin and soft tissue. K: Hypodermic needle inserted into T10 vertebra with affixed accelerometer

ii) Photo of in-situ setup

3.3.8 Accelerometer Position Tests (Invasive Contact Tip)

The previously described position testing was repeated using the invasive contact tip.

As a final measurement, the previously inserted needle-mounted accelerometer assembly was removed from the T10 spinous, and the accelerometer was re-glued to the skin in its original position. This was performed to obtain a vibration response measurement at the T10 vertebra from a skin-mounted accelerometer using the invasive tip.

3.3.9 Data Analysis Techniques

A number of objectives were incorporated into this protocol, necessitating a variety of data analysis techniques to be used to draw conclusions.

To analyze the data, the FRFs were first smoothed using a Savitzky-Golay filter of polynomial 3, with a span of 27.

3.3.9.1 Determining Repeatability of Tests

To determine the correlation of repeated tests, the Window-Averaged Global Shape Criteria (GSC) and Window-Averaged Global Amplitude Criteria (GAC)

were used. The GSC and GAC, previously described in Section 2.8.2 of the literature review, were calculated for each set of 5 repeated tests.

3.3.9.2 Determining Correlation of Two Signals

The calculation of the correlation between any two signals was performed using the D-statistic, previously described in Section 2.8.3 of the literature review (Chapter 2). The calculations were performed on the 5 repeated tests, for the particular situation of interest.

3.3.9.3 Determining Qualitative Differences between Signal Positions

To determine the effect of the changing accelerometer position on the acquired vibration response signal, a principal components analysis (PCA) was performed. The technique of PCA was previously described in Section 2.8.2 of the literature review. To perform the PCA on changing accelerometer positions, all 30 FRFs from each of the accelerometer positions (5 FRFs x 5 positions, plus 5 from the repeated replacement back to position A) were performed. The principal components of the variation between the signals were calculated, and were also analyzed qualitatively using the graphical technique described in Section 2.8.2.

3.3.9.4 Statistical Analysis

All statistical analyses in this protocol were performed using PASW Statistics 17 (SPSS Inc, Chicago, Illinois, USA).

3.4 Results

3.4.1 Repeatability of Tests - Single Transducer Results

For each position test and for each contact tip type, five repeated tests were performed. The repeated measures from each sensor, for both types of contact tip, were individually graphed, and graphed as a mean with standard deviation. Representative results are shown below in Figures 3.6-3.9.

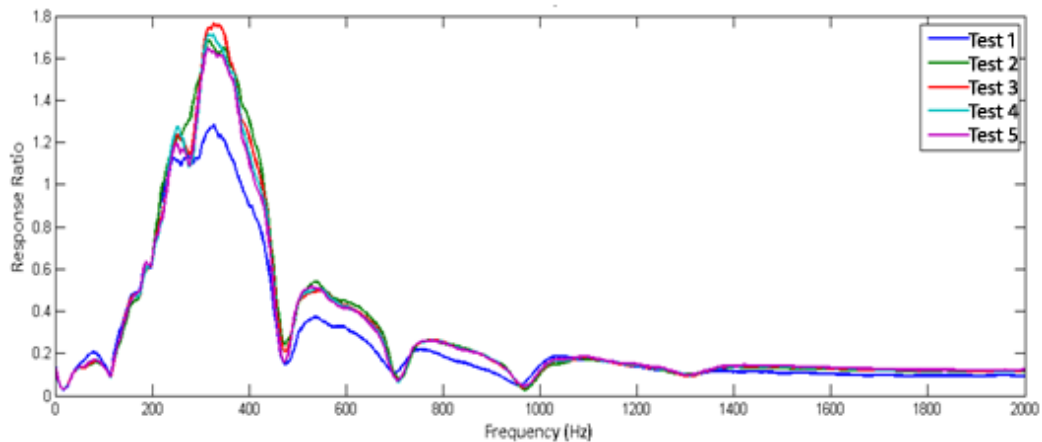


Figure 3.6: Repeated FRFs obtained from Subject 1, T9 Position A, using the non-invasive contact tip

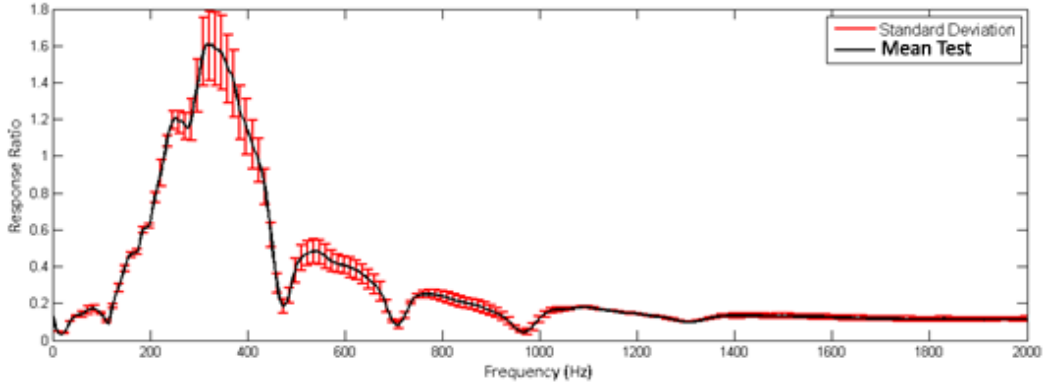


Figure 3.7 : Mean repeated test (FRF) with standard deviation on the 5 repeated measures for subject 1, T9 Position A, using the non-invasive contact tip.

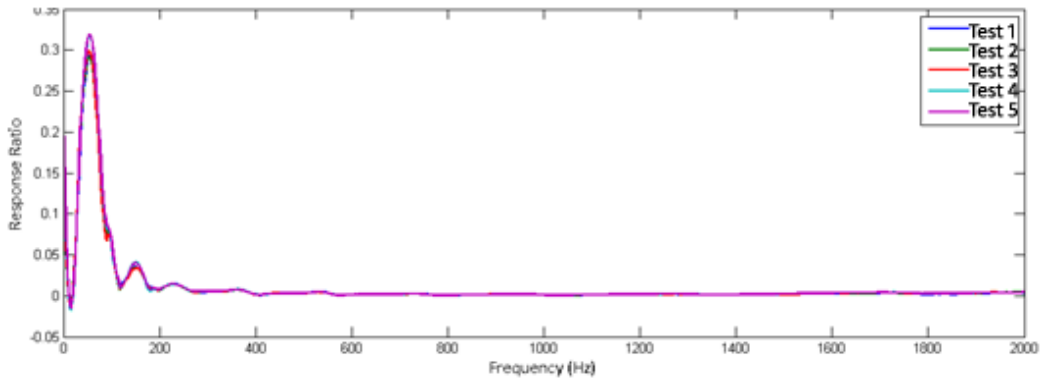


Figure 3.8: Repeated tests obtained from subject 1, T9 Position A, using the invasive contact tip.

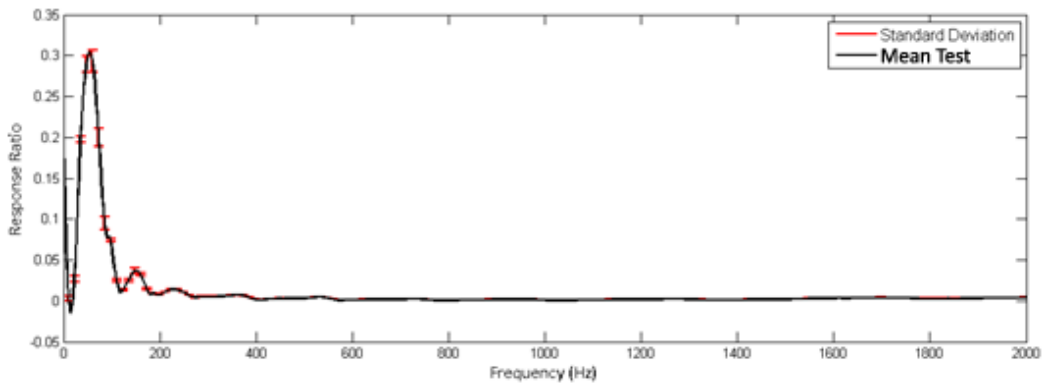


Figure 3.9: Mean repeated test (FRF) with standard deviation on the 5 repeated measures for subject 1, T9 Position A, using the non-invasive contact tip.

Uncharacteristically low repeatability existed only in one subject, with one FRF at position C, using the non-invasive contact tip. Figure 3.10 below shows this deviation. The cause of the deviation is unknown.

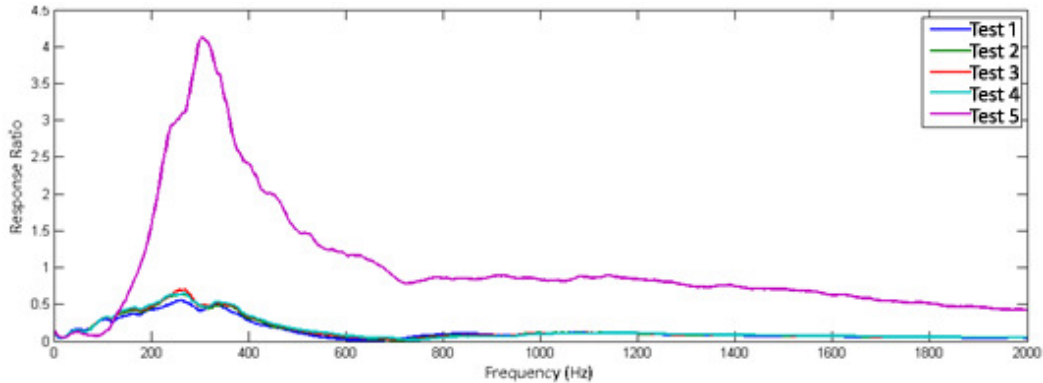


Figure 3.10: Repeated tests obtained from subject 1, T9 Position C, using the non-invasive contact tip

3.4.2 Repeatability of Tests - Multiple Transducer Results

Repeatability was also measured for the global system of transducers used in this protocol (T-9 Skin, T-9 Bone, T-10 Skin, T-10 Bone) , using the GSC and GAC. The GSC or GAC was calculated at each frequency for the five repeated measures, for each subject, each time the T-9 accelerometer was moved to a new placement. The results are summarized in Table 3.1 below for the non-invasive contact tip and Table 3.2 for the invasive contact tip.

Table 3.1: Mean GSC and GAC on global sensor system using the non-invasive contact tip, averaged over position tests.

Position		NI Tip GSC	Upper 95% CI	Lower 95% CI	NI Tip GAC	Upper 95% CI	Lower 95% CI
Pos. A	Subj. 1	0.999	1.000	0.994	0.997	1.000	0.988
	Subj. 2	1.000	1.000	0.999	0.999	1.000	0.994
	Subj. 3	1.000	1.000	0.998	1.000	1.000	0.997
	Subj. 4	0.999	1.000	0.976	0.998	1.000	0.981
	Subj. 5	0.999	1.000	0.994	0.997	1.000	0.988
Pos. A'	Subj. 1	1.000	1.000	0.999	1.000	1.000	0.997
	Subj. 2	1.000	1.000	0.995	0.999	1.000	0.995
	Subj. 3	1.000	1.000	0.996	0.999	1.000	0.994
	Subj. 4	1.000	1.000	0.991	0.999	1.000	0.990
	Subj. 5	1.000	1.000	0.999	1.000	1.000	0.997
Pos. B	Subj. 1	1.000	1.000	0.997	1.000	1.000	0.996
	Subj. 2	1.000	1.000	0.998	1.000	1.000	0.997
	Subj. 3	1.000	1.000	0.996	1.000	1.000	0.997
	Subj. 4	0.999	1.000	0.986	0.999	1.000	0.988
	Subj. 5	1.000	1.000	0.997	1.000	1.000	0.996
Pos. C	Subj. 1	0.977	1.000	0.880	0.987	1.000	0.930
	Subj. 2	1.000	1.000	0.997	1.000	1.000	0.998
	Subj. 3	1.000	1.000	0.994	1.000	1.000	0.996
	Subj. 4	0.999	1.000	0.984	0.999	1.000	0.985
	Subj. 5	0.977	1.000	0.880	0.987	1.000	0.930
Pos. D	Subj. 1	1.000	1.000	0.999	1.000	1.000	0.998
	Subj. 2	1.000	1.000	0.999	1.000	1.000	0.997
	Subj. 3	0.999	1.000	0.996	0.999	1.000	0.997
	Subj. 4	1.000	1.000	0.994	0.999	1.000	0.995
	Subj. 5	1.000	1.000	0.999	1.000	1.000	0.998
Pos. E	Subj. 1	1.000	1.000	0.999	1.000	1.000	0.999
	Subj. 2	1.000	1.000	0.999	1.000	1.000	0.998
	Subj. 3	1.000	1.000	0.996	1.000	1.000	0.996
	Subj. 4	1.000	1.000	0.993	0.999	1.000	0.994
	Subj. 5	1.000	1.000	0.999	1.000	1.000	0.999

Table 3.2: Mean GSC and GAC on global sensor system using the invasive contact tip, averaged over position tests.

Position		Inv. Tip GSC	Upper 95% CI	Lower 95% CI	Inv. Tip GAC	Upper 95% CI	Lower 95% CI
Pos. A	Subj. 1	0.999	1.000	0.985	0.999	1.000	0.990
	Subj. 2	0.999	1.000	0.99	0.999	1.000	0.984
	Subj. 3	1.000	1.000	0.996	0.999	1.000	0.995
	Subj. 4	1.000	1.000	0.993	1.000	1.000	0.995
	Subj. 5	0.999	1.000	0.985	0.999	1.000	0.990
Pos. A'	Subj. 1	1.000	1.000	0.990	0.999	1.000	0.991
	Subj. 2	1.000	1.000	0.994	0.999	1.000	0.986
	Subj. 3	1.000	1.000	0.994	1.000	1.000	0.996
	Subj. 4	1.000	1.000	0.998	1.000	1.000	0.998
	Subj. 5	1.000	1.000	0.990	0.999	1.000	0.991
Pos. B	Subj. 1	1.000	1.000	0.994	0.999	1.000	0.994
	Subj. 2	1.000	1.000	0.997	0.999	1.000	0.995
	Subj. 3	1.000	1.000	0.999	1.000	1.000	0.999
	Subj. 4	1.000	1.000	0.995	1.000	1.000	0.997
	Subj. 5	1.000	1.000	0.994	0.999	1.000	0.994
Pos. C	Subj. 1	0.998	1.000	0.903	0.997	1.000	0.951
	Subj. 2	1.000	1.000	0.997	0.999	1.000	0.996
	Subj. 3	1.000	1.000	0.998	1.000	1.000	0.999
	Subj. 4	1.000	1.000	0.995	1.000	1.000	0.997
	Subj. 5	0.998	1.000	0.930	0.997	1.000	0.951
Pos. D	Subj. 1	0.999	1.000	0.959	0.999	1.000	0.971
	Subj. 2	0.999	1.000	0.988	0.999	1.000	0.985
	Subj. 3	1.000	1.000	0.995	1.000	1.000	0.996
	Subj. 4	1.000	1.000	0.998	1.000	1.000	0.999
	Subj. 5	0.999	1.000	0.959	0.999	1.000	0.971
Pos. E	Subj. 1	1.000	1.000	0.988	0.999	1.000	0.992
	Subj. 2	1.000	1.000	0.992	0.999	1.000	0.985
	Subj. 3	0.999	1.000	0.99	0.997	1.000	0.987
	Subj. 4	1.000	1.000	0.999	1.000	1.000	0.998
	Subj. 5	1.000	1.000	0.988	0.999	1.000	0.992

The Upper CI is truncated at 1.000, as this represents perfect criteria matching. The range of GSC and GAC for the non-invasive tip was 0.977-1.000 and 0.987-1.000 respectively, and was 0.998-1.000 and 0.999-1.000 for the invasive tip.

3.4.3 T-9 Accelerometer Placement Results

3.4.3.1 T-9 Placement Results Skin signal placement comparisons

The T-9 vibration response was measured by a skin mounted accelerometer at 5 different positions over top of the spinous process, and again at position A upon replacing the accelerometer (denoted herein as A'). Typical position comparison examples, taken from subject 2, are shown below in Figures 3.11-3.14.

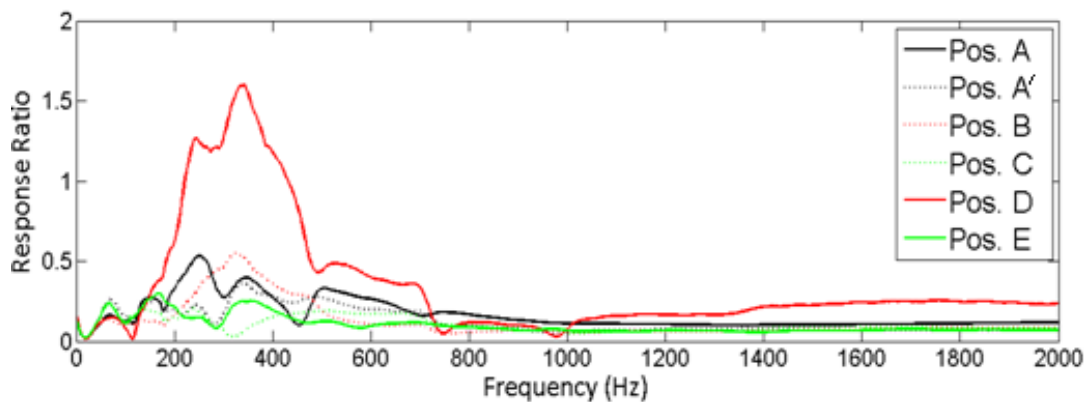


Figure 3.11: Mean position tests (FRFs) at T-9 vertebra taken using the non-invasive contact tip. Black signals indicate the accelerometer in position A, green indicates positions lateral to position A, and red indicates positions rostro-caudally located to position A.

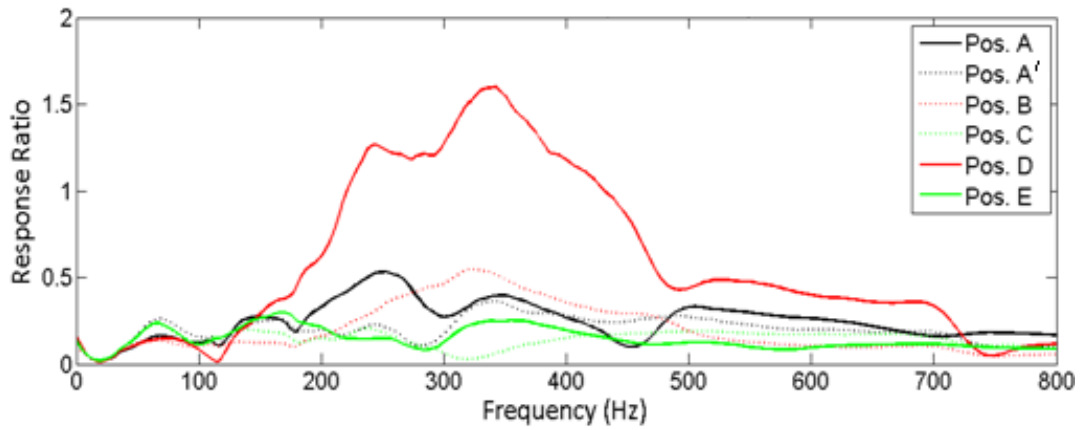


Figure 3.12: Figure 3.11 truncated to 800 Hz to show detail in low frequency vibration response

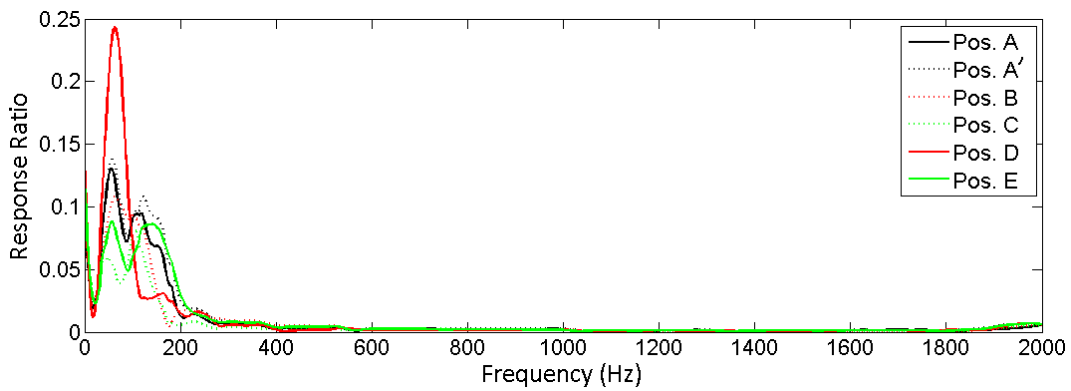


Figure 3.13: Mean position tests (FRFs) at T-9 vertebra taken using the invasive contact tip. Black signals indicate the accelerometer in position A, green indicates positions lateral to position A, and red indicates positions rostro-caudally located to position A.

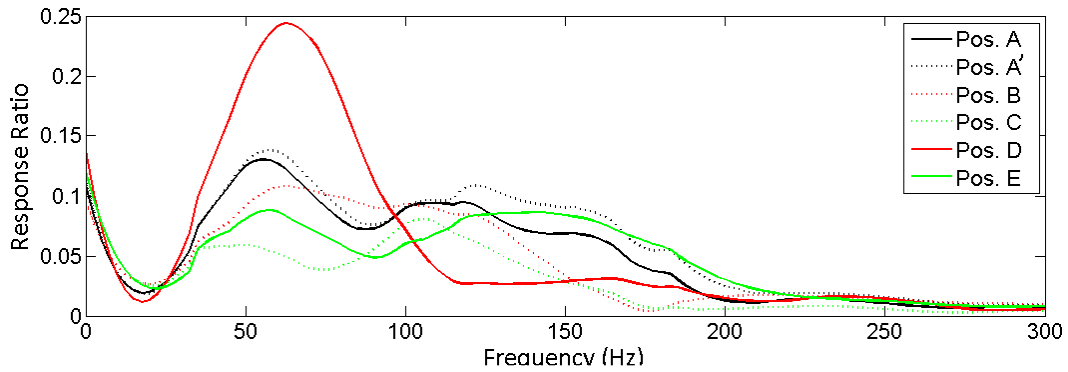


Figure 3.14: Figure 3.13 truncated to 300 Hz to show detail in low frequency vibration response

The graphs show increased peak amplitude at position D for both the invasive and non-invasive contact tips. This was typical for all subjects, except for subject 4 with the invasive contact tip; in this case, both position B and position A' showed peaks with higher amplitudes.

To determine the main mechanisms of variance in the set of 6 peaks, a principal component analysis (PCA) was performed. Each set of 5 repeated tests, for all 6 positions, was entered into the PCA for analysis. Representative graphs for PC1 for the invasive and non-invasive contact tip are shown below in Figure 3.15 and Figure 3.16, respectively.

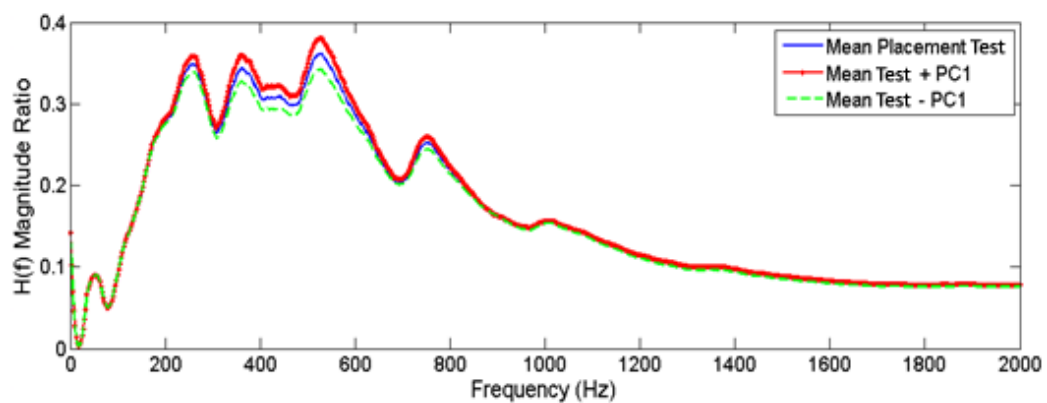


Figure 3.15: Mean non-invasive contact tip placement test with PC1 loading vector added and subtracted. Data taken from subject 1.

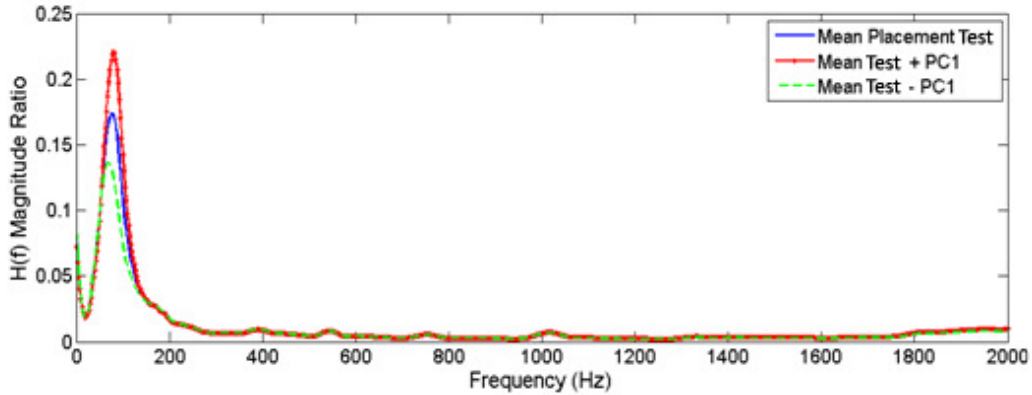


Figure 3.16: Mean invasive contact tip placement test with PC1 loading vector added and subtracted. Data taken from subject 1.

As was described in Section 2.8.2 of the literature review, each principal component represents a certain portion of the variance in the signals. These percentages are summarized below in Table 3.3.

Table 3.3: Percentage of variance accounted for by PC1 in each subject.

	Invasive Tip (%)	Non-Invasive Tip (%)
Subj. 1	72.2	98.2
Subj. 2	69.6	94.5
Subj. 3	57.8	94.5
Subj. 4	46.1	95.0
Subj. 5	87.2	97.2

A paired t-test was run between the invasive and non-invasive contact tip PC1 values. The non-invasive contact tip ($M=0.96$, $SE=0.01$) produced significantly higher values for PC1 % variance accounted for than the invasive contact tip ($M=0.66$, $SE=0.07$, $t(4)=-4.519$, $p=0.011$, $r=0.914$, $power=0.247$).

From each subject, a number of key qualitative features were noted for each PC figure. The number of peaks in the signal, plus the features shown by PC1 to be

affected, is noted for each subject. They are summarized below in Table 3.4 and Table 3.5, for the non-invasive contact tip and invasive contact tip, respectively.

Table 3.4: Description of mean placement FRF features, and signal effect represented by PC1, for the non-invasive contact tip

	Remarks
Subj. 1	Peaks at 52.5, 260, 360, 525, 750 Amplitude increase effect on 260, 360, 525, and 750 peaks
Subj. 2	Peaks at 65, 165, 245, 340 Amplitude increase effect on 245 and 340 peaks
Subj. 3	Peaks at 67.5, 135, 230, 325, 485 Amplitude increase effect on 230, 325, and 485 peaks
Subj. 4	Peaks at 77.5, 262.5 and 365 Amplitude increase on 262.5-365 peaks
Subj. 5	Peaks at 52.5, 262.5 and 320 Hz Amplitude increase effect on main peak (262.5- 320)

Table 3.5: Description of mean placement FRF features, and signal effect represented by PC1, for the invasive contact tip

	Remarks
Subj. 1	One peak at 77.5 hz Amplitude increase effect on main peak , possible widening effect on right side
Subj. 2	One main peak 60 hz with second peak at 120 Hz Amplitude increase effect on main peak, decrease effect on second peak
Subj. 3	Two main peaks (52.5, 102) Amplitude decrease effect on second peak only
Subj. 4	One main peak at 62.5 Hz Amplitude increase effect on main peak Right side of main peak has narrowing effect
Subj. 5	One main peak at 52.5 Hz Amplitude decrease effect on main peak only

3.4.3.2 T-9 Placement Results Skin and Bone Signal Comparisons

Comparisons were made to determine the effect of changing the T9 skin mounted accelerometer placement on the correlation of this signal with the T9 bone mounted accelerometer signal. To compare the two signals, the D-statistic was calculated. Figures 3.17-3.20 show examples of this analysis comparing the mean position A skin mounted accelerometers to the confidence interval on the corresponding bone-mounted accelerometer signals, using both the non-invasive and invasive contact tips. Representative data is shown from subject 4.

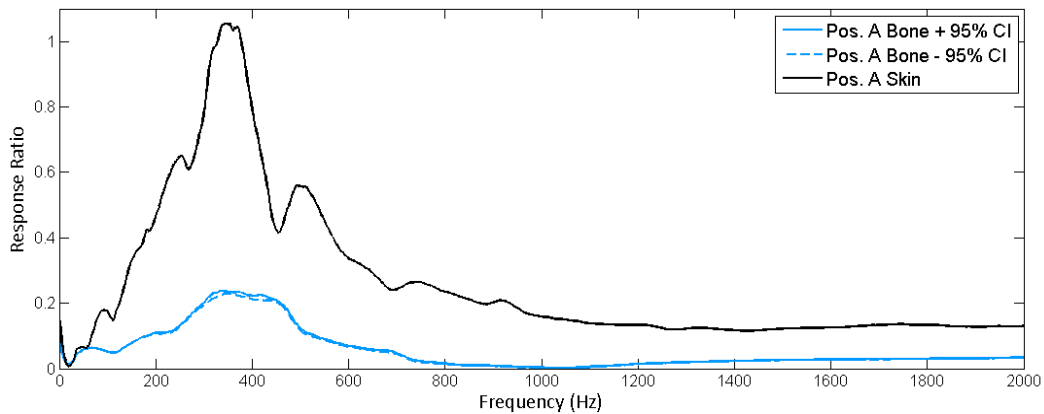


Figure 3.17: Comparison of position A skin-mounted to confidence interval on corresponding bone-mounted accelerometer signals, using the non-invasive contact tip. D-statistic is 0.12%.

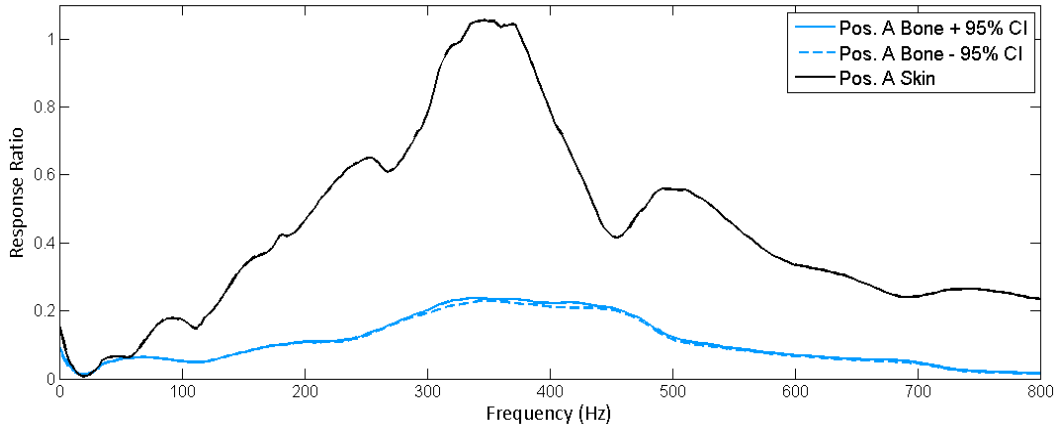


Figure 3.18: Enlargement of Figure 3.37 to 800 Hz to show low frequency detail

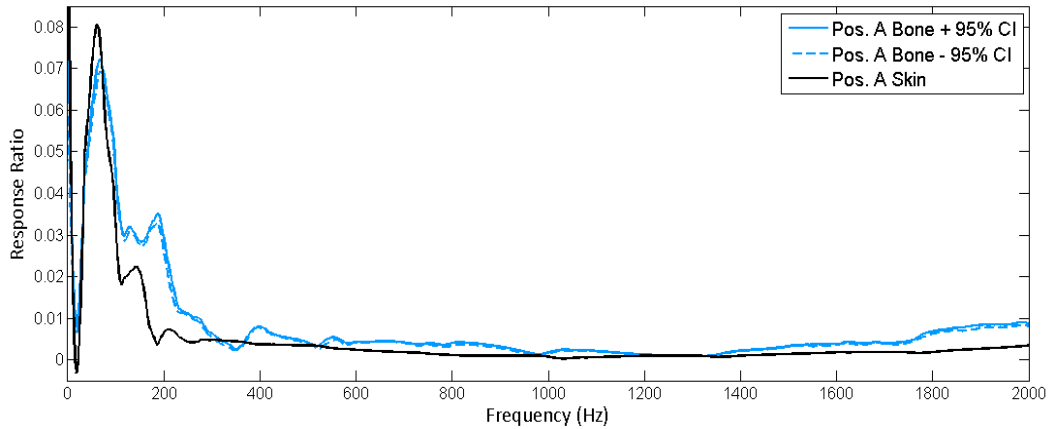


Figure 3.19: Comparison of position A skin-mounted to confidence interval on corresponding bone-mounted accelerometer signals, using the invasive contact tip. D-statistic is 4.24%.

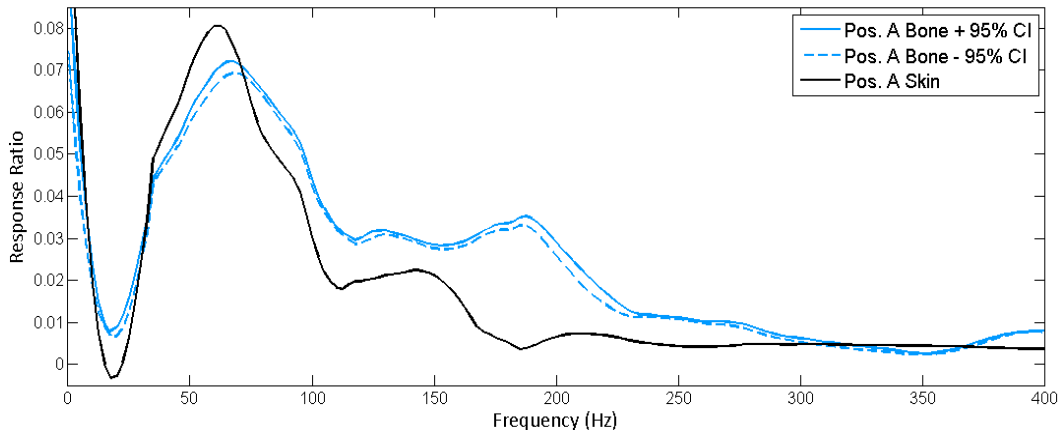


Figure 3.20: Enlargement of Figure 3.39 to 400 Hz to show low frequency detail

Results of all positions from all subjects for the non-invasive contact tip are shown below in Table 3.6, and in Table 3.7 for the invasive contact tip.

Table 3.6: Non-invasive contact tip D-statistic values between mean skin-mounted accelerometer and 95% confidence interval on bone-mounted accelerometer signals.

	Pos. A (%)	Pos. A' (%)	Pos. B (%)	Pos. C (%)	Pos. D (%)	Pos. E (%)
Subj. 1	1.37	0.62	0.75	1.62	0.00	7.12
Subj. 2	1.12	2.37	0.75	1.50	0.25	1.00
Subj. 3	0.25	0.12	1.50	1.75	0.12	0.75
Subj. 4	0.12	0.75	1.12	0.50	0.00	0.00
Subj. 5	1.37	0.12	0.75	0.00	0.00	0.87

Table 3.7: Invasive contact tip D-statistic values between mean skin-mounted accelerometer and 95% confidence interval on bone-mounted accelerometer signals.

	Pos. A (%)	Pos. A' (%)	Pos. B (%)	Pos. C (%)	Pos. D (%)	Pos. E (%)
Subj. 1	8.86	10.11	5.74	13.36	5.12	6.12
Subj. 2	0.37	1.00	0.12	0.25	0.25	0.25
Subj. 3	7.37	1.87	3.37	3.12	2.37	5.12
Subj. 4	4.24	1.62	3.62	3.12	1.50	2.00
Subj. 5	0.12	0.00	0.50	0.12	0.12	0.12

The results shown in Tables 3.6 and 3.7 were pooled together to run a repeated measures ANOVA, with within-subject factors of contact tip type and position. Mauchly's test indicated that sphericity had not been violated ($\chi^2=0.00$); therefore, no correction to the degrees of freedom was required for calculating the significance of the results. At $\alpha=0.05$, no significant differences in the D-statistic measures were found for contact tip ($F(1,4)=2.688$, $p=0.176$, effect size $r=0.634$, power = 0.245), skin accelerometer position ($F(5,20)=1.908$, $p=0.138$, effect size $r=0.295$, power=0.522), or the interaction effect ($F(5,20)=0.771$, $p=0.582$, effect size $r=0.193$, power = 0.221) between the two factors. The between subjects factor was not found to be significant ($F(1,4)=5.777$, $p=0.074$, effect size $r=0.76$, power = 0.449).

3.4.4 Results of Replacement Tests

In addition to repeatability of signals obtained from individual placements, the ability to replace the accelerometer back to the original placement A was investigated. Figures 3.21-3.22 below display representative data from subject 1.

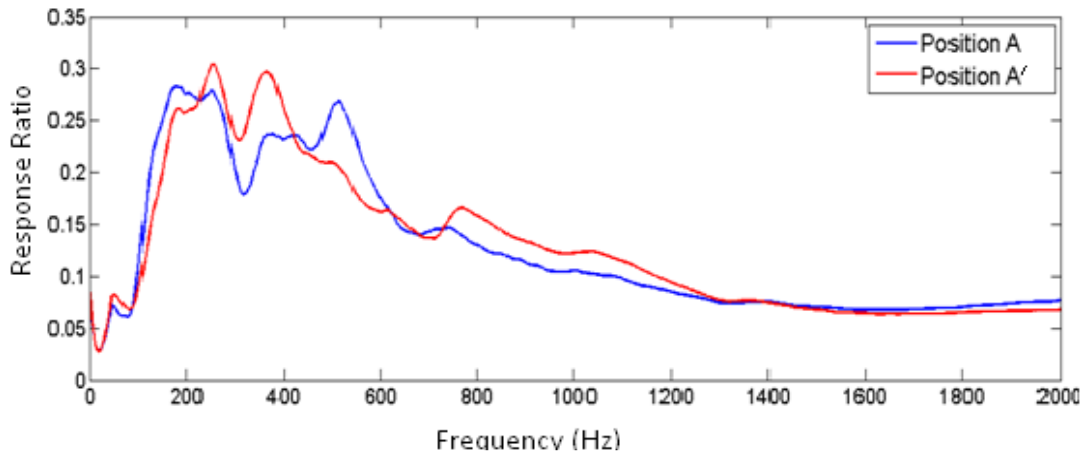


Figure 3.21: *Vibration response of the T9 vertebra using the non-invasive contact tip. Measurements were taken with the skin-mounted accelerometer Position A, and at Position A again (A') after all other placements had been completed. Data taken from subject 1.*

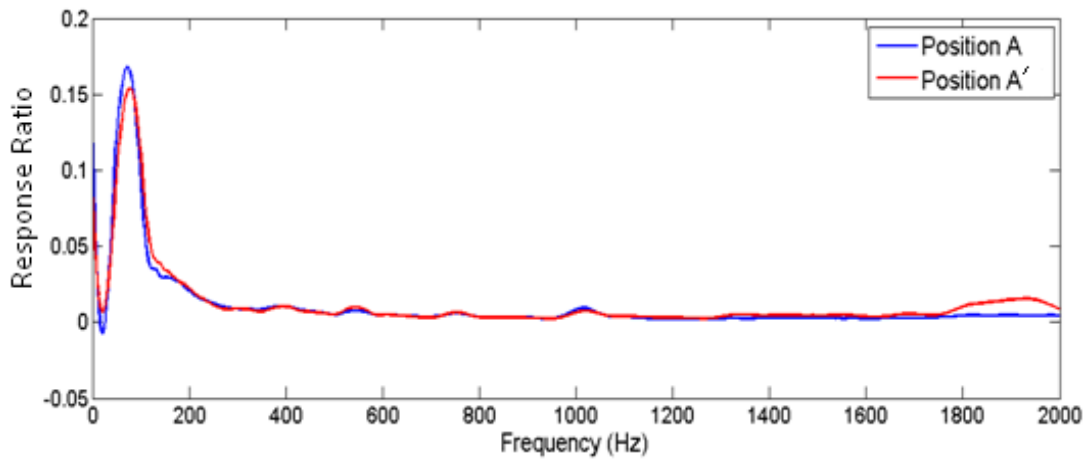


Figure 3.22: *Vibration response of the T9 vertebra using the invasive contact tip. Measurements were taken with the skin-mounted accelerometer Position A, and at Position A again (A') after all other placements had been completed. Data taken from subject 1.*

To quantitatively compare Position A to the replacement, Position A', the D-statistic was calculated, and results are summarized below in Table 3.8, and graphed in Figure 3.23.

Table 3.8: D-Statistic values comparing Position A and Position A'

	Invasive Contact Tip	Non-Invasive Contact Tip
Subject 1	21.22	3.87
Subject 2	14.36	1.75
Subject 3	14.73	4.24
Subject 4	22.60	0.00
Subject 5	16.48	15.36

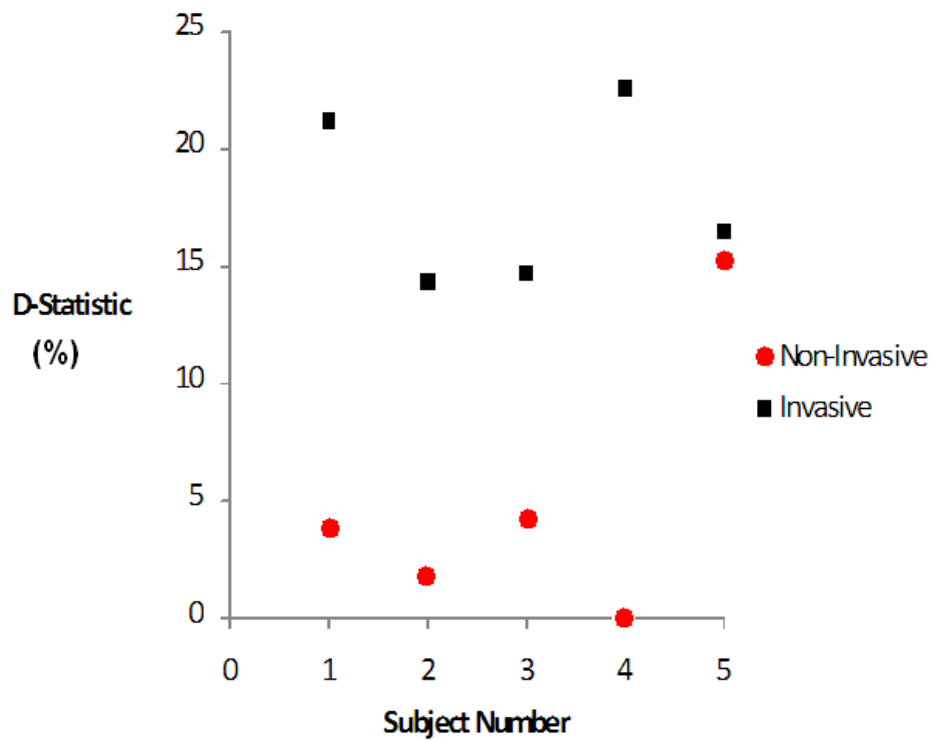


Figure 3.23: D-Statistic values comparing Position A and Position A'

These results show that, within subjects, the invasive contact tip produced a higher D-statistic when comparing A to A'. A two tailed, paired t-test ($\alpha=0.05$) shows that invasive contact tip (M=17.88, SE=2.69) produced significantly higher D-statistic values than the non-invasive contact tip (M=5.04, SE=1.69, $t(4)=-3.57$, $p=0.023$, $r=0.872$, power=0.230).

3.4.5 Comparison of T-10 Needle and Bone Mounted Accelerometer Signals

A needle-mounted accelerometer was dorsally implanted into the T-10 spinous process to determine whether a needle-mounted accelerometer could measure the T-10 bone vibration response.

To evaluate the two signals, the D-statistic was calculated by comparing the mean needle-mounted accelerometer FRF to the 95% confidence interval on the corresponding bone-mounted accelerometer FRFs. Measurements were taken with both the non-invasive contact tip and the invasive contact tip. Figure 3.24 and Figure 3.25 below show the results of this analysis taken from subject 3.

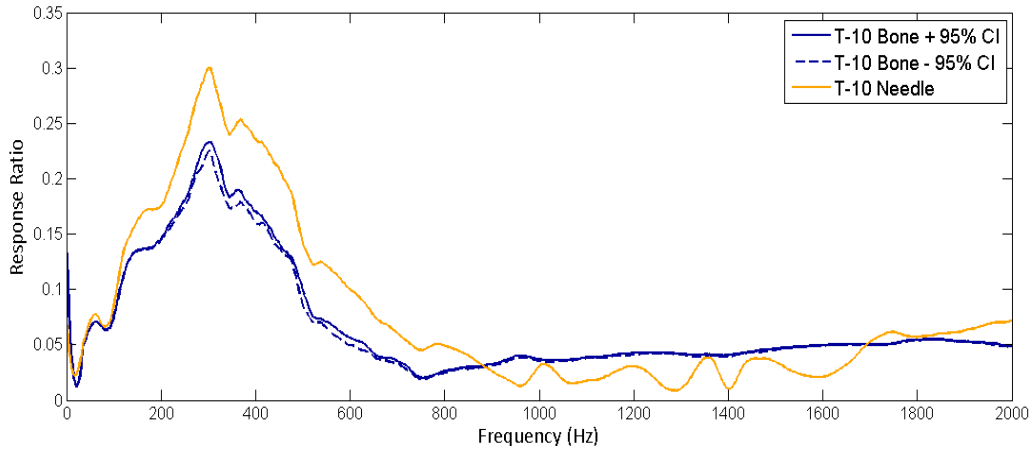


Figure 3.24: *D-statistic on the measurement of the T-10 vibration response using the non-invasive contact tip. The statistic was calculated using the mean needle-mounted FRF and the 95% confidence interval on the FRFs measured from the bone-mounted accelerometer. $D= 0.12\%$*

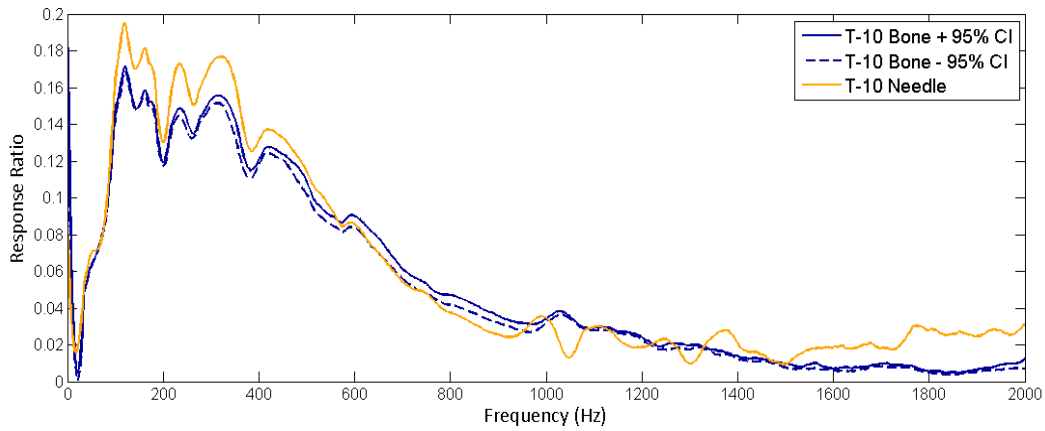


Figure 3.25: *D-statistic on the measurement of the T-10 vibration response using the invasive contact tip. The statistic was calculated using the mean needle-mounted FRF and the 95% confidence interval on the FRFs measured from the bone-mounted accelerometer. $D= 9.99\%$*

The full results for all subjects are summarized below in Table 3.9.

Table 3.9: D-statistic results for all subject using both the non-invasive and invasive contact tips, comparing the needle-mounted accelerometer signal to bone-mounted accelerometer signal.

	NI Tip (%)	Inv. Tip (%)
Subj. 1	0.00	2.37
Subj. 2	52.43	5.12
Subj. 3	0.12	9.99
Subj. 4	1.62	1.25
Subj. 5	2.62	2.37

Using a two tailed paired t-test ($\alpha=0.05$), the D-statistics summarized in Table 3.9 were determined to not be statistically different between the non-invasive contact tip (M=11.36, SE=10.28) and the invasive contact tip (M=4.22, SE=1.58, $t(4)=0.699$, $p=0.52$, $r=0.330$, power=0.075).

A significantly increased D-statistic can be seen for subject 2 when using the non-invasive contact tip. The signals used to calculate the confidence interval for this calculation are shown below in Figure 3.26.

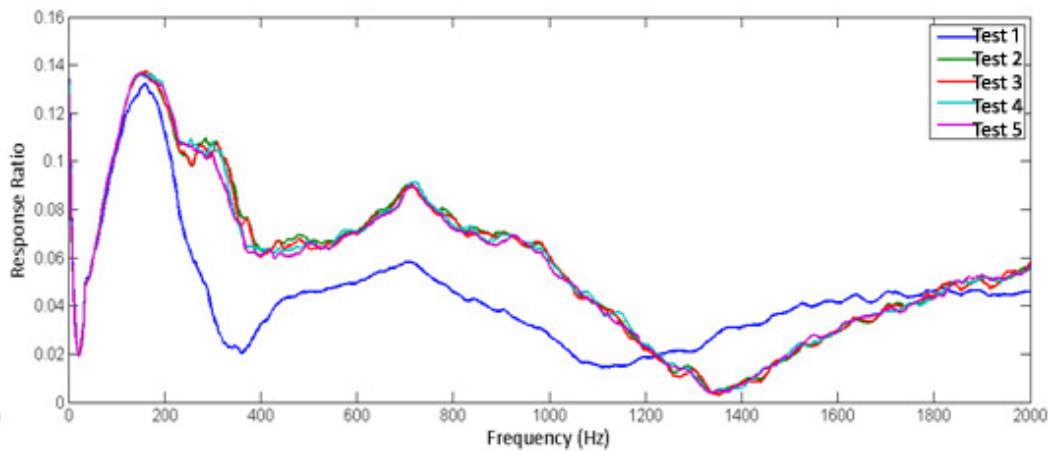


Figure 3.26: The 5 repeated measures taken of the T-10 bone signal using the non-invasive contact tip in subject 2.

Figure 3.26 shows that the first test measured is significantly different than the remaining 4 repeated measures. The cause of this significant difference is unknown. The difference between this signal and the remaining 4 signals created a wider confidence interval, thus increasing the D-statistic calculation when it was compared to the mean needle-mounted accelerometer signal.

3.4.6 Statistical Results Summary

The results of the statistical tests run to analyze the data in this protocol are summarized below in Table 3.10.

Table 3.10: Summary of statistical tests run in Protocol 1. Significant results are indicated by *. All ANOVAs were run at $\alpha=0.05$.

Description of Stat. Test	Factor	Source	p-value	Power
Paired T-Test on PC1 Values	PC1 Values	Tip Type	0.011*	0.247
RM ANOVA on D-statistic Matching T-9 Placement Signals	D-statistic Within Subjects	Tip Type	0.176	0.245
		Accel. Position	0.138	0.522
		Interaction	0.582	0.221
	D-statistic Between Subjects		0.074	0.449
Paired T-Test on D-Statistic of Replacement from A-A'	D-Statistic Values	Tip Type	0.023*	0.230
Paired T-Test on Needle-Bone Matching at T-10	D-Statistic Values	Tip Type	0.052	0.075

3.5 Discussion

Discussion of the results is presented below in order of the goals of the protocol.

3.5.1 Signal Smoothing

To improve the signal to noise ratio of the FRFs, data were smoothed using a Savitzky-Golay filter. This technique is known to remove noise in the data while preserving high-frequency features [Savitzky and Golay 1964;Steinier et al. 1972]. This filter is ideal for signals with a number of frequency elements caused by sharp resonance peaks which require preservation [Nakajima et al. 2001;Press et al. 1999]. In using this smoothing technique, the user determines a span of data points to which a polynomial of chosen degree is fitted using a least-squares error method. A degree of 3 and span of 27 was chosen.

A tradeoff occurs when deciding on these values. A higher order filter will better preserve narrow features, but performs poorly at smoothing broad features. An increased span can aid in this area, by smoothing out broader features [Press et al. 1999]. It is therefore left to the investigator to test which combinations of degree and span are optimal. The combination of polynomial of degree 3 and span 27 provided adequate smoothing, but still preserved important features in the data.

3.5.2 Repeatability of Measured Signals

As shown in by Figures 3.6-3.10, the repeatability of signals was good [Heylen and Lammens 1996]. Viewing the mean and standard deviation from single accelerometers, the confidence interval on repeated measures was very small. Very few exceptions to this result occurred, but examples of these exceptions are shown in Figures 3.10 and 3.26. Presently, the cause of the deviation of these signals is unknown. The GSC and GAC were calculated for the global system of sensors, based on the 5 repeated measures of each test. The results shown in Tables 3.1 and 3.2 indicate all mean GSC and GAC values were greater than 0.977. The lowest bound of the 95% CI, of any test, reached 0.88, an acceptably high value to constitute good repeatability [Heylen and Lammens 1996]. Previous invasive experiments performed in the Spinal Function Lab at the University of Alberta also showed comparably good repeatability values using fully invasive sensors and contact tip [Kawchuk et al. 2008]. These experiments demonstrate the ability of the system to attain high levels of repeatability using a semi or fully non-invasive system. The consistently high repeatability of the signals indicates that visco-elastic changes in the system likely do not have a significant influence over the short period of time taken to obtain the five signals.

3.5.3 T-9 Accelerometer Placement

3.5.3.1 T-9 Placement: Skin Accelerometer Placement Comparisons

The repeated measures ANOVA showed that no significant differences occurred between D-statistic values for either of the within subjects factors (contact tip

type or accelerometer position). As shown from the analysis, the power of these statistical tests was less than or equal to 0.522, which is considered to be of poor statistical power level [Field 2009]. This low power is likely due to the small sample size.

Figures 3.11 and 3.13 show the mean test (FRF) taken from each of the 5 placement positions A-E, plus the signal obtained upon replacement to position A. Using the non-invasive contact tip, changes in the rostro-caudal direction (positions D and A) tended to produce a signal amplitude effect. In all 5 subjects, position D showed an amplitude increase compared to position A. Comparing position B to position A, signals showed either a decrease in amplitude or comparable amplitudes in all 5 subjects. Signals from positions C and E were less than or equal to those of position A in amplitude. Using the invasive contact tip, signals obtained from position D were again greater in amplitude than those of position A. However, signals obtained from position B, C and E did not show a systematic effect with respect to amplitude. The principal component analysis performed on this data confirms that the amplitude effect is the greatest source of variation between the position data.

The accelerometers were moved 7.1 mm rostro-caudally in either direction, or 9.9 mm laterally in either direction; however, these small distances created significant differences in the measured vibration response, particularly when using the non-invasive contact tip. These results indicate the importance of precision when placing the accelerometers for measurement of the underlying vertebral vibration response when using the non-invasive contact tip.

The effect of the type of contact tip on the placement results is apparent from Figures 3.21 and 3.22. The non-invasive contact tip appears to have a systematic effect on the measured vibration response when the position of the

accelerometer is changed. Rostro-caudal changes in the position of the accelerometers produced an effect whereby the amplitude of the signal tends to decrease with increasing distance from the contact tip. Changes in the lateral positioning of the accelerometer also demonstrate this effect. If vibration is assumed to be distributed radially from the contact tip, the lateral positioning of the accelerometers places them slightly further away from the point of vibration input, meaning they should show decreased amplitude in comparison to position A. The decreasing amplitude of the signal with increasing distance from the contact tip is supported by the literature. Sörensson et al. tested vibration travelling through an arm via a hand gripping a vibrating handle [Sörensson and Burström 1997]. Measurements by skin-mounted accelerometers at the knuckle, wrist, and elbow showed decreasing signal energy with increasing distance from the handle. A study by Zhang et al used a laser vibrometer and a non-invasive contact tip to measure vibration in various parts of the body [Zhang et al. 2008]. Measuring from 2 mm-12mm, they found that a steady state input vibration had linearly decreasing velocity and phase with increasing distance from the vibration input point.

The only systematic effect apparent from the invasive contact tip tests appeared between position A and position D, with position D signals consistently showing a higher amplitude response than position A signals. Position D was located directly beside the portion of skin that had been cut away so as to insert the invasive contact tip. The removal of this skin could have changed some of the motion constraints on the remaining skin close to the D position. The skin would have been less constrained in its vibration response, causing the amplitude of the measured D position signal to increase.

These results show the impact of the non-invasive system on the measured vibration response of the spine. Using the non-invasive contact tip, vibration is

transmitted to the spine through the skin. However, the interfacing of the tip and the skin also allows for vibration to be transmitted directly through the skin to the accelerometer, bypassing the spine entirely. Steele et al. note that, for very thick skin, the measured vibration response may measure both the response of the bone and the skin to the vibration [Steele et al. 1988]. Lundberg also notes that when using skin-mounted markers in regions of thick skin in kinematic testing, the sensor tends to measure the movement of the skin instead of the underlying bone [Lundberg 1996]. A measurement of tissue thickness over the spinous process, taken upon removing soft tissue when installing the invasive contact tip in subject 1, showed the uncompressed thickness of this tissue to be 0.5 in. thick. Unfortunately, vibration testing of skin only was not performed; therefore, the exact contribution of the skin to the measured vibration response is unknown.

Results showed that, although PC1 accounted for amplitude variance using both the non-invasive and invasive contact tips in the experiments, the percentage of variance accounted for when using the non-invasive contact tip was significantly higher than the percentage accounted for when using the invasive contact tip. This is further evidence that the vibration response of the skin may be an overwhelming component of the total measured vibration response when using the non-invasive contact tip.

The effect of preload magnitude of the contact tip, or simply applying preload to the accelerometers was not investigated in this protocol. However, preloading may aid in future investigations. Thompson et al. investigated the role of preload on measuring the vibration response of the ulna, and determined that increasing the preload of the contact tip on the skin, when measuring the vibration response at the input point brings the measured response close to that of the actual bone response [Thompson et al. 1976]. Only a single preload of 30N was

tested at the input point. Furthermore, the accelerometers used in the protocol in this thesis were not preloaded to the skin in any way. These two factors suggest that the vibration of the skin may be an important component of the total measured vibration response. Preliminary testing of an accelerometer preloading technique using an elastic band was performed; however, results from these investigations were inconclusive. A full systematic study of this technique, as well as the effect of contact tip preloading, is warranted.

The accelerometer placement results show that the correct placement of accelerometers on the skin is important in obtaining viable measurements of the spinal vibration response. Development of a reliable placement technique will be crucial to the success of a non-invasive spinal diagnostic device. A limitation in performing the placement portion of the protocol was the accuracy of position A centralization over the spinous process, from which all other positions (B-E) were measured. Position A was determined solely by the investigator using palpation techniques, and therefore may not have been entirely centered over the spinous process. This technique could be aided in future experiments using ultrasound as a quick and efficient method of locating the spinous process boundaries.

3.5.3.2 T-9 Placement Results: Skin and Bone Signal Comparisons

Quantitatively, no significant difference was found between skin accelerometer position and bone accelerometer D-statistic values. Qualitatively analyzing the graphs provides a different account. Viewing the graphs of signals measured using the non-invasive contact tip, the features of the skin and bone signals are generally dissimilar in both shape and amplitude.

Conversely, the graphs of signals taken using the invasive contact tip are similar in amplitude, and contain many similar shape features. Examples demonstrating these observations are shown below in Figures 3.27 and 3.28.

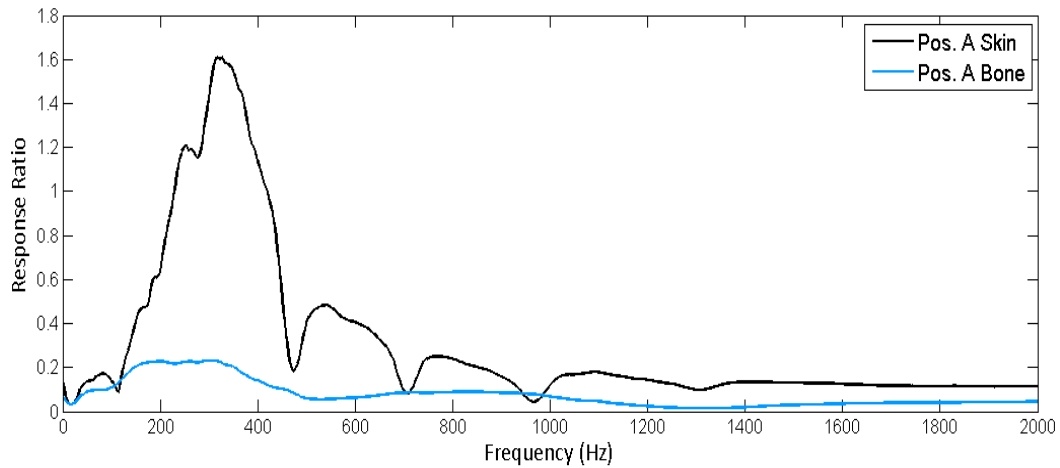


Figure 3.27: Comparison of measured skin and bone T-9 vibration response using the non-invasive contact tip

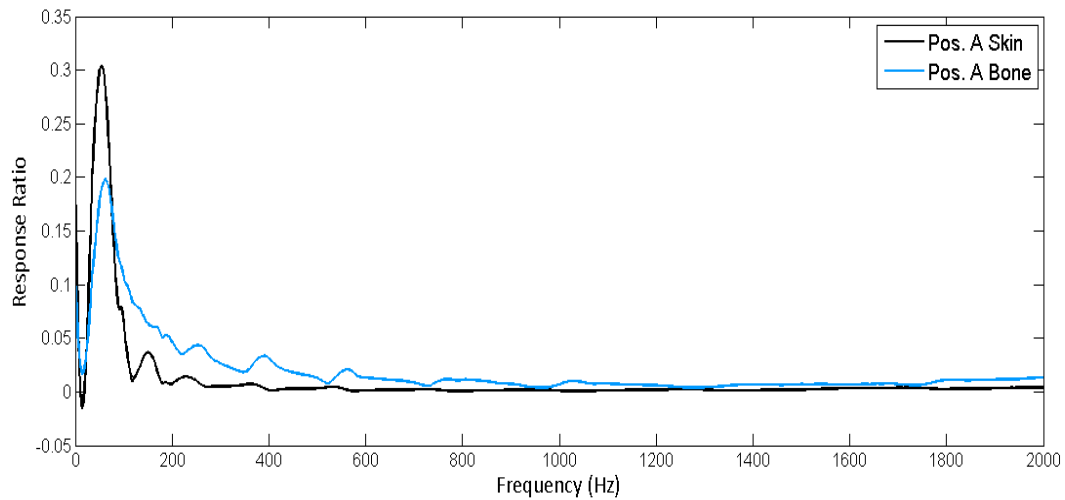


Figure 3.28: Comparison of measured skin and bone T-9 vibration response using the invasive contact tip

Figure 3.27 shows dissimilar matching of the peaks in both shape and amplitude, where Figure 3.28 shows both skin and bone signals with similar amplitude and main peak shape. These results provide further evidence that the non-invasive contact tip excites vibration modes in the skin and soft tissues surrounding the spine. The skin vibration response, when measured using the invasive contact tip, provides an approximation to the bone vibration response. However, vibration transmitted from the spine through the soft tissue still has the ability to excite the skin. Based on the results of the position tests, it appears that vibration transmitted through the skin by the non-invasive contact tip is damped out with increasing distance from the tip. Because the skin is a visco-elastic structure, this vibration could excite additional modes of vibration of the skin, or alter it through amplification or phase shifting of the signal. Wu et al. have demonstrated that the Poisson's ratio of the skin is dependent on the strain rate of the skin, while the volumetric compression is a non-linear property, dependent on loading rate and compression stress [Wu et al. 2003]. Dellaleau et al. found a non-linear behaviour exhibited by the skin under tension [Dellaleau et al. 2008]. The vibrating soft tissues in these experiments would undergo both types of stress locally. Therefore, the bone vibration response, transmitted through the skin, could have been altered by the time it reached the skin mounted accelerometer.

The results of the placement and skin-bone signal comparisons illuminate a key area for further investigation in the development of a non-invasive diagnostic device in the spine. Methods of reducing the unique vibration response of the skin, measured by skin-mounted accelerometers, should be investigated.

3.5.4 Replacement of A-A'

The correlation of the vibration response measured from position A and A' was compared using both the invasive and non-invasive contact tips. This comparison will be referred to as 'replaceability'. In the non-invasive contact tip tests, replaceability was poor. In the invasive contact tip tests, the replaceability was shown to improve.

The low replaceability found in these experiments could be due to a number of factors. As previously discussed, the graphs shown in Figure 3.11 demonstrate that the non-invasive contact tip tests are highly sensitive to changes in placement in comparison to the results of the invasive contact tip tests. Therefore, experimenter error in replacing the accelerometer precisely to its original position could contribute to differences in the signals. Though positions were marked on the skin, the sensitivity of the system to small changes in placement has been demonstrated. This error would not be as pronounced in the invasive tests due to the decrease in magnitude of the overall response, as well as due to smaller relative amplitude changes that occur as shown through positioning tests; however, some error is apparent in both the non-invasive and invasive tests. Another source of error between the two signals could be due to changes in the visco-elasticity of the system. Rubin et al. have demonstrated a relaxation effect in human tissues undergoing cyclic loading [Rubin et al. 1998]. Though the vibrations in these experiments were small in amplitude, the repeated nature of the testing could have induced such a relaxation effect in the soft tissues, causing changes in their mechanical response to vibration. This effect likely would not have shown up in the bone-mounted accelerometers due to the rigid nature of the bone.

A limitation of this study with respect to placing accelerometers on the skin was the inability to control the horizontal incline of skin-mounted accelerometers. The horizontal incline angle of the accelerometer was not measured upon replacing it to position A'. The small size of these accelerometers made them susceptible to rotation from their cables that attached them to the breakout box. Small rotations caused by moving the accelerometer to different placements and replacing it to the skin could have caused some of the signal discrepancies in the A-A' signal comparisons.

These results have significant implications for the implementation of a non-invasive spinal diagnostic device. In these controlled experiments, very little time passed between the testing at A, and again at A'. Furthermore, the ideal positioning of the accelerometer was marked directly on the skin. In a clinical situation, days or weeks could pass between testing times, and the positioning would not remain marked on the skin. These results show that it would be difficult to know whether actual changes had occurred in the spinal vibration response, or simply whether poor replacement of the accelerometer had occurred.

3.5.5 Needle and Bone Vibration Response Measurement Comparisons

Comparisons were made between the vibration response signal measured from a needle-mounted accelerometer that had been inserted into the T-10 spinous process, and the response signal measured from the T-10 bone mounted accelerometer.

Quantitatively, there was fairly poor correlation between the signals. However, qualitatively viewing the signals shows that while the needle and bone signals were dissimilar in amplitude, they contain similar shape features. There could be a number of reasons for this amplitude discrepancy. The difficulty of installing the needle in the bone was problematic, due to the small width of the spinous process and the depth of insertion required to reach the underlying bone. While every effort was made to install the needle such that the needle mounted accelerometer axis was aligned with the bone accelerometer measurement axis, the axes could not be perfectly aligned in most cases. Therefore, the off-axis measurements may be a significant factor in the discrepancy between the two measurements.

The similarity in signal shapes between the bone-needle signals indicates that it is likely that any vibration modes of the needle were not measured. The needle diameter was 0.82 mm (21 gage). Previous studies that have used such methods to measure bone movement have used intracortical pins of at least 1.6-3 mm in diameter [Arndt et al. 2004;Nokes et al. 1984;Gal et al. 1997;Rostedt et al. 1995]. Rostedt et al. tested three different diameters of pins inserted into the spinous processes of vertebrae to determine the relationship between their length and exposed frequency [Rostedt et al. 1995]. Pins were inserted into the spinous processes with varying distance between the accelerometer and the bone (20-30 mm), as well as varying the exposed length of pin above the accelerometer (50-120 mm). They determined that increasing pin diameter, decreasing the distance between the spinous and the accelerometer, and decreasing exposed pin above the accelerometer increased the resonant frequency of the pin. There were no results for diameters matching the needles used in this thesis. The situation most closely resembling this study was a pin with accelerometer distance of 20 mm and pin length of 5 mm, of 2 mm diameter, resulting in a natural frequency of 102 Hz. However, the accelerometer setup used in Rostedt's experiment

weighed approximately 27 g, while the accelerometer used in this protocol weighed 0.8 g. Therefore, the results cannot be directly compared. Based on the equation of natural frequency alone $\left(\omega = \sqrt{\frac{k}{m}}\right)$, the natural frequency of the pin system would be increased by a factor of 5.81 due to the accelerometer mass factor, negating the mass of the pin itself (see Appendix F for calculation). The natural frequency of the system would be decreased by smaller diameter of the pin, but would be increased due to the decreased overall pin length. The magnitude effect of these two parameters is unknown. However, the apparent high degree of shape correlation between the measured bone and needle signals indicates that modes of vibration in the needle-accelerometer assembly were likely not excited. To test the natural frequency of the needle, the procedure used by Rostedt et al. could be adapted. Using an impulse excitation or a pluck excitation of the needle, the implantation depth and the surrounding soft tissue (or synthetic soft tissue) could be systematically varied to determine their influence on the needle's natural frequency.

After reviewing the literature, hypodermic needles do not appear to have been used before as a substitute for bone pins in the measurement of skeletal motion. Therefore, the effect of simply installing the needle by tapping it into the bone, instead of the screw implantation used by traditional intracortical pins, is unknown. While the pins were tested by hand to ensure they were implanted into the bone adequately, there was no method of determining their security during testing, and whether this may have impacted the vibration response measurements.

A number of factors may have influenced the measurement of bone vibration using the needle-mounted accelerometer. The damping effect of the surrounding soft tissues may have impacted the needle-mounted accelerometer

measurements. The needle was inserted directly through the skin into the bone without removing any of the surrounding soft tissue. Measurements of skin and soft tissue were taken from the tissue removed when changing to the invasive contact tip. With measurements of the skin thickness at approximately 0.5 inches, this amount of skin may have impacted the needle-mounted accelerometer measurements, and contributed to the small shape discrepancies between the two signals. Rostedt et al. speculated that the skin may change the resonant frequency of bone pins due to its damping properties [Rostedt et al. 1995]. Furthermore, it has been shown that from the experiments in this protocol, vibration travels directly through the skin and soft tissues. It may also be possible that vibration could be transferred from the soft tissues back into the needle. Future experiments could explore this skin effect by removing the skin immediately surrounding the needle. This option was not viable for these experiments, as the replacement of the accelerometer to the skin after performing the needle tests required that the skin be intact.

The type of contact tip used in this protocol did not appear to affect the correlation between the needle-mounted accelerometer measurement and the bone-mounted accelerometer measurement. However, the physical shapes of the measured signals are different when comparing between the non-invasive and invasive contact tips. This difference in shape may indicate that the vibration input signal is altered as it passes from the non-invasive contact tip to the spine. The difference could additionally be due to an alteration of the spinal vibration response. The non-invasive contact tip is significantly preloaded onto the spine, whereas the invasive contact tip is not preloaded at all. This change in preload would likely cause a difference in the structural parameters influencing the spine. For instance, the extra preload would provide damping, or would constrain the movement of the spine, and hence would alter the spinal vibration response.

The lack of significant shape difference between the needle-mounted accelerometer signals and bone-mounted accelerometer signals, using both the invasive and non-invasive contact tips, indicates that the majority of variance between skin-mounted and bone-mounted accelerometer signals is accounted for by the skin and soft tissues alone.

These results show that with further investigation into the relationship between the needle and the surrounding skin, as well into needle installation techniques, a hypodermic needle may be suitable for use in the measurement of the bone vibration response.

3.6 Conclusions

Acceptably high repeatability of a measured vibration response signal from the spine can be obtained when using both a non-invasive vibration input contact tip, and a skin-mounted accelerometer.

Changes in the skin-mounted accelerometer position over the spinous process significantly affect the measured signal. Specifically, increasing distance between the point of vibration application and the skin-mounted accelerometer decreases the amplitude of the measured response. Furthermore, the changes in measured signals with changes in accelerometer position are primarily found when using a non-invasive contact tip. The non-invasive contact tip excites modes of vibration in the skin and soft tissues covering the spinous process, which are then transmitted to the skin-mounted sensor.

Finally, the invasive or non-invasive nature of the contact tip plays a significant role in the way the spine vibrates in response to the given input from the tip.

Two factors may contribute to these differences: A) The soft tissues between a skin-mounted accelerometer and the underlying vertebra may alter the measured vibration response signal; B) The preload of the contact tip on the spine likely affects the boundary conditions of the spine.

3.7 References

Arndt A, Westblad P, Winson I, Hashimoto T, Lundberg A. Ankle and subtalar kinematics measured with intracortical pins during the stance phase of walking. *Foot Ankle Int* 2004;25(5):357-364.

Delalleau A, Josse G, Lagarde JM, Zahouani H, Bergheau JM. A nonlinear elastic behavior to identify the mechanical parameters of human skin in vivo. *Skin Res Technol* 2008;14(2):152-164.

Ewins DJ, editor. *Modal testing*. Wiley; 2000. 562 p.

Field. Field A, editor. *Discovering Statistics Using SPSS*. 2 ed. Sage Publications Ltd; 2009. 821 p.

Gal J, Herzog W, Kawchuk G, Conway P, Zhang YT. Measurements of vertebral translations using bone pins, surface markers and accelerometers. *Clin Biomech (Bristol)* 1997;12(5):337-340.

Georgiou AP, Cunningham JL. Accurate diagnosis of hip prosthesis loosening using a vibrational technique. *Clin Biomech (Bristol)* 2001;16(4):315-323.

Gluser R, Sennerby L, Meredith N, Rée A, Lundgren A, Gottlow J, Hämmerle CHF. Resonance frequency analysis of implants subjected to immediate or early functional occlusal loading. Successful vs. failing implants. *Clin Oral Implants Res* 2004;15(4):428-434.

Hamza M, editor. FRAC: A consistent Way of Comparing Frequency Response Functions. Proceedings of the International Conference on Identification in Engineering Systems; Innsbruck, Australia: 1996. 48 p.

Holden JP, Orsini JA, Siegel KL, Kepple TM, Gerber LH, Stanhope SJ. Surface movement errors in shank kinematics and knee kinematics during gait. *Gait and Posture* 1997;5:217-227.

Holzapfel G. Biomechanics of Soft Tissue. In: Lemaître J, ed. *Handbook of materials behavior models*. Academic Press; 2001:1200.

Jurist JM. In vivo determination of the elastic response of bone. I. Method of ulnar resonant frequency determination. *Phys Med Biol* 1970;15(3):417-426.

Kawchuk GN, Decker C, Dolan R, Carey J. Structural health monitoring to detect the presence, location and magnitude of structural damage in cadaveric porcine spines. *J Biomech* 2009;42(2):109-115.

Kawchuk GN, Decker C, Dolan R, Fernando N, Carey J. The feasibility of vibration as a tool to assess spinal integrity. *J Biomech* 2008;41(10):2319-2323.

Keller TS, Colloca CJ. Dynamic dorsoventral stiffness assessment of the ovine lumbar spine. *J Biomech* 2007;40(1):191-197.

Lundberg A. On the use of bone and skin markers in kinematic research. *Hum Mov Sci* 1996;15:411-422.

Meredith N, Alleyne D, Cawley P. Quantitative determination of the stability of the implant-tissue interface using resonance frequency analysis. *Clin Oral*

Implants Res 1996;7(3):261-267.

DSP Technology in Wearable Satellite Terminals for ETS-VIII. DSP 2001 - Seventh International Workshop on Digital Signal Processing Techniques for Space Communications; Sesimbra, Portugal: 2001.

Nokes L, Fairclough JA, Mintowt-Czyz WJ, Mackie I, Williams J. Vibration analysis of human tibia: the effect of soft tissue on the output from skin-mounted accelerometers. J Biomed Eng 1984;6(3):223-226.

Savitzky-Golay Smoothing Filters. In: Press WH, Teukolsky SA, Vetterling WT, Flannery BP, ed. *Numerical recipes in C*. Cambridge University Press; 1999:650-655.

Ranken MD, C G J Baker, Kill RC, editor. Food Industries Manual 1997. Aspen Publishers; 1997.

Rosenstein AD, McCoy GF, Bulstrode CJ, McLardy-Smith PD, Cunningham JL, Turner-Smith AR. The differentiation of loose and secure femoral implants in total hip replacement using a vibrational technique: an anatomical and pilot clinical study. Proc Inst Mech Eng [H] 1989;203(2):77-81.

Rostedt M, Broman H, Hansson T. Resonant frequency of a pin-accelerometer system mounted in bone. J Biomech 1995;28(5):625-629.

Rubin MB, Bodner SR, Binur NS. An elastic-viscoplastic model for excised facial tissues. J Biomech Eng 1998;120(5):686-689.

Savitzky A, Golay M. Smoothing and differentiation of data by simplified least

squares procedures. 1964;36(8):1627-1639.

Steele CR, Zhou LJ, Guido D, Marcus R, Heinrichs WL, Cheema C. Noninvasive determination of ulnar stiffness from mechanical response--in vivo comparison of stiffness and bone mineral content in humans. *J Biomech Eng* 1988;110(2):87-96.

Steinier J, Termonia Y, Deltour J. Comments on Smoothing and Differentiation of Data by Simplified Least Square Procedure. *Anal Chem* 1972;44(11):1906-1909.

Sörensson A, Burström L. Transmission of vibration energy to different parts of the human hand-arm system. *Int Arch Occup Environ Health* 1997;70(3):199-204.

Thompson GA, Young DR, Orne D. In vivo determination of mechanical properties of the human ulna by means of mechanical impedance tests: experimental results and improved mathematical model. *Med Biol Eng* 1976;14(3):253-262.

Wu JZ, Dong RG, Smutz WP, Schopper AW. Nonlinear and viscoelastic characteristics of skin under compression: experiment and analysis. *Biomed Mater Eng* 2003;13(4):373-385.

Yrjämä M, Tervonen O, Kurunlahti M, Vanharanta H. Bony vibration stimulation test combined with magnetic resonance imaging. Can discography be replaced? *Spine* 1997;22(7):808-813.

Yrjämä M, Vanharanta H. Bony vibration stimulation: a new, non-invasive method for examining intradiscal pain. *Eur Spine J* 1994;3(4):233-235.

Zhang X, Kinnick RR, Pittelkow MR, Greenleaf JF. Skin viscoelasticity with surface wave method. Proceedings - IEEE Ultrasonics Symposium 2008;2008:651-653.

Chapter 4: Protocol 2 – Effect of Contact Tip Shape on Correlation between Skin and Bone Vibration Response Signals

4.1 Overview

The results of the Protocol 1 experiments (Chapter 3) detected that skin and soft tissue significantly affect the measured vertebral vibration response from a skin-mounted accelerometer. Furthermore, these results also demonstrated that a non-invasive contact tip further alters the vibration signal recorded by a skin-mounted accelerometer.

As a result, the following protocol was developed to determine whether contact tip interface shape influences the correlation between a skin-mounted sensor FRF and a bone-mounted sensor FRF. To this point at the Spinal Function Lab, protocols have only been performed in porcine subjects. Therefore, for this protocol, experiments were performed in both porcine and human cadavers to explore similarities and differences between subject types. In addition to testing contact tip shapes, the replaceability of an accelerometer to a skin position was investigated at three different vertebral levels to determine whether a distance effect between the accelerometer and contact tip occurred.

4.2 Introduction

As shown in Protocol 1 (Chapter 3), non-invasive vibration testing complicates the application methods of inputting and measuring vibrations due to soft tissue effects. Specifically, the effect of varying skin-mounted accelerometer placements, as well as the effect of using a non-invasive contact tip decreased the accuracy of the measured bone vibration response. These results suggested three different issues that warranted further investigation.

First, it was found that the non-invasive contact tip added signal noise to the measured vibration response of the bone. Therefore, an investigation into whether the shape of the contact tip affected the measured vibration response was warranted. Steele et al have provided a small summary of tips used to investigate the stiffness of the human ulna, concluding that a broad, curved tip shape reduced skin resonances [Steele et al. 1988]. However, this prior study did not elaborate on any effect of changing the radius or width of tip. Therefore, investigation of changes in these parameters is warranted.

Second, previous invasive experiments [Kawchuk et al. 2008;Kawchuk et al. 2009], as well as the experiments performed for Protocol 1 (Chapter 3) of this thesis were performed in porcine cadavers. The device used in these protocols had not yet been tested in human cadavers or live humans. Human skin has a significantly different structure and physical properties than porcine skin, in part due to a greater thickness of the stratum corneum layer [Montagna and Yun 1964]. It is unknown whether the observations made in porcine cadavers in Protocol 1 would be present in human cadavers. Therefore, this new protocol was devised and performed in both porcine and human cadavers to determine whether results were similar between cadaver types.

Third, the previous protocol also showed that the magnitude of the added signal noise decreased with increasing distance between the skin-mounted accelerometer and the non-invasive contact tip. Therefore, to investigate the dissipation of signal noise in both porcine and human cadavers, measurements were taken at 3 vertebral levels, each of increasing distance from the contact tip. Sörensson et al, have shown that vibration travelling through the human upper extremity significantly decreases in energy with increasing distance from the vibration input point, due to attenuation by soft tissues [Sörensson and Burström 1997]. Therefore, investigation into the degree of correlation between the skin-mounted and bone-mounted accelerometer at different distances from the vibration input point was performed.

4.2.1 Protocol Goals and Hypotheses

This experiment aimed to achieve a number of goals:

1. Quantify the signal correlation between skin mounted accelerometer and a needle mounted accelerometer in measuring vertebral vibration.
2. Given the above, determine whether the vertebral level, and hence distance from the contact tip, is a significant factor in the degree of signal correlation.
3. Determine, through signal correlations, which contact tip shape allows for the highest correlation of the needle-mounted accelerometer and skin mounted accelerometer signals.
4. Determine whether similar levels of signal correlation and contact tip performance were achieved in porcine and human cadavers.
5. Determine the correlation between the mean signal obtained from a skin-mounted accelerometer, and the mean signal from the same

accelerometer once removed and replaced to the same position. Performance of this test at 3 different vertebral levels of increasing distance from the contact tip will determine whether replaceability of the accelerometer is affected by distance from the contact tip.

For each of these goals, a general hypothesis was formulated. Goals 1 and 2 are summarized in hypothesis 1:

1. Increasing distance between the vertebral level and contact tip input point will increase the correlation between a skin-mounted accelerometer and a needle-mounted accelerometer signal.
2. Alteration of the contact tip shape parameters will significantly affect the degree of correlation between the FRF obtained from a skin mounted accelerometer, and that of a bone mounted accelerometer.
3. The overall correlation between skin-bone mounted accelerometers in human cadavers will improve over that of porcine cadavers due to the increase in compliance and elasticity of human skin; however, the variance in correlation values will increase due to the heterogeneity in human cadaver specimens.
4. A high correlation will occur between two FRFs from skin-mounted accelerometer measurements, taken before and after removing and replacing the accelerometer to the same position.

4.3 Methods

4.3.1 Porcine Cadaver Setup

Experiments on porcine cadavers were performed at the University of Alberta Swine Research and Technology Centre. Permission to use cadaveric porcine tissues was obtained from the Animal Policy and Welfare Committee of the Faculty of Agriculture, Forestry, and Home Economics at the University of Alberta (Appendix E). For the experiments described in Protocol 2, five pigs of breed Large White x Landrace or Duroc x (Large White x Landrace), each of 50-60 kg, were used. The gender of the cadavers was unknown. Each animal was first euthanized and eviscerated according to approved protocols at the University of Alberta Swine Research and Technology Centre. It was then placed on adjustable lift table, with rear legs overhanging the end of the table. A device consisting of two rigidly secured planks was designed to secure the rostral portion of the cadaver in place. The securing planks were applied at approximately the T12 vertebra rostrally. To support the rear of the cadaver, a rope-hoist system was devised. A rope was looped under the hip crease and was adjusted to lift the rear of the cadaver into a neutral position. This positioning equipment is shown below in Figure 4.1.

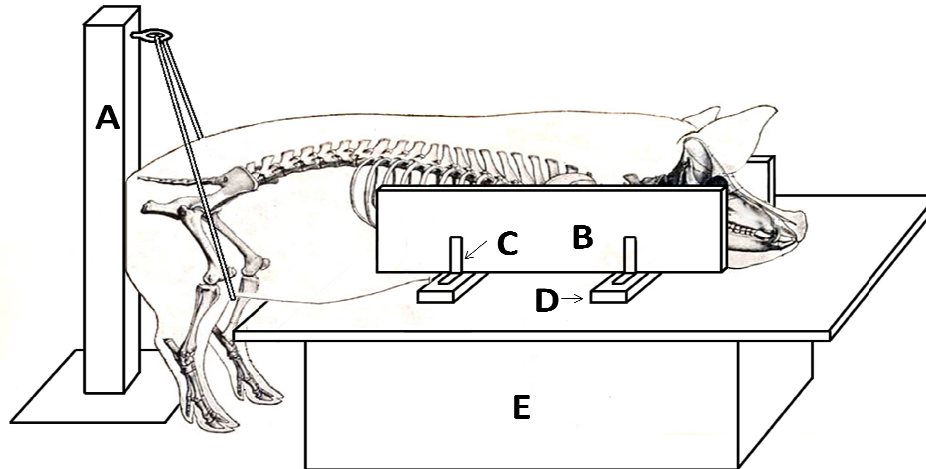


Figure 4.1 Porcine cadaver setup. A) Rope-hoist system; B) Lateral clamping wood; C) Hinged locking bracket; D) Cross-brace plank; E) Adjustable lift table

The 5 hour preparation and experimentation began immediately after euthanization of each animal, and was performed at approximately room temperature. Rigor mortis in adult pigs sets in at approximately 12-24 hours after death [Ranken et al. 1997]; The extent of the rigor in each animal was unknown, but is not likely to have been a significant factor in these experiments.

4.3.2 Human Cadaver Setup

Two female and three male human cadavers were also used for the experiments performed in Protocol 2. Human cadavers were obtained through the University Of Alberta Division of Anatomy's Anatomical Gifts Program. Permission to use human cadavers was obtained from the Health Research Ethics Board (Biomedical Panel) at the University of Alberta (Appendix D). All 5 unembalmed cadavers had been deceased for 24-72 hours at the time of testing. Human rigor mortis sets in at approximately 3-8 hours after death, and begins to disappear at

approximately 24 hours *post mortem* [Urdang 2004]. Experiments took approximately 4 hours to perform; however, it is unknown whether significant changes in rigor may have occurred over this time period. The age, sex, and physiologic condition of the cadavers were not pre-determined, and medical conditions such as cause of death were also unknown. Cadavers were placed in a prone position on the walled tray of an adjustable cadaver lift table. Cadavers were positioned with arms at their sides, and feet in a plantar-flexion position. Testing was performed in the Division of Anatomy Morgue at the University of Alberta, where cadavers were stored at approximately 68°F.

4.3.3 Equipment Setup

The equipment setup for porcine cadavers and human cadavers was identical, except where noted below. The skin of each cadaver was shaved, and then cleaned using a rubbing alcohol swab. The spinous processes of the lumbar vertebrae were next located by palpating the low back. The sacrum and the lowest ribs (joining at T-12 in humans, T-14 in pigs) were used as landmarks for this process. Upon locating the contours of each spinous process, the locations of the ends of the process were marked on the skin using a permanent marker. Hypodermic needles (21 gauge, 1.5 in, BD, Franklin Lakes, NJ) were installed into each of the L2, L3, and L4 spinous processes in a vertical fashion. A hammer was used to tap the needle into the spinous to ensure that the needle was securely embedded in the bone. One uniaxial accelerometer (model 352A24, PCB Piezotronics, Depew, NY) was glued to the hub of each needle using cyanoacrylate adhesive. A uniaxial accelerometer was glued to the skin over top of each of the L2, L3, and L4 spinous processes, in a rostral position with respect to the correspondingly installed needle. Care was taken to ensure the

accelerometer was positioned as close to the insertion point of the needle as possible without touching the needle stem.

Vibrations applied to the spine were created using an electrodynamic shaker (PA-138, Labworks, Costa Mesa, CA, USA), mounted to the crossbeam of an inverted U-shaped positioning frame positioned over the cadaver. To transmit the vibration to the spine, a number of components were fastened together in series. A stainless steel stinger rod of 30 cm in length was first screwed into the bottom of the shaker. Attached to the stinger was an impedance head (Model 288D01, PCB Piezotronics, Depew, New York), which was used to measure the vibration input to the spine. In porcine cadavers, a static load cell (Model ELFS-T3, Entran Sensors & Electronics, Fairfield, NJ, USA) connected to an oscilloscope (Model TDS 3014B, Tektronix, Inc., Beaverton, OR, USA) was screwed into the bottom of the impedance head, and was used to measure the static preload of the system on the spine. In human cadavers, a compression spring device was designed to measure the static preload on the spine. Further description of this device can be found in Appendix B. Finally, a Lexan contact tip was screwed to the bottom of the static load cell, and was used as the interface point to the spine. A number of different shapes of contact tip were used in this experiment, and will be discussed later in the methods. The full setup is shown below in Figure 4.2.

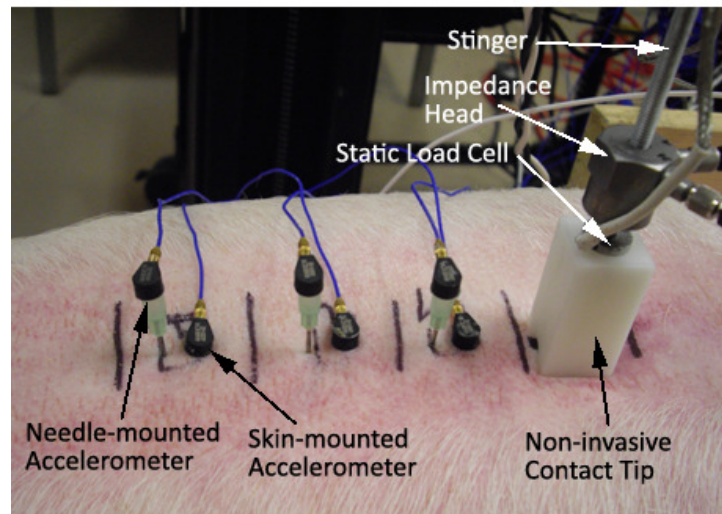
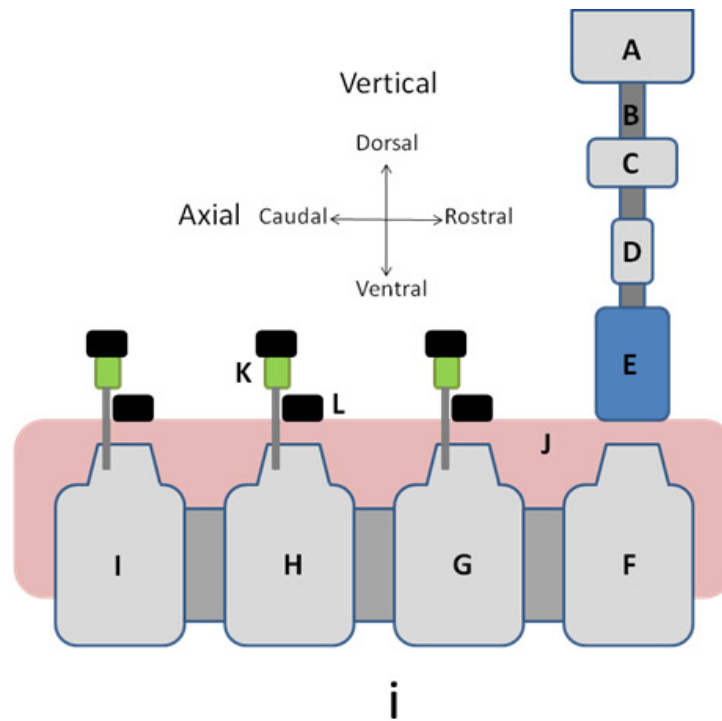


Figure 4.2 :i) Setup of non-invasive contact tip with skin-mounted accelerometers and needle mounted accelerometers. A: Shaker B: Stinger rod. C: Impedance head. D: Static load cell. E: Non-invasive contact tip. F: L1 Vertebra. G: L2 vertebra. H: L3 vertebra. I: L4 vertebra. J: Skin and soft tissue. K: Hypodermic needle inserted into vertebra with affixed accelerometer. L: Skin mounted accelerometer

ii) Photo of in-situ setup

To control the output of the electrodynamic shaker, PUMA Vibration Control and Analysis Software (Spectral Dynamics, San Jose, CA, USA) was used. A random burst protocol was selected from the software output options. Vibration of 0-2000 Hz was used in porcine subjects, while vibration of 0-1000 Hz was used in humans. The decision to reduce the frequency range in human cadavers was made based on preliminary cadaver testing, which showed no notable features above 1000 Hz. A resolution of 800 frames was used, meaning that in porcine subjects, frequency response measurements were taken every 2.5 Hz, while in humans, measurements were taken every 1.25 Hz. Due to the burst nature of the signal, no windowing was required. This signal was transmitted from the computer's D/A board to a linear power amplifier (PA-138, Labworks, Costa Mesa, CA). The linear power amplifier transmitted the signal to the shaker, which then produced the vibration output. Measurements of this output were taken from the uniaxial accelerometers, which were then passed to a breakout box. The breakout box returned the output signal to the computer, where the measurements were registered by the PUMA software.

4.3.4 Experiment Procedure

The contact tip was lowered onto the L1 spinous process. It was preloaded to 30 N in porcine cadavers, and 20 N in human cadavers. The decrease in preload for human cadavers was made due to the thinner skin in the human as well as the reduced amount of soft tissue posterior to each spinous process. To obtain the vibration response of the spine, 10 bursts of vibration were applied to the spine in porcine cadavers, and 20 bursts to human cadavers. The decision to change from 10 to 20 bursts was to obtain a more representative average signal. The response measured by the accelerometers and impedance head from these

bursts were averaged using an exponential averaging algorithm proprietary to the PUMA software. The averaged response comprised one 'test'.

Six different contact tips were used in these tests, each with varying shape at the spine interface end. Features of the tips were varied to determine how variations in the characteristics of the shape affected the measured vibration response. The six different contact tip shapes are shown below in Figure 4.3.

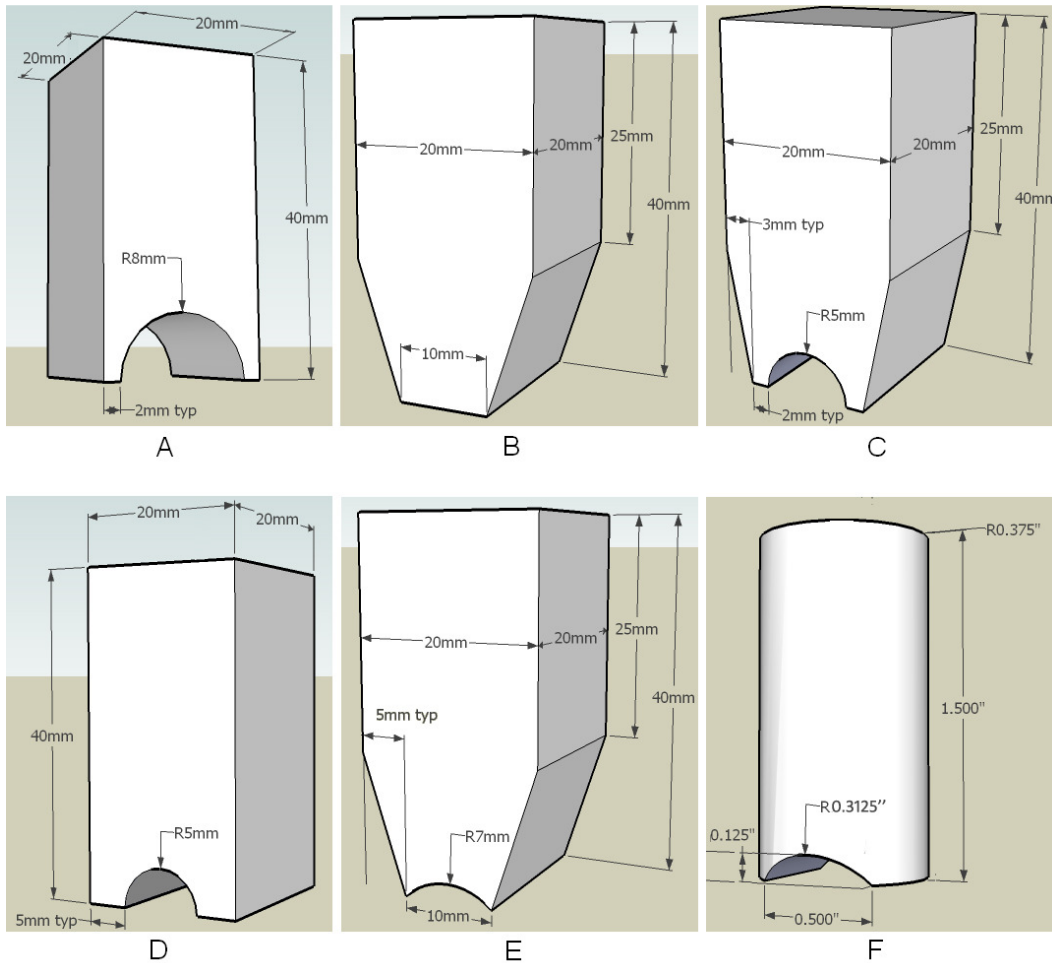


Figure 4.3: Contact tip shapes used in the Protocol 2 experiments.

For each contact tip shape, 5 tests were performed to obtain repeatability data. The order in which contact tips A, B, C, D, and F were used was randomized to reduce the chances of systematic effects occurring in the results. Testing always ended with contact tip E so as to perform replaceability testing that was comparable between subjects.

The replaceability of sensors to the skin was investigated next. Upon finishing the 5 repeatability tests using contact tip E, the skin-mounted accelerometers were removed from their initial skin positions, cleaned with acetone, and were re-adhered to the initial positions. Five more tests were taken. This replacement, re-adherence, and repeatability testing was performed one additional time. In total, each skin-mounted accelerometer was removed and replaced to its supposed initial position twice.

4.3.5 Data Analysis Techniques

A number of data analysis techniques were used to compare the obtained vibration response signals in this experiment.

To determine the correlation between skin and needle based accelerometers, the Global Shape Criteria and Global Amplitude Criteria were used. These techniques were previously described in Section 2.8.1 of the literature review.

The D-statistic was also used to determine the correlation of any two signals. To calculate the D-statistic, the 95% confidence interval of a set of original or baseline signals is first calculated. Next, the mean signal of a set of experimental signals is calculated. The percentage of the mean experimental signal that falls

within the 95% confidence bounds of the baseline signals is known as the D-statistic.

All statistical analyses in this protocol were performed using PASW Statistics 17 (SPSS Inc, Chicago, Illinois, USA). Mauchly's test was performed to determine whether sphericity was a factor in testing. Sphericity is the assumption that the variances of the differences between data taken from the same subject are equal [Field 2009]. For significant within subjects effects, a Bonferroni correction was applied to the significance level α . This correction was used to reduce the potential for Type 1 error by decreasing the α , and is a standard correction when multiple significance tests are performed on a set of data, as in a repeated measures ANOVA with multiple within subject factors [Field 2009].

Finally, data was only analyzed to 1000 Hz in porcine cadavers, though data was collected up to 2000 Hz. There were two reasons for this decision. Primarily, it was found that noteworthy vibration response did not occur past 1000 Hz in porcine cadavers. An example of this is shown in Figure 4.4. As this was also found to be the case in human cadavers, data was only recorded up to 1000 Hz in these subjects. Therefore, a secondary reason was to be able to compare results between cadaver types, the same frequency range was required for analysis.

4.4 Results

4.4.1 Repeatability of Tests

As previously mentioned, for each type of contact tip, 5 repeated tests were performed in all subjects. The repeated tests (FRFs) were measured at each of

the 6 accelerometers. Examples of these repeated measures are shown below in Figures 4.4-4.5, taken from subject 1 of the porcine experiments, and Figures 4.6-4.7, taken from subject 1 of the human experiments.

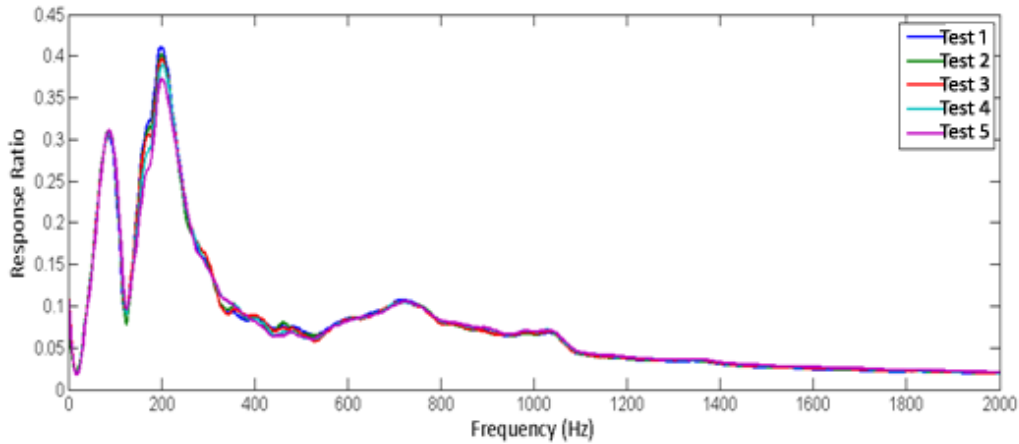


Figure 4.4: The 5 repeated tests measured at the L2 skin mounted accelerometer. Data taken from porcine subject 1.

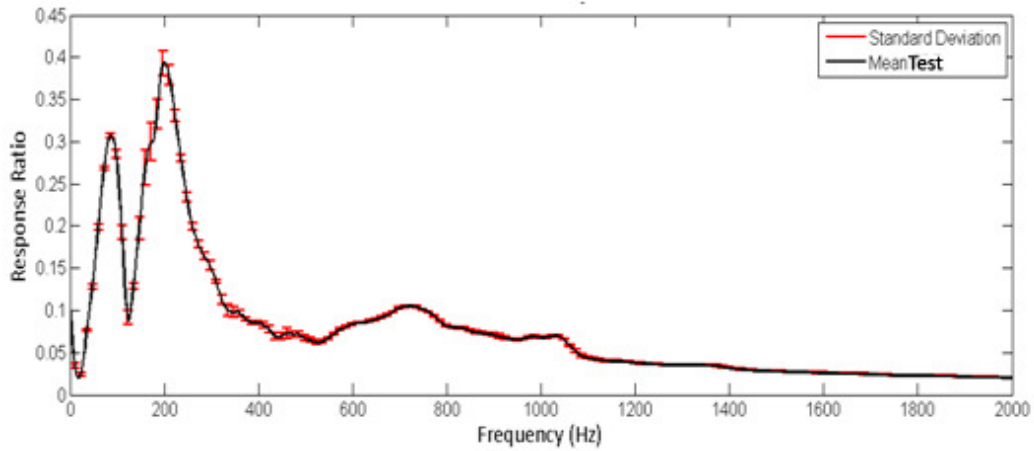


Figure 4.5: Mean FRF and standard deviation on the 5 repeated tests in Figure 4.4

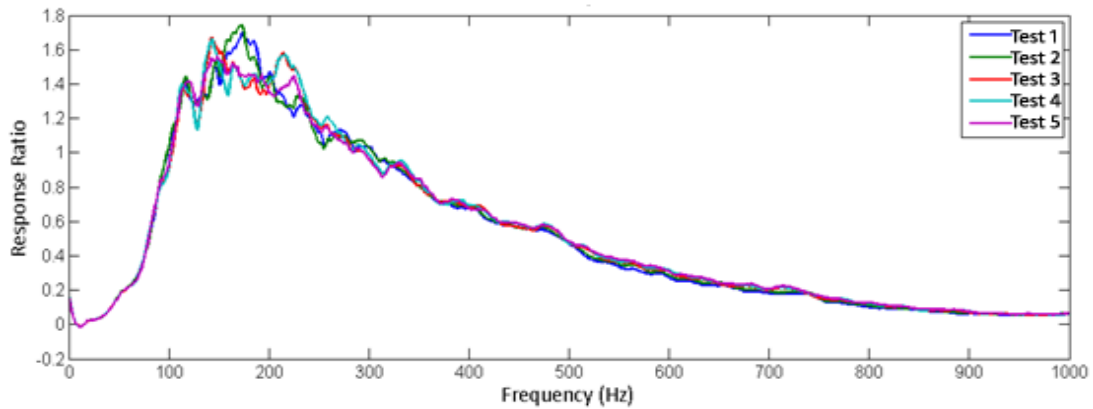


Figure 4.6: The 5 repeated tests measured at the L2 skin mounted accelerometer. Data taken from human subject 1.

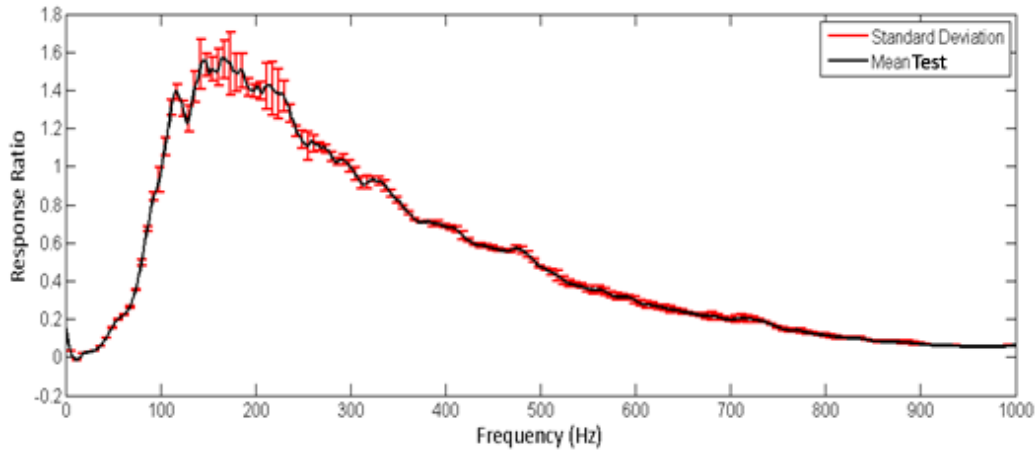


Figure 4.7: Mean FRF and standard deviation on the 5 repeated tests in Figure 4.6

The level of standard deviation indicated in each graph was typical for all subjects. For example, the average standard deviation was 0.0161 for Figure 4.7. Only one irregular signal occurred, in porcine subject 4, using contact tip B. An example test from this subject, from the L2 skin-mounted accelerometer is shown below in Figure 4.8.

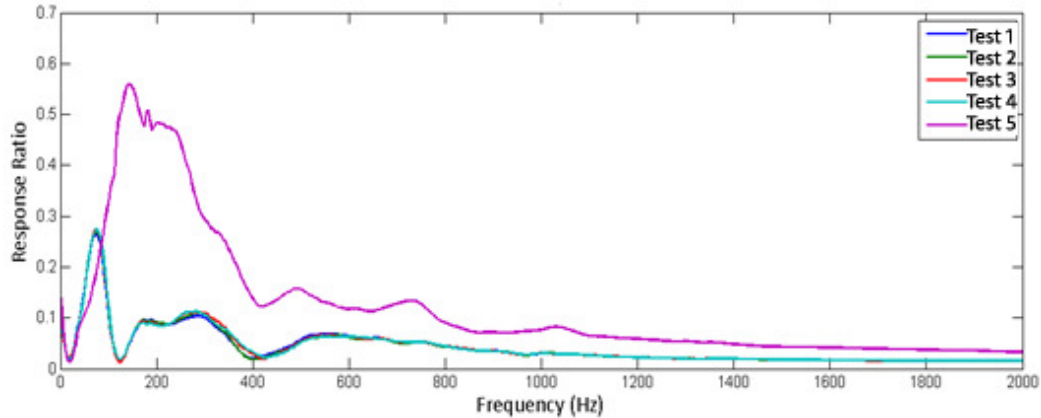


Figure 4.8: The five repeated measures FRFs taken from pig Subject 4, L2 skin-mounted accelerometer using contact tip B. Test 5 shows an outlier response.

As can be seen from Figure 4.8, the fifth test performed does not align well with the previous four tests. This effect occurred in all six accelerometer measurements. Upon reviewing the test notes, no anomalies in the test were noted. The cause of this significantly different measurement is unknown.

Due to the high repeatability of the signals, the Global Shape Criteria and Global Amplitude Criteria were used to calculate a global measure of repeatability for each contact tip in each subject. Table 4.1 below shows the mean GSC and GAC with 95% confidence interval for the cadaveric porcine experiments. Upper confidence intervals were truncated at 1.000, which represents perfect criteria matching.

Table 4.1: Results of GSC and GAC for the global accelerometer system in cadaveric porcine experiments.

		Mean GAC	Upper CI (95%)	Lower CI (95%)	Mean GSC	Upper CI (95%)	Lower CI (95%)
Tip A	Subj. 1	0.999	1.000	0.996	0.999	1.000	0.997
	Subj. 2	0.999	1.000	0.995	0.999	1.000	0.995
	Subj. 3	0.999	1.000	0.996	1.000	1.000	0.998
	Subj. 4	0.999	1.000	0.996	0.999	1.000	0.997
	Subj. 5	0.991	1.000	0.964	0.996	1.000	0.982
Tip B	Subj. 1	0.996	1.000	0.981	0.994	1.000	0.969
	Subj. 2	0.999	1.000	0.994	0.999	1.000	0.995
	Subj. 3	0.999	1.000	0.996	0.999	1.000	0.997
	Subj. 4	0.896	1.000	0.524	0.858	1.000	0.356
	Subj. 5	1.000	1.000	0.997	1.000	1.000	0.998
Tip C	Subj. 1	0.996	1.000	0.982	0.994	1.000	0.975
	Subj. 2	0.999	1.000	0.996	0.999	1.000	0.997
	Subj. 3	0.999	1.000	0.996	1.000	1.000	0.999
	Subj. 4	0.998	1.000	0.985	0.998	1.000	0.988
	Subj. 5	0.999	1.000	0.996	0.999	1.000	0.997
Tip D	Subj. 1	0.999	1.000	0.996	0.999	1.000	0.995
	Subj. 2	0.999	1.000	0.994	0.999	1.000	0.994
	Subj. 3	0.997	1.000	0.990	0.999	1.000	0.995
	Subj. 4	0.999	1.000	0.998	0.999	1.000	0.997
	Subj. 5	0.998	1.000	0.993	0.999	1.000	0.997
Tip E	Subj. 1	0.999	1.000	0.997	1.000	1.000	0.998
	Subj. 2	0.999	1.000	0.997	0.999	1.000	0.996
	Subj. 3	0.999	1.000	0.996	1.000	1.000	0.997
	Subj. 4	0.999	1.000	0.996	0.999	1.000	0.997
	Subj. 5	0.998	1.000	0.992	0.998	1.000	0.992
Tip F	Subj. 1	0.993	1.000	0.978	0.993	1.000	0.976
	Subj. 2	0.992	1.000	0.971	0.996	1.000	0.985
	Subj. 3	0.999	1.000	0.997	0.999	1.000	0.997
	Subj. 4	0.998	1.000	0.993	0.999	1.000	0.997
	Subj. 5	0.998	1.000	0.992	0.998	1.000	0.994

Similarly, Table 4.2 below shows the GSC and GAC results for the human cadaver experiments.

Table 4.2: Results of GSC and GAC for the global accelerometer system in cadaveric human experiments.

		Mean GAC	Upper CI (95%)	Lower CI (95%)	Mean GSC	Upper CI (95%)	Lower CI (95%)
Tip A	Subj. 1	0.995	1.000	0.960	0.998	1.000	0.952
	Subj. 2	0.988	1.000	0.938	0.998	1.000	0.980
	Subj. 3	0.989	1.000	0.961	0.994	1.000	0.975
	Subj. 4	0.994	1.000	0.972	0.997	1.000	0.979
	Subj. 5	0.996	1.000	0.980	0.997	1.000	0.981
Tip B	Subj. 1	0.994	1.000	0.965	0.999	1.000	0.983
	Subj. 2	0.985	1.000	0.935	0.997	1.000	0.977
	Subj. 3	0.976	1.000	0.911	0.988	1.000	0.917
	Subj. 4	0.990	1.000	0.958	0.996	1.000	0.963
	Subj. 5	0.988	1.000	0.941	0.995	1.000	0.975
Tip C	Subj. 1	0.989	1.000	0.935	0.995	1.000	0.937
	Subj. 2	0.992	1.000	0.962	0.999	1.000	0.980
	Subj. 3	0.987	1.000	0.946	0.991	1.000	0.946
	Subj. 4	0.993	1.000	0.969	0.997	1.000	0.977
	Subj. 5	0.993	1.000	0.967	0.995	1.000	0.963
Tip D	Subj. 1	0.990	1.000	0.924	0.995	1.000	0.947
	Subj. 2	0.995	1.000	0.974	0.999	1.000	0.988
	Subj. 3	0.994	1.000	0.980	0.997	1.000	0.985
	Subj. 4	0.993	1.000	0.967	0.996	1.000	0.974
	Subj. 5	0.994	1.000	0.974	0.996	1.000	0.972
Tip E	Subj. 1	0.996	1.000	0.977	0.999	1.000	0.977
	Subj. 2	0.978	1.000	0.892	0.996	1.000	0.963
	Subj. 3	0.994	1.000	0.968	0.997	1.000	0.977
	Subj. 4	0.988	1.000	0.950	0.996	1.000	0.968
	Subj. 5	0.991	1.000	0.962	0.993	1.000	0.966
Tip F	Subj. 1	0.998	1.000	0.986	0.999	1.000	0.992
	Subj. 2	0.989	1.000	0.965	0.996	1.000	0.985
	Subj. 3	0.989	1.000	0.938	0.991	1.000	0.928
	Subj. 4	0.997	1.000	0.985	0.998	1.000	0.987
	Subj. 5	0.992	1.000	0.965	0.995	1.000	0.966

The overall GSC and GAC ranged from 0.356-1.000 and 0.524-1.000 respectively in porcine cadavers, and 0.988-1.000 and 0.979-1.000 respectively in human cadavers.

4.4.2 Skin and Needle Mounted Accelerometer Correlations

The correlation between each needle-mounted accelerometer and its corresponding skin-mounted accelerometer was determined using the D-statistic. Table 4.3 below summarizes the D-statistic calculations on porcine cadaver subjects, calculated using the signal only up to 1000 Hz. Table 4.4 summarizes the same results for human cadaver subjects.

Table 4.3: D-statistic values comparing mean skin-mounted accelerometer FRF to the mean needle-mounted accelerometer FRF in porcine cadaver subjects.

		L2	L3	L4
Tip A	Subj. 1	1.25	1.00	0.00
	Subj. 2	0.00	0.50	0.00
	Subj. 3	0.00	2.49	16.96
	Subj. 4	0.25	0.00	0.00
	Subj. 5	0.50	0.75	4.24
Tip B	Subj. 1	0.00	0.50	0.25
	Subj. 2	0.25	0.75	0.25
	Subj. 3	6.48	0.25	0.50
	Subj. 4	13.22	0.75	2.24
	Subj. 5	0.00	0.00	0.50
Tip C	Subj. 1	4.74	0.75	0.75
	Subj. 2	2.24	0.75	0.25
	Subj. 3	0.50	6.23	2.74
	Subj. 4	0.00	0.00	1.00
	Subj. 5	2.24	0.50	1.50
Tip D	Subj. 1	1.50	0.75	1.50
	Subj. 2	0.75	0.00	1.00
	Subj. 3	0.25	2.00	17.46
	Subj. 4	0.00	0.50	0.50
	Subj. 5	6.48	0.00	0.50
Tip E	Subj. 1	0.00	1.25	0.00
	Subj. 2	1.25	0.25	0.75
	Subj. 3	1.25	0.25	0.25
	Subj. 4	0.25	0.00	0.50
	Subj. 5	2.74	0.00	0.75
Tip F	Subj. 1	6.73	6.23	0.25
	Subj. 2	1.75	0.50	0.75
	Subj. 3	6.98	0.00	2.74
	Subj. 4	10.47	0.25	0.25
	Subj. 5	1.25	1.25	3.99

Table 4.4: D-statistic values comparing mean skin-mounted accelerometer FRF to the mean needle-mounted accelerometer FRF in human cadaver subjects.

		L2	L3	L4
Tip A	Subj. 1	0.00	0.25	0.50
	Subj. 2	0.12	0.37	1.50
	Subj. 3	0.50	14.23	6.99
	Subj. 4	0.50	0.87	4.99
	Subj. 5	1.37	10.74	0.50
Tip B	Subj. 1	1.37	1.37	2.62
	Subj. 2	0.00	1.50	0.12
	Subj. 3	0.12	8.86	0.00
	Subj. 4	1.25	1.50	15.61
	Subj. 5	3.62	0.12	0.00
Tip C	Subj. 1	0.25	0.75	4.49
	Subj. 2	0.00	1.87	1.12
	Subj. 3	9.99	5.62	8.86
	Subj. 4	0.37	0.62	8.11
	Subj. 5	6.62	0.12	0.12
Tip D	Subj. 1	1.50	0.25	1.87
	Subj. 2	0.12	0.37	2.37
	Subj. 3	0.25	7.24	6.12
	Subj. 4	0.75	0.62	4.87
	Subj. 5	2.50	5.74	0.37
Tip E	Subj. 1	0.00	0.62	2.00
	Subj. 2	0.00	3.12	0.00
	Subj. 3	0.37	0.50	2.62
	Subj. 4	0.75	2.25	6.24
	Subj. 5	12.98	0.12	0.87
Tip F	Subj. 1	0.00	0.87	4.00
	Subj. 2	0.12	3.00	6.87
	Subj. 3	2.12	3.12	6.12
	Subj. 4	0.12	1.62	5.87
	Subj. 5	5.24	0.25	0.25

A repeated measures ANOVA was run on the D-statistic values, separately on the porcine cadaver subjects and human cadaver subjects ($\alpha=0.05$).

In porcine cadavers, Mauchly's test of sphericity indicated that the assumption of sphericity had not been violated ($\chi^2(2)=1.943$, $p>0.05$). The results show that measured D-statistic was not significantly affected by contact tip type, $F(5, 20)=.991$, $p=0.448$, effect size $r=0.217$, power=0.2799, vertebral level of measurement, $F(2, 8)=1.195$, $p=0.352$, effect size $r=0.361$, power=0.193, or the interaction effect, $F(10, 40)=1.366$, $p=0.231$, effect size $r=0.18$, power=0.595. The between subjects effect was found to be significant ($F(1,4)=12.719$, $p=0.023$, effect size $r=0.87$, power=0.76).

In human cadavers, Mauchly's test of sphericity indicated that the assumption of sphericity had not been violated ($\chi^2(2)=1.246$, $p>0.05$). The results show that measured D-statistic was not significantly affected by contact tip type, $F(5, 20)=0.269$, $p=0.925$, effect size $r=0.0.115$, power=0.101, vertebral level of measurement, $F(2, 8)=0.633$, $p=0.556$, effect size $r=0.271$, power=0.122, or the interaction effect, $F(10, 40)=1.281$, $p=0.274$, effect size $r=0.176$, power=0.561. The between subjects effect from the repeated measures ANOVA was found to be significant ($F(1,4)=17.031$, $p=0.015$, effect size $r=0.563$, power=0.863).

Figures 4.9-4.14 below show the D-statistic graphs for each of contact tips A-F from human subject 1, at the L4 vertebral level.

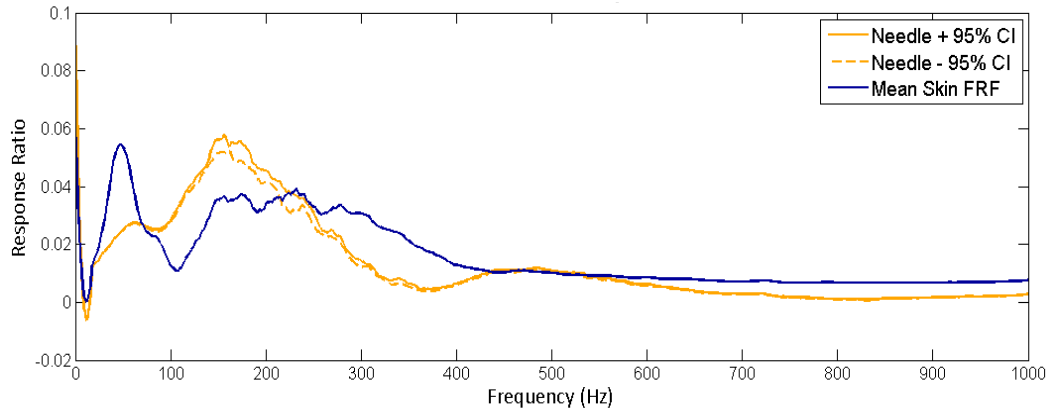


Figure 4.9: *D*-statistic on the measurement of the L4 vibration response using contact tip A in human subject 1. The figure shows the mean needle-mounted accelerometer FRF of the 5 repeated tests and the 95% confidence interval on the bone-mounted accelerometer FRFs of the 5 repeated tests. $D=0.5\%$

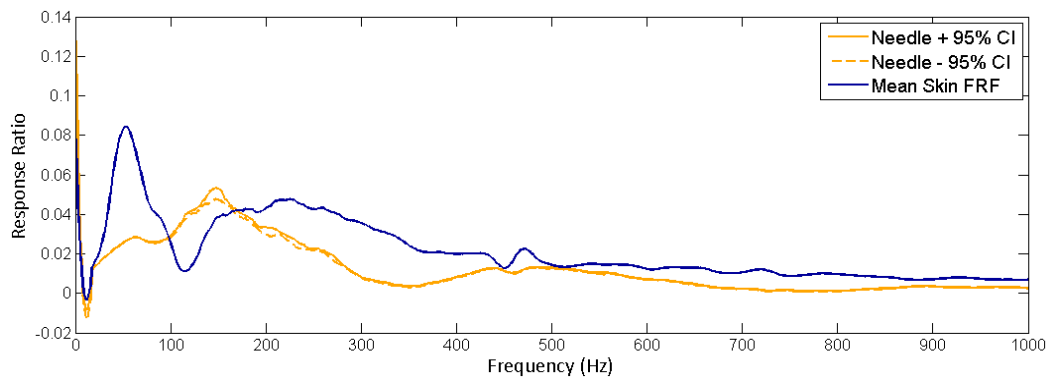


Figure 4.10: *D*-statistic on the measurement of the L4 vibration response using contact tip B in human subject 1. The figure shows the mean needle-mounted accelerometer FRF of the 5 repeated tests and the 95% confidence interval on the bone-mounted accelerometer FRFs of the 5 repeated tests. $D=2.62\%$

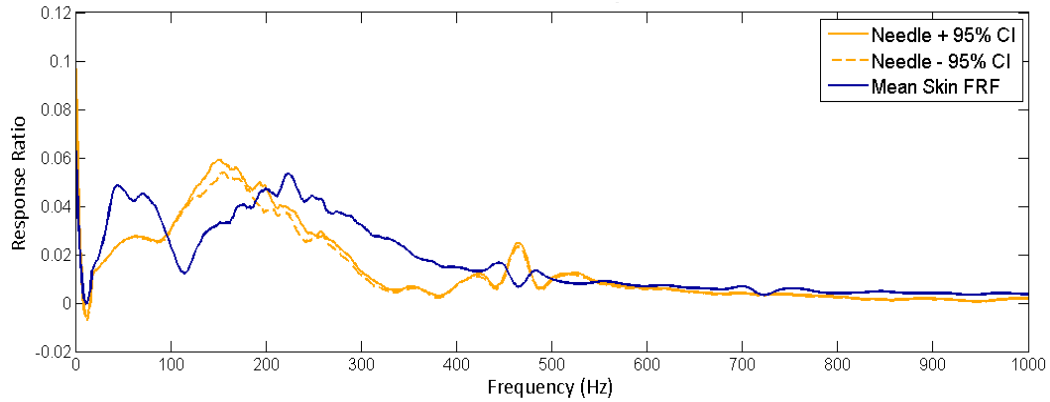


Figure 4.11: D-statistic on the measurement of the L4 vibration response using contact tip C in human subject 1. The figure shows the mean needle-mounted accelerometer FRF and the 95% confidence interval on the bone-mounted accelerometer FRFs. $D=4.49\%$

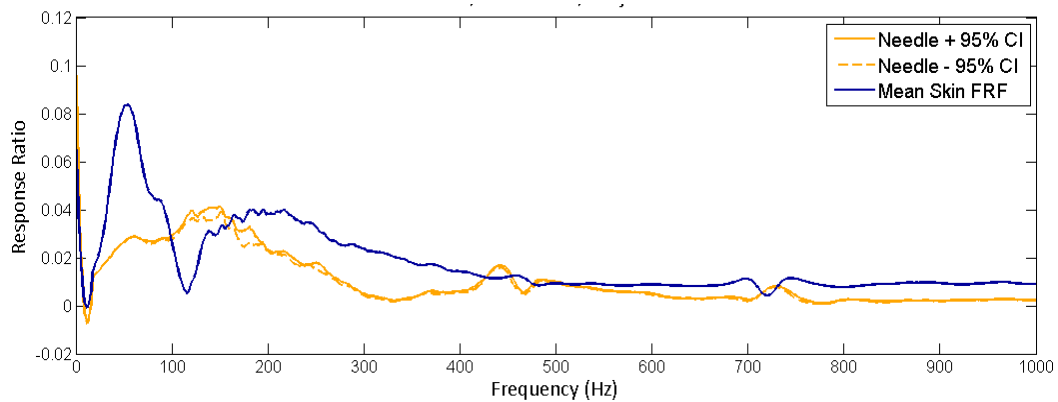


Figure 4.12: D-statistic on the measurement of the L4 vibration response using contact tip D in human subject 1. The figure shows the mean needle-mounted accelerometer FRF and the 95% confidence interval on the bone-mounted accelerometer FRFs. $D=1.87\%$

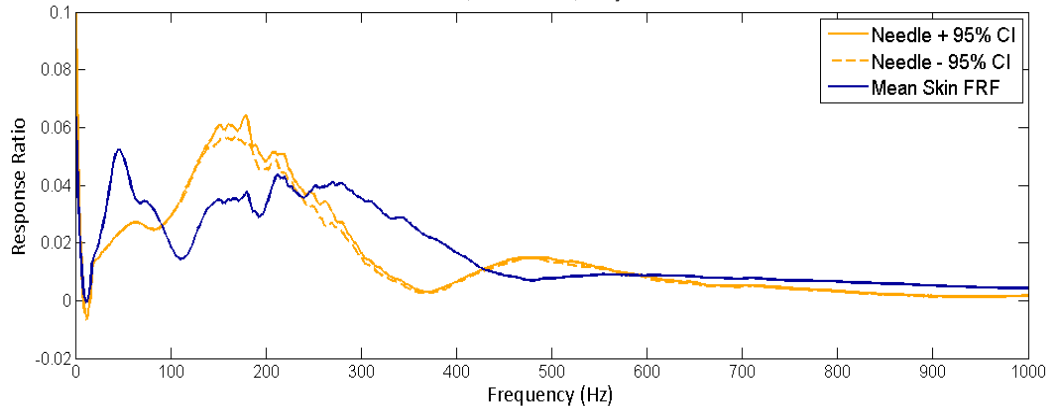


Figure 4.13: *D-statistic on the measurement of the L4 vibration response using contact tip E in human subject 1. The figure shows the mean needle-mounted accelerometer FRF of the 5 repeated tests and the 95% confidence interval on the bone-mounted accelerometer FRFs of the 5 repeated tests. $D=2.00\%$*

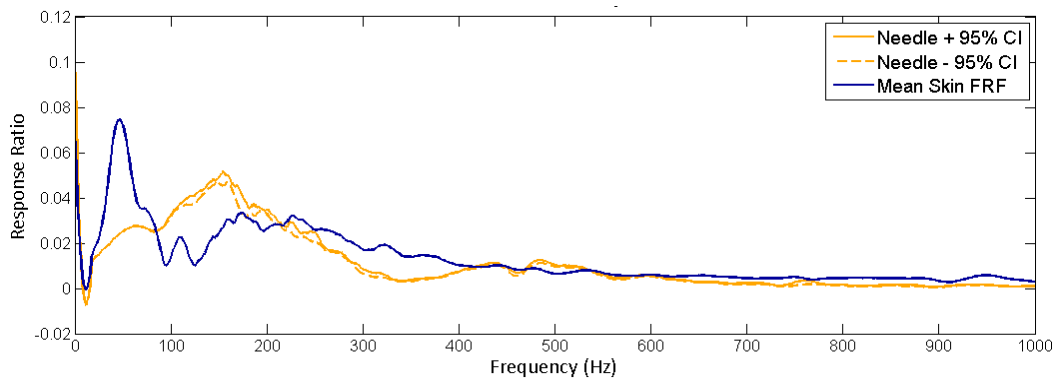


Figure 4.14: *D-statistic on the measurement of the L4 vibration response using contact tip F in human subject 1. The figure shows the mean needle-mounted accelerometer FRF of the 5 repeated tests and the 95% confidence interval on the bone-mounted accelerometer FRFs of the 5 repeated tests. $D=4.00\%$*

4.4.3 Replaceability of Skin-Mounted Accelerometers

Each of the skin-mounted accelerometers were removed from the skin, cleaned, and re-glued to their original positions over top of their respective vertebrae. This procedure was performed twice. Figure 4.15 below shows the three signals

obtained from the L4 skin-mounted accelerometer, from human cadaver subject 1.

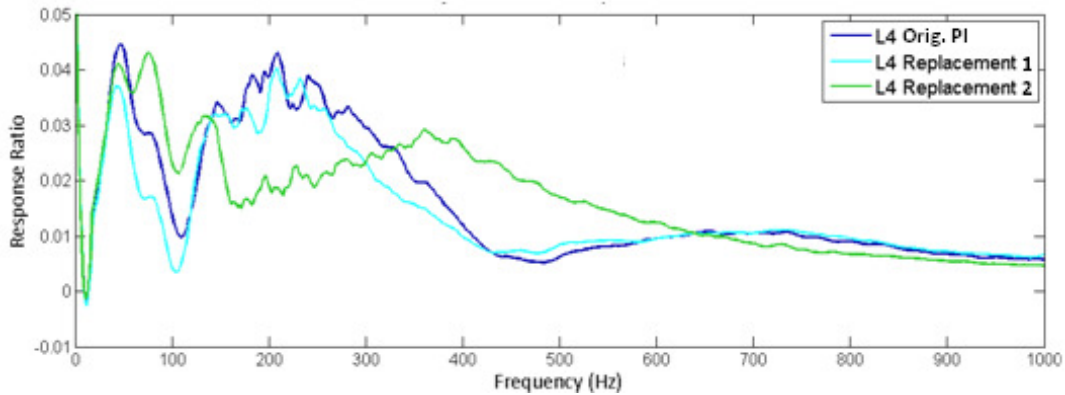


Figure 4.15: Three replacement signals obtained from the L4 skin-mounted accelerometer. Orig. PI. is the original signal, where replacement 1 and replacement 2 are signals obtained after removing and replacing the accelerometer to the skin.

The D-statistic was calculated to compare each mean ‘replacement’ signal (Rep. 1 or 2) to the original mean placement signal. The graphs depicting the confidence interval on the original placement were graphed with Rep. 1 and Rep. 2 mean FRFs, and are shown respectively in Figures 4.16 and 4.17 below.

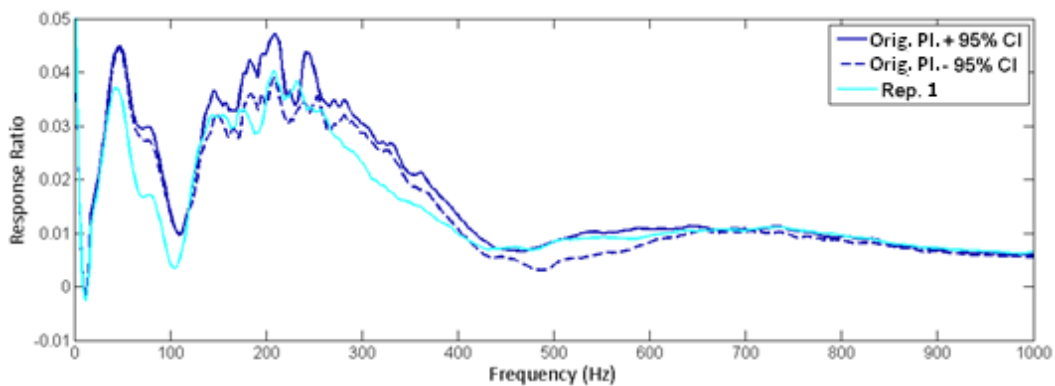


Figure 4.16: The 95% confidence interval on the original signal, compared to the first replacement signal (Rep. 1). $D = 36.45\%$

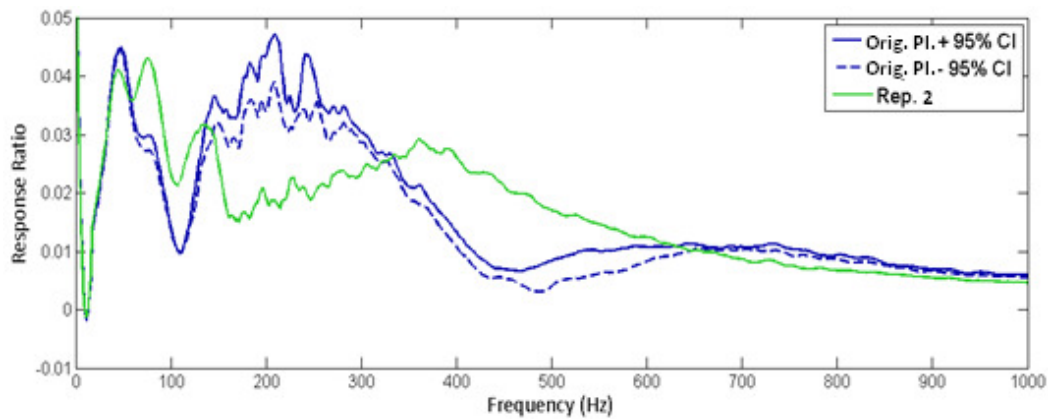


Figure 4.17: The 95% confidence interval on the original signal, compared to the second replacement signal (Rep. 2). $D = 4.24\%$

The full results of the D-statistic calculations are shown below in Table 4.5.

Table 4.5: D-statistic on replacements of the skin-mounted accelerometer to its original position in human cadaver subjects.

	L2 (%)		L3 (%)		L4 (%)	
	Rep. 1 - Rep. 2	Rep. 1 - Rep. 3	Rep. 1 - Rep. 2	Rep. 1 - Rep. 3	Rep. 1 - Rep. 2	Rep. 1 - Rep. 3
Subj. 1	14.36	0.62	5.12	9.61	36.45	4.24
Subj. 2	18.35	11.86	6.99	26.59	20.10	13.73
Subj. 3	25.47	19.60	24.59	9.11	21.85	19.60
Subj. 4	6.12	1.12	7.74	7.37	44.94	11.61
Subj. 5	16.35	25.22	9.24	38.20	17.60	8.61

A repeated-measures ANOVA was run on the data from Table 4.5, with $\alpha=0.05$. Mauchly's test of sphericity indicated that the assumption of sphericity had not been violated between repeats ($\chi^2(2)=0.638$, $p=0.808$) or for the interaction effect ($\chi^2(2)=3.889$, $p=0.143$). The results show that measured D-statistic was not significantly affected by repeat number, $F(1, 4)=2.979$, $p=0.159$, effect size $r=0.653$, power=0.265, vertebral level of measurement, $F(2, 8)=2.634$, $p=0.132$, effect size $r=0.498$, power=0.380, or interaction between the two effects, $F(2,$

8)=1.497, p=0.280, effect size r=0.397, power=0.232. Tests of between subjects effects showed a significant result (F(1,4)=97.694, p=0.001, effect size r=0.979, power=1.000).

4.4.4 ANOVA Results Summary

The results of the individual RM ANOVAs run in Protocol 2 are summarized below in Table 4.6.

Table 4.6: Summary of RM ANOVA findings for Protocol 2 results. Significant results are indicated by *. All ANOVAs were run at $\alpha=0.05$.

Description of ANOVA	Factor	Source	Pigs – p-value/power	Humans - p-value/power
RM ANOVA on D-statistic Matching Skin and Bone Signals	Within Subjects	Vertebral Level	0.352/0.449	0.556/0.122
		Tip Type	0.448/0.279	0.925/0.101
		Interaction (Level*Type)	0.231/0.595	0.274/0.561
	Between Subjects		0.023*/0.760	0.015*/0.863
RM ANOVA on D-statistic Matching Replacement of Skin mounted accel signals	Within Subjects	Vertebral Level	-	0.159/0.265
		Repeat	-	0.132/0.380
		Interaction (Level*Rep)	-	0.280/0.232
	Between Subjects		-	0.001*/1.000

4.5 Discussion

4.5.1 Repeatability of Measured Signals

As shown in Tables 4.1 and 4.2, the repeatability of signals was acceptably high. One notable exception occurred in porcine subject 4, contact tip B. Barring this exception, the confidence interval on any given subject did not fall below 0.892 in humans, and 0.969 in porcine subjects. These values constitute good repeatability [Heylen and Lammens 1996]. Furthermore, these values are consistent with values obtained in the Protocol 1 experiments.

The cause of the anomalous FRF in subject 4 contact tip B is unknown, but as the irregular signal was found in all channels, the cause was likely due to the vibration input and not the sensors. A potential cause of this issue may be due to the contact tip shape. Contact tip B has a fully flat bottom, with no curvature to secure it over the spinous process. It is possible that, for a number of the vibration bursts performed in creating the FRF signal, the tip may have slipped off the side of the spinous process unnoticed, causing a significant change in the input vibration to the system and therefore changing the measured amplitude ratio.

4.5.2 Effect of Distance between Contact Tip and Accelerometer

A representative graph showing the vibration response measured by the skin mounted accelerometers at each of L2, L3, and L4 in porcine subject 1 is shown below in Figure 4.18.

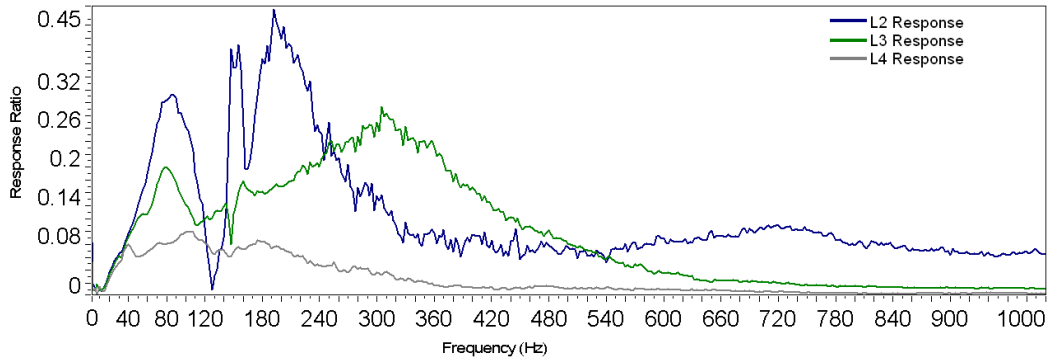


Figure 4.18: Measured vibration response at L2, L3, and L4 by skin-mounted accelerometers. Data taken from porcine subject 1, using contact tip A.

The graph shows that with increasing distance from the contact tip, the amplitude response decreases.

This type of behaviour is supported by the literature. Zhang et al. measured skin surface waves transferred to the skin by a small mechanical shaker at various points in the body, such as the mid-back, forearm, and calf [Zhang et al. 2008]. By measuring a steady state 200 Hz propagating surface wave at 2 mm increments, they were able to determine that the waves had roughly linearly decreasing phase with increasing distance from the skin contact tip. Therefore, the waves were attenuated to some degree by the skin and soft tissues. A study by Sörensson et al. describes the transmission of random vibration from the knuckle to the elbow of a hand gripping a handle [Sörensson and Burström 1997]. Comparing the energy transmission at each of the knuckle, wrist, and elbow, it was found that 50% of the signal energy had been absorbed by the time it reached the knuckle, 85% before the wrist, and 90% before the elbow. This further supports the theory of vibration attenuation by soft tissues.

The attenuation of the vibration transmitted through the skin did not increase the correlation between the skin-mounted accelerometer and needle-mounted

accelerometer at each vertebral level, as no significant findings occurred when a repeated-measures ANOVA was run. While amplitudes of the two signals became more comparable with increasing distance, signal shapes remained dissimilar. Representative graphs showing the attenuation of the signal in human cadaver subject 1 using contact tip A are depicted below in Figures 4.19-4.21, for the L2, L3, and L4 vertebrae respectively.

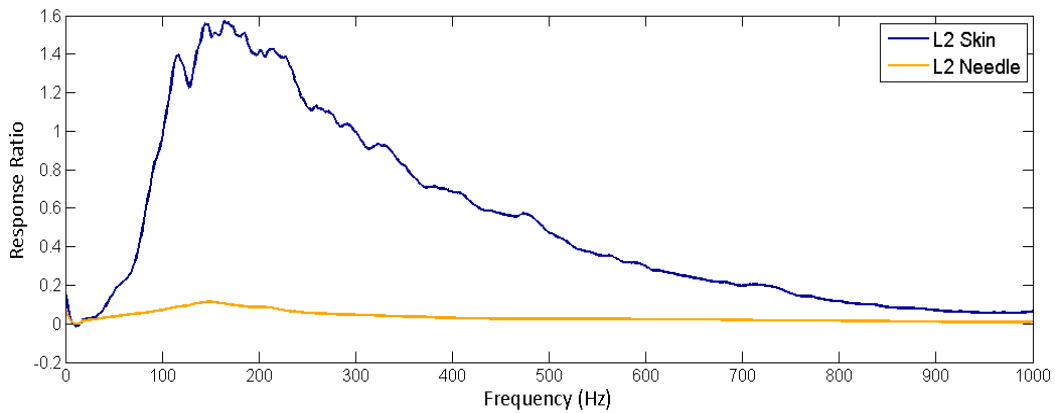


Figure 4.19: L2 Skin-mounted accelerometer (blue) and bone-mounted accelerometer (orange) mean FRF of the 5 repeated tests using contact tip A. The mean of all tests is shown for both signals.

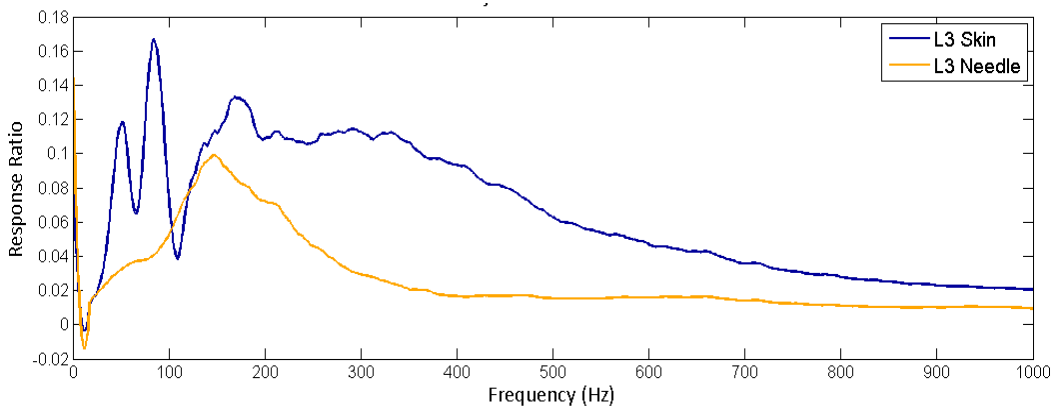


Figure 4.20: L3 Skin-mounted accelerometer (blue) and bone-mounted accelerometer (orange) mean FRF of the 5 repeated tests using contact tip A. The mean of all tests is shown for both signals.

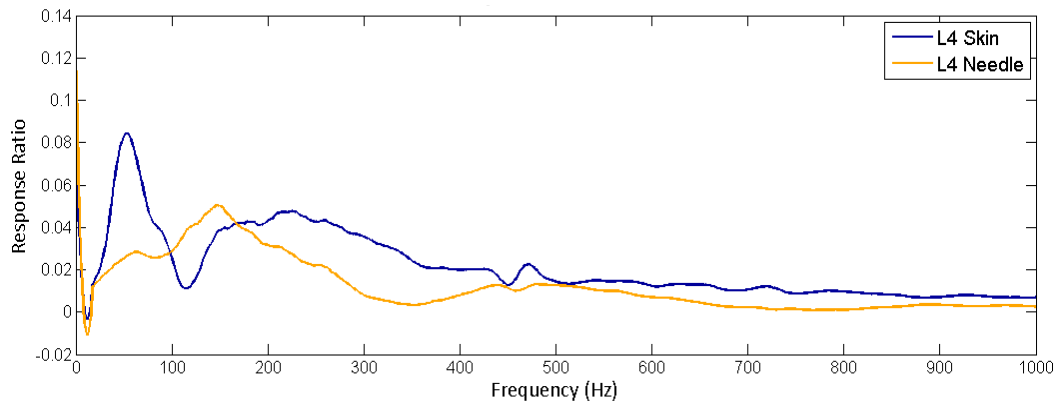


Figure 4.21: L4 Skin-mounted accelerometer (blue) and bone-mounted accelerometer (orange) mean FRF of the 5 repeated tests using contact tip A. The mean of all tests is shown for both signals.

4.5.3 Contact Tip Shape Effect

The results in Tables 4.3 and 4.4 demonstrate that changes in contact tip shape did not change the level of correlation between the skin-mounted accelerometer FRFs and their corresponding bone-mounted accelerometer FRFs. There were no significant differences found between tip shapes or vertebral levels, in either porcine cadavers or human cadavers. Figures 4.22-4.24 below show a comparison of signals taken from human cadaver subject 1 at each of the L2-L4 vertebrae.

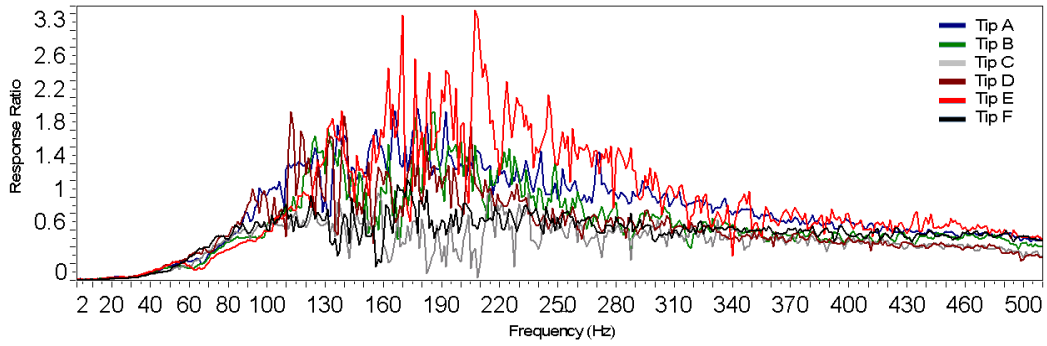


Figure 4.22: Signals taken from human subject 1 at the L2 vertebra for each of the contact tips used. Data shown to 500 Hz.

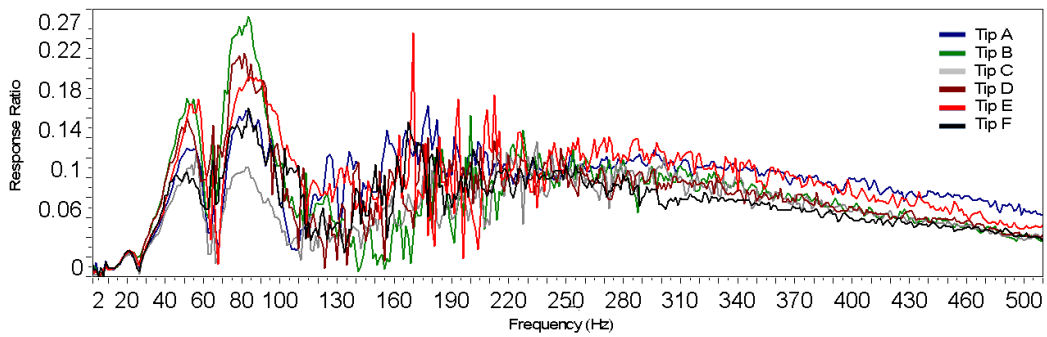


Figure 4.23: Signals taken from human subject 1 at the L3 vertebra for each of the contact tips used. Data shown to 500 Hz.

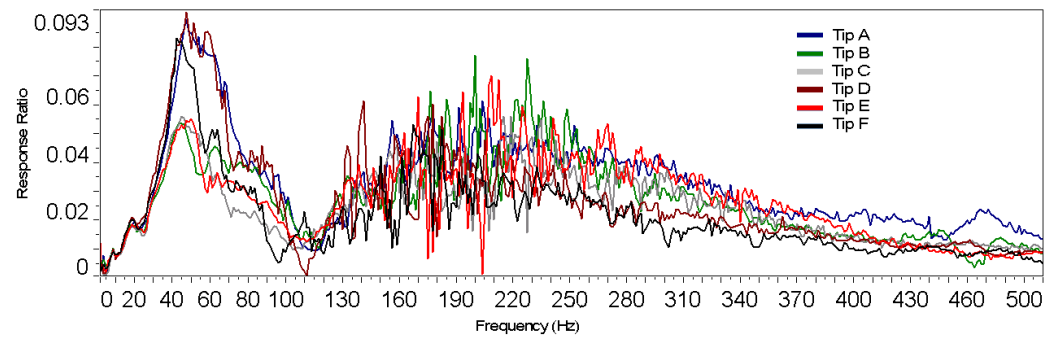


Figure 4.24: Signals taken from human subject 1 at the L4 vertebra for each of the contact tips used. Data shown to 500 Hz.

These signals all show somewhat similar response shapes, while different in amplitude.

To the knowledge of the investigator, there have been no full-scale studies investigating the impact of contact tip shapes on the measured vibration response. Steele et al. summarize the effect of a number of tip shapes used in vibration experiments evaluating the stiffness of the human ulna, shown in Figure 4.25 [Steele et al. 1988].

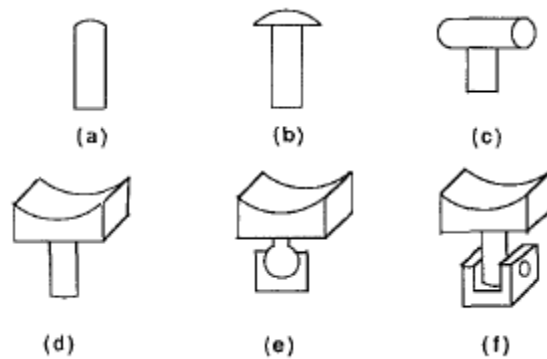


Figure 4.25: Evolution of contact tip shapes used by Thompson et al. and Steele et al. [Thompson et al. 1976]. Tips a) and b) were found to be painful and induced secondary resonances of the skin. Tip c) eliminated this problem, but tips d) e) and f) were found to attain the highest repeatability in data. Figure taken from Steele et al. [Steele et al. 1988]

The contact tips in Steel et al.'s investigation were placed on the ulna and vibration up to 1000 Hz was inputted. The impedance of the system was measured at the contact tip. They determined that probe tips with a small circular surface area tended to increase the preload pressure beyond the pressure-pain threshold, and created a secondary resonance that may have been caused by side-slipping of the skin on the bone. It was discovered that a curved tip, such as those shown in d), e), and f), adequately contacted the skin uniformly without causing discomfort or interfering with the measurements. However, the

impact of these tips on creating surface waves on the skin is unknown. Though the tips used in Protocol 2 were of similar shape, a direct comparison of their impact on measurements cannot be made, as the measurements by Steele et al. were made at positions not in-line with the tips. It should be noted that tips d), e), and f) from Steele et al. are similar in shape to those used in this protocol.

Though the D-statistic calculations did not turn out to be significantly different, the shapes of both the skin and bone signals shown in Figures 4.9-4.14 clearly have some differences between contact tips used. For example, in these graphs, contact tip C has two equal peaks at 50-60 Hz, while all other tips have one main peak with a much smaller secondary peak. The D-statistic is highly dependent on the level of repeatability of the bone signal; a high repeatability with a tight confidence interval may inevitably create a lower D-statistic. Therefore, subtle changes caused by the contact tip shape differences may not be adequately detected using this analysis technique. Analysis techniques to aid in the discovery of subtle differences in the FRF signals should be sought. No satisfactory techniques were available at the time of analysis, to the investigator's knowledge. This difficulty is discussed further in Chapter 5.

4.5.4 Correlation of Skin and Bone signals in Porcine vs. Human Cadavers

There was no significant difference found in the correlation level between porcine and human cadavers. This result was unexpected. Dellaleau et al. showed that, for optimal correlation between a skin and bone signal, the skin thickness had to be accounted for [Delalleau et al. 2008]. The porcine cadavers had a roughly homogeneous body type and skin thickness, potentially due to their similarities in breeding factors (breed, age), as well as their environment

and lifestyle (feeding amounts and times, activity levels, living environment). It was hypothesized that, due to the highly heterogeneous physical characteristics of the human cadavers, the level of correlation would vary significantly. The human cadavers used were found to be highly heterogeneous, with two males and three females, age range from 62-97 years old, and weight range of 125-190 lbs. Additionally, the observed skin condition in the lumbar area ranged from very thin, loose, and inelastic, to thick and highly elastic. Because of these factors, it was hypothesized that a minimal between-subjects effect would be observed in porcine cadavers, while it would be significant in human cadavers. The results show that significant between-subjects effects were found in both types of cadaver. Differences in subject musculature may account for some of these discrepancies, particularly in human subjects. Cornelissen et al. discovered that muscle mass surrounding the human tibia significantly influenced the level of damping and the resonant frequency of the bone [Cornelissen et al. 1987]. It follows that this type of behaviour may apply to other areas of the body, such as the spine. Furthermore, Cornelissen et al. also found that the resonant frequencies were not as affected when the tibia was left in a free-free state during testing, versus whether the limb was supported (thereby having significant boundary conditions). In the experiments performed for this protocol, supports were used at both ends of the spine. While the setup performed for each subject was similar (within cadaver type), measurements of forces or specific loading on the spine caused by the supports were not taken. Therefore, this could have caused significant differences between subjects, even in porcine cadavers apparently similar in body type.

It was further hypothesized that comparisons of the skin FRFs to the bone FRFs would have overall higher correlation in human subjects than in porcine subjects. Potts et al. showed that low-frequency vibration travelled through the stratum corneum layer of the skin, which is significantly thicker in porcine subjects than in humans. They also showed that high frequency vibration

travelled through the deeper tissues below the stratum corneum layers [Potts et al. 1983;Potts et al. 1984]. Due to the increased stratum corneum and thickness of soft tissue surrounding the spine in porcine cadavers, it was thought that the vibration carried through the skin would increase, thereby producing poorer D-statistic correlation between skin and bone signals in porcine cadavers. However, the overall level of correlation did not improve when moving from porcine to human cadavers. Potts et al. also showed that younger, more moist skin was able to damp out low frequencies much quicker than older, dryer skin [Potts et al. 1984]. This finding is supported by Elsner, who noted that skin with more moisture content causes the skin to be softer and more elastic [Elsner et al. 2001]. Potts tested an age range of 24-63 years old. The age range of our cadavers was from 62-97 years old. Extrapolating from Potts' results, it could be that the vibration was not readily damped out in our elderly human subjects. In addition to age related effects on the vibration signal, the moisture content in the skin of the cadavers may have been somewhat reduced due to illness before death, or may have decreased in the time between death and testing due to natural dehydration. The skin moisture level was not quantified in these experiments. Therefore, the potential improvements in the D-statistic correlation due to the thinner stratum corneum may have been negated by the dryness or age of the skin.

The small number of subjects tested in these experiments did not allow for generalizations to be made about the influences of subject musculature or body fat content. An expanded study size would greatly aid in this area. Proper measurements and analysis of body fat content, musculature, skin moisture content and skin elasticity would greatly aid in creating generalized theories on the influence of skin and soft tissues in spinal vibration response testing.

The technique of measurement of bone vibration using needle-mounted accelerometers requires further investigation, as was discussed in Protocol 1.

The issues encountered in performing Protocol 2 experiments are much the same as those found in Protocol 1. These issues are briefly reviewed here. In Protocol 2 experiments, the needle installation technique did not allow the needle-mounted accelerometer axes to be fully aligned with the skin-mounted accelerometers in their axes of measurement. Therefore, some of the differences between the skin signals and the bone/needle signals may be attributed to slightly misaligned sensor axes. Future work to investigate the significance of this factor could include a simple experiment involving measuring a known vibration input into a sawbones spine through accelerometers mounted to the vertebrae. The angles of the accelerometers could be incrementally changed to determine the effect of misalignment on the measurement of the spinal vibration response. An investigation into improved methods of installation, for example drilling pilot holes, would aid in solidifying the hypodermic needle as a viable technique for measuring the bone vibration response. Furthermore, it is not known whether the natural resonance of the needle played a role in altering the measured bone signal. Future testing could investigate the influences on the natural frequency of the needle by testing using a protocol similar to that of Rostedt et al. [Rostedt et al. 1995]. Using an impulse or pluck excitation to induce needle vibration, different needle installation depths compared systematically with different thicknesses of soft tissue covering the bone could be used to determine the natural frequency of the needle.

Finally, as noted in the discussion of Protocol 1, the low D-statistic values may simply have been a result of the nature of the calculation. The D-statistic relies on a 95% confidence interval based on repeated measures of a control signal (bone/needle signal), compared to the mean measure of an experimental signal (skin signal). Due to the extremely high repeatability of the vibration response measurements, the confidence interval on the needle mounted accelerometer's measured vibration response was very tight. This tight confidence interval would

mean that even small deviations in the skin-measured signal would produce a poor correlation.

4.5.5 Replaceability of Skin-Mounted Accelerometers

It was hypothesized that the correlation would be excellent between two FRFs from skin-mounted accelerometer measurements, taken before and after removing and replacing the accelerometer to the same position. Table 4.5 showed the repeatability of replacing the sensors back to their original positions to be highly variable, and generally poor. The mean replaceability D-statistic values in this Protocol (performed in human cadavers only) ranged from 10.74-28.19, while, in Protocol 1 (performed in porcine cadavers only), the mean repeatability D-statistic value was 5.04 %. Therefore, there may be improved replaceability in human cadaver subjects.

As in Protocol 1, there may be similar reasons for the low replaceability. It was found through those experiments that non-invasive contact tip testing is highly sensitive to changes in the placement of the accelerometers. Though the placement of the accelerometers was marked on the skin, experimenter error in replacing the accelerometer precisely to its original position could contribute to differences in the signals. Furthermore, the skin in the human cadaver subjects was able to be shifted small distances over top of the bone without rebounding to its original position. Therefore, small movements of the skin caused by removing and/or replacing the accelerometer to the skin may have caused changes in the measured FRFs.

As previously noted in the discussion of Protocol 1, these results have significant implications when considering the use of skin-mounted sensors in a spinal

diagnostic device. Changes in the FRF measured from a skin-mounted accelerometer would be assumed to be due to changes in the spinal vibration response. Differences in the FRFs caused by small variances in the placement of the accelerometers would make changes in the spinal vibration response immeasurable. Determination of the cause of the differences in the placement signals should be a primary focus of future investigations. One potential cause, the influence of cadaveric tissues, was previously noted in the discussion of Protocol 1. Testing in Protocol 1 and Protocol 2 occurred in cadaveric tissues. Shifting of the skin that may have occurred during the removal or replacement of the accelerometer may not return to its original position in the way a live tissue would. Therefore, replaceability tests should be performed in live human subjects to determine whether the replaceability improves in these subjects.

4.6 Conclusions

An acceptably high repeatability of a measured vibration response signal can be obtained from both porcine and human cadavers using a non-invasive contact tip.

It was hypothesized that the correlation between the skin-mounted and bone-mounted accelerometers would increase with increasing distance from the contact tip. Furthermore, it was hypothesized that contact tip shape would make a significant difference in the correlation between these two accelerometers. However, it was concluded that contact tip shape did not significantly affect the correlation between a skin-mounted and needle-mounted accelerometer. The type of cadaver used (human or porcine) did not affect the level of correlation, contrary to our hypothesis.

Finally, as initially discovered in Protocol 1 and confirmed here in Protocol 2, the removal and replacement of a skin mounted accelerometer to its original skin position yields poor D-statistic correlation values.

4.7 References

Cornelissen M, Cornelissen P, van der Perre G, Christensen AB, Ammitzboll F, Dyrbye C. Assessment of tibial stiffness by vibration testing in situ--III. Sensitivity of different modes and interpretation of vibration measurements. *J Biomech* 1987;20(4):333-342.

Delalleau A, Josse G, Lagarde JM, Zahouani H, Bergheau JM. A nonlinear elastic behavior to identify the mechanical parameters of human skin in vivo. *Skin Res Technol* 2008;14(2):152-164.

Elsner P, Berardesca E, Maibach HI, editor. *Bioengineering of the skin: skin biomechanics*. CRC Press; 2001.

Field. Field A, editor. *Discovering Statistics Using SPSS*. 2 ed. Sage Publications Ltd; 2009. 821 p.

Hamza M, editor. *FRAC: A consistent Way of Comparing Frequency Response Functions*. Proceedings of the International Conference on Identification in Engineering Systems; Innisbruck, Australia: 1996. 48 p.

Kawchuk GN, Decker C, Dolan R, Carey J. Structural health monitoring to detect the presence, location and magnitude of structural damage in cadaveric porcine spines. *J Biomech* 2009;42(2):109-115.

Kawchuk GN, Decker C, Dolan R, Fernando N, Carey J. The feasibility of vibration as a tool to assess spinal integrity. *J Biomech* 2008;41(10):2319-2323.

Montagna W, Yun JS. The Skin of the Domestic Pig. *J Invest Dermatol* 1964;42:11-21.

Potts RO, Buras EM, Chrisman DA. Changes with age in the moisture content of human skin. *J Invest Dermatol* 1984;82(1):97-100.

Potts RO, Chrisman DA, Buras EM. The dynamic mechanical properties of human skin in vivo. *J Biomech* 1983;16(6):365-372.

Ranken MD, C G J Baker, Kill RC, editor. *Food Industries Manual* 1997. Aspen Publishers; 1997.

Rostedt M, Broman H, Hansson T. Resonant frequency of a pin-accelerometer system mounted in bone. *J Biomech* 1995;28(5):625-629.

Steele CR, Zhou LJ, Guido D, Marcus R, Heinrichs WL, Cheema C. Noninvasive determination of ulnar stiffness from mechanical response--in vivo comparison of stiffness and bone mineral content in humans. *J Biomech Eng* 1988;110(2):87-96.

Sörensson A, Burström L. Transmission of vibration energy to different parts of the human hand-arm system. *Int Arch Occup Environ Health* 1997;70(3):199-204.

Thompson GA, Young DR, Orne D. In vivo determination of mechanical properties of the human ulna by means of mechanical impedance tests: experimental results and improved mathematical model. *Med Biol Eng* 1976;14(3):253-262.

Urdang L, editor. The Bantam medical dictionary. Bantam; 2004. 713 p.

Zhang X, Kinnick RR, Pittelkow MR, Greenleaf JF. Skin viscoelasticity with surface wave method. Proceedings - IEEE Ultrasonics Symposium 2008;2008:651-653.

Chapter 5: Discussion of Overall Results

5.1 Introduction

In Chapters 3 and 4, discussions were presented regarding individual protocol elements as well as a discussion of support for or against the hypotheses presented in each chapter. This chapter will integrate the aspects of Chapters 3 and 4 when they are considered together. Specifically, novel discussion will be presented that revolves around similarities, dissimilarities and synergies between Chapters 3 and 4 that were not addressed in the individual chapters. In addition, this chapter will discuss the project as a whole in terms of overall strengths, weaknesses, and assumptions. Finally, the significance of the work as a whole will be put into perspective, and future directions for this topic area will be discussed.

5.2 Discussion of Overall Results

5.2.1 Signal Attenuation Due to Soft Tissues

5.2.1.1 Overview of Findings

The dissipation of vibration with increasing distance from the contact tip was demonstrated through two different mechanisms observed separately in Protocols 1 and 2: dissipation of vibration transmitted through the skin and soft tissues, and dissipation of vibration transmitted through the spine. Specifically, in

Protocol 1, vibration was shown to travel to a skin based accelerometer via the skin and soft tissues. This was shown by systematically changing the placement of a skin-mounted accelerometer and comparing the resulting FRFs. An amplitude effect on placement changes was shown when performing the experiments with a non-invasive contact tip, while no amplitude effect was observed on placement changes when using the invasive contact tip. In Protocol 2, measurements of the spinal vibration response were taken by both skin-mounted and needle-mounted accelerometers at each of the L2-L4 vertebrae. Vibration was applied at L1, to determine whether distance between the measurement and vibration application points made a difference on the vibration transmitted through the skin. From these results, it was shown that much of the vibration signal transmitted through the soft tissue dropped off quickly over the length of one spinous process. This demonstrated that vibration transmitted to the spine decreased in amplitude with increasing vertebral distance from the contact tip, as was shown in Figure 4.18. This type of behaviour was found in both porcine and human cadavers. Despite the decreasing signal amplitude, it was found that the spinal vibration response could be measured at least 3 segments away (i.e. at L4) from the contact tip input point (i.e. at L1).

5.2.1.2 Discussion of Findings

Given the above, several statements can be made with some degree of confidence. First, vibration propagation through the skin created by the non-invasive contact tip is likely damped by the skin itself. Vibration propagation through the spine is likely damped by both the compliance of the soft tissues of the spine itself, as well as the surrounding fat and musculature [Cornelissen et al. 1987].

In both cases, this damping by soft tissues can be explained by the equations for damping ratio and spring constant, which are respectively:

$$\zeta = \frac{c}{2\sqrt{km}}$$

(12)

Where

$$k = \frac{F}{x}$$

(13)

Where ζ is the damping ratio, c is the damping coefficient of the system, k is the spring constant of the system, m is the mass under oscillation, F is the applied force to the mass, and x is the displacement of the mass from its equilibrium position. It can be seen from equation 13 that as more force is required to move a mass a given distance, the spring constant increases; more 'elastic' substances are likely to have lower spring constants. Keeping this in mind with respect to equation 12, we see that smaller k values produce larger damping ratios. The effect of changing damping ratios is shown below in Figure 5.1.

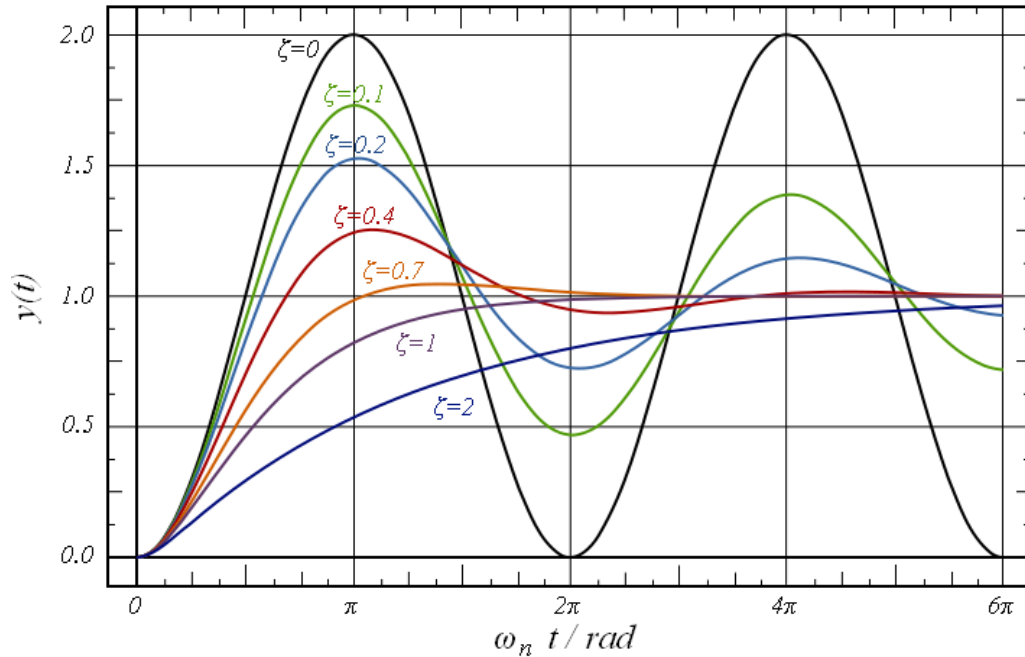


Figure 5.1: Amplitude response of a perfectly oscillating signal under various damping conditions. Increasing damping ratio ζ decreases the time taken to reach a steady response.

Figure 5.1 shows the effect of changing the damping ratio on the response of a signal undergoing a step change of 1. The effect of the damping ratio can easily be seen; that is, larger damping ratios reduce the amplitude of oscillation sooner than smaller damping ratios. As previously discussed, the damping ratio is affected by the elasticity of the system, where more elastic substances produce larger damping ratios. Therefore, an elastic substance like skin and soft tissue is likely to reduce the amplitude of vibration carried through it. Vibration transmitted through the skin is likely to be damped out quickly due to the low modulus of the structure ($E=0.042\text{-}0.85$ MPa [Agache et al. 1980;Elsner et al. 2001]). Vibration transmitted through the spine may be damped out less quickly, as the spine is made of stiffer structures such as bone ($E=11.3$ GPa [Rao and Dumas 1991]) and intervertebral discs ($E=1.0\text{-}1.8$ GPa [Rao and Dumas 1991]). The data from Protocol 1 and Protocol 2 appear to support these suggestions, as

the bulk of vibration transmitted through the skin was dissipated over the L2 vertebra, while vibration transmitted through the spine was still viably measured at the L3 and L4 vertebrae. The damping of vibration with increasing distance from the vibration input point has been previously demonstrated in studies by Zhang et al. and Sörensson et al. [Zhang et al. 2008;Sörensson and Burström 1997].

The large amount of damping of the skin-transmitted vibration signal over the distance of one vertebra indicates that vibration measurements should not be taken at vertebrae directly adjacent to the contact tip, as there may be a degree of contamination of the signal due to vibration of the skin. The distance at which viable vibration response information can no longer be obtained above regular signal noise is not known. In these protocols, measurements from at least three vertebral levels away from the contact tip were shown to contain measurable vibration response information.

5.2.1.3 Concluding Message

Vibration is damped out at different rates depending on the elasticity of the tissue through which it is transmitted. A large bulk of the vibration transmitted through the skin is damped out within one vertebral segment of the contact tip input point, while measurable vibration is transmitted through the spine to at least 3 vertebral lengths away from the contact tip input.

5.2.2 Signal Correlation Methods

5.2.2.1 Overview of Findings

The protocols performed in this thesis primarily used the D-statistic to analyze the data. The D-statistic is a measure that employs a simple method of comparing one set of repeated signals to another. To review, it determines the percentage of the mean of one set of signals that could be classified as a repeated measure of another set of signals. While this method is logical, the repeated measures on the bone signals, coupled with the poor matching of the skin and bone signals gave D-statistic values that were very low in many cases.

Section 5.2.1 discussed the fact that skin noise was damped out with increasing distance between the accelerometer and the contact tip. Despite the lessening of this vibration, the D-statistic values did not improve.

5.2.2.2 Discussion of Findings

The D-statistic was developed by Zennaro et al. as a component of an algorithm designed to detect changes in the shape of measured EMG signals from motor units [Zennaro et al. 2002]. The D-statistic values were fed into the algorithm with a number of other parameters to discriminate between and classify motor unit waveforms in decomposed EMG signals. The D-statistic method has not been previously applied as a stand-alone signal correlation measure, and is believed to be a novel implementation in the case of this thesis. Unfortunately, Zennaro et al. did not report their D-statistic values; thus, there is no previous data to compare against the results of this thesis. While there is no precedent for the use of this kind of analysis in vibration response testing, the D-statistic was

chosen due to the logical simplicity of the calculation. The D-statistic represents a straightforward method of determining the percentage of an experimental signal that could be classified as a control signal, theoretically making it a satisfactory 'correlation' criterion.

The low D-statistic values were likely due to a combination of two factors. First, qualitatively viewing the results shows that signal matching between skin and bone-mounted accelerometer signals was in many cases poor. The low D-statistic values were reasonable in these cases. Second, the high repeatability of each of the measured bone signals generally created a very tight confidence interval on the mean. This left very little room for error between the skin and bone/needle signals. For example, Figure 5.2 below shows data taken from human cadaver subject 2 at the L4 vertebra using contact tip C.

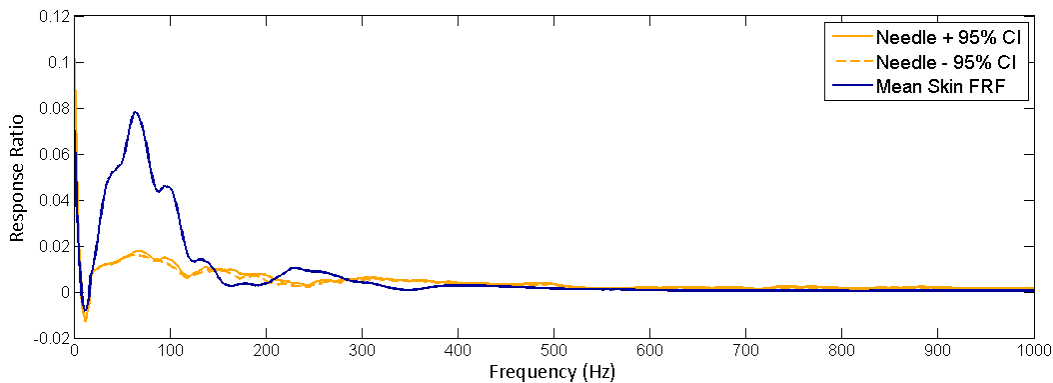


Figure 5.2: Mean skin-mounted accelerometer FRF graphed with 95% confidence interval on the needle-mounted accelerometer measurements at L4 using contact tip C in human cadaver subject 1. D=1.12%

The D-statistic value for this comparison was 1.12%. It can be seen that from approximately 400-1000 Hz, the signals are almost identical in shape and amplitude. However, due to the small confidence interval on the needle signals, the D-statistic for this section of the curve is 0%.

The D-statistic values do not provide further information as to why two signals correlate poorly, or where the range of poor correlation occurs. Furthermore, the D-statistic does not delineate the severity of the poor correlation. For example, the D-statistic will be 0% for both a skin signal that may fall just outside the bone signal CI, and a signal that has 1000% greater amplitude than the upper CI on the bone signal.

Unfortunately, an exhaustive search of correlation methods for two signals, or two sets of signals, did not produce any alternative methods with superior qualities to the D-statistic. For example, the concept of transmissibility was investigated. Transmissibility simply divides the 'experimental' (i.e., skin accelerometer signal) response ratio by the 'control' (i.e. bone accelerometer signal) response ratio at each frequency [Bressel et al. 2010]. For perfect matching, the transmissibility at a given frequency is 1. When comparing two signals, the average transmissibility of all the frequencies can be computed by simply adding the transmissibility values from each frequency together and dividing by the number of frequencies measured. However, this technique is very insensitive to local discrepancies in the signals. An example of this situation can be explained by two signals, measured at two frequencies. The transmissibility at frequency 1 could be 0.0001, while the transmissibility at frequency 2 could be 1.9999. Clearly, these two signals do not match at either frequency, but their average transmissibility (ie: 1) would mislead a reader to thinking the signals matched perfectly.

A satisfactory method of signal correlation previously used by the Spinal Function Lab was found in using the Global Shape Criteria (GSC), and Global Amplitude Criteria (GAC) [Kawchuk et al. 2008;Kawchuk et al. 2009]. These criteria determine the correlation in a set of signals separately in shape and amplitude. Unfortunately, these techniques are formulated to apply to signals obtained from a global system of sensors, rather than repeated measures

obtained from two individual sensors. For example, the GSC compares the 'shape' between sensors – that is, the operating deflection shape of the vibrating object, rather than the shapes of the individual FRFs [Friswell].

One solution this signal analysis problem may be to further the use of PCA in the analysis of the data in conjunction with the D-statistic. PCA played a minor role in the analysis of Protocol 1 by qualitatively analyzing the variance between the T-9 skin-mounted accelerometer placement signals. This method of analysis showed that PCA could be used to determine the greatest areas of variance between signals, as well as to determine the percentage of total variance that each mode of variance accounted for. PCA was not performed further in this thesis as a method to compare the large number of graphs generated by the analysis has not yet been devised. For example, in the Protocol 2, there are potentially 360 graphs (5 pig and 5 human cadaver subjects x 3 measured vertebrae x 6 contact tips x 2 PCs (min.)) that require comparison of numerous features in shape and amplitude. An efficient and effective method must be devised to summarize the differences in the graphs to provide a meaningful result for interpretation. It is recommended that this undertaking be performed as a devoted project.

PCA appears to be a promising alternative method of analysis for changes between skin and needle/bone mounted accelerometer signals. However, this method does appear to be highly time consuming and open to investigator interpretation. Therefore, alternative methods of quantitative signal correlation are still desirable. Developments in signal processing methods that improve comparisons between two given signals should be monitored for potential future use.

5.2.2.3 Concluding Message

The low D-statistic values found in the results of this thesis were likely due to two main factors: A) the poor matching of skin-mounted and bone-mounted accelerometer signals, and B) the high repeatability of the bone-mounted accelerometer signals creating an extremely tight 95% confidence interval. To analyze differences in the signals further, a method that can analyze qualitative signal differences, such as principal component analysis, could be used.

5.2.3 Comparison of Skin and Reference Signals

5.2.3.1 Overview of Findings

Protocol 1 and 2 results both showed poor correlation between reference accelerometers (needle/bone) and skin accelerometers when using a non-invasive contact tip. As previously discussed in Chapters 3 and 4, some of the factors that may have contributed to this poor correlation were:

- Vibration travelling through the skin, interfering with the skin-mounted accelerometer's measurement of the bone vibration
- D-statistic dependence on confidence interval on the mean of a set of control signals
- Poor alignment of measurement axes of skin mounted and reference accelerometers

5.2.3.2 Discussion of Findings

Section 5.2.2 has already discussed methods of improving the issues encountered in using the D-statistic. This discussion will primarily center on the issues involved in measurement of the signals and physical installation of the sensors.

The alignment of the measurement axes of needle-mounted accelerometers with both bone mounted accelerometers in Protocol 1 and with skin mounted accelerometers in Protocol 2 was not optimal due to problems installing the needles in the spinous processes. Difficulty installing the needles in the bone occurred for a number of reasons. Primarily, the small width of the spinous processes made it difficult to install the needle deeply and securely in the spinous. This was more apparent in the human cadavers, where the spinous processes were smaller than in the porcine cadavers. Frequently, the needle would penetrate out the side of the spinous, damaging and presumably tearing the supraspinous structures which then loosened the needle implantation. This required the needle to be removed and re-implanted. The difficulty of securely installing the needle at a given angle on this small portion of bone did not leave room for a large number of attempts, as each attempt caused further damage to the underlying spinous. Therefore, the angle of the needle installation was compromised against the security of the needle in the bone. A second difficulty of installing the needle was due to subject anatomy. In one human subject, the soft tissue and skin covering the spinous processes was so thick, it was difficult to ensure the security of the needle in the bone without the hub of the needle touching the skin. A third difficulty encountered in some human subjects was the calcification of the bone. In one subject in particular, the bone was so hard that the needle would not penetrate the spinous easily, and a number of needles had to be removed due to the needles being bent during installation attempts.

Given the above difficulties, improved techniques on the installation of needles into the spinous processes are required. One method of improvement could involve the use of ultrasound and a mechanically guided installation apparatus. This technique would first use an ultrasound device to characterize the shape of the spinous process. From this, the investigator would determine the optimal area on the spinous for installation of the needle. The needle would then be held by a device that rigidly constrained the needle such that it would be installed at the identified location, aligned with the skin accelerometer measurement axis. The investigator could then tap the needle into position with a hammer.

As discussed in section 3.5.3.1, preloading of the accelerometers should also be investigated to compress the skin below the accelerometers. A study by Nokes et al. demonstrated the effect of preloading skin-mounted accelerometers to improve the correlation with a bone signal [Nokes et al. 1984]. The time response of the human tibia to an impulse vibration was measured using a skin-mounted accelerometer and an accelerometer screwed into the bone. The preload on the skin-mounted accelerometer was varied from 3.2-6 N using a mass weighting arm. Subject skin thicknesses varied from 2-11 mm at the measurement site. This study showed that with too little preload (3.2 N), the effect of soft tissue resonance was still apparent in the skin accelerometer signal. However, with too much preload (6 N), the bone and mass weighting arm became a rigid system, and the vibration of the weighting arm was apparent in the measured signal. Therefore, an optimal preload likely existed somewhere in between the two measures, depending on the subject morphology. A further study by Cornelissen showed that heavy preloading of an accelerometer can cause a shift in the resonant frequencies, presumably for the same reasons as discovered by Nokes et al. [Cornelissen et al. 1987]. However, it is unknown whether a similar result would be obtained for an elastically preloaded accelerometer, which would not have the same weighting effects. As was mentioned previously in Chapter 3, preliminary testing of an accelerometer

preloading technique using an elastic band was performed. However, results from these investigations were inconclusive. This was due to the lack of ability to measure the level of preload on the accelerometers; therefore no systematic preload effect could be determined. From Nokes et al., it is apparent that preloading may hold some merit in increasing the correlation between skin and bone mounted accelerometers [Nokes et al. 1984;]. Therefore, systematically testing different preload levels on accelerometers should be performed to determine the potential for improving this correlation. It is suggested that both mass preloading and elastic preloading be investigated to determine whether the preloading method contributes to potential changes in correlation. Furthermore, tissue thickness over the spinous process should also be measured in these experiments to determine its influence on the changes in signal correlation.

A further, digital alternative for correcting the correlation between skin and reference signals could also be considered. Currently, it is thought that the signal obtained from a skin-mounted accelerometer is noisy due to vibration transmitted through the skin from the contact tip. If the noise were systematic in nature, this component of the measured signal could be removed to reveal the estimated reference signal. An example of a systematic noise component would be: for a given skin thickness, moisture content, subcutaneous fat amount, and elasticity measurement, a certain frequency range and amplitude of vibration is measured by the skin-mounted accelerometer. Many have previously tried to model the behaviour of the skin [Oomens et al. 1987;Rubin et al. 1998;Wu et al. 2003;Zhang et al. 2008;Delalleau et al. 2008]. Dellaleau et al. are likely the most successful in their attempt, and have modeled the skin as a non-linear elastic material [Delalleau et al. 2008]. They validated their model through testing on the volar forearm of 30 subjects using a traditional suction cup-deformation method to measure the experimental skin parameters. If this model could be applied to determine the theoretical vibration response of the skin and soft

tissues, then the theoretical skin response could be subtracted from the response measured by a skin-mounted accelerometer to reveal the true vertebral (bone) vibration response.

As previously mentioned in the literature review, Kitazaki and Griffin had some success with individualized inverse transfer functions applied to the data to remove the skin effects, but their results were not validated *in vivo*, and were only applicable up to 35 Hz. Currently, only one method of signal filtering on skin to improve the correlation between skin and reference signals has had adequate success. Developed by Andriacchi et al., a multitude of skin-based markers were used to detect non-rigid body motion of a moving limb (ie, skin motion), from which the skin artifact could be removed [Andriacchi et al. 1998]. Unfortunately, this method required a minimum of 8 sensors to characterize one limb, and is therefore not applicable in individual vertebrae due to space issues. An algorithm that does not appear to have been explored for skin measurements is the Kalman filter. The purpose of the Kalman filter is to take signals with noise and estimate the true underlying signal, using repeated measures over time to refine the estimate [Welch and Bishop 2006]. However, the nature of the statistical distribution of the skin signal noise must first be delineated, as the Kalman filter assumes a normal distribution of the noise.

If the noise in the signal is not systematic and cannot be removed, it is likely this technique will not succeed in a non-invasive format. Changes caused by vibration travelling through the skin in these measurements would not be differentiated from actual changes in the spinal vibration response.

Briefly, the alternative of simply abandoning the skin-mounted accelerometer could be used. Patients could be given local anesthetic, and needle-mounted accelerometers could be installed in the vertebrae. However, development of the needle installation technique must be refined, as was discussed in Section

4.4.4. Furthermore, installation of the needle into the spinous would damage the bone of the vertebra, as well as the tissues overlaying the tip of the spinous process such as the supraspinous ligament. In the studies performed for this thesis, bleeding occurred at a number of needle installation sites in both porcine and human cadavers; it is assumed that this would likely also happen in live patients. While healing time of the bone from such a procedure could take 6 weeks [Walker 2007], the healing of damage to the tissues overlaying the top of the spinous is unknown. It is unknown whether this damage would have significant lasting consequences. Therefore, a cost-benefit analysis would need to be performed by the doctor and patient before undertaking such a procedure.

5.2.3.3 Concluding Message

A number of topics were broached in this discussion on comparing skin and reference signals. First, the difficulty of installing hypodermic needles into the spinous processes of cadavers requires further development of installation techniques to improve the viability of the signals obtained. Second, the effect of vibrating skin interfering with skin-mounted accelerometer measurements requires mitigation. Therefore, physical techniques such as preloading of the accelerometers, as well as digital filtering techniques should be explored to improve on this problem. If the vibration response of the skin only cannot be filtered out from the total measured vibration response, it is likely that this technique will not be a viable method of detecting spinal dysfunction.

5.3 Strengths and Weaknesses of the Study

5.3.1 Strengths

The tests performed in this thesis have provided a path for future development of the technique by identifying a number of key problem areas in the implementation of the testing in a non-invasive manner.

Testing in Protocol 2 involved a randomization process to determine the order of the contact tip use. This further strengthens the results of the contact tip testing by eliminating any potential order effects that may have been introduced by the different shapes.

Testing was performed on fresh human cadavers that had not been previously frozen or embalmed, nor were they thought to have been affected by the effects of rigor mortis. This factor left the tissues in a natural state as close to *in vivo* as possible. This is a strength of the study because the results are likely to be more applicable to live humans; however, the impact of these results in live humans could be changed by effects such as muscle activation, breathing, or tissue hydration/rehydration.

The fact that many of the findings in this study were demonstrated by previous investigators may be considered by some to be a weakness; however, the impact of these behaviors with respect to the technique under development was unknown, and their characterization through the work in this thesis should be considered a strength. Furthermore, the majority of these previous results were found in long bone testing of the tibia or ulna. Only one report of specific mechanisms of soft tissue vibration in the spine in the context of a non-invasive vibration technique had been performed by Zhang et al. [Zhang et al. 2008]. The confirmation of the impact of these previously discovered phenomena in the

context of the current technique set-up has will help shape the future development of the technique.

Despite the need for further study of needle-mounted accelerometer techniques, the results of Chapter 3 and 4 showed the technique could provide a suitable measure of the vertebral vibration response. This should be considered a strength of the study, as the potential impact of this technique for use in future experiments is important. The needle is significantly smaller, less invasive, and with refinement of the technique could be easier to install than the medical bone pins frequently used by other researchers [Rostedt et al. 1995;Gal et al. 1997;Nester et al. 2007].

5.3.2 Weaknesses

There are a number of weaknesses that should be considered when reviewing the data in this thesis. The small sample size used in each protocol limited the generalizability of the results. For example, trends in the measured vibration response based on contact tip type may have come to light with a greater number of cadavers tested. Therefore, future work could expand to include a larger sample size to improve the generalizability of results. Sample size for this study was decided upon by two factors. First, previous invasive work had a similar size with significant results. Second, the nature of the experiments performed in Protocol 1 and Protocol 2 was exploratory and performed primarily to obtain pilot data. This pilot data was instrumental in determining the future recommendations for the overarching vibration diagnostic technique project.

A further issue related to sample size is the power of the study. From results shown in Tables 3.10 and 4.6 summarizing the repeated measures ANOVAs run

on the D-statistic results, it can be seen that the power of the statistical tests ranged between 0.101-0.561. It is generally recommended that adequate statistical power of an analysis be at least 0.8 [Field 2009]. The study lacked sufficient power in most cases to validate a significant effect. Evidence of this can be seen from the calculated effect sizes. For example, in Protocol 1 T-9 placement testing, the effect size measuring the effect of contact tip type was 0.634, which can be considered moderate. However, the power of this test did not allow for a significant effect to be detected ($p=0.176$). Power is largely influenced by sample size [Field 2009]; therefore, due to the small number of cadavers tested in this study, it is likely that small or moderate significant effects could not be detected. The study could be expanded to a larger sample size to help determine whether these effects exist.

The lack of control over the cadaver characteristics further contributed to the lack of generalizability of results. The studies examined in the literature review have shown soft tissue and skin factors to be a highly important variable in non-invasive human kinematic testing. These factors include muscle/soft tissue mass surrounding the spine, skin age, and skin moisture content. The soft tissue characteristics of the cadavers used in these protocols was not quantified. Furthermore, both male and female cadavers were used, and their medical condition at time of death was not provided. It is unknown whether these potential differences of the skeleton or soft tissues had an effect on the vibration response capabilities.

While the D-statistic provides a suitable method for comparing two signals, its usefulness is highly dependent on the repeatability of the data. Data with very high repeatability, such as the signals found in the protocols performed in this thesis, can produce a poor D-statistic even if the signals are similar in shape but not in amplitude. Therefore, simply viewing the D-statistic values does not always provide an accurate picture of how similar two signals are. Further

analysis using PCA or alternative measures of signal correlation should be sought.

In Protocol 1 (Chapter 3), there were significant differences in the measured vibration response when comparing between the invasive and non-invasive contact tips. As was previously discussed in that chapter, a number of sources could have contributed to those differences, one of these being the level of preloading on the spine from the non-invasive or invasive contact tip. Figure 5.3 below shows the differences between signals measured from T-9 bone mounted accelerometers using both the invasive and non-invasive contact tips.

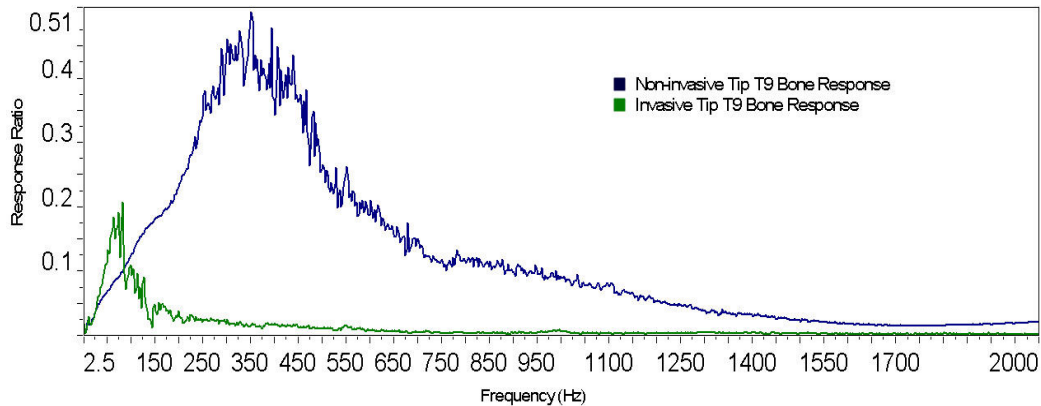


Figure 5.3: Comparison of T-9 bone-mounted accelerometer response taken using the non-invasive (blue) and invasive (green) contact tips. Data taken from subject 1, Protocol 1 porcine data.

Figure 5.3 shows a significant dependence of the bone vibration response on the type of contact tip used. A flaw of Protocol 1 was that the level of preloading on the spine was not the same for the invasive and non-invasive contact tips. Not only could this have changed the boundary conditions on the spine, but also could have changed the level of force imparted to the spine during vibration. The literature review (Chapter 2) mentions that the basic formulation of an FRF is a ratio between the output acceleration and the input force to the spine, known as accelerance. It follows that changes in the input force levels between these two

types of contact tip would significantly affect the measured FRF. A strict comparison of the forces imparted to the spine in these experiments was not performed for this thesis. Therefore, this factor must be considered when making interpretations between non-invasive and invasive contact tip signals.

5.4 Influence of Study Assumptions

This study made a number of key assumptions. It was estimated that the response of the system did not contain significant non-linearities in the response. Research has shown that the non-linearity of the human body is primarily in relation to the magnitude of the vibration input [Matsumoto and Griffin 2002;Hinz and Seidel 1987]. The magnitude of the vibrations in these protocols was not fully controlled, due to the random burst nature of the signal. However, the non-linearity within a signal may not be a significant factor for a number of reasons. First, the repeatability of the vibration response was shown to be very high. Therefore, differing magnitudes of vibration at each frequency did not affect the final frequency response function. Second, comparisons were made only within subjects, not between subjects; therefore, the non-linear response of the spine, thought to be due to the soft tissues and skin, would remain the same within subjects and would not influence comparison of results.

The second assumption made was that the systems were time-invariant. While the vibration may have induced small visco-elastic changes in the tissues, the overall vibration response did not appear to be affected by time. Figure 5.4 below shows the two signals taken from Protocol 1. The first signal was taken from the T9 bone-mounted accelerometer at the beginning of testing with the non-invasive contact tip, when the skin-mounted accelerometer was in position A. The second was taken from the bone-mounted accelerometer when the skin-

mounted accelerometer had been replaced, position A'. The time difference between these two signal measurements was approximately one hour.

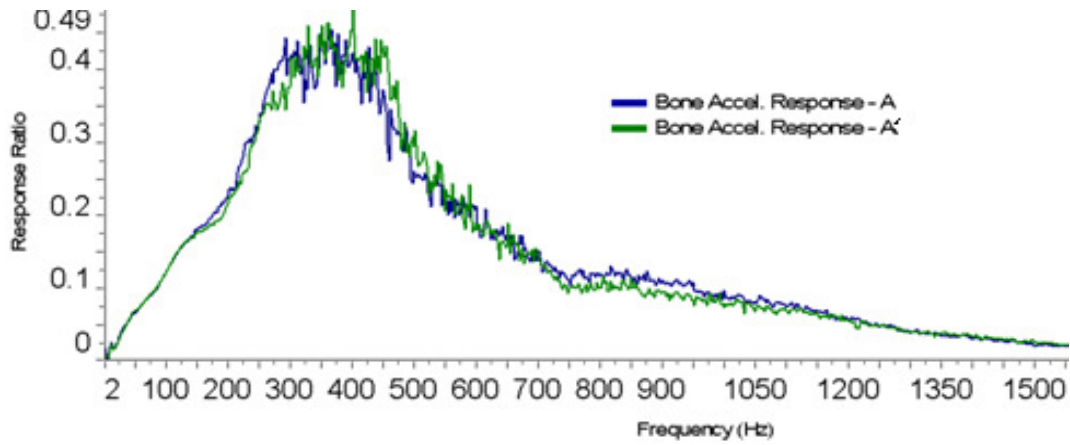


Figure 5.4: T-9 bone-mounted accelerometer vibration response at two time intervals. Blue - skin-mounted accelerometer was placed at position A. Green – skin-mounted accelerometer was placed replaced, position A'

Figure 5.4 shows that time-variant factors were likely not a significant source of variance in the measured FRFs from the bone. A similar degree of signal correlation was found when comparing the skin-mounted accelerometer signals from the T-10 vertebra. However, due to the changes in placement of the accelerometer on the T-9 vertebra, it is unknown whether these signals could have been affected by time-dependent visco-elastic changes. Rubin et al found that tissues undergoing cyclic loading had visco-elastic change over time [Rubin et al. 1998]. Vibration travelling through the skin may have had a more significant effect on the skin and soft tissues at T-9 than T-10, due to the vibration being damped out with increasing distance from the contact tip.

A further assumption inherent in all vibration response testing is the assumption of reciprocity. The assumption of reciprocity states that an excitation at point 1 produces a response at point 2 and point 1. An excitation at point 2 produces the

same responses at point 1 and point 2 [Brown et al.]. Due to the single input point tested, it is not known whether this assumption was violated.

5.5 Significance of the Study

This study confirms the results of prior investigations using skin-mounted sensors [Holden et al. 1997]. It was known prior to performing these experiments that skin would have an influence on the measured vibration response. The protocols in this thesis were designed to determine the extent of the influence of the skin and soft tissues in the specific context of the non-invasive spinal diagnostic technique. A number of discoveries were made with respect to the specific technique at hand.

The protocols in this project have provided the first data on the implementation of the Spinal Function Lab's non-invasive vibration technique in human cadavers. The successful collection of this data provides precedent for collecting data in live humans. An important yet basic consideration in investigating the employment of the non-invasive vibration testing protocol was whether the measurements of the spinal vibration response from the skin-mounted accelerometers were repeatable. It was found that the repeatability of measured signals was very high. Therefore, reliable measurements can be obtained non-invasively in subjects for a given accelerometer set-up.

The results suggested that the measured signal is highly sensitive to skin mounted accelerometer placement. Position testing in Protocol 1, as well as replaceability testing in Protocol 1 and 2 showed that small changes in the placement of an accelerometer, or possibly disturbances of the skin caused by the removal and replacement of an accelerometer, can greatly impact the

measured vibration response. These results are very significant in the context of a potential diagnostic technique. To be able to monitor a patient's condition over time, clinicians must be certain that changes in the measured vibration response are not due to variation in the setup of the sensors, but rather are due to the phenomenon they are intended to measure. For this non-invasive diagnostic technique to become a viable product, an effective method of replacing skin-mounted accelerometers to obtain repeatable measurements must be developed. The technique must be easy to implement as well as accurate. A potential method to solve this problem involves the use of a hand-held ultrasound device. Previously, the accelerometer had been replaced to the same segment of *skin* over top of the spinous. However, the skin is not affixed rigidly to the underlying bone, and can therefore move and slide from its original position when a force is applied to it. The use of ultrasound could guide the clinician in placing the accelerometer over the same segment of spinous process, instead of placing the accelerometer on the same segment of skin. This may improve the correlation in measurements obtained in replacement testing, if it is assumed that the 'new' skin overlaying the spinous is roughly analogous in structure and properties to the 'old' skin. This method would require the development of a spatial reference frame between the ultrasound image and the subject's spine to ensure accurate placement of the accelerometer. It is likely that this aspect of the solution would require significant development before becoming a viable solution, as the ultrasound head itself has the potential to move the skin while being used. One drawback to the ultrasound solution in terms of the clinical technique is that clinicians would be required to own or purchase an ultrasound machine in conjunction with the vibration technique/device. Furthermore, the addition of this extra step in the use of the technique takes away from its potential advantages over imaging modalities such as MRI and x-ray, in that it becomes more complicated and time consuming than the original stand alone vibration technique.

As previously discussed in Section 5.2.1, it was found that vibration of the skin and soft tissues affects the measured vibration response. This result has a great impact on the clinical development of this technique. Improvements to the skin-mounted accelerometer measurement technique must be made before this approach can be viable in a clinical setting. Mechanical techniques such as preloading of the accelerometers, as well as digital techniques like Kalman filtering should be investigated to improve the measured vibration response. However, it was found that increasing distance between the contact tip and skin-mounted accelerometer by one vertebra did decrease the amount of measured signal noise. Though there was no difference in the D-statistic values, this effect could easily be seen by viewing the resulting graphs. Therefore, by simply inputting the vibration at increased distances from the spinal area of interest, a large amount of signal noise can be immediately reduced.

The effect of contact tip shape did not make a significant difference in increasing the correlation between the signals from a skin-mounted accelerometer and a needle-mounted accelerometer. Therefore, a contact tip that is securely stationed over the spinous process (ie, some form of arch shape) that also maximizes patient comfort should be used.

5.6 Future Considerations

A number of key future considerations have been generated by this project that each relate to the current system evolving into a viable diagnostic technique.

The most important future consideration is dealing with the vibration response of the skin/soft tissue from a skin mounted accelerometer. The results presented in this thesis show that soft tissue has a significant influence on the measured

vibration response from skin-mounted accelerometers. Future work should center on finding mechanical and digital methods of minimizing the soft tissue vibration component of the measured spinal response.

A second critical consideration is the replaceability of the accelerometer on the skin to obtain repeatable measurements. It was found that accelerometers removed and replaced to the same skin position obtained variable FRF measurements of the spinal vibration response. For the development of a viable diagnostic technique, the clinician must be certain that changes in the measured FRFs are due to structural or functional changes in the spine and not due to changes in the experimental setup. In this thesis, accelerometers were replaced to the same *skin* position. However, it is possible that the skin may have moved between placements, which would introduce error in the measurements. Future methods should focus on ways to replace the accelerometer over the same *bone* position.

A number of less critical future directions have also been identified. Further methods of comparing two FRF signals should be investigated. As previously discussed in section 5.3.2, the D-statistic is an overall measure of the correlation between two signals. New research in signal processing and analysis should be monitored for developments that may aid in this comparison. Furthermore, the use of PCA may be helpful in determining qualitative differences in the FRFs.

Human anatomic factors such as sex, skin elasticity, body composition (% muscle and fat), and BMI were not considered in this study. Future studies should investigate these factors in relation to non-invasive spinal vibration response testing to determine their impact on the measurement capability of the system. Because of the successful implementation of the non-invasive technique in human cadaveric subjects, the technique should next be tested in live human subjects to investigate these factors.

5.7 References

Agache PG, Monneur C, Leveque JL, De Rigal J. Mechanical properties and Young's modulus of human skin in vivo. *Arch Dermatol Res* 1980;269(3):221-232.

Andriacchi TP, Alexander EJ, Toney MK, Dyrby C, Sum J. A point cluster method for in vivo motion analysis: applied to a study of knee kinematics. *J Biomech Eng* 1998;120(6):743-749.

Bressel E, Smith G, Branscomb J. Transmission of whole body vibration in children while standing. *Clin Biomech (Bristol)* 2010;25(2):181-186.

Modal Analysis: Theory and Application. International Modal Analysis Conference XXVII; Feb 6-7, 2009; Society for Experimental Mechanics;

Cornelissen M, Cornelissen P, van der Perre G, Christensen AB, Ammitzbohl F, Dyrbye C. Assessment of tibial stiffness by vibration testing in situ--III. Sensitivity of different modes and interpretation of vibration measurements. *J Biomech* 1987;20(4):333-342.

Delalleau A, Josse G, Lagarde JM, Zahouani H, Bergheau JM. A nonlinear elastic behavior to identify the mechanical parameters of human skin in vivo. *Skin Res Technol* 2008;14(2):152-164.

Elsner P, Berardesca E, Maibach HI, editor. *Bioengineering of the skin: skin biomechanics*. CRC Press; 2001.

Field. Field A, editor. Discovering Statistics Using SPSS. 2 ed. Sage Publications Ltd; 2009. 821 p.

Friswell M. Personal Correspondence. 29/4/2010.

Gal J, Herzog W, Kawchuk G, Conway P, Zhang YT. Measurements of vertebral translations using bone pins, surface markers and accelerometers. "Clin Biomech (Bristol 1997;12(5):337-340.

Hinz B, Seidel H. The nonlinearity of the human body's dynamic response during sinusoidal whole body vibration. Ind Health 1987;25(4):169-181.

Holden JP, Orsini JA, Siegel KL, Kepple TM, Gerber LH, Stanhope SJ. Surface movement errors in shank kinematics and knee kinematics during gait. Gait and Posture 1997;5:217-227.

Kawchuk GN, Decker C, Dolan R, Carey J. Structural health monitoring to detect the presence, location and magnitude of structural damage in cadaveric porcine spines. J Biomech 2009;42(2):109-115.

Kawchuk GN, Decker C, Dolan R, Fernando N, Carey J. The feasibility of vibration as a tool to assess spinal integrity. J Biomech 2008;41(10):2319-2323.

Matsumoto Y, Griffin MJ. Non-linear characteristics in the dynamic responses of seated subjects exposed to vertical whole-body vibration. J Biomech Eng 2002;124(5):527-532.

Nester C, Jones RK, Liu A, Howard D, Lundberg A, Arndt A, Lundgren P, Stacoff A, Wolf P. Foot kinematics during walking measured using bone and surface

mounted markers. *J Biomech* 2007;40(15):3412-3423.

Nokes LD. The use of low-frequency vibration measurement in orthopaedics. *Proc Inst Mech Eng [H]* 1999;213(3):271-290.

Nokes L, Fairclough JA, Mintowt-Czyz WJ, Mackie I, Williams J. Vibration analysis of human tibia: the effect of soft tissue on the output from skin-mounted accelerometers. *J Biomed Eng* 1984;6(3):223-226.

Oomens CW, van Campen DH, Grootenboer HJ. A mixture approach to the mechanics of skin. *J Biomech* 1987;20(9):877-885.

Rao AA, Dumas GA. Influence of material properties on the mechanical behaviour of the L5-S1 intervertebral disc in compression: a nonlinear finite element study. *J Biomed Eng* 1991;13(2):139-151.

Rostedt M, Broman H, Hansson T. Resonant frequency of a pin-accelerometer system mounted in bone. *J Biomech* 1995;28(5):625-629.

Rubin MB, Bodner SR, Binur NS. An elastic-viscoplastic model for excised facial tissues. *J Biomech Eng* 1998;120(5):686-689.

Sörensson A, Burström L. Transmission of vibration energy to different parts of the human hand-arm system. *Int Arch Occup Environ Health* 1997;70(3):199-204.

Turek SL, Weinstein SL, Buckwalter JA, editor. *Turek's Orthopaedics*. Lippincott Williams & Wilkins; 1994. 708 p.

Walker B, editor. *The Anatomy of Sports Injuries*. 2007. 244 p.

Welch G, Bishop G. An Introduction to the Kalman Filter. 2006;

Wu JZ, Dong RG, Smutz WP, Schopper AW. Nonlinear and viscoelastic characteristics of skin under compression: experiment and analysis. Biomed Mater Eng 2003;13(4):373-385.

Zennaro D, Laubli T, Wellig P, Krebs D, Schnoz M, Klipstein A, Krueger H. A method to test reliability and accuracy of the decomposition of multi-channel long-term intramuscular EMG signal recordings. International Journal of Industrial Ergonomics 2002;30:211-224.

Zhang X, Kinnick RR, Pittelkow MR, Greenleaf JF. Skin viscoelasticity with surface wave method. Proceedings - IEEE Ultrasonics Symposium 2008;2008:651-653.

Chapter 6: Summary of Conclusions

6.1 Protocol 1 Conclusions

The measured signal from a skin-mounted accelerometer, a bone-mounted accelerometer, and a needle-mounted accelerometer can all obtain acceptably high repeatability when using both a non-invasive and an invasive contact tip.

Changes in the skin-mounted accelerometer positioning over the spinous process produce considerable changes in the measured FRF in both shape and amplitude. Increasing the distance between the skin-mounted accelerometer and the contact tip decreases the amount of signal noise measured. Signal noise is created as a result of modes of vibration being excited in the skin and soft tissues dorsal to the spine.

The vibration signal transmitted from the contact tip to the spine is impacted by the type of contact tip used. The non-invasive contact tip noticeably excites modes of vibration in the skin and soft tissues covering the spine, where the invasive contact tip does not. Furthermore, the different levels of preloading on the spine used for the two different contact tips likely changed the structural boundary conditions of the spine, providing different levels of damping on the spine.

6.2 Protocol 2 Conclusions

An acceptably high repeatability of a measured vibration response signal from both skin-mounted accelerometers and needle-mounted accelerometers can be obtained from both human and porcine cadaver subjects.

Small changes in the interface shape of the contact tip do not significantly influence the level of correlation between a skin-mounted and needle-mounted accelerometer at any given vertebral level. This conclusion was reached in both porcine and human cadavers. Furthermore, the type of cadaver tested does not influence the level of correlation between the two signals.

Testing concluded that the replaceability of a skin mounted accelerometer to its original position yields poor correlation between the measured vertebral vibration response signals.

6.3 Overall Conclusions

Vibration transmitted to a spine is damped out at different rates depending on the tissue through which it is travelling. The majority of vibration transmitted through the skin and dorsal soft tissues is damped out within one vertebral segment of the contact tip location, while vibration travelling through the spine can be measured at least three vertebral segments away from the contact tip input.

Two main factors likely contributed to the low D-statistic values in the results of this thesis. First, the poor matching of skin-mounted and bone-mounted accelerometer signals were a valid but poor result. Second, the high repeatability

of the bone-mounted accelerometer signals created an extremely tight 95% confidence interval, which left a very small margin of error between the skin and reference accelerometer signals.

The issues in the comparison of skin and reference signals led to a number of conclusions. First, the utilization of a needle-mounted accelerometer has potential to measure the vibration response of bone; however, the installation techniques of the needle must be improved upon to obtain accurate results in the future. Second, the vibration transmitted through the skin when using a non-invasive contact tip significantly affects the measured vibration response of the spine.

Appendix A: Principal Component Analysis Calculation

A.1 Calculation

Principal component analysis (PCA) is a multivariate analysis technique that can be used to reduce the size of large data sets, and describe the mechanisms of variance within the data.

Typical data sets for which PCA is used are comprised of a number of observations, and a number of variables within each observation. For example, when measuring the vibration response of the spine, the observation would be the frequency response function (FRF), and the variables would be the frequencies at which the FRF was measured. The actual data within the FRF is the value of the frequency response.

To illustrate the calculation of PCA, we will use the example of performing a PCA on data taken from skin mounted accelerometers and bone mounted accelerometers, to discover how these signals differ. In this example, we have 10 FRFs – 5 from each type of accelerometer, each consisting of measurements at 801 frequencies. Therefore, we have an $n \times p$ matrix ' X ', where $n = 10$ and $p = 801$.

The mechanism of PCA calculation described here illustrates the method used by Matlab R2009a [The Mathworks], to remain consistent with the data analysis performed for this thesis.

First, the data is centered such that for the columns of X , $\bar{X}_p = 0$. Next, singular value decomposition (SVD) is performed on this centered \bar{X} matrix [Wallisch et al., 2009]:

$$\bar{X}_{n \times p} = U_{n \times n} \Sigma_{n \times p} V_{p \times p}^T$$

(14)

Where U and V are known as the left and right singular vectors, respectively, and Σ is a diagonal matrix of singular values. The eigenvectors of $\bar{X}\bar{X}^T$ comprise the columns of U , and the eigenvectors of $\bar{X}^T\bar{X}$ comprise the columns of V [Baker, 2005; Ewins, 2000]. To calculate the eigenvectors and eigenvalues, we use the equation:

$$A\vec{v} = \lambda\vec{v}$$

(15)

Where A is either $\bar{X}\bar{X}^T$ or $\bar{X}^T\bar{X}$, λ is an eigenvalue of the matrix, and \vec{v} is the corresponding eigenvector [Baker, 2005]:

$$\vec{v} = \begin{bmatrix} x_1 \\ \vdots \\ x_{n,p} \end{bmatrix}$$

(16)

To solve for the eigenvalues and eigenvectors, we treat the system as a set of linear equations and solve for the unknowns. This process will not be detailed

here. As a final step, each eigenvector is orthonormalized such that the magnitude of each vector is 1.

The eigenvalues of the U and V matrix are identical. To create Σ , the square-root of each eigenvalue is placed in on the diagonal of the matrix, with all other entries being 0. The root-eigenvalues are arranged from largest to smallest, starting in the top left of the matrix Σ . As previously mentioned, the orthonormalized eigenvectors are summarized column vectors which comprise the matrices U and V, and are arranged to correspond with their matching eigenvalue. Thus, the 3 components (U, Σ , and V) of the SVD are created.

Simply by calculating the SVD, we already have two important components of PCA. The matrix $V_{p \times p}^T$ contains the principal component coefficients or PCs, and Σ , which contains the square roots of the eigenvalues. The eigenvectors, or coefficients (PCs), contain information about the variance at each of the p variables. The corresponding eigenvalue to each eigenvector describes the importance of that eigenvector in describing the variance between the n observations (ie: the percentage of variance in the 10 FRF signals described by that eigenvector) [Jolliffe and Morgan, 2002].

The final step in PCA is to calculate the importance of each of the PCs with respect to each of the original observations, known as the PC scores. To compute these scores, the diagonal elements of the Σ matrix are extracted to form a single column vector. Each row in the U matrix is multiplied by the corresponding element of the column vector matrix.

In Matlab R2009a, the function to perform the PCA is:

[coeff score latent]=princomp(X)

where *coeff* is the matrix of PC coefficients, *score* is the PC scores, and *latent* is a single array of the eigenvalues.

The magnitude of the eigenvalues is not important; rather, it is the relative magnitudes of these values which determine how much variance is accounted for by each eigenvector. Therefore, the magnitude of each eigenvalue can be expressed as a percentage of the total magnitude of the eigenvalue array. When paired with the corresponding eigenvector (ie: PC coefficients), this percentage describes the percentage of variance accounted for by the particular eigenvector.

To determine the variance that each eigenvector describes, a visual analysis may be performed, as described by Ramsay et al. [Ramsay and Silverman, 2005]. First, a constant *C* is defined as:

$$C^2 = \frac{\|\hat{u} - \bar{u}\|^2}{n}$$

(17)

Where \hat{u} is the mean value of all observations at a given variable *p*, \bar{u} is the mean value of all observations for all variables, and *n* is the number of variables. A plot with 3 curves is created: \hat{u} , and $\hat{u} \pm aC\gamma$, plotted as a function of frequency (in the case of the example data in this Appendix). The variable γ represents the vector of PC coefficients, and *a* is a constant chosen by the investigator to give easily interpretable results. Adjustments of *a* may be made depending on the nature of the data [Ramsay and Silverman, 2005].

A.2 References

Baker K. 2005. Singular Value Decomposition Tutorial. Ohio State University, USA.

Ewins DJ, editor. 2000. Modal testing. Wiley. 562 p.

Jolliffe IT, Morgan BJ. Jolliffe IT, editor. 2002. Principal component analysis. Springer Verlag. 487 p.

Ramsay JO, Silverman BW, editor. 2005. Functional data analysis. Springer Us. 426 p.

The Mathworks I. 'princomp' function- Principal component analysis on data - Revision: 2.9.2.10 Date: 2007/08/03.

Wallisch P, Lusignan M, Benayoun M, Dickey AS, editor. 2009. MATLAB for neuroscientists. Academic Press. 384 p.

Appendix B: Compression-Spring Force Gage

Below is the CAD image used to create the force gage (Figure B.1). The components of the gage are labeled. Two of the dimensions are given for an idea of scale.

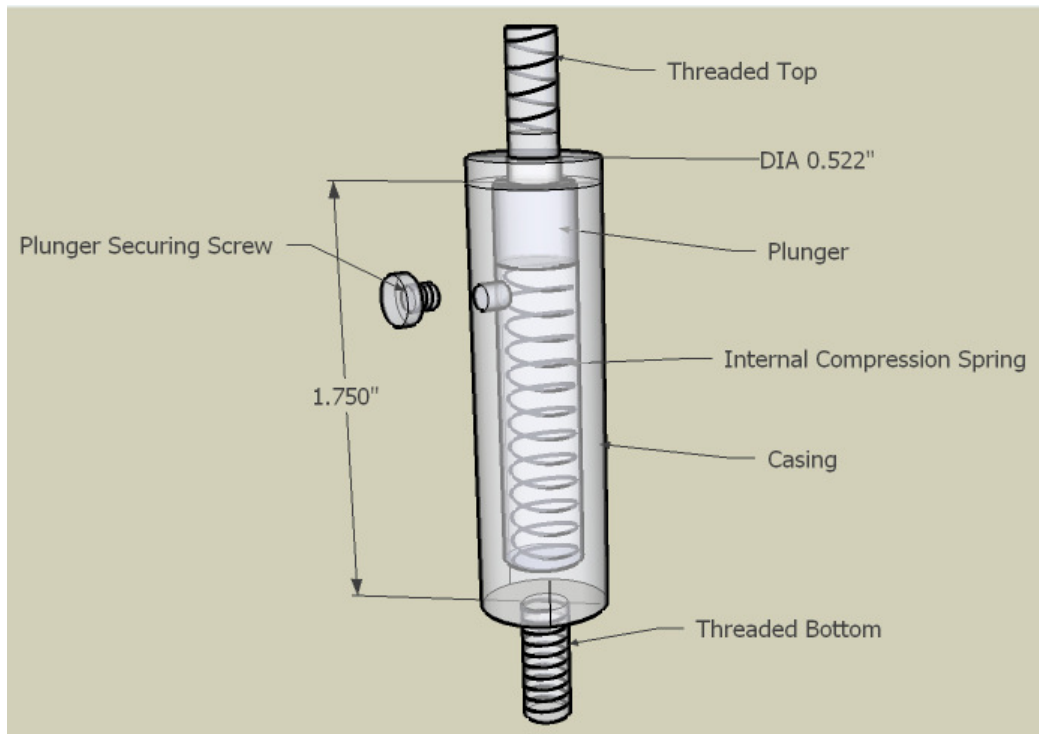


Figure B.1: Compression spring force gauge.

The spring constant of the compression spring was calibrated by Dr. Jason Carey in the Department of Mechanical Engineering at the University of Alberta. The load/extension curve in Figure B.2, used to calculate the spring constant, is shown below.

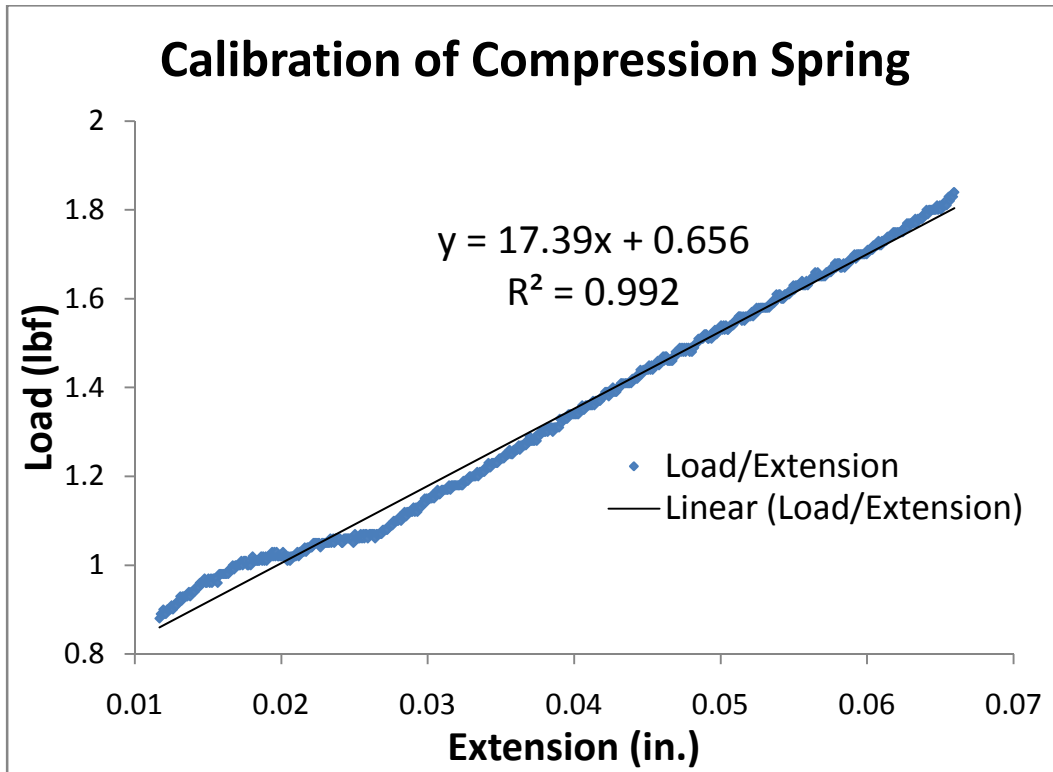


Figure B.2: Calibration curve of the compression spring used in the force gauge

Therefore, linear fit to the curve shows the spring constant to be 17.39 lbf/in. The R-squared value of 0.992 shows this to be an excellent fit.

To determine the preload on a subject, a ruler was marked on the side of the casing of the gauge. The plunger was used to compress the spring a known depth, corresponding to a pre-determined preload force. When the plunger reached the desired depth, a securing screw was maximally hand tightened to secure the plunger in place for the duration of the testing.

A photograph of the finished and installed design is shown below in Figure B.3.



Figure B.3: Compression spring force gauge in its experimental setup state.

Appendix C: Vibration System Technical Background

C.1 Overview

The vibration system used in this thesis consists of a number of basic elements: Control software, a signal generator, amplifier, electrodynamic shaker, and vibration sensors. The vibration system used in these experiments is designed as a single input, multiple output (SIMO) system. The signal generator creates a voltage signal in the desired vibration pattern, given through parameters in the testing control software. The vibration signal is then sent to an amplifier, which increases the gain on this signal. This electrical signal is transmitted from the amplifier to the electrodynamic shaker. The electrodynamic shaker attaches to the test object to which it inputs vibration. Transducers are placed on the test object to measure the response to vibration. This response is translated back to a computer, where analysis software can be used to extract pertinent signal information. Analysis software will not be discussed further as these techniques, beyond what is discussed in Chapter 2, are typically proprietary. Some of the advantages and disadvantages of the components are discussed in the following section in the context of the experiments performed for this thesis.

C.2 Vibration Input/Output Techniques

A number of vibration input/output configurations are used in vibration testing, with advantages and disadvantages to each. A single-input, single-output (SISO) system uses a single vibration excitation point to create input vibration, and a

single transducer to measure the vibration response of the object. The SIMO system also uses a single vibration excitation point; however, this input vibration is then measured at multiple locations on the test object through sensors. A multiple input, single output (MISO) system utilizes more than one vibration excitation point on the test object, while still measuring the vibration response from a single transducer. Finally, a multiple input, multiple output (MIMO) system utilizes more than one excitation point on the test object, while measuring the vibration response from multiple transducers [Ewins, 2000; Brown et al.].

The SIMO method is advantageous over a single input, single output (SISO) system, as it reduces testing time by measuring at multiple locations simultaneously [Brown et al.]. The simultaneous measurements do not have the potential for time-related effects such as creep or tissue dehydration, which could occur between location measurements in a SISO system. Additionally, the potential for measurement error in the vibration response is reduced by fixing the location of the sensors, as properties of the system could change due to the movement of the transducer mass [Allemang]. The SIMO system does not have the advantages of multiple-input systems (MISO, MIMO). The multiple excitation points allow for input vibration to be more evenly distributed over the object, with better energy distribution [Allemang; Brown et al.]. This reduces the need for high-amplitude vibration input, which minimizes the chance of non-linearities in the system. A multiple input system was not used in the spine due to the limited vertebral space available to which equipment could be attached. The contact tip currently used to input vibration takes up the entire spinous process of one vertebra. With only 5 lumbar vertebrae available for measurement, the addition of an excitation point decreases the number of vertebrae to measure the vibration response from; therefore, a SIMO system was chosen for the investigations in this thesis. Future investigation with MIMO techniques should include inputting vibration at non-lumbar skeletal points, such as the sacrum or

thoracic spine, so as to leave unaffected the number of vertebrae available for response measurement.

C.3 Electrodynamic Shaker and Stinger

The electrodynamic shaker acts in a similar manner to an audio speaker, and is shown below in Figure C.1.

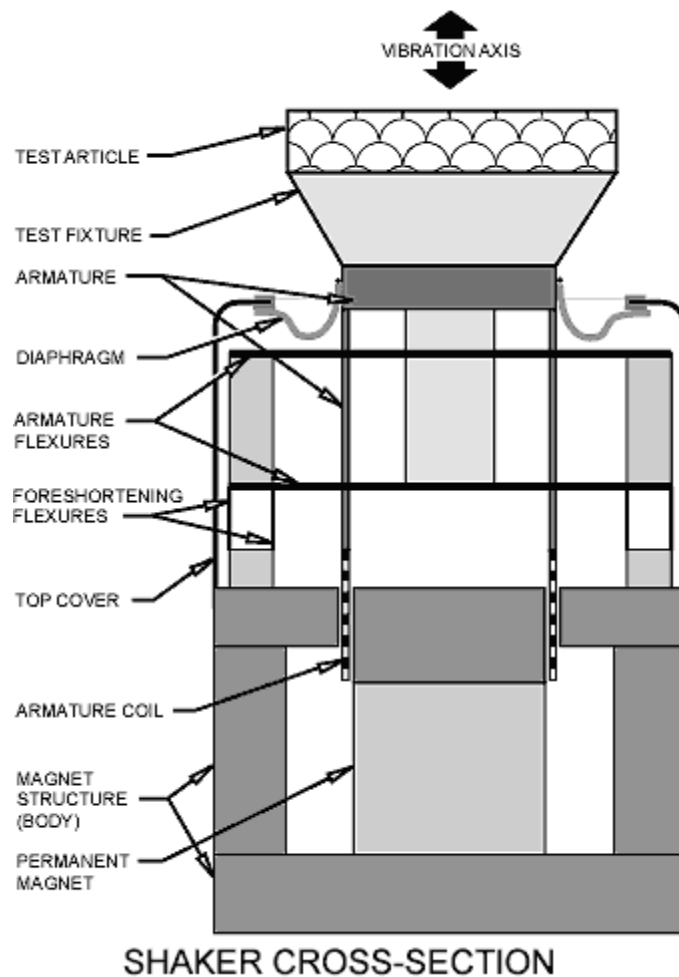


Figure C.1: Electrodynamic shaker schematic. Image from Labworks [Labworks, 2010]

The current received from the amplifier is sent through a movable armature coil, which is stationed around an affixed magnet. The presence of the current in the field of the magnet creates a force between the armature and the stationary magnet, causing the armature to move. The armature is connected to a diaphragm and mounting plate, to which test objects can be affixed via a stinger rod. By varying the applied current through the armature, the desired vibration output is created. The use of the current signal in an electrodynamic shaker offers a higher degree of signal control over that of a mechanical exciter, which uses an off-balance rotating mass to create vibrations [Ewins, 2000]. Therefore, an electrodynamic shaker was chosen for the experiments in this thesis.

The stinger rod is typically used to transmit vibrations to the test object from the electrodynamic shaker. This rod is an exceptionally important part of the vibration input system. When vibration is inputted to an object, the electrodynamic shaker typically creates the vibration on a rigid single axis only. However, the object will typically respond to this vibration in 3 axes of motion, as well as 3 rotational axes. If an inflexible stinger rod is used to connect the rigid shaker to the object, the multi-axial vibration response of the test object causes moments to be generated by the stinger/shaker, which are then exerted back on the test object as a secondary input vibration [Ewins, 2000]. These secondary input vibrations are not measured by the input system, but are measured by the sensors placed on the test object. This causes inaccurate frequency response function measurements. To reduce the effect of the secondary input vibrations, a stinger rod that is rigid in the axis of vibration input, but somewhat flexible in the remaining axes should be used. These stinger rods are typically made from Plexiglas, or stainless steel as with the experiments performed for this thesis. The length and flexibility of the rod must be carefully accounted for; if the rod is too flexible or too long, its own modes of vibration may be introduced to the test object [Ewins, 2000].

C.4 Vibration Excitation Signals

The pattern of excitation input to the system is a crucial decision in any vibration experiment. Vibration excitation signals are typically grouped into three different categories: periodic, transient, and random [Ewins, 2000; Brown et al.]. Periodic signals, such as a stepped sine, sine sweep, or chirp signals are characterized by a continuous, patterned signal, in which the vibration response of the system is averaged over a number of excitations. For instance, in a chirp signal, an input sine wave steadily increases in frequency over the given test period, from a specified low to high frequency. These types of signals are advantageous for use in detecting non-linearities of structures due to the systematic nature of the signal. Consequently, when the minimization of non-linearities in the vibration response is desired, periodic signals or random signals do not perform this task well. An additional disadvantage of some periodic signals is the length of time required to execute them, such as in stepped-sine testing, where steady state vibration response must be reached at each input frequency before moving on to higher frequencies [Ewins, 2000]. Random signals avoid linearity effects and steady state response issues by inputting purely random frequencies to the system in a continuous signal. However, the disadvantage of this continuous excitation is that transforming the signal to the frequency domain becomes extremely difficult. The steady state signal response must be truncated as a discrete signal in time so as to perform the Fourier Transform required to create an FRF. Therefore, the whole input signal is not observed within the transformation window, which can lead to an inaccurate FRF [Brown et al.]. This phenomenon is known as leakage error, and can be observed from any form of steady state input signal. To overcome the problem of leakage error, a transient signal such as a burst random or impact signal can be used. To create impact signals, an impact hammer instead of a shaker device is used to strike the test object. Unfortunately, the range of input frequencies is limited and uncontrolled,

as they are dictated by the material properties of the hammer [Ewins, 2000]. A random burst signal outputs discrete random frequencies to a test object. This type of signal has similar advantages to the random steady state signal, in that it reduces non-linear responses of the test object. However, it has the added benefit of being a discrete signal in time, which minimizes leakage error in the FRF [Ewins, 2000; Brown et al.; Allemang]. Because of these advantages, the random burst signal was chosen for the experiments performed in this thesis.

A summary of the full characteristics of each type of input signal is shown in Table C.1.

Table C.1: Excitation Signal Characteristics (Adapted from Allemang [Allemang et al])

Excitation Signal Characteristics								
	Steady State Sine	Pure Random	Pseudo Random	Periodic Random	Fast Sine	Impact	Burst Sine	Burst Random
Minimize Leakage	No	No	Yes	Yes	Yes	Yes	Yes	Yes
Signal-to-Noise Ratio	Very High	Fair	Fair	Fair	High	Low	High	Fair
Test Measurement Time	Very Long	Good	Very Short	Fair	Fair	Very Short	Very Short	Very Short
Controlled Frequency Content	Yes	Yes *	Yes *	Yes *	Yes *	No	Yes *	Yes *
Controlled Amplitude Content	Yes	No	Yes *	No	Yes *	No	Yes *	No
Removes Distortion	No	Yes	No	Yes	No	No	No	Yes
Characterize Nonlinearity	Yes	No	No	No	Yes	No	Yes	No

* Special Hardware Required

C.5 Transducers

A minimum of two transducers are required for any vibration testing experiment. The first transducer is required to measure the excitation input signal, and must be placed in line with the stinger, between the shaker and the test object. The transducer is placed in-line as close to the test object as possible, so as to gain the most accurate reading of the input vibration [Ewins, 2000]. The second transducer, or in the case of SIMO, transducers, are placed at points of interest on the test object. For example, when testing in the spine, transducers are affixed to vertebrae in invasive testing, or are placed directly on the skin atop the vertebrae in non-invasive testing.

Typically in vibration testing, accelerometers are used to measure the vibration response of the object, while impedance heads or dynamic force sensors are used to measure the input excitation [Ewins, 2000].

C.6 References

Allemang R. University of Cincinnati ME663 - Vibrations III Course Notes - CH5
Frequency Response Function Measurements. 79.

Brown D, Allemang R, Avitabile P. Modal Analysis: Theory and Application.
International Modal Analysis Conference XXVII, Society for Experimental
Mechanics, 2009.

Ewins DJ, editor. 2000. Modal testing. Wiley. 562 p.

Labworks I. 2010. Shaker Engineering Information - Electrodynamic Shakers.
http://www.labworks-inc.com/enginfo/shaker_eng.htm

Appendix D: Human Cadaver Ethics Documents

Budget

Project: The effect of human skin on non-invasive vibration analysis
Date: Thursday, January 08, 2009
Project Investigators: Dr. Gregory Kawchuk, Principal Investigator, Colleen Decker, M.Sc student

Item	Item Description	Cost Per Item	Number of Items	Total Items Cost
Anatomical Gifts Program Donation	Cadavers and facility are free for use, donations are encouraged according the users' ability to pay. Our donation will be \$100/cadaver for 6 cadavers	\$100.00	6	\$600.00
Box Nitrile Gloves	Gloves for investigator health protection	\$13.77	1	\$13.77
Box 18 GA Needles	Needles to implant into cadaver spine to measure spine movement	\$12.17	1	\$12.17
Cyanoacrylate Glue	Glue used to affix accelerometers to needles/skin on cadavers	\$4.00	1	\$4.00
Equipment Transportation	Supply management services moving equipment from current location to morgue. Rate supplied is hourly, est. 2 hrs moving time	\$74.00	2	\$148.00
			Total:	\$777.94

Budget Note: Measurement equipment (computer, analysis software, signal amplifier, sensors (accelerometers) and associated cables/attachments have already been purchased for use in previous experiments and have not been included as a cost in this budget)

Application Additional Documentation Notes

We wish to note the following items as additional information for our application:

1. As per Dr. D.J. Livy, Acting Director of the Department of Anatomy, we have obtained official approval to use cadavers from the Anatomical Gifts Program.
2. We wish to request an expedited approval of this application due to the minimally invasive nature of the experiments, as well as the cadaveric nature of the subjects.

ID: Pro00004279

Status: Approved

1.1 Study Identification

All questions preceded by a **red asterisk *** are required fields. Other fields may be required by the REB in order to evaluate your application. Please answer all presented questions that will reasonably help to describe your study or proposed research.

- 1.0 * Short Study Title (restricted to 250 characters):**
The effect of human skin on non-invasive vibration analysis
- 2.0 * Long Study Title (can be exactly the same as short title):**
The effect of human skin on the detection of the lumbar spine frequency response in non-invasive vibration analysis
- 3.0 * Select the appropriate Research Ethics Board:**
HREB Biomedical
- 4.0 * Which office requires notification of ethics approval to release funds or finalize the study contract? (It is the PI's responsibility to provide ethics approval notification to any office other than the ones listed below)**
University of Alberta - Research Services Office (RSO)
- 5.0 * Name of Principal Investigator (at the University of Alberta, Covenant Health, or Alberta Health Services):**
[Gregory Kawchuk](#)
- 6.0 Investigator's Supervisor (Required for graduate students and trainees NOT applying to the Health Research Ethics Board (HREB). The HREBs do not accept graduate students or trainees as Principal Investigators in an ethics application. Please enter your supervisor as the PI and yourself as a co-investigator in your application for HREB.)**
- 7.0 * Type of research/study:**
Graduate Student - Thesis, Dissertation, Capping Project
- 8.0 Study Coordinators/Assistants (will have access to and can edit this application and will receive all notifications for this study):**
- | Name | Employer |
|-------------------------------|----------|
| There are no items to display | |
- 9.0 Co-Investigators (Authorized List):** The following people can act as co-authors to this application: they will have access to, and can edit, this ethics application online. Co-investigators do not receive HERO notifications about the progress of the applications unless they are added to the study email list.
- | Name | Employer |
|----------------|----------|
| Colleen Decker | Student |
- 10.0 Study Team (co-investigators, supervising team, other study team members who do not require access to this application or to receive notifications):**
- | Last Name | First Name | Organization | Role | Phone | Email |
|-------------------------------|------------|--------------|------|-------|-------|
| There are no items to display | | | | | |

1.2 Additional Approval

- 1.0 * Departmental Review:**

RM Physical Therapy

2.0

Internal Review:

1.3 Study Funding Information

1.0

* Type of Funding:

Grant (external to the institution)

If OTHER, provide details:

2.0

Funding Source

2.1 Select all sources of funding from the list below:

NSERC - Natural Sciences And Engineering Research Council NSERC

2.2 If not available in the list above, write the Sponsor/Agency name(s) in full (you may add multiple funding sources):

There are no items to display

3.0

Location of funding source (required if study is funded):

Canada

4.0

RSO University-Managed Funding

4.1 If your funds are managed by the Research Service Office (RSO), select the project ID and title from the lists below to facilitate release of your study funds. (Not available yet)

4.2 If not available above, provide all identifying information about the study funding:

Project ID	Project Title	Speed Code	Other Information
[View] 239194-05	Determinants of Spinal Stiffness	56171	

1.4 Conflict of Interest

1.0

* Are any of the investigators or their immediate family receiving any personal remuneration (including investigator payments and recruitment incentives but excluding trainee remuneration or graduate student stipends) from the funding of this study that is not accounted for in the study budget?

Yes No

If YES, explain:

2.0

* Do any of investigators or their immediate family have any proprietary interests in the product under study or the outcome of the research including patents, trademarks, copyrights, and licensing agreements?

Yes No

3.0

Is there any compensation for this study that is affected by the study outcome?

Yes No

4.0

Do any of the investigators or their immediate family have equity interest in the sponsoring company? (This does not include Mutual Funds)

Yes No

- 5.0 Do any of the investigators or their immediate family receive payments of other sorts, from this sponsor (i.e. grants, compensation in the form of equipment or supplies, retainers for ongoing consultation and honoraria)?
- Yes No
- 6.0 Are any of the investigators or their immediate family, members of the sponsor's Board of Directors, Scientific Advisory Panel or comparable body?
- Yes No
- 7.0 Do you have any other relationship, financial or non-financial, that, if not disclosed, could be construed as a conflict of interest?
- Yes No

If YES, explain:

Important

If you answered YES to any of the questions above, you may be contacted by the REB for more information or asked to submit a Conflict of Interest Declaration.

1.5 Study Locations and Sites

- 1.0 * Specify research locations: Enter all locations where the research will be conducted under this Research Ethics Approval (eg. university site, hospital, community centre, school, classroom, participant's home, in the field, clinician's private office, internet website, etc. - provide details):
The Division of Anatomy and Faculty of Medicine morgue will be used as the facility in which to perform the experiments. A morgue technician must and will be on hand to supervise the work. Cadavers, supplied by the morgue facility and the Anatomical Gifts Program (Division of Anatomy), will be used as test subjects.
- 2.0 * Please check if your study will utilize or access facilities, programmes, resources, staff, students, specimens, patients or their records, at any of the sites affiliated with the following (select all that apply):
Not applicable
- Details must be provided if Alberta Health Services and/or Covenant Health and/or Capital Care selected:
- 3.0 If the study involves researchers in other institution(s), will ethics approval be sought from other institutions/organizations (eg. another university, Alberta Cancer Board, school district board, etc)?
Not Applicable
- If YES, provide a list:
Name
There are no items to display

2.1 Study Objectives and Design

- 1.0 Proposed Start Date:
1/12/2009
- 2.0 Proposed start date for working with human participation (can be the same as item 1.0):
1/12/2009

3.0 **Proposed end date for working with human participation:**
3/31/2009

4.0 *** Provide an abstract or lay summary of your proposed research (restricted to approx. 300 words):**

Low back pain is thought to be caused by mechanical dysfunction of the spine. The development of a new non-invasive diagnostic instrument to obtain functional information about the spine is the focus of this investigation.

In a prior study, we applied vibration to the spine using equipment attached directly to the spinal vertebrae. This study concluded that the vibration response of the spine could be used to correctly identify the location and nature of structural alterations of the spine.

In this study, we aim to adapt the described invasive test setup to a non-invasive setup for use in humans. Preliminary work performed in cadaveric pigs has shown that non-invasive vibration applied to the spine is partially transmitted through the skin, bypassing the spine.

Because human skin is significantly less thick over the spine compared with that of pigs, we seek to understand the effect of human skin on spinal vibration testing. We hypothesize that thinner, more elastic human skin will allow the input vibrations to be transferred more effectively to the spine, and less so through the skin.

To investigate this question, the following protocol will be used. An 18 gauge needle will be inserted through the skin into each of the L2, L3, and L4 vertebrae with an accelerometer attached to the needle hub. In addition, 3 accelerometers will be glued to the skin over the centre of the L2, L3, and L4 spinous processes. Once all accelerometers are applied, vibration will be applied by 6 different shaped shakers that will contact the skin overlying the L1 spinous process. The spine will be vibrated from 0-2000 Hz, which will be repeated for each shaped shaker. The correlation level of resulting frequency response functions (FRFs) from skin mounted accelerometers and bone mounted accelerometers will be calculated to determine the ability of skin-mounted accelerometers to represent underlying vertebral vibrations.

5.0 *** Provide a description of your proposed research (study objectives, background, scope, methods, procedures, etc) (restricted to approx. 1,000 words):**

Study Objective: To understand the effect of human skin on spinal vibration testing.

Background: Low back pain is a highly prevalent problem in society affecting up to 80% of individuals at some point in their lives. It is thought to be caused by mechanical dysfunction of the spine. The development of a new diagnostic instrument to obtain functional information about the spine is under investigation in this study. The instrument involves the application of structural health monitoring techniques for use in the lumbar spine. Structural health monitoring is a well known civil engineering technique used to determine the severity and location of damage, if any, to buildings, bridges, etc. Adapting this approach to a structure such as the spine would be extremely valuable in helping clinicians diagnose the causes of low back pain. Imaging techniques such as MRI and X-ray provide anatomical information but may not provide functional information. A new device which can determine the structural/functional state of the spine would be an advantageous diagnostic tool.

Previous work (invasive porcine testing): A vibration shaker device was attached directly to the L3 lumbar vertebra, with accelerometers screwed directly into each of the L1-L5 vertebrae. The spine was vibrated from 0-2000 Hz under different imposed perturbations to the spine. These conditions included disc transections, ligament transections, and simulated fusions between adjacent vertebral bodies. The acceleration response of each lumbar vertebra to the imposed vibrations (known as the frequency response function or FRF) was recorded. Using the frequency response data, a neural networking computer program was able to classify any given FRF with its correct perturbation type and severity. From this study, it was concluded that the frequency response data could be used to correctly identify the location and nature of each type of perturbation.

Previous work (non-invasive porcine testing): An accelerometer was glued to the skin centred over each of the T9 and T10 vertebrae (Thoracic vertebrae were used instead of lumbar due to thinner skin in this area, closer to that of humans). The vibration shaker was pre-loaded onto the skin over top of the T8 vertebra using a shaker head roughly formed to the underlying spinous shape. Accelerometers were also embedded into the anterior side of each of the T9 and T10 vertebrae to measure true bone movement. The spine was shaken from 0-2000 Hz. Comparison of a skin mounted accelerometer FRF to the corresponding true bone movement FRF showed poor correlation between the two. It was determined that vibrations from the shaker were being transmitted directly through the skin to the skin mounted accelerometer, bypassing the spine entirely and distorting that vibration signal. We believe that the thickness and inelastic nature of pig skin may play a role in the cause of this distortion, and thus testing is required on a human specimen.

Rationale: Measurements in our previous experiments have shown the skin to be approximately 1 inch thick over top of the T8 spinous process in a 60 kg pig which is not comparable to the skin thickness in humans of similar mass. We hypothesize that the thinner, more elastic human skin will allow the input vibration to be transferred more effectively to the spine and dampen any vibration in the skin itself, reducing noise in the skin accelerometer FRF signal.

Human Experiment Protocol: The following methods are adapted from the previously described non-invasive cadaveric pig tests. An 18 gauge needle will be inserted through the skin of human cadavers into each of the L2, L3, and L4 spinous processes with an accelerometer glued to the top of each. Three uniaxial accelerometers will be glued to the skin and centred over top of each of the L2, L3, and L4 spinous processes. The non-invasive vibration shaker will then be pre-loaded onto the skin over top of the L1 spinous process to a force of approximately 40 N. Four different non-invasive shaker heads, each with a different skin contact shape, will be tested to determine the most effective shape for inputting vibration to the spine. The spine will be vibrated from 0-2000 Hz and repeated 5 times per shaker head. FRF data will be taken from each of the skin mounted accelerometers and compared to the corresponding needle mounted accelerometer.

Data Analysis: Data will be analyzed using a computer program (created in-house) which measures the correlation in shape and amplitude between two given FRFs. Using this program, we will be able to quantify the differences and similarities between the true bone movement and the perceived bone movement picked up by the skin mounted accelerometer. The FRF correlation features of interest are: 1) Improvement or deterioration in the correlation of the skin accelerometer signal to the bone accelerometer signal (as compared to testing in cadaveric pigs); 2) Effect of shaker head design on the FRF signal correlation, and thus, the ability of the shaker head to transmit vibration directly to the spine.

- 6.0 **Describe procedures, treatment, or activities that are above or in addition to standard practices in this study area** (eg. extra medical or health-related procedures, curriculum enhancements, extra follow-up, etc):
N/A
- 7.0 **If this research proposal has received independent scientific or methodological review, provide information** (eg. names of committees or individuals involved in the review, whether review is in process or completed, etc):
N/A
- 8.0 **If this application is related to or builds upon a previously approved application not captured in HERO, provide the study title and approval number if available:**
We have obtained a "general use permission for porcine tissues" from the Faculty Animal Policy and Welfare Committee of the Faculty of Agriculture, Forestry, and Home Economics. This approval is dated June 20, 2006 and has no expiry. Our approval is deemed a category 'A' procedure, in which we acquire cadaveric porcine tissue from animals regularly euthanized by the Swine Research Technology Centre. There is no study title or approval number. Approval was granted by Dr. Doug Korver of the Department of Agricultural, Food and Nutritional Science / The Alberta Veterinary Research Institute. A copy of this approval will be uploaded with this application.

3.1 Risk Assessment

- 1.0 *** After reviewing the Minimal Risk Criteria provided in User Help, provide your assessment of the risk classification for this study:**
Minimal Risk
- 2.0 *** In a scale of 0 to 10 where 0 = No Likelihood, 5 = Moderate Likelihood and 10 = Extreme Likelihood, put a numerical rating in response to each of the following:**
- | Rate | Description of Potential Risks and Discomforts |
|------|--|
| 0 | Psychological or emotional manipulations will cause participants to feel demeaned, embarrassed, worried or upset |
| 0 | Participants will feel fatigued or stressed |
| 0 | Questions will be upsetting to the respondents |
| 0 | Participants will be harmed in any way |
| 0 | There will be cultural or social risk – for example, possible loss of status, privacy, and/or reputation |
| 0 | There will be physical risk or physiological manipulations, including injury, infection, and possible intervention side-effects or complications |
| 0 | The risks will be greater than those encountered by the participants in everyday life |
- 3.0 *** Provide details of short- and long-term risks and discomforts:**
N/A
- 4.0 *** Describe how you will manage and minimize risks and discomforts, as well as mitigate harm:**
N/A - Although there are no risks to the cadavers in terms of traditional concerns, precautions are in place to minimize damage to the cadavers themselves and those working on them. Cadavers will be stored, handled and moved as per morgue protocol, with the assistance and supervision of a morgue technician.
- Needles will be placed through the skin into the spinous processes of the lumbar vertebrae. To mitigate damage to the cadaver, needle placement will be carefully landmarked before insertion. The needle will be placed directly into the skin, and will be removed directly out. The needles will not be moved during the experiment. In previous porcine experiments, this has resulted only in a

small needle-thickness hole in the skin and spinous process.

Our test apparatus is non-invasive. The test requires the skin in the test area to be shaved. Only the necessary areas of skin will be shaved.

Our non-invasive test apparatus will press a shaker device onto the skin over top of the lumbar spinous process. Previous testing in cadaveric pigs has shown that the device does not break the skin. However, there may be a mark left on the skin due to the pressure of the shaker device on the skin (similar to marks left by wearing goggles, etc).

The shaker device will not cause any structural damage to the cadavers. The program which drives the shaker device is programmed to abort if a certain force input or displacement input is reached. These cut off levels have been pre-determined to standards that will not cause structural or tissue damage to the cadavers.

- 5.0 *** If your study has the potential to identify individuals that are upset, distressed, or disturbed, or individuals warranting medical attention, describe the arrangements made to try to assist these individuals. Explain if no arrangements have been made:**
N/A

3.2 Benefits Analysis

- 1.0 **Describe any benefits of the proposed research to the participants:**
Cadaveric study - N/A

- 2.0 *** Describe the scientific and/or scholarly benefits of the proposed research:**
Our lab is working towards developing a new device to be used in the diagnosis of mechanical spinal dysfunction using vibration analysis.

Vibration analysis has been investigated and successfully used in many diagnostic situations (dental and hip implant security, monitoring the healing of long bone fractures). The use of vibration analysis as a diagnostic tool has not yet been investigated in the spine. Our work is the first in this area, adding new scientific knowledge and literature.

More importantly, the development of a new diagnostic tool to aid in diagnosing mechanical dysfunction would be valuable to the scientific medical community. Imaging techniques (x-ray, CT, MRI) are only able to describe the anatomical state of the spine. The information obtained through our device gives researchers and clinicians insight into the structural and functional state of the spine in a rapid, non-invasive manner.

- 3.0 **Describe any benefits of the proposed research to society:**
Up to 80% of people will experience low back pain in their lifetime. In many back pain cases, the cause of the pain cannot be determined using imaging technology (x-ray, CT, MRI). The development of a new tool which provides functional information about the spine would aid clinicians in these situations, allowing for more informed diagnoses. An accurate diagnosis would allow patients to receive the correct treatment for their condition sooner, potentially improving their pain quicker and reducing long term treatment costs.

Because of these reasons, it is imperative that we continue the development of our new device. We have proven the viability of the concept using cadaveric pigs, and we now must move to testing human subjects. Testing in human cadavers will allow us to determine issues in testing in human subjects, and will allow us to improve the device so that we may begin testing in live human subjects.

- 4.0 **Benefits/Risks Analysis - describe the relationship of benefits to risk of participation in the research:**
Up to 80% of people will experience low back pain at some point in their lives. Though there is no risk to the participants of our study (as they are cadaveric), there is a great potential benefit to the greater world population. Continuing research on this device will eventually allow us to develop it as a viable tool to aid clinicians in their diagnoses of the causes of low back pain.

4.1 Participant Information

- 1.0 **Describe and justify the inclusion criteria for participants (eg. age range, health status, gender, etc):**
We will be using full adult cadavers. The age range will be any cadaver greater than 18 years old. This ensures that the spine is fully developed to adult size. Male or female cadavers may be used. Gender does not matter, as we are only testing the relationship of perceived bone

movement from a skin mounted accelerometer to the true underlying bone movement.

2.0 Describe and justify the exclusion criteria for participants:

Cadavers must have no skin conditions in the low back area. Cadavers will be in a pre-embalmed state. We will be testing the damping effect of skin on our vibration signal, and thus require regularity between test subjects. Because of this, any cadaver with a condition which would alter the regular behaviour of the skin (psoriasis, etc) cannot be included. Subjects must have been in good spinal health before becoming deceased. Cadavers will be excluded if they have altered structural integrity of the spine (scoliosis, spinal surgeries, etc). We would like the spine to have 'normal' healthy anatomy for the tests so as to be able to test our experimental equipment without introducing factors which may cause variability in our results.

3.0 Are there any direct recruitment activities for this study?

Yes No

4.0 Participants

Total number of participants you expect to enroll (including controls, if applicable):

6

Of these how many are controls, if applicable (Possible answer: Half, Random, Unknown, or an estimate in numbers, etc).

Descriptive study - N/A

If this is a multi-site study, how many participants (including controls, if applicable) do you anticipate will be enrolled in the entire study?

5.0 Justification for sample size:

This is a descriptive study. As our previous porcine studies related to this proposed experiment have used 5-6 animals/study, we have requested the same number of human subjects.

6.0 If possible, provide expected start and end date of the recruitment/enrollment period:

Expected Start Date:

Expected End Date:

4.2 Recruit Potential Participants

1.0 Recruitment

1.1 Will potential participants be recruited through pre-existing relationships with researchers (eg. employees, students, or patients of research team, acquaintances, own children or family members, etc)?

Yes No

1.2 If YES, identify the relationship between the researchers and participants that could compromise the freedom to decline (eg. professor-student). How will you ensure that there is no undue pressure on the potential participants to agree to the study?

2.0 Outline any other means by which participants could be identified (eg. response to advertising such as flyers, posters, ads in newspapers, websites, email, listservs; pre-existing records or existing registries; physician or community organization referrals; longitudinal study, etc):

Cadavers will be selected from the morgue by morgue staff based on availability, inclusion/exclusion criteria, and pre-deceased indication that the body is to be donated for medical research purposes. The morgue staff will have a pre-existing record of bodies which are to be donated for medical research purposes.

4.3 Recruitment Contact Methods

1.0 How will initial contact be made? Select all that apply:

Contact will be made through an intermediary

2.0 If contact will be made through an intermediary (including snowball sampling), select one of the following:

Intermediary provides potential participant's contact information to researchers with participant's informed consent for release of contact information

- 3.0 **If contact will be made through an intermediary, explain why the intermediary is appropriate and describe what steps will be taken to ensure participation is voluntary:**
Use of cadavers for medical research is handled by the Division of Anatomy in the Faculty of Medicine and Dentistry. We will use the cadavers selected by the staff as appropriate for us to use. Subjects will have given consent for their bodies to be used for medical research before becoming deceased.

- 4.0 **Provide the locations where participants will be recruited, (i.e. educational institutions, facilities in Alberta Health Services or Covenant Health, etc):**
University of Alberta Hospital morgue

4.4 Informed Consent Determination

- 1.0 *** Describe who will provide informed consent for this study:**
All participants will be competent to give informed consent

- 2.0 **How is consent to be indicated and documented?**
Signed consent form

- 3.0 **What assistance will be provided to participants, or those consenting on their behalf, who have special needs (eg non-English speakers, visually impaired, etc):**
As we will be using cadaveric subjects, consent issues will have been dealt with before death. Consent issues are handled by the hospital and the Faculty of Medicine and Dentistry.

- 4.0 **If at any time a participant wishes to withdraw or not participate in certain aspects of the research, describe the procedures and the last point at which it can be done:**
See 3.0

- 5.0 **Describe the circumstances and limitations of data withdrawal from the study, including the last point at which it can be done:**
N/A

- 6.0 **Will this study involve an entire group where non-participants are present?**
 Yes No

- 7.0 **Describe the incentives and/or reimbursements, if any, to participants and provide justification:**
No incentives or reimbursements are provided.

4.8 Study Population Categories

- 1.0 *** This study is designed to TARGET or specifically include the following (does not apply to co-incident or random inclusion). Select all that apply:**
Not applicable

5.1 Research Methods and Procedures

- 1.0 *** This study will involve the following (select all that apply)**
The list only includes categories that trigger additional page(s) for an online application. For any other methods or procedures, please indicate and describe in your research proposal in the Study Summary, or provide in an attachment:
Biohazardous Substances

- 2.0 **Does this study involve a Clinical trial (includes any research study that prospectively assigns human participants or groups of humans to one or more health-related intervention(s) to evaluate the effects on health outcomes; does not include randomized controlled trials – RCT – outside of clinical settings)?**

Yes No

3.0 For registered clinical trial(s), provide registry and registration number, if available:

4.0 Internet-based research

4.1 Will you be doing any internet-based research that involves interaction with participants?

Yes No

4.2 If YES, will these interactions occur in private spaces (eg. members only chat rooms, social networking sites, email discussions, etc)?

Yes No

4.3 Will these interactions occur in public space(s) where you will post questions initiating and/or maintaining interaction with participants?

Yes No

5.0 If you are using any tests in this study diagnostically, indicate the member(s) of the study team who will administer the measures/instruments:

Test Name	Test Administrator	Organization	Administrator's Qualification
There are no items to display			

6.0 If any test results could be interpreted diagnostically, how will these be reported back to the participants?

5.13 Biohazard Safety

1.0 **AMENDMENT OR RENEWAL:** If this application is for the amendment or renewal of a pre-existing clinical study, have new biohazards and/or manipulations been added to the research that were not identified in the original study protocol?

* **NOTE:** If this application is for a new study or a pre-existing non-clinical study, please select "Not Applicable".

If you selected **NO**, this amendment or renewal is exempt from requiring further review by the EHS Biosafety Division and the *original biohazard approval remains valid*. You do not need to respond to any of the questions below.

2.0 Will your research involve the use of one or more of the following? Provide a response for each item.

Answer	Description
<input type="radio"/> Yes <input checked="" type="radio"/> No	Risk group 2, 3 or 4 viruses, bacteria, fungi, parasites or eukaryotic cell lines
<input type="radio"/> Yes <input checked="" type="radio"/> No	Environmental specimens suspected to contain risk group 2, 3 or 4 microbes
<input type="radio"/> Yes <input checked="" type="radio"/> No	Large-scale single volume culture in excess of 10 litres for any microbe or eukaryotic cell line
<input type="radio"/> Yes <input checked="" type="radio"/> No	Microbial toxins
<input checked="" type="radio"/> Yes <input type="radio"/> No	Human clinical specimens, including blood or other body fluids, or primary culture of human cells
<input type="radio"/> Yes <input checked="" type="radio"/> No	Xenotransplant studies involving vertebrate donors and/or recipients
<input type="radio"/> Yes <input checked="" type="radio"/> No	Genetic therapy studies involving vertebrate donors and/or recipients
<input type="radio"/> Yes <input checked="" type="radio"/> No	Genetic manipulation involving virulence genes from risk group 2, 3 or 4 microbes, mammalian oncogenes, mammalian cytokine or interleukin genes, or microcide resistance genes

If you have any questions or concerns regarding the biohazard approval process, please contact:

Dr. Daniel Dragon
Biosafety Officer
Environmental Health and Safety
780-492-3142
EHS_RSR@ehs.ualberta.ca
Campus Mail: MS Code 287

In a cover letter, be sure to include the Principal Investigator's name and department, the project title, and the name of the grant, if applicable

6.1 Data Collection

- 1.0 *** Will the study team know the participants' identity at any stage of the study?**
 Yes No
- 2.0 **Primary/raw data collected will be (check all that apply):**
Anonymous
Confidential
All personal identifying information removed
- 3.0 **If identifying information will be removed at some point, when and how will this be done?**
We will not know the identity of the cadavers used. Cadavers will not have any identifying information associated with them available to the study investigators.
- 4.0 **If this study involves secondary use of data, list all sources:**
none
- 5.0 **In research where total anonymity and confidentiality is sought but cannot be guaranteed (eg. where participants talk in a group) how will confidentiality be achieved?**
n/a

6.2 Data Identifiers

- 1.0 *** Personal Identifiers:** will you be collecting any of the following (check all that apply):
None
If OTHER, please describe:
- 2.0 **Will you be collecting any of the following (check all that apply):**
There are no items to display
If OTHER, please describe:
n/a
- 3.0 **If you are collecting any of the above, provide a comprehensive rationale to explain why it is necessary to collect this information:**
n/a
- 4.0 **Specify information that will be RETAINED once data collection is complete, and explain why retention is necessary. Include the retention of master lists that link participant identifiers with de-identified data:**
n/a
- 5.0 **If applicable, describe your plans to link the data in this study with data belonging to another organization:**
n/a

6.3 Data Confidentiality and Privacy

- 1.0 *** How will confidentiality of the data be maintained? Explain the steps you propose to maintain data confidentiality and privacy.** (For example, study documents must be kept in a locked filing cabinet and computer files encrypted, etc.)
Physical lab documentation pertaining to each test along with the corresponding experimental data will be kept in a separate notebook which will be kept in a locked filing cabinet. Computer files and physical lab documentation do not have any personal identifiers associated with them, only raw data measurements.
- 2.0 **What privacy education/training do members of the team have prior to their access to data?**
NIH Human subjects training (Kawchuk)
- 3.0 **If you involve colleagues, assistants, transcribers, interpreters and/or other personnel to carryout specific research tasks in your study, how will you ensure that they properly understand and adhere to the University of Alberta standards of data privacy and confidentiality?**
N/A - Essential personnel (investigators named in this study) only are permitted in the morgue. There are no other assistants or colleagues involved in this project.
- 4.0 **Data Access**
- * 4.1 Will the researcher make raw data that identify individuals available to persons or agencies outside of the research team?**
- Yes No
- 4.2 If YES, describe in detail what identifiable information will be released, to whom, why they need access, and what safeguards will be used to protect the identity of subjects and the privacy of their data.**
n/a
- 4.3 Provide details if identifiable data will be leaving the institution, province, or country (eg. member of research team is located in another institution or country, etc.)**
n/a

6.4 Data Storage, Retention, and Disposal

- 1.0 **Where will the research data be stored? Specify the physical location and how it will be secured to protect confidentiality.**
Research notes will be stored in a dedicated lab notebook which will be kept in a locked filing cabinet. Research data obtained digitally through testing will be kept on a password protected lab computer. No personal data concerning the cadaver subjects is collected in this study.
- 2.0 **Describe what will happen to the data once the study is completed. Indicate your plans for the destruction of the identifiers at the earliest opportunity consistent with the conduct of the research and/or clinical needs:**
No identifiers are recorded in the study. Raw data from testing will be stored on our password protected lab computer.
- 3.0 **You must keep your data for a minimum of 5 years according to GFC Policy 96.2. How will you provide for data security during this time?**
No identifiers are recorded in the study. Raw data from testing will be stored on our password protected lab computer.

7.1 Documentation

Add documents in this section according to the headers. Use Item 12.0 "Other Documents" for any material not specifically mentioned below.

Sample templates are available in the [HERO Home Page in the Forms and Templates](#), or by clicking [HERE](#).

Important: Please do not use .docx files as attachments. It is recommended you convert these files first to .doc (standard Word document files) before attaching.

1.0	Recruitment Materials:			
	Document Name	Version	Date	Description
	There are no items to display			
2.0	Letter of Initial Contact:			
	Document Name	Version	Date	Description
	There are no items to display			
3.0	Informed Consent / Information Document(s):			
	3.1 What is the reading level of the Informed Consent Form(s):			
	3.2 Informed Consent Form(s)/Information Document(s):			
	Document Name	Version	Date	Description
	There are no items to display			
4.0	Assent Forms:			
	Document Name	Version	Date	Description
	There are no items to display			
5.0	Questionnaires, Cover Letters, Surveys, Tests, Interview Scripts, etc.:			
	Document Name	Version	Date	Description
	There are no items to display			
6.0	Protocol:			
	Document Name	Version	Date	Description
	There are no items to display			
7.0	Investigator Brochures/Product Monographs (Clinical Applications only):			
	Document Name	Version	Date	Description
	There are no items to display			
8.0	Health Canada No Objection Letter (NOL):			
	Document Name	Version	Date	Description
	There are no items to display			
9.0	Confidentiality Agreement:			
	Document Name	Version	Date	Description
	There are no items to display			
10.0	Conflict of Interest:			
	Document Name	Version	Date	Description
	There are no items to display			
11.0	Other Documents:			
	<i>For example, Study Budget, Course Outline, or other documents not mentioned above</i>			
	Document Name	Version	Date	Description
	Study Budget 	0.01	1/20/2009 2:40 PM	
	Additional Study Notes 	0.01	1/20/2009 2:39 PM	
	Previous ethics approval - for general use of cadaveric porcine tissues 	0.01	1/7/2009 11:01 AM	
	Biohazard approval to work with human body substances 	0.01	1/7/2009 10:52 AM	

Final Page

You have completed your ethics application! Please select "Exit" to go to your study workspace.

This action will NOT SUBMIT the application for review.

Only the Study Investigator can submit an application to the REB by selecting the "SUBMIT STUDY" button in My Activities for this Study ID:Pro00004279.

You may track the ongoing status of this application via the study workspace.

Please contact the REB Administrator with any questions or concerns.

ETHICS APPROVAL FORM - DELEGATED REVIEW

Date: February 14, 2009

Principal Investigator: [Gregory Kawchuk](#)

Study ID: [Pro00004279](#)

Study Title: The effect of human skin on the detection of the lumbar spine frequency response in non-invasive vibration analysis

Sponsor/Funding Agency: NSERC - Natural Sciences And Engineering Research Council NSERC

Thank you for submitting the above study to the Health Research Ethics Board (Biomedical Panel). Your application to use skin from cadavers, obtained under the Anatomical Gifts Program, has been reviewed and approved on behalf of the committee. We should point out that the consent questions on the application imply that specific consent is being obtained from the subject for this research project. However, we think this was a misinterpretation on your part and is meant to indicate that the subjects gave consent for their bodies to be used for research purposes. Please confirm that we are correct. An appropriate update to the application can be submitted as an administrative amendment.

This approval will expire on February 3, 2010. A renewal report or closure notice must be submitted next year prior to the expiry of this approval. You will receive electronic reminders at 60, 30, 15 and 1 day(s) prior to the expiry date. If you do not renew on or before that date, you will have to submit a new ethics application.

Approval by the Health Research Ethics Board does not encompass authorization to access the patients, staff or resources of Capital Health or other local health care institutions for the purposes of research. Enquiries regarding Capital Health administrative approval, and operational approval for areas impacted by research, should be directed to the Capital Health Regional Research Administration office, #1800 College Plaza, phone 407-1372.

Sincerely,

J. Stephen Bamforth, MD
Associate Chair, Health Research Ethics Board (Biomedical Panel)

Note: This correspondence includes an electronic signature (validation and approval via an online system).

Appendix E: Porcine Cadaver Tissues Permission

The following pages contain letters pertaining to permission to use porcine cadaver tissues.



20 June 2006

Dr. Greg Kawchuk
Canada Research Chair in Spinal Function
Assistant Professor, Faculty of Rehabilitation Medicine
University of Alberta

RE: Obtaining Animal Tissues

Dr. Kawchuk,

Thank you for your letter requesting cadaveric spines from regularly euthanized swine at the SRTC. As this is a category "A" procedure, you may obtain any amount of tissue as required for your research and FAPWC does not need to record the amount, protocol numbers or investigators that correspond to the tissue harvest. Please follow up with Jay Willis, Unit Manager, SRTC, to confirm what records he might need to keep or report.

Any need to obtain spines that requires that animals be euthanized specifically for this purpose will require a completed and approved animal ethics form submitted to FAPWC with the form available at <http://www.fapwc.afhe.ualberta.ca>.

The Committee has no concerns regarding this research and there is no expiry to this letter. If you have any questions, please contact me at 492-3990 or via email doug.korver@ualberta.ca if I can be of further assistance.

Sincerely,

Doug Korver,
Chair, FAPWC

cc: Jay Willis, Unit Manger, SRTC
Loren Kline, Chair, HSAPWC

Faculty Animal Policy Welfare Committee

Faculty of Agriculture, Forestry and Home Economics,
4-10 Agriculture Forestry Centre, University of Alberta, Edmonton, Alberta T6G 2P5
Phone: 780-492-1587 Fax: 780-492-4265, E-mail: fapwc@afhe.ualberta.ca



UNIVERSITY OF ALBERTA

July 7, 2006

Dr. Greg Kawchuk
Canada Research Chair in Spinal Function
Assistant Professor, Faculty of Rehabilitation Medicine
University of Alberta
2-28 Corbett Hall

Dear Dr. Kawchuk:

Thank you for your letter, dated June 20, 2006, requesting tissues from swine that are regularly euthanized at the SRTC and for keeping Health Sciences Animal Policy and Welfare Committee (HSAPWC) informed of your intentions. We are in agreement with the recommendations described by Dr. Korver in his letter dated June 20, 2006.

Please contact the HSAPWC office at 492-5322 if you have any questions or concerns.

Yours truly,

A handwritten signature in black ink, appearing to read "Kathryn Todd", written over a large, stylized circular flourish.

Kathryn Todd, PhD
Acting Chair
Health Sciences Animal Policy
& Welfare Committee
skr

Health Sciences Animal Policy and Welfare Committee

Appendix F: Calculation of Accelerometer Weight Factor

The accelerometer used by Rostedt et al. was 27 g. The needle diameter used in this thesis was 0.8 g.

To calculate the increase in the natural frequency due to the accelerometer weight factor, we use equation (3), the natural frequency of the system:

$$\omega = \sqrt{\frac{k}{m}}$$

Assuming that the spring constant of the system remains invariable, the increase in natural frequency will be due to an increase in mass by a factor of:

$$\frac{\sqrt{\frac{k}{m_2}}}{\sqrt{\frac{k}{m_1}}} = \sqrt{\frac{m_1}{m_2}} = \sqrt{\frac{27}{0.8}} = 5.81$$